

Université du Québec
Institut National de la Recherche Scientifique
Centre Armand Frappier

APPLICATION OF CNCs FOR PRESERVATION OF FOOD MATRICES

Par
Maria Paula Criado Cabrales

Mémoire ou thèse présentée pour l'obtention du grade
de Philosophiae Doctor (Ph.D.)
en Biologie

Jury d'évaluation

Président du jury et
Examineur interne

Steven Laplante
INRS-Institut Armand Frappier

Examineur externe

Valérie Orsat
University McGill

Examineur externe

Tatjana Stevanovic
University of Laval

Directeur de recherche

Monique Lacroix
INRS-Institut Armand Frappier

Codirecteur de recherche

Carole Fraschini
FPInnovations

INDEX

ACKNOWLEDGMENTS	vii
RÉSUMÉ	viii
SUMMARY	xi
LIST OF TABLES	xiv
LIST OF FIGURES	xv
ABBREVIATIONS	xvii
1. FOOD SPOILAGE	18
1.1 Presence of Pathogenic Bacteria.....	19
1.1.1 <i>Escherichia coli</i>	20
1.1.2 <i>Listeria monocytogenes</i>	20
1.1.3 <i>Salmonella</i>	21
1.2 Mesophilic Total Flora (MTF) and Food Shelf Life	21
1.3 Lipid Oxidation and Food Quality.....	22
1.4 Available Tests for the Determination of Lipid Oxidation	24
1.5 Active Biopolymeric Matrices in Food Industry.....	26
1.6 Existing Natural Antimicrobial Compounds from Plant Origin for Food Preservation.....	31
1.7 Encapsulation of Essential Oils by Biopolymers and Combination of Treatment	32
2. APPLICATIONS OF CELLULOSE NANOCRYSTALS IN FOOD PACKAGING	35
2.1 Cellulose Nanocrystals	35
2.2 Extraction of Cellulose Nanocrystals (CNCs).....	37
2.3 Microscopic Features and Morphology	39
2.4 Applications of CNCs in Food Biopolymers.....	40
2.4.1 CNCs' Role in Mechanical Properties of Biopolymers	40
2.4.2 CNCs' Role in Oxygen Barrier Capacity	41
2.4.3 CNCs' Role in Controlled Release	44
2.4.4 Modification of CNCs	45
2.5 Wholesomeness/toxicity of CNCs for Food Applications.....	48
3. GENERAL OBJECTIVE, HYPOTHESIS, SPECIFIC OBJECTIVES AND METHODOLOGIES	51
3.1 General Objective.....	51
3.2 Hypothesis.....	51
3.3 Specific Objectives	51

3.4 Methodologies	52
4. PUBLICATION 1: FREE RADICAL GRAFTING OF GALLIC ACID (GA) AND EVALUATION OF ANTIOXIDANT REINFORCED GELLAN GUM FILMS	54
CONTRIBUTION OF THE AUTHORS	55
RÉSUMÉ	56
ABSTRACT	56
4.1 Introduction.....	57
4.2 Experimental Section.....	59
4.2.1 Materials	59
4.2.2 Modification of CNCs	59
4.2.3 Ion Exchange (protonation) Treatment.....	61
4.2.4 Characterization of CNCs by Fourier Transform Infrared (FTIR)	61
4.2.5 Carboxylic Acid Content Determination by Conductometric Titration.....	62
4.2.6 Thermo Gravimetric Analysis (TGA).....	62
4.2.7 Free Radical Scavenger Properties	63
4.2.8 Mechanical Properties of Films	64
4.2.9 Water Vapor Permeability (WVP) of Films.....	65
4.3 Statistical Analysis.....	65
4.4 Results	65
4.4.1 FTIR analysis.....	65
4.4.2 Conductometric Titration of CNCs.....	67
4.4.3 Thermogravimetric Analysis.....	68
4.4.4 Radical Scavenging (RS) Capacity of CNCs	69
4.4.5 Radical Scavenging (RS) Properties of Gellan-based Films.....	71
4.4.6 Effect of Modified CNC on Mechanical Properties of Gellan Films	71
4.4.7 Water Vapor Permeability (WVP).....	74
4.5 Conclusions.....	75
4.6 Acknowledgements	76
4.7 References	77
5. PUBLICATION 2: GAMMA-IRRADIATION OF CELLULOSE NANOCRYSTALS (CNCs): INVESTIGATION OF PHYSICO-CHEMICAL AND ANTIOXIDANT PROPERTIES.....	82
CONTRIBUTION OF AUTHORS	83
RÉSUMÉ	84
ABSTRACT	84

5.1 Introduction.....	85
5.2 Materials.....	87
5.3 Methods	87
5.3.1 Preparation of CNCs Suspensions.....	87
5.3.2 Carboxylic Acid Content Determination by Conductometric Titration.....	88
5.3.3 Aldehyde Content Determination by Purpald [®] Reagent.....	88
5.3.4 Fourier Transform Infrared (FTIR) Spectroscopy	89
5.3.5 Fluorescence Spectroscopy.....	89
5.3.6 Cellulose Degree of Polymerization Determination	89
5.3.7 Chain Scission Number (CSN).....	90
5.3.8 Thermogravimetric Analysis (TGA)	90
5.3.9 Contact Angle	91
5.3.10 Transmission Electron Microscopy (TEM)	91
5.3.11 Antiradical Properties.....	91
5.4 Statistical Analysis.....	92
5.5 Results	93
5.5.1 Determination of Carboxyl Groups Content by Conductometric Titration...	93
5.5.2 Determination of Aldehyde Content by the Purpald [®] Method	94
5.5.3 Determination of Total Sulphur Content by ICP-AES	95
5.5.4 Fourier Transform Infrared (FTIR) Spectroscopy of Irradiated CNCs	95
5.5.5 Fluorescence Spectroscopy of Irradiated CNCs.....	96
5.5.6 Degree of Polymerization of Cellulose Chains	97
5.5.7 Effect of Irradiation on the Chain Scission Number (CSN)	98
5.5.8 Thermogravimetric Analysis (TGA)	99
5.5.9 Hydrophilic Character of Irradiated CNCs by Contact Angle	100
5.5.10 Transmission Electron Microscopy (TEM).....	101
5.5.11 Radical Scavenging Properties of Irradiated CNCs	102
5.6 Conclusions.....	104
5.7 Acknowledgements	105
5.8 References.....	106
6. PUBLICATION 3: EFFECT OF CELLULOSE NANOCRYSTALS ON THYME ESSENTIAL OIL RELEASE FROM ALGINATE BEADS: STUDY OF ANTIMICROBIAL ACTIVITY AGAINST LISTERIA INNOCUA AND GROUND MEAT SHELF LIFE IN COMBINATION WITH GAMMA IRRADIATION.....	111
CONTRIBUTION OF AUTHORS	112

RÉSUMÉ	113
ABSTRACT	113
6.1 Introduction.....	114
6.2 Materials and Methods	116
6.2.1 Materials	116
6.2.2 Bacteria Strain	117
6.2.3 Preparation of Alginate Emulsion Loaded with Different Concentrations of Thyme EO and CNCs	117
6.2.4 Preparation of Thyme Oil Loaded Beads	118
6.2.5 Particle Size of Alginate Emulsions.....	118
6.2.6 Encapsulation Efficiency and Loading Capacity of Thyme EO in Alginate Beads	118
6.2.7 <i>In vitro</i> Release Study of Thyme EO in Food Simulating Solvent for Ground Meat (Ethanol 10% v/v).....	119
6.2.8 <i>In vitro</i> "Agar Diffusion Assay".....	120
6.2.9 Volume of Alginate Beads.....	120
6.2.10 Transmission Electron Microscopy (TEM) of Alginate Beads	120
6.2.11 Fourier Transform Infrared Spectroscopy Analysis of Alginate Beads ...	121
6.2.12 In situ Test of Optimized Beads Introduced in Ground Meat	121
6.2.13 Gamma Irradiation and Thyme EO Combined Treatment	121
6.2.14 Mesophilic Total Flora (MTF) of Ground Meat.....	122
6.3 Statistical Analysis.....	122
6.4 Results and Discussion	122
6.4.1 Effect of Microfluidization on Thyme Emulsion Particle Size	122
6.4.2 Encapsulation Efficiency and Loading Capacity	124
6.4.3 <i>In vitro</i> Release Study.....	126
6.4.4 <i>In vitro</i> Test in "Agar Diffusion Assay" of Alginate Beads	129
6.4.5 Volume of Alginate Beads.....	129
6.4.6 Transmission Electron Microscopy (TEM).....	130
6.4.7 Fourier Transform Infrared Spectroscopy.....	131
6.4.8 Effect of Thyme EO loaded Alginate Beads and Gamma irradiation on <i>Listeria innocua</i> Inoculated Ground Meat.....	134
6.4.9 Effect of Combined Treatment in Mesophilic Total Flora (MTF) on Ground Meat	137
6.5 Conclusions.....	141
6.6 Acknowledgements	141

6.7 References	142
7. PUBLICATION 4: CELLULOSE NANOCRYSTALS (CNCs) LOADED ALGINATE FILMS AGAINST LIPID OXIDATION OF CHICKEN BREAST	147
CONTRIBUTION OF AUTHORS	148
RÉSUMÉ	149
ABSTRACT	149
7.1 Introduction.....	151
7.2 Materials and Methods	152
7.2.1 Chemicals	152
7.2.2 Preparation of Alginate-based Films Loaded with Cellulose Nanocrystals (CNCs)	152
7.2.3 Characterization of Alginate-based Films	153
7.2.4 Lipid Oxidation Tests of Food Matrices	154
7.3 Statistical Analysis.....	156
7.4 Results	157
7.4.1 Light Transmittance, Morphology of Films, and Birefringence of Alginate Solutions Loaded with CNCs	157
7.4.2 Oxygen Permeability of Alginate-based Films Loaded with Cellulose Nanocrystals (CNCs)	159
7.4.3 Lipid Peroxide Values of Chicken Coated Samples.....	161
7.4.4 TBAR Substances of Chicken Breast Coated with Alginate Films	163
7.4.5 Color of Coated Chicken Breast.....	165
7.5 Conclusions.....	166
7.6 Acknowledgements	167
7.7 References	168
GENERAL DISCUSSION AND CONCLUSIONS.....	174
REFERENCES	178
PUBLICATIONS AND CONTRIBUTIONS	199

ACKNOWLEDGMENTS

First and foremost, I would like to thank Pr. Monique Lacroix and Dr. Carole Fraschini for giving me this opportunity. During this rewarding experience, they taught me that when passion meets perseverance and hard-work one can get to achieve set goals and pass through any obstacles. Thanks for all the valuable guidance, support, and advice given in the development of this project.

Through this work, I had the opportunity to work with Damien and Philippe with whom I shared great discussions about materials and characterization. Thanks to them for the guidance they provided me with and the industrial point of view they brought into our discussions.

Special thanks to Stéphane for his help and discussions about protocols, results and his constant enthusiasm. To all the people I had the chance to meet at Laboratoire de Recherche en Sciences appliquées à l'alimentation de Laval and to Yosra, Amina, and Farah for the co-working and friendship developed over the years.

I cannot forget to thank Myriam for her constant hospitality and kind advice when challenging times occurred from time to time.

To all the students who contributed to this project: Dorra, Francisco, Daniela, Kelly, Anthony, Ianja, Sarah, Natacha, and Affef for their involvement in some parts of the project and the responsibility taken during their internship period. I am deeply grateful for your help and all the things I learnt from each of your experiences.

Thanks to Michel who has been always available for a hint during my bibliography research, for his support on managing and looking for the best data that could fit the field I was working on. I would like also to extend my deep thanks to Mme Philippon and Mme Chantal for their administrative help supplied during these years.

Finally, I would like to express my profound gratitude and thanks to Enrique, Margarita, Camargo-Higuera's family, Lubin, Ahmed, Samia, Dominique, and Marie-Christine, thank you for all your continued support, comprehension and encouragement throughout this experience. To my parents, Jairo, Carmen Cecilia, my brother Daniel, and family Denisse and Danielle to whom I owed my motivation and constant inspiration.
Gracias !

RÉSUMÉ

La recherche de nouveaux matériaux est en constante évolution, parfois dans le but d'augmenter la diversité des emballages biodégradables offerts, de lutter contre la pollution par les matières plastiques, de réduire la quantité de matériaux utilisés ou simplement de minimiser le gaspillage des aliments. Les nanocristaux de cellulose (CNCs) représentent un matériau innovant extrait de plantes, d'animaux marins, constitué majoritairement de cellulose, l'un des polymères d'origine naturelle les plus abondants au monde. En raison de leurs caractéristiques exceptionnelles telles que leur rigidité, leur dispersibilité dans les systèmes aqueux, leurs propriétés de renforcement/barrière et leur large surface spécifique pouvant offrir une multitude de fonctionnalités, les CNCs ont démontrés un grand potentiel en tant que nanoparticule de renforcement dans des matériaux nanocomposites.

Le but de ce projet était d'étudier la contribution et les performances des CNCs lorsqu'ils sont intégrés dans des polymères utilisés dans des systèmes alimentaires afin de préserver la qualité des aliments. Les deux premiers chapitres représentent la revue de littérature. Afin d'atteindre les objectifs et de répondre aux hypothèses du projet, des méthodologies ont été proposées et considérées dans le troisième chapitre. Dans le quatrième chapitre, nous avons examiné la possibilité de modifier chimiquement les CNCs à l'aide de la technologie d'irradiation gamma, avec comme objectif de leur conférer des propriétés antiradicalaires. L'irradiation gamma et le couple rédox initiateur (peroxyde d'hydrogène et acide ascorbique) ont tous deux conduit à la formation de sites actifs et facilité l'insertion d'acide gallique (GA), un composé phénolique aux propriétés antioxydantes. Un test à base de N,N-diéthyl-p-phenylènediamine (DPPD) a été utilisé pour analyser les propriétés antiradicalaires des CNCs. Dans une phase préliminaire, les suspensions de CNCs irradiées ont montré des propriétés antiradicalaires élevées de 1.92 (pour CNC- γ) à 8.20 mM eq Trolox/mg (pour CNC-H₂O₂-AA- γ -GA) comparé à 0 mM eq Trolox/mg pour les CNCs non-modifiés. En caractérisant les modifications chimiques des CNCs modifiées (CNC- γ et CNC-H₂O₂-AA- γ -GA), il a été observé qu'une concentration élevée en groupements acide carboxylique (environ 132-134 mmol COOH/kg de CNC) était formée par rapport aux CNCs non-modifiés (49 mmol COOH/kg).

Avec l'objectif de vérifier les modifications induites par l'irradiation gamma, les CNCs ont été dispersés et irradiés à des doses croissantes (0 à 80 kGy). Ces travaux font l'objet du cinquième chapitre où nous avons démontré la formation de nouveaux groupes fonctionnels tels que des groupements carboxyliques et que leur concentration augmentait proportionnellement avec la dose d'irradiation. Par exemple, les CNCs irradiés de 0 à 80 kGy indiquaient des concentrations en groupes carboxyliques allant de 43 jusqu'à 631 mmol COOH/kg de CNCs, respectivement. Les groupes aldéhydes ont également été quantifiés et leur concentration accrue a été attribuée à une rupture des liaisons glycosidiques des chaînes de cellulose pendant l'irradiation. Les propriétés antiradicalaires des CNCs irradiés ont ensuite été analysées, montrant ainsi une concentration de 40 μM eq acide ascorbique (AA) à 80 kGy par rapport à une concentration de 3 μM eq AA à 0 kGy. Les différences au niveau des résultats des propriétés antiradicalaires observées dans cette section par rapport à la section précédente se basent sur le principe de deux tests. Le test de DPPH a comme finalité de stabiliser le radical DPPH comparé aux nombreuses espèces réactives de l'oxygène (ROS) (e.g., anion superoxyde ($\bullet\text{O}_2^-$), oxygène singulet ($^1\text{O}_2$), radicaux hydroxyles ($\bullet\text{OH}$), peroxyde d'hydrogène (H_2O_2) et ion hypochlorite (OCl^-)) issues de l'électrolyse ayant lieu dans le test de DPPD. Une réponse similaire a été rapportée dans les tests de capacité antioxydante totale (TOC) qui montrent pour les CNCs irradiées (80 kGy) une réponse de 800 μM AA eq comparée à 200 μM AA eq pour les CNCs natifs.

La capacité réductrice des fonctions aldéhydes a été suggérée comme étant responsable des nouvelles propriétés antiradicalaires des CNCs. Des tests physico-chimiques tels que les mesures d'angle de contact et l'analyse FTIR ont été utilisés pour confirmer les changements de propriétés hydrophobes (mouillabilité) de la surface des films et les modifications chimiques des CNCs irradiés, respectivement. De plus, les images de microscopie électronique par transmission (TEM) ont permis d'évaluer la morphologie des cristaux pour lesquels aucune altération de morphologie n'a été révélée.

Le sixième chapitre examine la capacité d'encapsulation et le profil de libération contrôlée que les CNCs peuvent générer dans un système de billes d'alginate réticulé au calcium. Lors de précédentes études sur l'efficacité connue de l'huile essentielle (EO) de thym en tant qu'agent antimicrobien, des billes d'alginate ont été chargées avec différentes concentrations de CNCs, puis la capacité d'encapsulation ainsi que le taux

de libération d'EO ont été analysés dans un milieu simulant la viande. Le modèle de Korsmeyer-Peppas a été appliqué pour étudier la cinétique de libération de l'EO dans le solvant de simulation. L'ajout de 30% de CNCs dans des billes contenant 3% d'EO a eu pour effet de retarder de 10% la libération cumulative d'EO et de réduire de 30% la constante cinétique par rapport aux échantillons témoins. Les images de la coupe transversale des billes ont affiché une morphologie à plus faible porosité en présence de CNCs par rapport aux billes témoins. Cette observation pourrait expliquer le délai de libération observé pour l'EO dans le milieu simulé. La formulation optimale des billes a été testée contre *Listeria* sur du porc haché, où une activité synergique avec l'irradiation gamma a été observée pendant la période d'entreposage.

Enfin, dans un septième chapitre, l'influence de la présence de CNCs dans des films d'enrobage à base d'alginate a été évaluée sur le degré d'oxydation des lipides dans la poitrine de poulet. La transmittance de la lumière et l'effet barrière à l'oxygène à 0, 50 et 70% d'humidité relative (RH) ont été évalués afin de caractériser les films d'enrobage. Les films les plus performants ont été testés sur la surface du poulet et les mesures de valeurs de peroxyde, de TBARS et de colorimétrie ont été réalisées pour évaluer l'effet des enrobages sur la qualité du poulet en cours d'entreposage. Les résultats ont montré qu'une concentration de 30% de CNCs permettait une réduction de la perméabilité à l'oxygène dans les films d'enrobage. Également, dans la poitrine de poulet enrobée, une réduction des lipides peroxydés et des TBARS a été observée au fil du temps sans aucun indice d'oxydation mesuré par colorimétrie.

SUMMARY

New materials are constantly developed, some of them with the aim of increasing the offer in biodegradable packaging with the ultimate goal to combat plastic pollution, to reduce the amount of materials used or to simply reduce food spoilage.

CNCs are an innovative material extracted from plants and marine animals and composed of cellulose, one of the most abundant polymers on earth. Because of their outstanding characteristics such as stiffness, dispersibility in aqueous systems, reinforcing ability, barrier properties and surface area, that offer a large number of sites for further chemical derivatization, CNCs have demonstrated their potential as filler in nanocomposite materials.

The purpose of this project was to understand the contribution that CNCs can bring in the performance of polymers applied in food systems to protect food quality. This purpose will be reviewed in the literature review presented in the first two chapters. In order to achieve the established objectives and answer the hypothesis related to this project, methodologies have been proposed and were considered in the third chapter. In the fourth chapter, the feasibility of altering the CNCs surface chemistry by means of gamma irradiation for antioxidant molecule insertion purposes was studied. Both, the use of gamma irradiation and the presence of a redox pair (e.g., hydrogen peroxide and ascorbic acid) served to induce the formation of active sites and facilitate the insertion of gallic acid (GA), a phenolic compound with antioxidant properties, on CNCs surface. The N,N-diethyl-*p*-phenylenediamine (DPPD) test was used to analyze the antiradical properties of pristine (non-modified) and modified CNCs. The modified CNCs showed high antiradical properties from 1.92 (for CNC- γ) to 8.20 mM Trolox eq/mg (for CNC-H₂O₂-AA- γ -GA) compared to 0 mM Trolox eq/mg reported for pristine CNCs. By monitoring the chemical changes of both CNC- γ and CNC-H₂O₂-AA- γ -GA, it was observed that the concentration of carboxylic acid groups was slightly increased to approximately 132-134 mmol COOH/kg compared to 49 mmol COOH/kg for pristine CNCs.

In order to verify and study the changes induced by gamma irradiation, CNCs were dispersed in water and irradiated at doses ranging from 0 to 80 kGy, which study is covered in the fifth chapter. It was observed that the increase in carboxylic acid groups

formed during irradiation was directly proportional to the irradiating dose. For instance, 0 and 80 kGy-irradiated CNCs showed 43 and 631 mmol COOH/kg CNCs, respectively. Aldehyde groups were also quantified and results showed that their concentration also increased which was ascribed to a cleavage of glycosidic bonds of the cellulose chains during irradiation. The antiradical properties of irradiated CNCs were then analyzed showing a concentration of 40 μM ascorbic acid (AA) at 80 kGy compared to 3 μM AA at 0 kGy. Differences with regard to the results observed in the fourth chapter were based on the capability of irradiated CNCs to stabilise the DPPH radical compared to the numerous reactive oxygen species (e.g., superoxide anions ($\bullet\text{O}_2^-$), singlet oxygen ($^1\text{O}_2$), hydroxyl radicals ($\bullet\text{OH}$), hydrogen peroxide (H_2O_2) and hypochlorite ion (OCl^-)) produced during electrolysis carried out in the DPPD test. Similar increased values of antiradical properties were observed in the total antioxidant capacity (TAC) with reported values of 200 μM AA eq and 800 μM AA eq for CNCs irradiated at 0 and 80 kGy, respectively. The reducing properties of aldehyde groups were suggested to be responsible for the new antiradical properties of CNCs. Physico-chemical tests were carried out using contact angle for determining hydrophobic changes (wettability) of CNCs film surface, FTIR was used to confirm the chemical changes of irradiated CNCs and TEM images of dried crystals studied the morphology of CNCs, revealing no changes.

The sixth chapter reviewed the encapsulation capacity and controlled release properties that CNCs can bring to a calcium cross-linked alginate bead system. With previous studies conducted on the efficiency of thyme essential oil (EO) as an antimicrobial agent, the beads were loaded with different concentrations of CNCs and then encapsulation efficiency and release of EO were analyzed in a meat simulating solvent. The Korsmeyer-Peppas model was applied in order to study the release kinetics of the EO in the solvent. The presence of CNCs in the bead system proved their efficiency by delaying by 10% the cumulative release of EO and decreasing by 30% the kinetic constant value when 3% thyme EO and 30% CNCs were used with respect to the control sample with 0% CNCs. Images of the bead cross-section exhibited the presence of smaller pores when CNCs were added to the beads compared to control. This phenomenon could explain the delay observed in the release of EO in simulated solvent. Optimal formulation of beads was tested in ground pork against *Listeria* and when used in combination with gamma irradiation, synergistic activity was observed during storage.

Finally, in the seventh chapter, the influence of CNCs incorporated in alginate-based edible coatings was evaluated against the degree of lipid oxidation in chicken breast. Light transmittance and oxygen barrier properties of edible films at 0, 50, and 70% RH were measured. Films showing the highest performance were tested on chicken breast surface and peroxide values, TBARS, and colorimetry tests were used to determine the effect of the coating on the meat quality during storage. Results showed that a concentration of 30% CNCs reduced the oxygen permeability of the coating and resulted in a reduction of lipid peroxide and TBARS in the coated chicken breast over the storage period. Non-oxidative response was suggested by colorimetric measurements of the chicken breasts.

LIST OF TABLES

Table 1 Sampling plan divided into two classes for qualification of food quality	22
Table 2 Length (L) and width (w) of CNCs extracted from different sources.	38
Table 3 Oxygen permeability (OP) of polymers with dispersed and coated CNCs.....	43
Table 4 Concentration of carboxylic acid groups introduced onto CNC surface.....	68
Table 5 Radical scavenging properties (mM Trolox eq/mg CNC) of CNCs derivatives	70
Table 6 Physicochemical characteristics of native and irradiated CNCs suspensions	93
Table 7 Radical scavenging properties of irradiated CNC expressed as ascorbic acid and Trolox equivalents (eq) in μM	102
Table 8 Principal components of <i>Thymus vulgaris</i> (thyme) EO analyzed by the provider <i>via</i> gas chromatography.....	118
Table 9 Encapsulation efficiency (%) and loading capacity (%) of different concentrations of thyme EO (prepared from 1 and 3% emulsion) in alginate beads containing 0-40% CNCs.....	125
Table 10 Release parameters of beads prepared from 1-3% thyme EO emulsion in simulating solvent (10% (v/v) ethanol). Parameters <i>n</i> and <i>k</i> represent exponent coefficient and release constant respectively.	128
Table 11 Agar diffusion assay of thyme oil loaded alginate beads inoculated with <i>Listeria innocua</i> on an initial well diameter of 8 mm.	129
Table 12 <i>Listeria innocua</i> growth on ground meat mixed with alginate beads prepared from 3% thyme EO emulsion at 0% (Thyme) and 30% CNCs (Thyme+CNC) treated with gamma irradiation doses from 0 to 3 kGy.....	135
Table 13 Oxygen permeability (OP) ($\text{cm}^3 \cdot \mu\text{m}/\text{m}^2 \cdot \text{day}$) of pure CNCs-based and alginate-based films containing 0 and 30% CNCs at characterized at different relative humidity (%) and comparison with the calculated OP values according to Eq. 23.	160

LIST OF FIGURES

Fig. 1 Examples of lipids: a) phospholipid and b) triglyceride. Phospholipid image was taken from "cell membrane structure" website retrieved from https://aecbio11.fandom.com/	23
Fig. 2 Schematic representation of the alginate macromolecule	28
Fig. 3 Schematic representation of chitin (a) and deacetylated chitosan (b)	29
Fig. 4 Schematic representation of low acyl gellan gum	30
Fig. 5 Schematic representation of the hierarchical structure of wood	35
Fig. 6 Number of publications (such as articles, conference papers, reviews, book chapters) related to cellulose nanocrystals. Data from Scopus database from 2007 to 2017.	36
Fig. 7 AFM and TEM images of CNCs extracted from wood by sulfuric acid hydrolysis. AFM and TEM images are taken from Sacui <i>et al.</i> (2014).....	39
Fig. 8 Representation of hydrogen bonding (Favier <i>et al.</i> 1995; Hamad, 2017; Lizundia <i>et al.</i> , 2016) and percolation phenomenon of cellulose nanocrystals embedded in a polymer matrix ...	41
Fig. 9 Polystyrene molecule (left) and poly(vinyl alcohol) (right).....	42
Fig. 10 Proposed reaction pathway of gamma-rays on C ₁ and C ₄ of cellulose adapted from (Ponomarev and Ershov, 2014, Sánchez Orozco <i>et al.</i> , 2012, Sokhey and Hanna, 1993, Sultanov and Turaev, 1996).	47
Fig. 11 Schema of proposed mechanism of reaction of gallic acid with CNC by means of a redox pair followed by gamma-irradiation.....	60
Fig. 12 Schema of treatments performed onto CNC	61
Fig. 13 Example of conductometric titration curve of protonated CNC containing weak acid groups	63
Fig. 14 FTIR spectra of CNC (Black), CNC-H ₂ O ₂ -AA (Green), CNC-γ (Yellow), CNC-H ₂ O ₂ -AA-γ (Blue) and CNC-H ₂ O ₂ -AA-γ-GA (Red).....	66
Fig. 15 Thermogravimetric analysis (TGA) of native CNC and its derivatives	69
Fig. 16 Radical scavenging capacity (RS in mM Trolox eq/100 mg of film) of 1% (w/v) gellan-based films with native CNC or CNC- H ₂ O ₂ -AA-γ-GA at different concentrations. The asterisk indicates the difference with respect to the control	71
Fig. 17 Tensile strength (MPa) for gellan gum films containing CNC or CNC-H ₂ O ₂ -AA-γ-GA.....	72
Fig. 18 Tensile modulus (MPa) for gellan gum films containing CNC or CNC-H ₂ O ₂ -AA-γ-GA.....	73
Fig. 19 Elongation at break (%) of gellan gum films containing CNC or CNC-H ₂ O ₂ -AA-γ-GA.....	74
Fig. 20 Water vapor permeability (WVP in g·mm/m ² ·day·pKa) of gellan films containing CNCs or CNC-H ₂ O ₂ -AA-γ-GA	75
Fig. 21 Proposed reaction pathway of gamma-rays on C ₁ and C ₄ of CNCs adapted from (Sokhey and Hanna 1993; Sultanov and Turaev 1996; Sánchez Orozco <i>et al.</i> 2012; Ponomarev and Ershov 2014).	94
Fig. 22 FTIR spectra of acid freeze-dried CNCs irradiated at 0 kGy (Black), 10 kGy (Blue), 20 kGy (Red), 40 kGy (Pink), 80 kGy (Green)	96
Fig. 23 Fluorescence spectroscopy of irradiated CNCs	97
Fig. 24 Molar mass distribution of CNCs irradiated at different doses	98
Fig. 25 Chain scission number (CSN) as a function of γ-irradiation dose.....	98

Fig. 26 Thermogravimetric curves of freeze-dried irradiated CNCs	99
Fig. 27 Contact angle measurements of films of irradiated CNCs	100
Fig. 28 TEM images (11,000x) of re-suspended native and irradiated CNCs neutralized with NaOH. The scale bar represents 500 nm.....	101
Fig. 29 Total antioxidant capacity and DPPH radical scavenging tests comparison performed in irradiated CNCs	103
Fig. 30 Effect of CNCs concentration (0-40 % wt. polymer dry weight) on homogenization (0 and 3 cycles at 15,000 psi) of 1 and 3% thyme EO emulsion.	123
Fig. 31 <i>In vitro</i> thyme oil release profile of alginate beads prepared from 1% thyme EO emulsion and 0-40% CNCs.....	126
Fig. 32 <i>In vitro</i> thyme EO release profile of alginate beads prepared from 3% thyme oil emulsion and 0-40% CNCs.....	127
Fig. 33 Calculated volume of beads containing 0-40% CNCs prepared from 0 and 3% of thyme EO emulsions.	130
Fig. 34 TEM images (2,000x) of the cross section of alginate beads prepared from 3% thyme EO-loaded emulsion with 0% (A) and 30% CNCs (B).	131
Fig. 35 Fourier Transform Infrared spectra of alginate beads containing 0-3% thyme EO - 0-30% CNCs.	133
Fig. 36 Mesophilic Total Flora (MTF) growth on ground meat without beads as a function of gamma irradiation doses (0-3 kGy).	138
Fig. 37 Mesophilic Total Flora (MTF) growth on ground meat mixed with alginate beads (prepared from 3% thyme EO emulsion and 0% CNCs) as a function of gamma irradiation doses (0-3 kGy).	139
Fig. 38 Mesophilic Total Flora (MTF) growth on ground meat mixed with alginate beads (prepared from 3% thyme EO emulsion and 30% CNCs) as a function of gamma irradiation doses (0-3 kGy).	140
Fig. 39 Optical transmittance of alginate-based films loaded with cellulose nanocrystals (CNCs)	157
Fig. 40 DIC microphotographs of CNCs films (A) and alginate films loaded with 0% CNCs (B), 10% CNCs (C), 20% CNCs (D), and 30% CNCs (E)	158
Fig. 41 Birefringence of CNC suspension at 0.6% w/w (A), alginate solution (B) and alginate solution with dispersed CNCs at 10% (C), 20% (D), and 30% w/w (E) as observed through cross-polarizers under magnetic stirring	159
Fig. 42 Peroxide values (mEq/kg) of chicken coated with alginate-based films loaded at different concentrations of CNCs (control, 0, 30% CNCs)	161
Fig. 43 Chicken meat water loss (%) without coating (control) and coated with alginate-based film (0% CNCs) and alginate based film loaded with CNCs (30% CNCs) (A). Water retention (%) of the system (meat and film) during storage of control and coated with film loaded with 0% and 30% CNCs (B)	162
Fig. 44 Thiobarbituric Acid Reagent Substances (TBARS) content of chicken breast coated with alginate-based film containing 0% and 30% CNCs during storage for 8 days at 4°C, compared to the control without coating.....	164
Fig. 45 Lightness (L*) and redness (a*) of chicken breast samples with and without alginate based coating loaded with 0 and 30% CNCs	165

ABBREVIATIONS

AA: Ascorbic acid	OP: Oxygen permeability
AFM: Atomic force microscopy	OTR: Oxygen transmission rate
Aw: Water activity	PCL: Polycaprolactone
CFU: Colony forming unit	PHB: Polyhydroxybutyrate
CNCs: Cellulose nanocrystals	PLA: Polylactic acid
CTC: Cellulose tricarbonyl	PV: Peroxide values
DMSO: Dimethyl sulfoxide	PVA: Polyvinyl alcohol
DP: Degree of polymerization	PPA: Phenyl acetic acid
DPPD: N,N-diethyl- <i>p</i> -phenylenediamine sulfate salt	RH: Relative humidity
DPPH: 2,2-diphenyl-1-picrylhydrazyl	ROS: Radical oxygen species
Eb: Elongation at break	RS: Radical scavenging
EE: Encapsulation efficiency	STEM: Scanning transmission electronic microscopy
EO: Essential oil	TBARS: Thiobarbituric reactive substances
FTIR: Fourier Transform Infrared	TEM: Transmission electronic microscopy
GA: Gallic acid	TGA: Thermogravimetric analysis
HDPE: High density polyethylene	THF: Tetrahydrofuran
LC: Loading capacity	TM: Tensile modulus
LDPE: Low density polyethylene	TS: Tensile strength
MAPAQ: Ministère de l'Agriculture, des Pêcheries et de l'Alimentation du Québec	TSB: Tryptic soy broth
MDA: Malondialdehyde	WVP: Water vapor permeability
MMT: Montmorillonite	
MTF: Mesophilic total flora	

LITERATURE REVIEW

1. FOOD SPOILAGE

Food is considered a biological product coming from living organisms. It is mainly constituted of water, proteins, carbohydrates and fats, which make food a valuable product and a source of energy for the biochemical transformations occurring during metabolism processes. In addition, food represents a source of essential minerals for daily intake where sodium, potassium, calcium, magnesium, and phosphorous are recommended at concentrations of 0.5-2.3, 1.2-2.3 (United States Department of Agriculture, 2010), 1 (Health Canada, 2008), 0.3 and 0.5-1 (Health Canada, 2005) g/day for adults, respectively. In addition to minerals and vitamins, amino acids coming from vegetal and animal proteins are also essential elements for a balanced nutritional diet without discriminating the energetic role given by lipids such as common polyunsaturated fatty acids.

Because of its content on carbon and energy source, food represents a suitable niche for the development of microorganisms or physicochemical changes which without adequate control it can lead to degradation and loss of its nutritional value. Environmental conditions such as temperature, humidity, oxygen, and light are influential agents on the acceleration of food degradation (Rahman, 2007). For instance, Ciftci and Ozilgen (2019) observed a direct effect of increased temperatures on the lipid oxidation process in almond pastes. In sprayed dried spinach juice, the authors Syamila *et al.* (2019), showed a decreasing concentration of β -carotene under the effect of light, oxygen, and temperature during storage period.

Previous examples are related to the influence of environmental parameters on food shelf-life, but also microbial spoilage can be presented in food. Soil, water, air, and animals are some of the sources of microorganisms (Rahman, 2007). These microorganisms can be transferred to food and while treating other non-contaminated products cross-contamination can be then produced. Constituting 25% of food-borne outbreaks (Tirado and Schmidt, 2001), cross-contamination takes place in equipment, or surfaces where products are transformed and treated. For example, it was studied that chicken filets and cucumber were contaminated with the transfer of pathogenic bacteria such *Salmonella*, *Staphylococcus aureus*, and *Campylobacter jejuni* from stainless steel surface (Kusumaningrum *et al.*, 2003).

Either by ingestion or direct contact, pathogenic bacteria can cause diseases and infections in humans. It has been reported that millions of food-borne diseases (Public Health Agency of Canada, 2015) highlight how food insecurity is impacting health and human development. With the purpose of mitigating these existing problems and preventing ingestion of contaminated food, associations such as World Health Organization, Food, and Agricultural Organization and Health Canada among others regularly issue recalls and safety alerts (Government of Canada, 2012). Even though, international associations are in vigilance of the food spoilage consequences, it is necessary to continuously find solutions from different points of view (e.g., industrial and/or academic) in order to prevent the contamination to reach the consumer. This chapter will introduce the different types of pathogenic bacteria in microbial contamination, the reactions during lipid oxidation, and the available tests. Finally, this chapter will end with a description of the principal encapsulating matrices, the efficiency of essential oils and their combined effect with a non-thermal treatment of gamma-irradiation.

1.1 Presence of Pathogenic Bacteria

According to Health Canada (2004), a food-borne disease (also known as food-borne illness or food-borne poisoning) is attributed when a person has been contaminated with a harmful micro-organism (e.g., bacteria, virus or parasite). It is then considered an outbreak when two or more people sharing a common exposure suffer similar symptoms with one of them being sick.

Food contamination can either come from an exogenous or endogenous origin. An exogenous origin represents contamination transferred from the external environment. Mostly, food is contaminated when it comes in contact with contaminated surfaces or external sources such as handling, chopping or any other processing technologies. On the other hand, endogenous contamination is considered when microorganisms come from the animal itself from whose digestive tract, anus, and oropharyngeal sphere represent appropriate sites for the development of millions of microorganisms, among them pathogenic bacteria. One of the best known reported cases of endogenous contamination was due to *Salmonella* infection in eggs (Louis *et al.*, 1988). The source of this infection was linked to either the transmission of the bacteria from the animal to

the egg during egg formation and/or the transfer of the bacteria on the surface of the eggshell during handling/processing (Whiley and Ross, 2015). Even though an exogenous source of contamination is more often observed than endogenous, one should be aware of the existence of both of them.

Pathogenic bacteria not only affect human health and food but also the total viable count (TVC) or microbiological organisms that co-exist in food and are responsible for textural changes, loss of color, apparition of visible colonies on surface without mentioning their influence on organoleptic aspects. Defined by the number of colonies forming units per m² or g of food, TVC in food establishes the limit tolerable in food. For this reason, its measurement remains as one parameter that includes all aerobic bacteria present in the product.

In the following section it will be described the most important pathogenic bacteria, their associated symptoms, as well as mesophilic total flora (MTF) growth in food as a regulation criterion for the evaluation of good manufacturing practices.

1.1.1 *Escherichia coli*

Escherichia coli is a gram-negative bacterium that can be found in the lower portion of the intestine of both animals and humans. Because of its capacity to grow under precarious environmental conditions such as those found in manure, water troughs, and other places in the farming environment (Mead and Griffin, 1998) *E. coli* can be transferred to food, water or through direct contact with infected animals and people (Hancock *et al.*, 1998). In a human infection caused by *E. coli*, after 3 to 9 days of incubation, the symptoms observed can vary from diarrhoea, haemorrhagic colitis, abdominal pain to in some cases haemolytic uremic syndrome (Jeantet *et al.*, 2006a).

1.1.2 *Listeria monocytogenes*

Listeria is an aerobic, facultative anaerobic and gram-positive bacterium first discovered in 1926 due to an outbreak in rabbits and guinea pigs (Murray *et al.*, 1926). The bacterium shows propensity to grow under adverse conditions such as low temperature (2-4°C) or a wide range of pH (3.9-9.6) but it can also be found on soil where it is then transmitted to animals or people. As a consequence *Listeria* has been found in several food matrices such as unpasteurized milk, meat, soft cheeses, and ready-to-eat food

where the water activity (a_w) is sufficient to allow its development (Asahata *et al.*, 2015). In addition, because of its ability to form bacterial biofilms on surfaces, areas such as slaughtering, cutting, packing, and processing represent a proper environment where *Listeria* can grow (Health Canada, 2011; Little *et al.*, 2009).

Its ingestion leads to gastroenteritis and the probability of mortality ranges between 20 to 30% on average for population contaminated with the bacterium and incubation time can vary from three to 70 days (Linnan *et al.*, 1988; Riedo *et al.*, 1994). Illness related to *Listeria* infection can severely affect pregnant women, elderly, and immuno-depressed people, as well as unborn babies and neonates.

1.1.3 *Salmonella*

Salmonella is a mesophilic and gram-negative bacterium. This pathogenic bacterium is divided into two groups –typhoid and non-typhoid– depending on its consequences on human health. The typhoid and paratyphoid A and B species are responsible for fevers and non-typhoid species cause food-borne diseases (Collins *et al.*, 2004). *Salmonella* species can grow in a wide range of temperatures from 10°C to 50°C and have the ability not only to survive in food for prolonged periods of time but also in the environment, vegetables, and animal faeces. In most cases, *Salmonella* is incubated in the digestive tube of humans or animals like chicken. When *Salmonella* resides in chicken, contamination is transmitted through the egg, as the yolk represents the most favourable conditions for growth. Incubation time ranges from 12 to 24 h and the symptoms associated with the illness are diarrhoea and vomiting but abdominal pain, fever, and vertigo can also be observed (Jeantet *et al.*, 2006b).

1.2 Mesophilic Total Flora (MTF) and Food Shelf Life

Aerobic mesophilic bacteria or mesophilic total flora (MTF) represents microorganisms that grow at temperatures between 25°C to 45°C, with a maximum growth rate at 37°C. MTF belongs to one of the groups of the total viable count of microorganisms found in food in addition to psychrotropic flora growing at 15°C, yeasts and moulds. Because of the appropriate growing conditions, it can be suggested that MTF allows the determination of sanitary aspects at which a product is submitted during processing (e.g., chain preservation, use of transport, equipment, and utensils) (Jeantet *et al.*, 2006a).

According to the Ministère de l'Agriculture, des Pêcheries et de l'Alimentation du Québec (MAPAQ), the content of mesophilic bacteria associated with good manufacture procedures can be divided into two classes (**Table 1**): **m*** which corresponds to the group of food with good manufacturing procedures and acceptable for consumption and **M*** which encloses the group of food where no control was taken and verifications followed by corrective actions are required. **Table 1** shows the MTF concentration tolerated for the group of foods of ham, pastrami, pasta, raw fish or meat according to MAPAQ.

Table 1 Sampling plan divided into two classes for qualification of food quality

m*	M*
Acceptable and good manufacture procedures. Ex. $1 \cdot 10^6$ CFU/g	No-control and required corrective actions on procedures. Ex. $1 \cdot 10^7$ CFU/g

Even if there is no specific relationship between MTF growth and pathogenic bacteria, a high number of MTF represents an appropriate condition to favour their development. In addition, it is important to highlight that a high concentration of MTF leads to noticeable physical changes in the product. For instance, Balamatsia *et al.* (2006) reported that sensorial analysis of chicken breast samples stored in air at 4°C passed from having an acceptable slight off-odour/off-flavour to an unacceptable quality and recognizable off-odour when MTF concentration increased from 7.2 and 7.9 log CFU/g, respectively. Therefore, MTF becomes an important parameter to consider.

1.3 Lipid Oxidation and Food Quality

In food, lipids add to the product flavour, texture, and nutritional value. They are present in more than 50% of products that are consumed by humans such as milk, nuts, eggs or meat (Jeantet *et al.*, 2006a). Being responsible for energy supply in living microorganisms, lipids also provide fat-soluble vitamins such as A, D, E, and K, and essential fatty acids. These molecules are known for being non-soluble in water and are composed of esters of long fatty acid chains, triacylglycerol, phospholipids, steroids, and carotenoids (St Angelo, 1996; Willey *et al.*, 2016). In **Fig. 1** two of the most common

lipids are depicted, phospholipids, and triglycerides. Phospholipids contain two hydrophobic tails of fatty acids with a hydrophilic head composed of a phosphate and choline groups with quaternary ammonium functionality. Triglycerides are made of a glycerol molecule esterified with three fatty acid chains (R group).

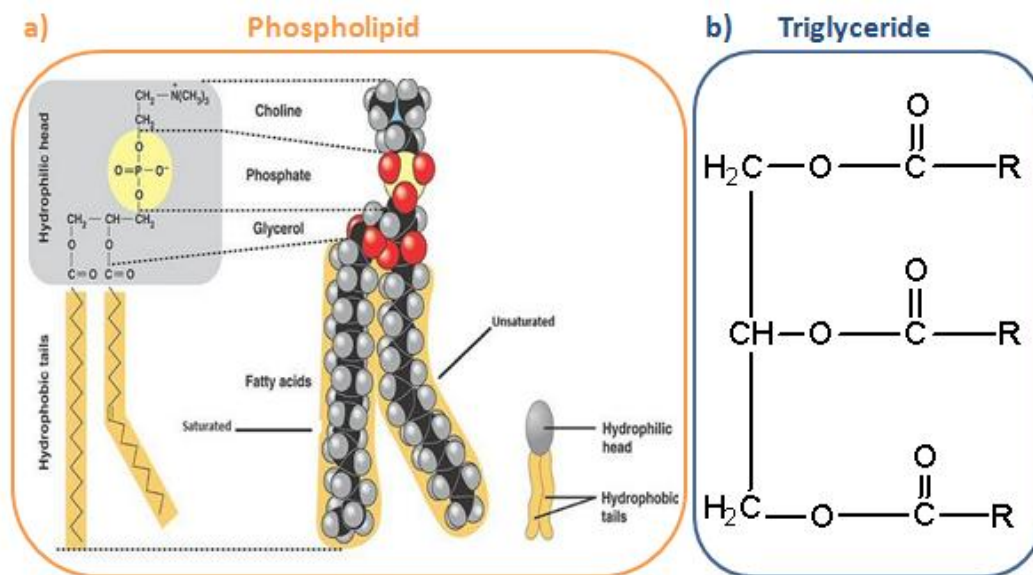


Fig. 1 Examples of lipids: a) phospholipid and b) triglyceride. Phospholipid image was taken from "cell membrane structure" website retrieved from <https://aecbio11.fandom.com/>

Because of the natural presence of unsaturated bonds, especially in polyunsaturated fatty acids, oxidative reactions can easily be initiated by factors such as light, temperature, metals, enzymes, and microorganisms.

Depending on the product, lipid oxidative phenomenon can be either desirable or undesirable. For instance, at a low level, oxidation reactions are responsible for the production of the pleasant flavour of fried food, cooked meats, roasted nuts or some cheeses such as cheddar and Roquefort (Gallois and Langlois, 1990). Auto-oxidation in chicken and fish might lead to the formation of 2-methylpropanal responsible for sweet and floral odours like caramel and cocoa (Frérot, 2017). However, exposing food to high oxidation levels leads to some undesirable off-flavours development (also called rancidity), production of toxic compounds, loss of colour and nutritional value deterioration, all causing the loss of food quality (Greene, 1969; Labuza and Dugan Jr, 1971). In meat, lipid oxidation is susceptible of two principal mechanisms: auto-oxidation (radical mechanism) and photo-oxidation (singlet oxygen-mediated mechanism). These

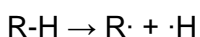
two mechanisms differ in their initiators: the presence of double bonds and the exposure to high temperatures are the precursors of auto-oxidation reactions, while light exposure and the presence of photosensitizers -chlorophyll, pheophytin, metalloporphyrin or riboflavin- are the initiators of photo-oxidation (Choe and Min, 2005; Min and Boff, 2002).

Lipid Oxidation Reactions

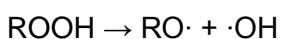
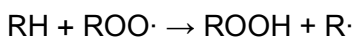
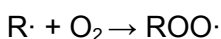
During oxidation three reactions occur simultaneously. The first reaction called initiation is based on the formation of two radicals ($R\cdot$ and $H\cdot$) formed from an unsaturated fatty molecule (R) by the action of an initiator such as light, heat or metal-proteins as shown in **Eq. 1**. In the propagation phase, a high number of radicals are formed, one example of these reactions is the formation of peroxy radical ($ROO\cdot$) issued from the reaction of a lipid radical ($R\cdot$) with oxygen (O_2) (**Eq. 2**), and the termination phase which is reached when two radicals react with each other, examples are given in **Eq.3**.

Lipid hydroperoxides ($ROOH$) are considered the primary oxidation products as they are the first compounds issued from the oxidative process. The decomposition of these compounds yields to the formation of aldehydes, ketones, alcohols, polymers or other compounds, known as secondary derivative compounds.

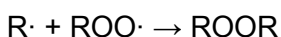
Initiation (1)



Propagation (2)



Termination (3)



1.4 Available Tests for the Determination of Lipid Oxidation

In order to control and understand the reactions occurring during lipid oxidation, tests are performed based on the quantification of the formation of primary and secondary products (da Silva *et al.*, 2018; Lee *et al.*, 2003; Serrano-León *et al.*, 2018). For primary

compounds, the determination of hydroperoxides content is prioritized but their instability should be taken into account. Hence, complementary tests are recommended and the quantification of aldehydes, ketones, alcohol, hydrocarbons, and epoxides can correlate the coexisting phenomena. Methods based on the identification of the type of compound formed are discussed and evaluated in the next sections.

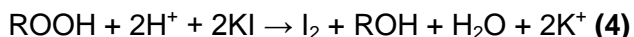
Primary Reactive Compounds

Analysis of Total Hydroperoxides

The peroxide value is a common method used for evaluating the extent of oxidation in fats, oils and food lipids based on iodometric, spectrophotometric or chromatographic techniques (Dobarganes and Velasco, 2002). The following section will review the principle of the redox techniques that allow the quantification of lipid peroxides.

Iodometric Titration Method

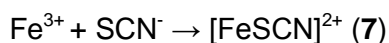
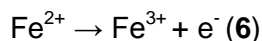
The iodometric titration method is a test used to determine the hydroperoxide content in fats and oils through the oxidation of iodide ion (I^-) to iodine (I_2) as it is shown in **Eq. 4** (Dobarganes and Velasco, 2002). The I_2 formed during the reaction is titrated against a standardized solution of sodium thiosulfate ($Na_2S_2O_3$) using starch as indicator (**Eq. 5**).



Because of the labour intensity (Ruiz *et al.*, 2001), the significant amount of fat samples required (Dobarganes and Velasco, 2002) and waste generated (Eymard and Genot, 2003), other methods such as ferric ion complexes are often used.

Ferric Ion Complexes

The ferric ion complex technique is based on the oxidation of ferrous ion (Fe^{2+}) to ferric ion (Fe^{3+}) by lipid hydroperoxides contained in fats, oils (Nourooz-Zadeh *et al.*, 1995), and food lipids (Burat and Borzkuć, 1996; Grau *et al.*, 2000). In the presence of acidic thiocyanate solution, the sample forms a complex with the ferric ion that can be detected at a wavelength of 510 nm. The chemical reactions are expressed by the following equations (**Eq. 6** and **7**):



Secondary Reactive Compounds

Thiobarbituric Reactive Substances (TBARS) Determination

The Thiobarbituric Acid Reactive Substances (TBARS) test is one of the most common tests used to detect malondialdehyde (MDA), a secondary component of oxidation of fatty acid which represents the best known marker (Barriuso *et al.*, 2013). During the colorimetric assay performed in the presence of thiobarbituric acid (TBA), MDA forms a pink colored complex with TBA which is detectable in the range of wavelength of 530-535 nm.

1.5 Active Biopolymeric Matrices in Food Industry

In order to overcome the numerous diseases and waste occasioned by food spoilage, the food industry is constantly looking for innovating solutions to reduce bacterial contamination, delay food deterioration or prevent the formation of undesirable off-odours or off-flavours.

With the growing demand for natural ingredients, biopolymers represent an alternative solution to help prevent spoilage problems due to their compatibility with food matrices. The use of active biopolymeric matrices or edible coating placed on surfaces has demonstrated its potential for preventing the formation of fatty acid oxidation byproducts in food containing unsaturated fats like chicken (Hassanzadeh *et al.*, 2017), salmon (Gennadios *et al.*, 1997), and beef (Vital *et al.*, 2016). Biopolymeric matrices have also been used for protecting the viability of lactic acid bacteria (Bekhit *et al.*, 2018) and essential oils (Serrano-León *et al.*, 2018). Their low toxicity, as well as the acceptance to be labelled as a food additive by governmental institution such as Health Canada (Government of Canada, 2013) demonstrate the capacity of biopolymers to be used for food matrices. Applications of edible films include coatings (Gennadios *et al.*, 1997; Hassanzadeh *et al.*, 2017; Vital *et al.*, 2016), edible beads (Huq *et al.*, 2014) or bioactive packaging films loaded with antioxidant and antimicrobial compounds (Grujic *et al.*, 2017).

With regard to edible coatings, authors reported noticeable changes in the appearance of food such as improvement of water retention, firmness, and glow during storage of fruits and vegetables. Indeed, the use of the first coating for fruit preservation was implemented in China during the 12th and 13th century and was based on the application of wax (Vukić *et al.*, 2017). Nowadays, not only wax but also biopolysaccharides or proteins have been used to improve the surface of fruits, vegetables, and meat products. For instance, carrageenan coated cherries showed 30% water loss reduction and higher brightness compared to the control (Larotonda, 2007). In meat, edible films made of polysaccharides or proteins provide gas barrier properties, bringing the advantage of adding bioactive compounds that can be diffused from the film to the product (Dehghani *et al.*, 2018). In addition, edible coating on meat shows improvement of appearance, reduction of juice drippings, rancidity, discoloration, and bacterial load (Gennadios *et al.*, 1997). With respect to loaded bioactive films, Vital *et al.* (2016) demonstrated the efficiency of loading oregano essential oil in alginate films during the storage of beef. The authors demonstrated not only the antioxidant capacity brought by the addition of the essential oil with 47% TBARS reduction, but also the ability of the alginate control film to maintain low concentration of TBARS, weight and colour of poultry samples during 14 days. The protective effect of active compounds contained in a matrix was proven by Serrano-Léon *et al.* (2018) with the study of chitosan based films loaded with pink pepper extract and peanut skin extract compared to the non-encapsulated antimicrobials against psychrotrophic counts in chicken.

In general, edible biopolymers play an important role against the formation of oxidation compounds, improve sensorial quality of samples, enhance colour, prevent water loss and protect active ingredients from pH changes, light degradation and volatilization, while maintaining the activity of major compounds against bacteria growth and reducing quality deterioration. Examples of some of the most common biopolymers used in food system are alginate, chitosan, and gellan gum which will be described in the following sections.

Alginate

Alginate is a polysaccharide extracted from brown algae or secreted by various bacteria such as *Azotobacter vineladii*, *Pseudomonas aeruginosa* (Pedersen *et al.*, 1990), and *P. syringae* (Yu *et al.*, 1999). It has demonstrated a large applicability in fields such as for

biomedical cell microencapsulation, drug delivery systems (Skaugrud *et al.*, 1999), dental impressions (Ertesvåg and Valla, 1998), wound dressings (Lee and Mooney, 2012), tissue engineering (Lee and Mooney, 2012), as well as industrial processes such as dye production (Jensen, 1993; Yamamoto *et al.*, 1991), and paper industry (Ham-Pichavant *et al.*, 2005; Rhim *et al.*, 2006). Some of the reported properties of alginate in food matrices are the ability to stabilize encapsulated compounds, to enhance viscosity or to add gelling effect in food products such as jam, jellies or fruit filling (Toft *et al.*, 1986). The alginate structure (**Fig. 2**) is composed of two types of units conforming the polymer, (67%) guluronic acid (G) and (33%) mannuronic acid (M) linked by glycosidic bonds. They can be found as blockwise homopolymers but also as alternating structure between G and M blocks as it is shown in the **Fig. 2**.

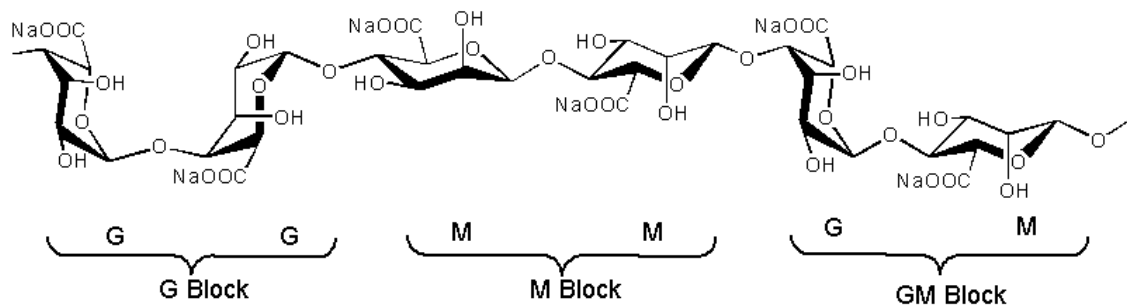


Fig. 2 Schematic representation of the alginate macromolecule

The worldwide commercial production of alginate is 30,000 metric tons per year from processed macroalgae (Rehm, 2009). Chemical extraction of alginate is performed in acidic media followed by addition of sodium carbonate to convert the alginic acid into its sodium salt form which allows solubilisation in water. Also called the egg-box model, alginate has shown the ability to form a gel structure by networking interactions between the acid groups present in alginate with divalent cationic ions. Among the most commonly used cations, non-toxic calcium ions are widely used in food applications (Ching *et al.*, 2017). So far, the cross-linking reaction of alginate with calcium ions has been highly studied in food-grade applications, for example in delivery systems for encapsulation of lipophilic compounds (Hosseini *et al.*, 2013; Huq *et al.*, 2014; Soliman *et al.*, 2013; Zeeb *et al.*, 2015), hydrosoluble compounds (Huq *et al.*, 2014; Le-Tien *et al.*, 2004) or living microorganisms (Bekhit *et al.*, 2018; Huq *et al.*, 2017).

Chitosan

Chitosan, a compound derived from chitin, has been categorized as a promising polysaccharide due to its active properties (Aider, 2010; Aziz and Karboune, 2018). Chitin (**Fig. 3a**) was first discovered by Braconnot (1811) in mushrooms, but a decade later Odier (1821) found it in the walls of insects giving the Greek name of "*khitōn*" referring to envelop. Nowadays, chitin is extracted from crustaceans shells such as crab, crawfish and shrimp (Younes and Rinaudo, 2005), and a subsequent alkaline treatment of chitin converts it into a partial (No and Meyers, 1997) or complete (Domard and Cartier, 1989; Mima *et al.*, 1983) deacetylated form composed of β -(1-4)-linked D-glucosamine or chitosan (**Fig. 3b**).

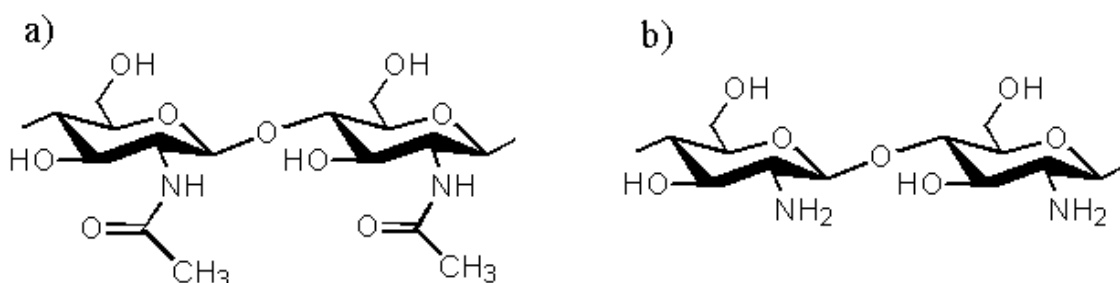


Fig. 3 Schematic representation of chitin (a) and deacetylated chitosan (b)

The principal characteristic of chitosan relies on the facility to be dissolved in acidic media under pH 6 due to the available amino group (Aziz and Karboune, 2018; Ravindra *et al.*, 1998). This amino group has demonstrated to contribute to the antimicrobial activities of chitosan against gram-positive and gram-negative bacteria (Jeon *et al.*, 2001; Rhoades and Roller, 2000). Despite the fact that the antimicrobial mechanism has not been completely understood, it is suggested that protonated amino groups react with negatively charged cellular membranes leading to leakage of intracellular parts of microorganisms, DNA fragmentation followed by apoptosis (Hasegawa *et al.*, 2001). Chitosan also demonstrated abilities to form films with increased oxygen barrier properties for prevention of oxidation in food matrices such as nuts. Compared to gelatin, chitosan coated nuts showed reduced peroxide values during 120 days of storage (Bonilla *et al.*, 2018). Chitosan also showed improvement of >35 days of shelf life of Halloumi cheese treated with 5 and 10% brine compared to 10 and 25 days in non-coated samples, respectively (Mehyar *et al.*, 2018).

Gellan Gum

Gellan gum is a polysaccharide composed of four repeating units: two glucose, one rhamnose and one glucuronic acid (**Fig. 4**). Gellan gum is a polysaccharide extracted by microbial fermentation of *Sphingomonas elodea* or *Pseudomonas elodea* (Warren and in het Panhuis, 2015) and in low yield, it can also be excreted by *Sphigomonas paucimobilis* ATCC 31461 (Morris *et al.*, 2012; Salunke and Patil, 2016; Wang *et al.*, 2016). The main characteristics of gellan gum are its non-toxicity (Warren and in het Panhuis, 2015), biodegradability (Karthika and Vishalakshi, 2015; Pacelli *et al.*, 2016, 2015), thermal response (Prezotti *et al.*, 2014; Sonje and Mahajan, 2016), and stability at low pH. Commercially, two types of gellan gum are found: the high acyl and low acyl gellan gum which both differ in their final properties. Flexible and soft hydrogels are obtained with the high acyl gellan gum and more rigid hydrogels are obtained with the low acyl gellan gum. Jellifying procedures also differ as cooling temperatures of high acyl gellan gum is about 65°C and about 40°C for low acyl gellan gum (Danalache *et al.*, 2015; Kirchmajer *et al.*, 2014). With the interest on rigid properties, the structure of the low acyl gellan gum is depicted in **Fig. 4**.

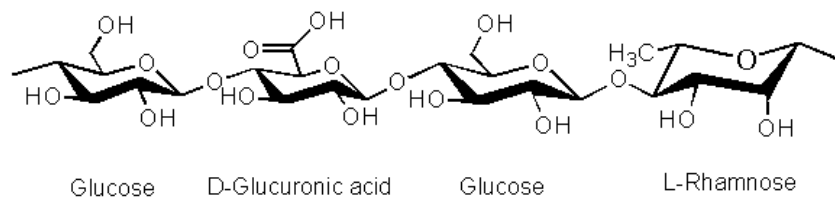


Fig. 4 Schematic representation of low acyl gellan gum

In the presence of divalent cations, the negative charges also allow gellan gum to form clear gels or polyelectrolyte complexes with oppositely charged polymers like chitosan. During the process of gelation, gellan gum chains pass from a coiled organization to a double helix structure forming a 3D complex. Applications of gellan gum range from water-based jellies (Moritaka *et al.*, 1999) to bakery filling and fluid gels for beverage dispersions (Sworn *et al.*, 1995).

1.6 Existing Natural Antimicrobial Compounds from Plant Origin for Food Preservation

The use of synthetic antimicrobial and antioxidant compounds has been reported to induce carcinogen effects. Antioxidants such as butylated hydroxyanisole and butylated hydroxytoluene or antimicrobial additives such as nitrites have been either abolished or their content reduced in food. Therefore, with the aim to ensure food quality by providing natural compounds the use of essential oils represents an alternative (Aziz and Karboune, 2018). In this section, the main characteristics and mechanism of action of essential oils are being described.

Essential Oils

As defined by the 7th edition of European Pharmacopoeia, essential oils are "odorant products, generally of a complex composition, obtained from a botanically defined plant raw material". In fact, essential oils (EO) are principally composed of terpenes, aldehydes, ketones, carboxylic acids, sulphides, disulphides and trisulphides substances (Voda *et al.*, 2003). Via steam distillation, essential oils are easily separated from the aqueous phase without affecting their chemical composition.

Among the well-known essential oils, *Thymus vulgaris* –common name Thyme- has demonstrated effective antimicrobial and antioxidant capacity. Thyme is a flowering plant belonging to the mint family *Lamiaceae* species native of Spain and Hungary. Its main components are thymol (35%), *p*-cymene (19%), γ -terpinene (20%), carvacrol (3%) among others terpene compounds. By evaluating the mechanism of antioxidant action of both thymol and carvacrol molecules, it was demonstrated by Yanishlieva *et al.* (1999) that the major compound of the essential oil, thymol, has a higher antioxidant activity compared to carvacrol.

As explained by Oussalah *et al.* (2006), the mechanism of action of thyme essential oil on bacteria induces pore formation on cell membrane leading to cytoplasmic leakage, intracellular ATP decrease and degradation and modification of muropeptides present in bacteria (Caillet and Lacroix, 2006).

1.7 Encapsulation of Essential Oils by Biopolymers and Combination of Treatment

Even though essential oils possess antimicrobial or antioxidant properties, their efficiency needs to be protected from external factors. It is known that EOs can suffer oxidation, isomerization, cyclization, or dehydrogenation led by either enzymatic or chemical reactions. As a consequence, these reactions can cause off-flavours (Sinki *et al.*, 1997), changes in colours (Preuss, 1964), and loss of product quality (Fincke and Maurer, 1974; Kubeczka, 1993).

In order to protect the essential oil quality, encapsulation is a technique that has been proposed to prevent damage or alteration of essential oil efficiency. Because of its capacity to enclose the bioactive compounds from external interactions such as food ingredients, encapsulated essential oil can increase its physical stability (volatility) and be delivered where bacteria is located (Weiss *et al.*, 2009).

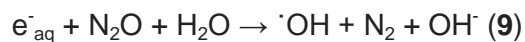
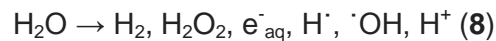
Biopolymers have demonstrated as being good candidates for the encapsulation of compounds. Because of their flexibility, mobility in chain length, and permeability, biopolymers allow the diffusion of compounds, especially essential oils and drugs (Wischke and Schwendeman, 2008). For instance, biopolymers such as chitosan used in beads or zein used in films showed protecting ability of *Citrus aurantium* oil (Karimirad *et al.*, 2018) and thymol (Mastromatteo *et al.* 2009) over time, respectively. To illustrate this phenomenon Karimirad *et al.* (2018) showed that when *C. aurantium* oil was encapsulated into the chitosan nanoparticles, the lightness of mushrooms was preserved for 15 days more than when the essential oil was in its non-encapsulated form. These values were also confirmed by the low polyphenoloxidase activity, responsible for the enzymatic browning of mushrooms observed in encapsulated systems.

Encapsulated Essential Oil and Combination of Treatment

In order to improve the protection against pathogenic bacteria, non-thermal treatments have been used on food samples. These non-thermal treatments are known for inactivating bacteria while being processed at ambient temperatures, avoiding extreme changes in flavour, colour or quality of food. Among the existing non-thermal treatments, gamma irradiation is a cold process currently used in different countries. For example, to delay the ripening of fruits and vegetables and deterioration of meat, United States of

America (USA) and Canada apply gamma-irradiation to fruits (Eustice, 2011) or potatoes, onions, wheat, spices, and ground beef (Government of Canada and Canadian Food Inspection Agency, 2012).

Measured in Gray (Gy) units, referring to 1 unit of energy (joules) per kg of product, the mechanism of action involved in bactericidal purposes of gamma irradiation is based on the radical-compound formation issued from water radiolysis. From the water radiolysis, reactive oxygen species are produced, among them, the radical hydroxyl groups ($\cdot\text{OH}$) (**Eq. 8**).



It has been stated that hydroxyl radicals are the influent compounds in the bactericidal mechanism of gamma irradiation that are capable of breaking DNA and bacteria membrane. Besides the water hydrolysis, the solvated electrons (e^-_{aq}), when reacting with nitrous oxide, are also able to produce 90% of hydroxyl radicals and 10% of hydrogen radicals (**Eq. 9**) (Von Sonntag, 1980).

Interest of gamma irradiation has increased over the years because of its ability to control food-borne diseases (Pujato *et al.*, 2019), to avoid food loss from infestation (Hossain *et al.*, 2019; Ricardo Machi *et al.*, 2019), and to delay food ripening (Zhao *et al.*, 1996). Gamma irradiation has been proposed in a large range of applications among one of them the conservation of food matrices.

However, due to its high energy, increasing gamma irradiation doses might result in nutrient and vitamins loss (Khattak and Klopfenstein, 1989; Horticulture and Forestry Science, 2012). Thus, in order to decrease side-effects of gamma-irradiation, the combination with other treatments such as addition of antimicrobial compounds (e.g., essential oil) has been proposed in literature (Caillet *et al.*, 2006a, 2006b; Ouattara *et al.*, 2001; Vu *et al.*, 2012, Severino *et al.*, 2014). For instance, Severino *et al.* (2014) observed that the required dose to eliminate one log CFU (D_{10} -value) of *L. monocytogenes* present in broccoli florets was decreased from 0.32 in irradiated control samples to 0.24 when samples were irradiated with mandarin EO-based coating. Similar synergy was obtained by Ouattara *et al.* (2001) who observed a complete inhibition (0 log CFU/g) of *Pseudomonas putida* in coated shrimp with essential oil (E018) after seven day storage compared to 2 log CFU/g growth observed in irradiated control samples.

Both authors, Ouattara *et al.* (2001) and Severino *et al.* (2014), agreed with the fact that combining gamma irradiation with active films improve the antimicrobial efficiency caused by their additive effect. In this thesis the incorporation of essential oils and the combined treatment with gamma irradiation will be studied.

2. APPLICATIONS OF CELLULOSE NANOCRYSTALS IN FOOD PACKAGING

2.1 Cellulose Nanocrystals

Cellulose is one of the most abundant natural polymers, being distributed in plants, algae, marine animals, fungi, bacteria, and protozoa (Habibi *et al.*, 2010). It consists of β -1, 4-glucopyranose units linked together with a degree of polymerization (DP) ranging from 2,900-11,000 in wood pulp, fibre, and ramie (Gralén and The Svedberg, 1943; Pettersen, 1984; Zografis and Kontny, 1986), close to 10,000-18,000 in *Valonia* (Marx-Figini, 1969), and 4,000-10,000 in bacterial cellulose (Kuga *et al.*, 1989; Tahara *et al.*, 1997; Watanabe *et al.*, 1998). Cellulose is found in a pure state in cotton but can also be extracted from wood, plant leaves, and stalks (Dufresne, 2017) where it co-exists with other natural compounds such as hemicellulose, lignin, and extractives like wax and fats. It constitutes the primary compound (65-75%) of the elementary fibres (Gorshkova *et al.*, 1996; McDougall, 1993) following a hierarchical structure from fibres to microfibrils as it is depicted in **Fig. 5**. These microfibrils, with a diameter of approximately 4 to 20 nm (Klemm *et al.*, 2011; Näslund *et al.*, 1988), are held together by a network of hydrogen bonds forming crystalline and amorphous regions.

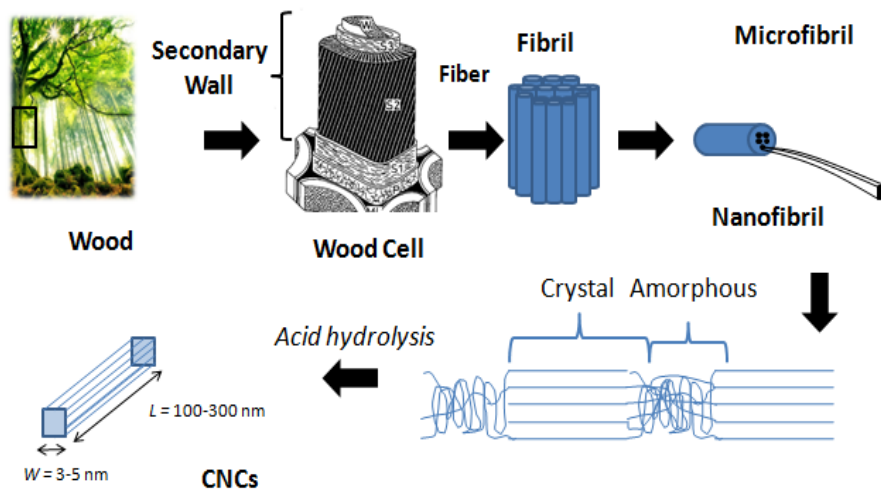


Fig. 5 Schematic representation of the hierarchical structure of wood

Cellulose nanocrystals (CNCs), also called cellulose whiskers, nanowhiskers or nanocrystalline cellulose (NCC), have gained particular attention and growing interest because of their light weight, nanometric dimensions and high mechanical strength

properties. Scopus database (**Fig. 6**) shows that the number of publications per year considering "CNCs" as a keyword has risen from 107 to 721 between 2010 and 2017. In different fields, attention is focused on the value added to materials such as stiffness, barrier properties, and dispersibility in aqueous media (Oksman *et al.*, 2008; Rampazzo *et al.*, 2017; Shoseyov *et al.*, 2015; Zhou and Wu, 2012).

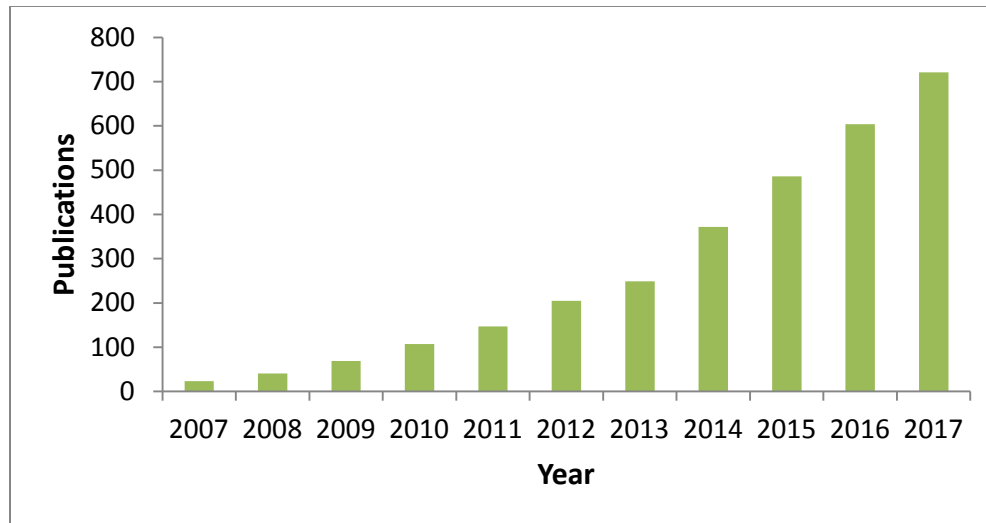


Fig. 6 Number of publications (such as articles, conference papers, reviews, book chapters) related to cellulose nanocrystals. Data from Scopus database from 2007 to 2017.

In the field of biopolymers applied for foods, the interest of adding nanoparticles in packaging materials has also been increasing (Azeredo, 2009; Bumbudsanpharoke *et al.*, 2015; Bumbudsanpharoke and Ko, 2015; Huang *et al.*, 2018). Food matrices such as fruit juices, carbonated beverages, and dairy products are examples of matrices that require appropriate oxygen control. Thus, the use of nanocomposite packaging materials can represent a potential direction where nanomaterials could offer the required quality parameters (Brody, 2007).

Due to the fact that high performing materials (i.e., that allow protection to food from external conditions bringing also activity against microorganism's growth and extension of shelf-life) are highly desired and because the use of CNCs can potentially bring some advantages, the next sections will shed some light as to how this nanomaterial could potentially be helpful. In the first section, the main characteristics of CNCs will be highlighted, followed by a brief description of the major types and morphological features of existing cellulosic derivatives.

2.2 Extraction of Cellulose Nanocrystals (CNCs)

The procedure to extract cellulose nanocrystals was first reported by Rånby (1949) who, by treating cellulosic material with sulfuric acid at boiling temperature, allowed the formation of colloidal particles with a crystalline character. This procedure called acid hydrolysis still represents the principal treatment to produce cellulose nanocrystals (CNCs). Strong mineral acids like sulfuric (Dong *et al.*, 1998), hydrochloric, but also phosphoric (Espinosa *et al.*, 2013; Lemke *et al.*, 2012), and hydrobromic acid (Filpponen and Argyropoulos, 2010; Sadeghifar *et al.*, 2011), have been applied for such purposes. However, dispersibility of CNCs in aqueous systems can be achieved using sulfuric acid (Revol *et al.*, 1992) and recent studies showed a slight dispersion of CNCs using phosphoric acid hydrolysis (Camarero-Espinosa *et al.* 2013; Vanderfleet *et al.* 2018) resulting with sulfate (-OSO₃H) and phosphate (-OPO₃H) half-ester groups grafted onto their surface. Due to the fact that CNCs obtained for this study are derived from sulfuric acid method, the following sections will mainly focus on this grade of CNCs.

Optimal hydrolysis conditions with a sulfuric acid concentration of 64% and a temperature of 45°C were reported by Hamad and Hu (2010) for wood derived CNCs. The authors obtained a degree of polymerization below 100, a crystallinity of approximately 80%, a crystallite size of 5 - 10 nm and a half-ester group content of 261 mmol per kg CNCs.

Literature shows that both morphology and dimensions of CNCs obtained after acid hydrolysis depend on the cellulosic source (Araki *et al.*, 2001; De Souza Lima *et al.*, 2003; Helbert *et al.*, 1996; Miller and Donald, 2003). **Table 2** reports different ranges of particle length (L) and width (w) for animal and plant-derived CNCs measured by microscopy techniques. Tunicate sea animal-derived CNCs showed dimensions of 15 - 30 nm in width and 1,000 - 3,000 nm in length which represent the longest known length of CNCs in comparison to wood derived CNCs with reported sizes of 3 - 4 nm and 100 - 200 nm for width and length, respectively.

Table 2 Length (L) and width (w) of CNCs extracted from different sources.

Cellulosic source	L (nm)	w (nm)
Bacterial cellulose	100-1000	10-50
Ramie	150-250	6-8
Sisal	100-500	3-5
	150-280	3.5-6.5
Tunicate	1000-3000	15-30
Valonia	1000-2000	10-20
Softwood	100-200	3-4
Hardwood	140-150	4-5

Adapted from Habibi *et al.* (2010)

In regard to CNCs morphology, the aspect ratio, defined as the length-to-width ratio, has some influence on the mechanical behavior of the materials into which CNCs are embedded. Thus, in order to confirm the relation between the stiffness and the size of CNCs, the authors Bras *et al.* (2011), evaluated the Young modulus of casted CNCs films extracted from different sources. The authors showed that films made from palm tree and sugar cane bagasse derived CNCs (aspect ratio of 47 and 13) exhibited Young modulus of 8 and 1 GPa, respectively. Therefore, it was suggested by Bras *et al.* (2011) that the improved films' mechanical properties had been affected by the large dimensions of the nanoparticles of the individual crystals.

It was also found that stiffness is a characteristic parameter of the nanoparticles. With the aim to evaluate the stiffness of a single particle Šturcová *et al.* (2005) and Rusli and Eichhorn (2008) reported estimated values of tensile modulus based on single tunicate- (aspect ratio 77) and cotton-derived (unspecified aspect ratio) CNCs tested by Raman spectroscopy. Results of these studies estimated elastic modulus values of 143 and 105 GPa for single tunicate- and cotton-derived CNCs, respectively. With these results, it was confirmed that individual CNCs, regardless of the source, possess a stiffness comparable with others nanofillers such as glass (69 GPa) and steel (200 GPa).

2.3 Microscopic Features and Morphology

Due to the importance of morphological features to understand the relationship between particle-particle and particle-matrix interactions, several imaging studies have been carried out on CNCs. Different techniques such as transmission electron microscopy (TEM) (El Achaby *et al.*, 2018; Shin *et al.*, 2018) and atomic force microscopy (AFM) (Salajková *et al.*, 2012) were used with the purpose to either analyze the crystal's morphology or determine their size distribution (Kaushik *et al.*, 2015).

Taking into account that each of these techniques possess their own advantages and disadvantages such as overestimation of dimensions by AFM (Kvien *et al.*, 2005), damage of samples caused by voltage exposition by TEM (Bengio *et al.*, 2014; Sacui *et al.*, 2014), precise images can still be obtained, succesfully presenting surface and structure of cellulose nanocrystals.

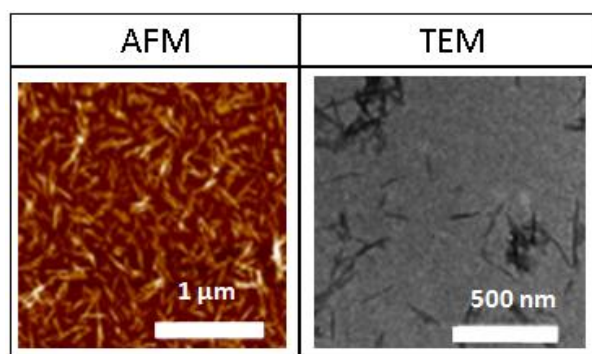


Fig. 7 AFM and TEM images of CNCs extracted from wood by sulfuric acid hydrolysis. AFM and TEM images are taken from Sacui *et al.* (2014)

Fig. 7 shows the rod-like morphology of wood-extracted CNCs obtained by AFM and TEM reported by Sacui *et al.* (2014). A rounded morphology of the crystals was observed in the AFM images which could have been ascribed to the irregular-shaped images issued from the technique whereas TEM images of CNCs were more thin-shaped particles. Some particle aggregation is noticeable in the TEM images. However, the authors Araki *et al.* (1998) suggested that the phenomenon could be the result of an aggregated state within the original suspension or occurred during the drying procedure of the sample on the grid.

2.4 Applications of CNCs in Food Biopolymers

The following sections will highlight how the addition of CNCs has contributed to the improvement of the mechanical resistance, the oxygen barrier properties, and the controlled release of bioactive compounds in biopolymers as well as the chemical functionalization that can be carried out on CNCs. The final section of this chapter will generally describe the reported studies that evaluate the wholesomeness/toxicity of the CNCs via *in vitro* tests and the performed tests on the overall migration of nanoparticles in simulated foods.

2.4.1 CNCs' Role in Mechanical Properties of Biopolymers

When it comes to the properties of CNCs in materials, first glance is given to the inherent stiffness of cellulose nanocrystals. However, preparing a film of pure CNCs results in a mechanically brittle material that might limit its application for film or coating purposes (Guidetti *et al.*, 2016; Liu *et al.*, 2017). On the other hand, the addition of CNCs to a material can result in an increase of the mechanical performance of the matrix into which they are embedded.

The characteristic stiffness of single crystals is a result of the hydrogen bonding network and their inherent crystallinity, and when CNCs are added to materials, the reinforcement effect can be explained by a percolation mechanism of the nanocrystals. The first study evaluating the effect of CNCs into polymeric materials was carried out by Favier *et al.* (1995) who showed an improvement of the mechanical properties by measuring the storage modulus (G) of poly(styrene-co-butyl acrylate) films with 0, 1, 3, and 6% tunicate derived CNCs. The authors observed a maximum G value of 8 when tunicate-derived CNCs at 6% (w/w) were added to the polymer matrix compared to the pure polymer. Lower incorporations of CNCs in films exhibited lower storage modulus.

The improvement of the mechanical performance of poly(styrene-co-butyl acrylate) was explained by the authors as attributed to the network formed by the crystals driven by hydrogen bonding as it is depicted in **Fig. 8**. Other examples of improvements of mechanical properties due to CNCs incorporation in biodegradable polymers include blends with polyhydroxybutyrate (PHB)/polycaprolactone (PCL) (Garcia-Garcia *et al.*, 2018), alginate (Huq *et al.*, 2012), chitosan (Khan *et al.*, 2012), and gellan gum (Criado

et al., 2016). In alginate matrices, Huq *et al.* (2012) showed that it was necessary to incorporate 5% CNCs to exhibit a maximum tensile modulus of 3.2 GPa compared to 1.8 GPa in the absence of CNCs. In chitosan films, the same concentration of CNCs showed an increase of tensile modulus from 1.6 GPa to 2.9 GPa when the same concentration was added to the films.

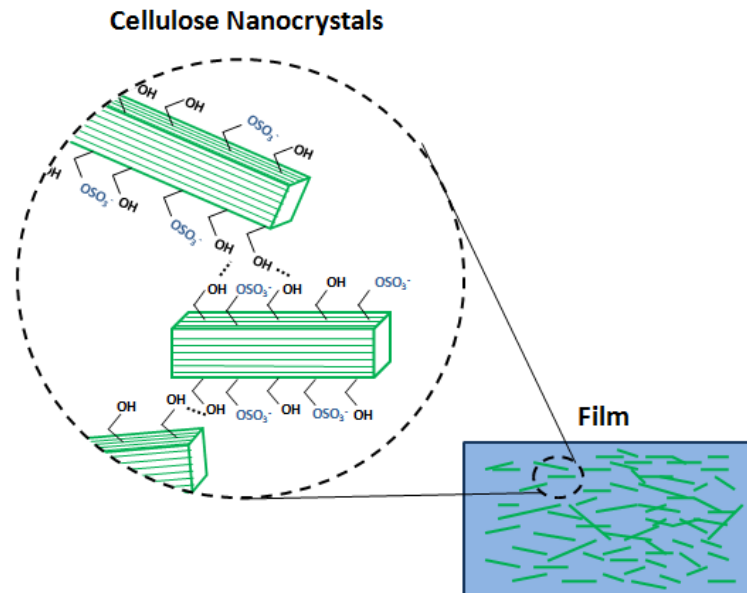


Fig. 8 Representation of hydrogen bonding (Favier *et al.* 1995; Hamad, 2017; Lizundia *et al.*, 2016) and percolation phenomenon of cellulose nanocrystals embedded in a polymer matrix

2.4.2 CNCs' Role in Oxygen Barrier Capacity

Oxygen is considered a critical factor affecting foods' longevity. In the packaging field, oxygen barrier properties were initially sought by the use of materials such as glass or metal (Akkapeddi and Gervasi, 1989). However, due to their high transportation cost and the arduous recycling procedures, developing plastic materials that are light and transparent became then highly desirable.

According to Catalá and Gavara (1996), the permeability of a gas through a polymeric matrix includes two phases: i) the adsorption of the permeant in the polymer and ii) its diffusion through the polymer matrix (Wang *et al.*, 2018).

This phenomenon expressed as the volume of gas going through the film per unit of film thickness, exposed area, time and driving force (partial pressure within the film) can be represented by the following equation (**Eq. 10**):

$$P = m \cdot l / t \cdot A \cdot \Delta p \quad (10)$$

where m is the quantity of gas, l is film thickness of the film, t is the time, A is the exposed surface area and Δp is the driving force in units of pressure.

Inherent properties and characteristics of the film are important to understand the diffusion of the permeant through the film. Parameters such as cohesive energy density (i.e., the measure of the polarity of a polymer free spaces and crystallinity of the material) play an important role in the definition of oxygen barrier properties (Miller and Krochta, 1997). To illustrate the phenomenon, films of poly(ethylene terephthalate), for example, show at 30% crystallinity an oxygen permeability (OP expressed in $\text{mL} \cdot \mu\text{m} / \text{m}^2 \cdot \text{d} \cdot \text{kPa}$) of 0.0024 compared to 0.0014 at 45% crystallinity. Thus, the higher the crystallinity is, the lower is the permeability of the material. Regarding the cohesive energy density, it is believed that increasing the polarity of the functional groups of the polymer backbone decreases the oxygen passage due to the dissimilarity of the polar groups with the non-polar oxygen molecule (Lagaron *et al.*, 2004). A good example is polystyrene (**Fig. 9 left**) possessing an OP of 0.168 $\text{mL} \cdot \mu\text{m} / \text{m}^2 \cdot \text{d} \cdot \text{kPa}$ compared to poly(vinyl alcohol) (PVA) (**Fig. 9 right**) with an OP of 0.0000016 $\text{mL} \cdot \mu\text{m} / \text{m}^2 \cdot \text{d} \cdot \text{kPa}$.

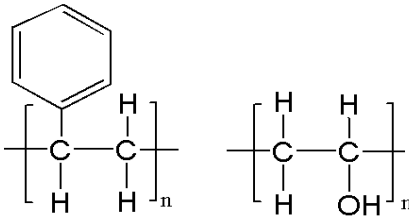


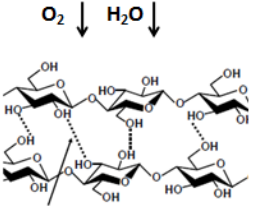
Fig. 9 Polystyrene molecule (left) and poly(vinyl alcohol) (right)

The use of nanofillers in polymers also affects the response of oxygen permeability. Examples of enhancement are observed in polymers like PVA (Sapalidis *et al.*, 2012) and polylactic acid (PLA) (Şengül and Dilsiz, 2014; Valapa *et al.*, 2015) where the presence of fillers results in a more crystalline and compact material.

Because the presence of nanofillers allows the creation of a tortuous pathway for the diffusing gas as described by García *et al.* (2004), the appropriate dispersion of CNCs in the polymer matrix might, in the same way, permit the creation of such tortuosity and lead to a decreased diffusion of the gas through the material (Dufresne, 2012). Examples of the oxygen permeability (OP) of polymers with dispersed or coated CNCs are reported in **Table 3** where it can be observed that OP decreases in presence of CNCs at the different tested conditions of relative humidity. According to Lagaron *et al.* (2004), the outstanding oxygen barrier capacities observed with the nanosized particles are explained by the loss of chain mobility and the lower free volume, thus resulting in less space available for the passage of oxygen through the matrix. Because of CNCs dimensions and the large hydrogen bonding (Favier *et al.* 1995; Hamad, 2017; Lizundia *et al.*, 2016) ability with compatible matrices, introduction of the nanoparticles result in an improvement of oxygen barrier properties in materials.

It is important to highlight that oxygen barrier properties are linked to experimental testing conditions such as the relative humidity (%RH). For instance, at high relative humidity, oxygen barrier properties tend to decrease due to the diffusion of moisture into the polymer. Therefore, for appropriate oxygen permeability measurements, it is critical to take into account parameters such as the water activity of the product as well as the storage conditions that will be used.

Table 3 Oxygen permeability (OP) of polymers with dispersed and coated CNCs

CNCs for Oxygen Barrier Properties	CNCs (coated/dispersed)	Polymer	OP (cc·µm/m ² ·d·kPa)	Ref.
 <p data-bbox="391 1465 641 1501">O₂ ↓ H₂O ↓</p> <p data-bbox="391 1680 641 1711">Hydrogen bond</p>	0 – 5% (dispersed)	Polylactic Acid (PLA)	1200 – 172 (24°C – 80% RH)	Sanchez-Garcia and Lagaron (2010)
	0 - 2% (dispersed)	PLA	1.4 – 0.4 (23°C -0% RH)	Karkhanis <i>et al.</i> (2018)
	0 – 4% (dispersed)	Collagen-glutaraldehyde	4-3 (23°C-0% RH)	Long <i>et al.</i> (2018)
	0 – 0.7% (dispersed)	Polypropylene Carbonate - Polyethylene Glycol	70 – 3 (23°C – 45% RH)	Jiang <i>et al.</i> (2017)
	0 – 8% CNCs (coated)	Poly (ethylene terephthalate)	20 – 0.012 (30°C – 0% RH)	Rampazzo <i>et al.</i> (2017)

2.4.3 CNCs' Role in Controlled Release

A food additive, according to Health Canada, represents any substance that when added to food becomes part of it. Food additives such as preservatives (i.e., antibacterial, antifungal and antioxidants), can become unstable or see their biological activity reduced by the presence of external factors, e.g., light (Conrad *et al.*, 2005; Yuan and Chen, 1998) or enzymes (Schneider *et al.*, 2011).

Similarly essential oils are prone to be oxidized due to exposure to temperature, oxygen, light, and irradiation (Turek and Stintzing, 2013; Velasco *et al.*, 2003).

In order to protect these active compounds from external conditions, their encapsulation and controlled release became an interest of study reported in literature by several authors (Del Toro-Sánchez *et al.*, 2010; Hsieh *et al.*, 2006). In food packaging, the controlled release is used to ensure a continuous provision of the active molecule for long periods of time, at minimal concentration while offering a protective role to the active compound from the external conditions (Appendini and Hotchkiss, 2002).

Because of their nanometric dimensions, the tortuosity brought by the presence of cellulose nanocrystals can prevent the leakage and rapid liberation of the active compounds. The use of CNCs for controlled release has been applied for the delivery of encapsulated drugs in matrices such as glutaraldehyde-gelatin hydrogels (Ooi *et al.*, 2016), polyvinyl alcohol (PVA) and poly(D,L-lactide-co-glycolide) (Jackson *et al.*, 2011).

In the food packaging field, recent research on the controlled release of essential oils trapped in polymeric matrices loaded with CNCs has demonstrated promising results (Alvarado *et al.*, 2018; Hossain *et al.*, 2018). For example, Alvarado *et al.* (2018) demonstrated that diffusion of thymol was reduced from $2.5 \cdot 10^{-13}$ to $5.5 \cdot 10^{-14}$ m²/s when pure PLA and PLA containing PVA nanofibers/CNCs films were used, respectively. Besides, Hossain *et al.* (2018) demonstrated that methylcellulose films loaded with 7.5% CNCs allowed a 10% decrease of the release of oregano: thyme EOs over 12 weeks. Both research groups described that the reduction of release was the result of the changes in the diffusion pathway or "increased tortuosity" created by addition of CNCs into the film.

In agricultural applications, the controlled release concept has also been studied by Li *et al.* (2016) who demonstrated that the release in water of phenylacetic acid (PAA)

encapsulated in cross-linked alginate-kaolin beads was decreased by approximately 5% in the presence of CNCs, after 48h. The authors confirmed that the presence of CNCs improved interactions with polyethylenimine, a cationic polyelectrolyte polymer, forming a denser structure of the bead and reducing liberation of PAA.

2.4.4 Modification of CNCs

Due to the large number of hydroxyl groups on their surface, CNCs are considered hydrophilic. However, in order not to limit their application to aqueous solutions, appropriate surface modification can improve their dispersion into hydrophobic matrices. Some of the major chemical modifications that occur with CNCs are acylation, polymer grafting, oxidation, layer-by-layer organization, cationic surface modification or radiation-induced graft polymerization reactions. In this section, only the reactions of CNCs with gamma irradiation, as well as the radical grafting mechanism of various compounds, will be reviewed.

Physical Methods for Cellulose Functionalization

In comparison to chemical modification of CNCs, physical methods are procedures that are considered less rigorous and where lower amounts of reagents are required to facilitate reactions. In cellulose, treatments such as plasma (Brioude *et al.*, 2015; Zhang *et al.*, 2018), electron beam, UV (Buesch *et al.*, 2016; Furtak-Wrona *et al.*, 2018; Hai and Bum Seo, 2017) and gamma irradiation (Henniges *et al.*, 2012) have been proposed for modification of cellulose. In this study, the use of gamma irradiation will be evaluated as a tool for oxidizing CNCs.

Gamma irradiation

Gamma irradiation is a process that uses the isotope cobalt⁶⁰ (Co⁶⁰) as a high energy source. Other sources of gamma-rays is the isotope of cesium¹³⁷ (Cs¹³⁷), however due to its limited capacity of being extracted, cobalt remains the main source of this type of irradiation (Satin, 1993). Gamma irradiation is characterized for its powerful penetration capability in materials, allowing the control of microorganism growth in food and also the

sterilization of medical devices (Nguyen *et al.*, 2007), pharmaceutical ingredients, excipients, and drugs (Hasanain *et al.*, 2014).

When applied to polymers, the use of gamma irradiation favours the formation of radicals, allowing cross-linking reactions such as vulcanization in rubber, polyethylene/ethylene-vinyl acetate blends (Martínez-Pardo and Vera-Graziano, 1995) or grafting of molecules on fibers (Le Moigne *et al.*, 2017; Roy *et al.*, 2009), and polysaccharides (Irimia *et al.*, 2017). Generally, grafting reactions using gamma irradiation occur at low doses (< 20 kGy) and two different methods exist (Roy *et al.*, 2009). The first method is called pre-irradiation which consists in irradiating a cellulose substrate followed by the introduction of monomers or reagents to the solution (Takács *et al.*, 2005). In the second method, called mutual irradiation, both a cellulose substrate and a monomer solution are irradiated simultaneously (Sonnier *et al.*, 2015). Both types of grafting reactions have been applied to cellulosic materials using either monomers such as acrylamide, acrylic acid or 2-hydroxypropylacrylate (HPA) through the pre-irradiation approach at irradiation doses of 5 - 40 kGy (Takács *et al.*, 2005) or phosphoric flame retardant molecule on flax fabric *via* mutual irradiation treatment at 50 kGy (Sonnier *et al.*, 2015).

In the paper industry, irradiation was first proposed for two purposes: as a treatment to prevent the microbiological attack by fungi and mold in confined paper (Butterfield, 1987; Sinco, 2000), and as a prevention of diseases for people in contact with the fungal issue (Gambale *et al.*, 1993). Results demonstrated that elimination of microbial charge was effective (Urban *et al.* 1978), but the irradiated paper showed a decrease in tear and fold resistance (Butterfield, 1987; Flores, 1976; Horáková and Martinek, 1984; Kubat *et al.*, 1968).

Since then, in order to understand the effect of gamma irradiation on cellulose itself and lignocellulosic material (jute), further studies have been performed (Glegg and Kertesz, 1957; Sultanov and Turaev, 1996; Takács *et al.*, 1999). At high doses, results show a decrease in the degree of polymerization of cellulose and the formation of carbonyl groups (Lee, 1987). As explained by Takacs *et al.* (1999) the radiation causes the formation of radicals on the main backbone chain (**Fig. 10**), resulting in anhydroglucose rings opening and rupture of glycosidic bonds. Henniges *et al.* (2012) were in agreement with the conclusions reported by Takacs *et al.* (1999) who found that doses of 10 kGy

increased by 60% the carbonyl groups content in bleached sulphite pulp and showed a decrease of molecular weight.

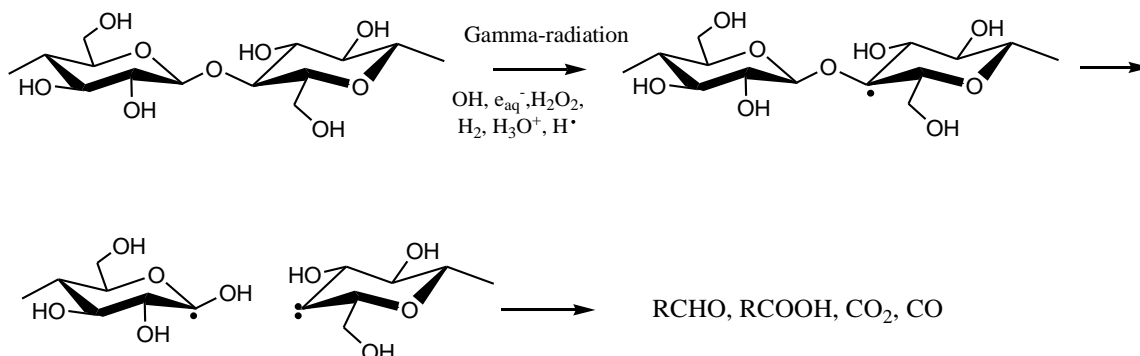


Fig. 10 Proposed reaction pathway of gamma-rays on C₁ and C₄ of cellulose adapted from (Ponomarev and Ershov, 2014, Sánchez Orozco *et al.*, 2012, Sokhey and Hanna, 1993, Sultanov and Turaev, 1996).

Like Henniges *et al.* (2012) and Takács *et al.* (1999), it was claimed that irradiation on cotton leads to the formation of carboxylic acid groups (Bouchard *et al.* 2006) close to 313 mmol COOH/kg at irradiating dose of 4.5 MeV and 140 kGy. Similar to gamma irradiation, chemical approaches reported changes on CNCs by using 2,2,6,6-tetramethylpiperidine-1-oxyl (TEMPO) in TEMPO-mediated oxidation (de Nooy *et al.*, 1994; Habibi *et al.*, 2006) leading to a concentration of 599 mmol COOH/kg CNCs after a reaction time of 4h without significant formation of aldehyde groups (Carlsson *et al.*, 2014). In agreement with these studies, Frascini *et al.* (2017) studied the formation of total acid groups on CNCs through TEMPO-oxidation, observing approximately 1200 mmol of total acid groups per kg CNC, without significant changes on the half-ester sulfate content or the crystalline structure of the crystals.

On the other hand, research studies performed on gamma irradiation of polysaccharides such as carrageenan (Abad *et al.*, 2013) or chitosan (Feng *et al.*, 2008) showed that the molecular weight of the polymer backbone decreases when irradiation increased. By testing the radical scavenging capacity, the authors observed that increasing irradiation doses led to high antioxidant properties. For example, irradiated chitosan at 2, 10, and 20 kGy showed radical scavenging (RS%) of 41, 47 and 64% compared to 20 % RS in pure chitosan (Feng *et al.*, 2008). This phenomenon was suggested by Feng *et al.* (2008) as a decrease of the intermolecular interactions and further availability of the functional amine group in chitosan polymers. Similar conclusions were made by Abad *et*

al. (2013) from whom the increased antioxidant capacity was ascribed to increased reducing capacity in the irradiated carragenan.

To the best of our knowledge, no study has been done before on gamma irradiation of CNCs with the aim to create new functional groups and by its functionalization the addition of new antioxidant properties to the nanoparticles. Based on published studies of irradiated cellulose and polysaccharides such as carrageenan and chitosan, one of the purposes of this thesis was to understand the changes in functionalities and properties of CNCs when gamma irradiation was applied.

2.5 Wholesomeness/toxicity of CNCs for Food Applications

As discussed in the previous sections, the presence of CNCs can bring many benefits in terms of performance in food packaging such as enhancement of mechanical properties, increased oxygen barrier, and contribution to antimicrobial and antioxidant activities. However, when nanometric particles (NPs) are embedded in a material, migration can occur, becoming a potential problem that should not be dismissed. Šimon *et al.* (2008) stated that small particles are prone to migrate when they are embedded in matrices of low viscosity with no interaction with the polymeric matrix.

In order to resolve any doubts related to particle migration, studies have been performed to understand the release of monomers from polymeric PLA material in food-simulating solvents (Conn *et al.*, 1995), and recent studies have been done on CNC migration from PHB and PLA matrices as examples (Dhar *et al.*, 2015; Dhar *et al.*, 2017). In CNCs-reported studies, the authors (Dhar *et al.*, 2015; Dhar *et al.*, 2017) were in agreement that the overall migrated amount of the films did not exceed the 10 mg/dm³ or the 60 mg/kg of simulant, as it was the limit established by the European Commission Directive 2002/72/EC (2002).

Despite the fact that migration might or might not occur through the food packaging, guidelines and regulations have been created based on the use of NPs in contact with food with the aim of guaranteeing the safety of the consumer. Being aware of the use of nanoparticles in food, agencies such as Food and Drug Administrations, in the United States, has published documents in order to guide manufacturers or end-users of food ingredients to assess the regulatory status of a food substance. Without declaring or categorically judging the technology as harmful or benign, these guidelines were stated to assess the safeness of the product by:

- 1) Declaring the identity of the substance (i.e., name, chemical formula (e), source, quantitative composition, impurities and contaminants, and its physical properties
- 2) Determining the technical effect or functionality of the substance in the food matrix
- 3) Establishing the self-limiting levels of use and the safety assessment of the food substance. For instance, if altering the size of the particle affects the palatability perspective or other parameters for self-limiting acceptance.
- 4) Evaluating the effect of the size on the bioavailability of the product through the absorption, distribution, metabolism, and excretion of the substance in the body. Thus, if higher rates of absorption due to changes of size are obtained, new required amounts of the final product should be reconsidered.
- 5) Declare the impurities/contaminants of the product that can affect its purity.

Even though, the evaluation of nanoparticles is a case-by-case situation, there have been advances in the scientific field that evaluate their toxicity. For example, in living organisms and cells, the effect of CNCs contact with dermal, oral system and human cells has been studied in literature (Cretu *et al.*, 2017; Du *et al.*, 2015; Harper *et al.*, 2016; Kovacs *et al.*, 2010; Menas *et al.*, 2017; Shvedova *et al.*, 2016; Weiss *et al.*, 2006). Dermal studies carried out by O'Connor *et al.* (2014) demonstrated that no effect was observed in mice treated with 25 μ L of CNCs at different concentrations from 2.5 to 10.7% applied on the ear dorsum. In the oral system, Roman (2015) suggested that the transfer of CNCs bearing negatively charged sulfate half-ester groups are less prone to pass through the gastrointestinal tract due to the slow diffusion in the negatively charged mucus. In the same system, acute oral toxicity tests were done to determine the maximum concentration of CNCs for the oral gavage of Cr1:CD(SD)BR rats. During the test period at feeding the rats with daily concentrations of 500; 1,000; and 2,000 mg/kg of CNCs, no adverse effects or toxicity were observed (O'Connor *et al.*, 2014).

Other authors have reported that at low concentration of CNCs no significant cytotoxicity in different cell types: human brain microvascular endothelial (Roman *et al.*, 2009), gingival fibroblast (Villanova *et al.*, 2011) L929 human brain microvascular endothelial (Dong *et al.*, 1998) and NIH 313 fibroblast (Yang *et al.*, 2013).

Even if previous studies demonstrated non-toxicity to human cells or the environment, parameters such as dispersibility, exposure time, sources, preparation, and surface

chemistry of the nanoparticles with the surrounding environment might be evaluated on a case-by-case basis in order to assess a complete safe evaluation of the CNCs when migrated from food. So far, new regulations and adequate techniques for evaluation of migration and safety remain under development.

3. GENERAL OBJECTIVE, HYPOTHESIS, SPECIFIC OBJECTIVES AND METHODOLOGIES

3.1 General Objective

The general objective of this research was to evaluate the potential use of cellulose nanocrystals as:

- an active surface to be functionalized by means of gamma irradiation,
- a reinforcing agent in biopolymeric networks to assure a controlled release of natural antimicrobial molecules over time,
- a potential antioxidant to insure food innocuity and stability during storage.
- To evaluate the combined treatments: active biopolymers and gamma irradiation to assure food safety.

3.2 Hypothesis

3.2.1) Gamma irradiation promotes the modification of cellulose nanocrystals which allows the improvement or permits the grafting of bioactive compounds to bring antioxidant properties.

3.2.2) The addition of CNCs enhances the mechanical properties of biopolymers.

3.2.3) The introduction of CNCs in biopolymer containing antimicrobial properties insures the controlled release and extends the bioactivity of active compounds during food processing and storage periods.

3.2.4) The addition of CNCs in biopolymer films improves their barrier properties and prevents oxidation of food components.

3.3 Specific Objectives

3.3.1) Determine the ability of gamma irradiation in combination with redox chemistry to introduce antioxidant functionality onto CNCs' surface.

3.3.2) Assess and quantify the functional groups grafted at the surface of CNCs.

3.3.3) Introduce CNCs in polymeric matrices and evaluate their reinforcing properties by standard techniques.

3.3.4) Develop a method to encapsulate essential oil in biopolymers using CNCs and evaluate the presence of these CNCs on the release of the bioactive compound (from the EO) in an *in vitro* simulated meat condition.

3.3.5) Determine the antimicrobial activity of encapsulated active molecules in nanocomposite biopolymers against pathogenic bacteria in meat and the possible synergistic effect with gamma irradiation.

3.3.6) Evaluate the oxygen permeability and UV light barrier of the biopolymer nanocomposite films loaded with CNCs and their capacity to limit the lipid oxidation of food matrices.

3.4 Methodologies

3.4.1) Functionalization of gamma irradiated CNCs was monitored by Purpald[®] test and conductometric titration (Metrohm, Canada) for quantification of aldehyde and carboxylic acid groups, respectively according to Quenseberry and Lee (1996) and Katz *et al.*, (1984).

3.4.2) Functionalization of modified CNCs by irradiation was determined by FTIR spectroscopy (Perkin-Elmer, Canada).

3.4.3) The determination of antioxidant properties of CNCs was performed by the antiradical tests DPPD (Han *et al.* 2011), DPPH assay, and the total antioxidant capacity was assessed according to Dasgupta and De (2004).

3.4.4) Mechanical properties (tensile strength, elongation at break, and Young modulus) of reinforced polymeric matrices loaded with CNCs were measured with a Universal Testing Machine Model H5KT (Tinius Olsen, USA) according to Huq *et al.* (2012).

3.4.5) Alginate polymer cross-linked with calcium chloride in a bead-shaped formulation and reinforced with CNCs was used for the encapsulation of bioactive compounds. Different concentrations of CNCs (0-30%) were added to this formulation. Analysis of the bioactive compound release was performed in 10% aqueous-ethanol as a simulating solvent for meat where the alginate beads were immersed in the ethanol solution according to Jamshidian *et al.* (2012). The cumulative release (%) of active compounds

over storage time was evaluated by UV spectroscopy (Scinco, ON, Canada) using an empirical model from Korsmeyer-Peppas (1983).

3.4.6) The antimicrobial properties against *Listeria* of active beads were evaluated as function of storage time in meat. The growth of total mesophilic flora (MTF) was calculated according to Dussault *et al.* (2012). The synergistic effect of the active beads with gamma irradiation on bacteria was also determined according to Huq *et al.* (2015).

3.4.7) Alginate films loaded with different concentrations of CNCs were prepared by casting and oxygen barrier properties testing and UV transmission were performed using an OX-TRAN Model 1/50 (Mocon, USA) at 0, 50 and 70% RH according to Fortunati *et al.* (2016) and a Cary 100 Bio UV-Visible spectrophotometer (Agilent technologies, Canada) according to Dai *et al.* (2016).

3.4.8) *In situ* antioxidant properties of the edible coating formulation based on alginate based films loaded with CNCs were evaluated using peroxide values (Bakota, 2014). The antioxidant properties were also evaluated by the analysis of the TBARS values on chicken (Oussalah *et al.*, 2004).

4. PUBLICATION 1: FREE RADICAL GRAFTING OF GALLIC ACID (GA) AND EVALUATION OF ANTIOXIDANT REINFORCED GELLAN GUM FILMS

Published in Journal Radiation Physics and Chemistry (2016), 118: 61-69

P. Criado¹, C. Fraschini², S. Salmieri¹, D. Becher¹, A. Safrany³ M. Lacroix¹

¹Research Laboratories in Sciences Applied to Food, Canadian Irradiation Centre (CIC), INRS-Institute Armand-Frappier, University of Quebec, 531 Boulevard des Prairies, Laval, Quebec, H7V 1B7, Canada

²FPIinnovations, 570 boulevard Saint Jean, Pointe-Claire, Quebec, H9R 3J9, Canada.

³International Atomic Energy Agency (IAEA), Division of Nuclear Sciences and Applications, Department of physical and Chemical Sciences, Section of Industrial Applications and Chemistry, Vienna International Centre, POB: 100, A-1400 Vienna, Austria A2371.

* * Author to whom correspondence should be addressed, Telephone: +1-450-687-5010;
Fax: +1-450-686-5501; E-mail: monique.lacroix@iaf.inrs.ca

The number of figures and tables were adjusted in this article in order to follow the sequence of the thesis document. The style of references was presented according to the guidelines of the journal.

CONTRIBUTION OF THE AUTHORS

During this proposed research work, Paula Criado, Dorra Becher and Stéphane Salmieri were working on preliminary experiments in the laboratory under the supervision of Pr. Monique Lacroix. The article was written by Paula Criado and support was given by Dr. Carole Fraschini to understand the behaviour of CNCs and the characterization of the modified material. Both Pr. Monique Lacroix and Dr. Carole Fraschini were constantly reviewing the scientific paper during its redaction. This work was done in collaboration with IAEA under supervision of Dr. Agnès Safrany.

RÉSUMÉ

Des propriétés antiradicalaires ont été conférées à des nanocristaux de cellulose (CNCs) par l'intermédiaire d'un couple redox initiateur et d'un traitement par irradiation gamma. Différentes procédures ont été testées sur des suspensions de CNCs, une réaction de 2 h avec le couple peroxyde d'hydrogène (H_2O_2)/acide ascorbique (AA) a été choisie comme étape préliminaire. Les CNCs ont ensuite été traités par irradiation gamma à une dose de 20 kGy puis l'acide gallique (GA) a été ajouté à la suspension. Après 24 h de réaction, le produit CNC- H_2O_2 -AA- γ -GA a été généré. La formation de nouveaux groupements carboxyliques et carbonyles a été caractérisée par analyse FTIR grâce à la présence de bandes à respectivement 1650 et 1730 cm^{-1} . Ces groupes ont été également quantifiés par titrage conductimétrique où une augmentation de 49 à 134 mmol COOH/kg a été observée pour les CNCs natifs et irradiés, respectivement. Une augmentation similaire du nombre de groupements carboxyliques (132 mmol/kg) a également été observée dans les échantillons CNC- H_2O_2 -AA- γ -GA qui ont démontré des propriétés antiradicalaires significatives (8 mM Eq Trolox/mg de CNCs). Une analyse thermogravimétrique a confirmé les changements structuraux des CNCs. Un film d'emballage à base de gomme gellane contenant 20% de CNC- H_2O_2 -AA- γ -GA a été préparé afin d'évaluer ses propriétés mécaniques. Une amélioration significative ($p \leq 0.05$) de la résistance à la traction (TS), du module de traction (TM), de l'allongement à la rupture (Eb) et la perméabilité à la vapeur d'eau (WVP) a été observée lorsque les CNC- H_2O_2 -AA- γ -GA ont été ajoutés au film d'emballage.

ABSTRACT

Antiradical properties were introduced on cellulose nanocrystals (CNCs) by redox pair (RP) initiator and γ -radiation treatments. Different procedures were tested on CNCs, first a 2 h reaction of hydrogen peroxide (H_2O_2)/ascorbic acid (AA) was performed on CNCs solution. γ -radiation treatment at 20 kGy dose was then applied and immediately after GA was reacted during 24 h with the pretreated CNCs, giving CNC- H_2O_2 -AA- γ -GA. The formation of new carboxylic acids and carbonyl groups were characterized by FTIR at 1650 and 1730 cm^{-1} respectively. Carboxylic acid functionalities were also analysed by conductometric titration where an increase from 49 to 134 mmol COOH/kg was found from native to irradiated CNCs. A similar increase of carboxylic acids (132 mmol/kg) was observed in CNC- H_2O_2 -AA- γ -GA, showing the highest radical scavenging properties (8 mM Trolox eq/mg CNC). Thermogravimetric analysis confirmed the structural changes onto CNCs are presented in the molecule. Film packaging containing 20% of CNC- H_2O_2 -AA- γ -GA was then added to a gellan based film packaging. A significant improvement ($p \leq 0.05$) of the tensile strength (TS), the tensile modulus (TM), and the elongation at break (Eb) and a water vapor permeability (WVP) reduction was observed when CNC- H_2O_2 -AA- γ -GA was added to the film packaging formulation.

4.1 Introduction

Currently, scientists challenge lies on the use of active biopolymers, which have the potential to preserve food and protect it from antimicrobial attack in food packaging (Bautista-Baños *et al.*, 2006). However, the use of a biodegradable film has some limitations such as poor vapor barrier, weak mechanical properties (Khan *et al.*, 2014) and weak antimicrobial effects (Zivanovic *et al.*, 2005). In order to improve the functionality of bio-polysaccharide based films, addition of active reinforcements has been proposed. Several composites have been developed by adding reinforcement agents such as clays, silica or silver to polymers in order to enhance their thermal, mechanical, and barrier properties (Azeredo, 2009). A uniform dispersion of these reinforcement particles in polymer matrices can lead to a better molecular mobility, relaxation behavior and the consequent thermal and mechanical properties of the material. According to Suyatma *et al.* (2005) a reinforcing agent increases the physico-chemical properties, acting as a lubricant in a polymer network. Taking into account that polymer-polymer interactions within polymer chains are made of hydrogen bonding and van der Waals forces, a reinforcing agent role is to break down these bonds and increase the flexibility of the polymer network. Ludueña *et al.* (2007) have demonstrated that the smaller the filler particles loaded in polymer matrices, the better the interaction in the polymer network and the higher the cost-price efficiency. In this context several nanoreinforcements have been interesting due to their high surface that provides better reinforcement effects (Ray *et al.*, 2006; Sun *et al.*, 2007; Azeredo *et al.*, 2009; Klemm *et al.*, 2009; Rhim *et al.*, 2013).

Interest has been found in using cellulose nanoreinforcements as the main components in the manufacture of biodegradable packaging materials (Erdohan and Turhan, 2005; Ye and Farriol, 2006; Shih *et al.*, 2009), in addition to the stimulating search for non-petroleum-based structural materials (Dufresne, 2012). Cellulose is an organic polymer known to occur in a wide variety of living species from the world of plants, bacteria and animals. Cellulose structure consists of a linear homopolymer of β -1, 4 linked units of glycopyranose (Ray *et al.*, 2006). It is important to underline that cellulose has the advantage of having an abundance of hydroxyl groups at its surface, thus, chemical modifications of these functional sites can be performed and other functionalities, besides mechanical, can be added to the polymer. Bioactive materials in polymer matrices can provide both high mechanical and biological potential. The attachment of

antioxidant and antimicrobial molecules to polymers has been applied by several authors (Curcio *et al.*, 2009; Spizzirri *et al.*, 2009, 2010; Cho *et al.*, 2011; Liu *et al.*, 2014). Based on the beneficial effect for human health and food conservation, the use of antioxidants has been suggested as promising treatment for diseases (Seifried *et al.*, 2007). Polyphenols are usually referred to have numerous biological activities, in particular as antimicrobials and antioxidants (Cho *et al.*, 2011). Gallic acid (GA) is a natural phenolic compound providing antioxidant properties. This compound is widely present in many plants and fruits as a secondary polyphenolic metabolite (Lu *et al.*, 2006). As an antioxidant, this compound can play an important role in nutraceutical, pharmacological and food applications for scavenging free radicals (Kanai and Okano, 1998; Dwibedy *et al.*, 1999).

Grafting antioxidant molecules to biopolymer backbone has been presented in literature by the authors Spizzirri *et al.* (2009), Curcio *et al.* (2009), and Liu *et al.* (2013). The suggested mechanism of reaction includes the formation of hydroxyl radicals created from a reduction-oxidation pair composed of peroxide hydrogen and ascorbic acid. The role of the redox pair (peroxide hydrogen and ascorbic acid) is based on the formation of hydroxyl radicals, generated by the oxidation of ascorbic acid into the formation of an intermediate molecule or called ascorbyl radical (Kitagawa and Tokiwa, 2006). It is then suggested that the produced hydroxyl radical interact with the polysaccharide backbone, allowing the grafting of macroradical polysaccharide with antioxidant molecules. However, a stronger grafting procedure can be carried out when gamma-irradiation is applied. Radiation technology has been considered as a tool for surface grafting and reactive improvement (Singh and Silverman, 1992; Woods and Pikaev, 1994; Zaharescu *et al.*, 1999). One of the advantages of using this method is the formation of strong bridges between molecules (Ratnam *et al.*, 2006).

The aim of this study was to evaluate the effect of the redox pair (hydrogen peroxide and ascorbic acid) and the gamma irradiation in order to enhance the antiradical properties of adding gallic acid to cellulose nanocrystals (CNCs). Thus, the modified CNCs were then used to prepare antioxidant based gellan film packaging and the radical scavenging, mechanical, and barrier properties were evaluated.

4.2 Experimental Section

4.2.1 Materials

3,4,5 trihydroxybenzoic acid anhydrate (gallic acid (GA)), L-ascorbic acid (AA), hydrogen peroxide (H_2O_2) (8M), sodium chloride, Dowex® Marathon C™ cation-exchange resin, sodium hydroxide, N,N-diethyl-*p*-phenylenediamine sulfate salt (DPPD), 6-hydroxy-2,5,7,8-tetramethylchroman-2-carboxylic acid (Trolox®) were purchased from Sigma Aldrich chemie GmbH (Oakville, ON, Canada). Freeze-dried CNCs were kindly provided by FPIinnovations (Pointe-Claire, QC, Canada) from where CNCs was produced according to the modified procedure described in literature (Dong *et al.* 1998).

For the preparation of the films, gellan gum Kelcogel® F was kindly given by CPKelco (San Diego, California, USA), calcium chloride and glycerol were purchased from MAT laboratory (Quebec, QC, Canada).

Methods

4.2.2 Modification of CNCs

CNCs were treated by different procedures in order to produce a new nanomaterial with antioxidant properties. CNCs derivatives were studied after treatments such as gamma irradiation, chemical reaction with the redox pair peroxide hydrogen and ascorbic acid, and the antioxidant gallic acid (GA). Thus, CNCs were irradiated at 20 kGy (CNC- γ) or reacted with the redox pair (RP) for 2 h (CNC- H_2O_2 -AA) under magnetic stirring. By combining these methods, RP was firstly added to CNCs and after 2 h of reaction the solution was irradiated at 20 kGy (CNC- H_2O_2 -AA- γ).

A 100 mL solution of CNCs at 0.5% (w/w) was prepared in deionized water. Vacuum and oxygen-free nitrogen gases were passed through the solution for a minimum of 5 minutes before irradiation. The irradiation treatment was immediately followed at the Canadian Irradiation Center in a gamma ray Underwater Calibrator-15A irradiator equipped with a ^{60}Co source and having a dose rate of 16.536 kGy/h (0.2756 kGy/min) (Nordion Inc., Kanata, ON, Canada). The sample of CNC- H_2O_2 -AA was reacted with 135 mg of ascorbic acid and 567 μL of hydrogen peroxide (8 M) at 25 °C for 2 h under magnetic stirring. The addition of 0.75 g of gallic acid was done immediately after

irradiation and the solution was then stirred for 24 h (CNC-H₂O₂-AA-γ-GA). The proposed mechanisms of reaction and treatment procedures are shown in **Figures 11** and **12**. The grafted CNCs were dialyzed against distilled water for 48 h in 12-14 kDa membranes in order to eliminate unreacted products, and then freeze-dried.

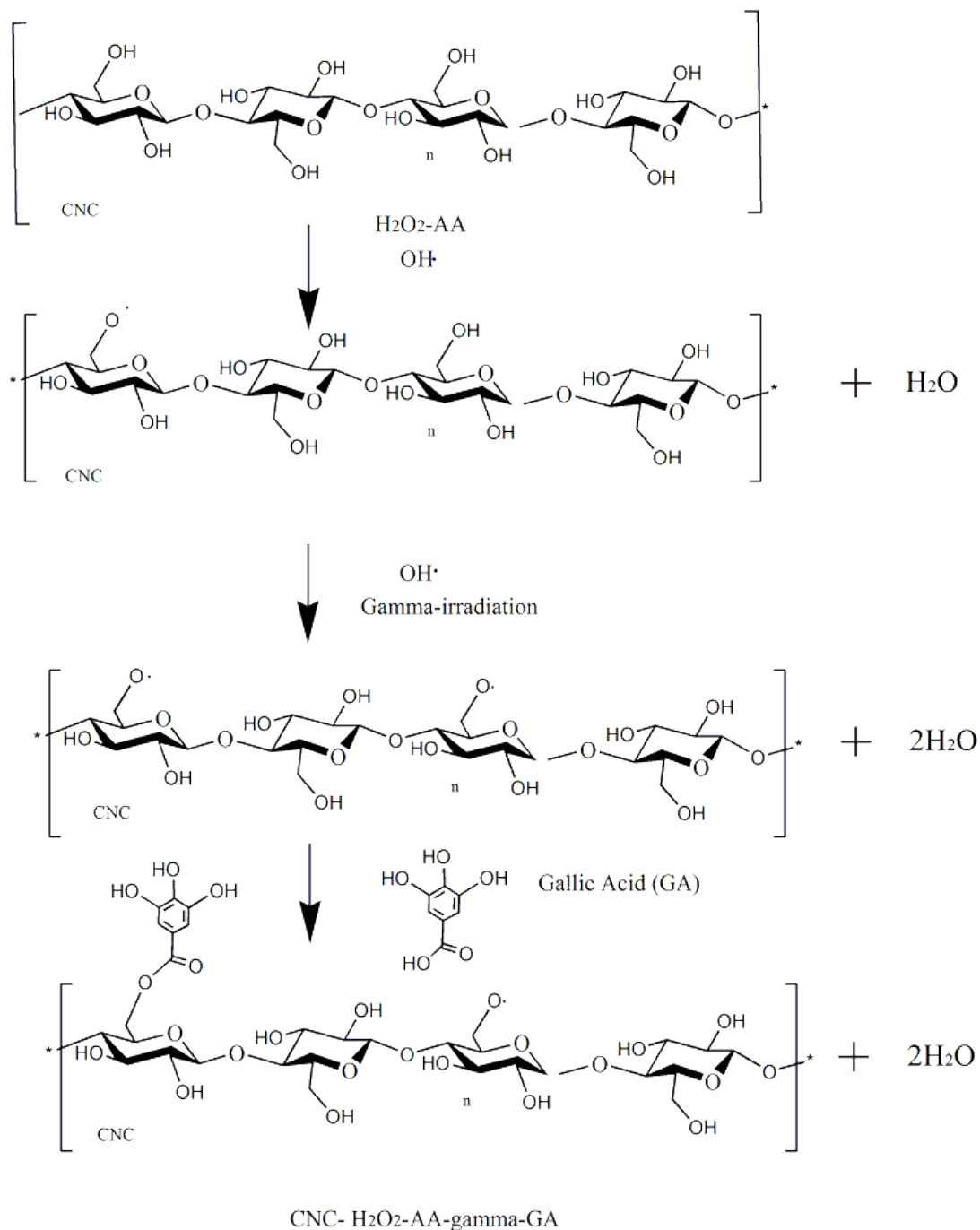


Fig. 11 Schema of proposed mechanism of reaction of gallic acid with CNC by means of a redox pair followed by gamma-irradiation

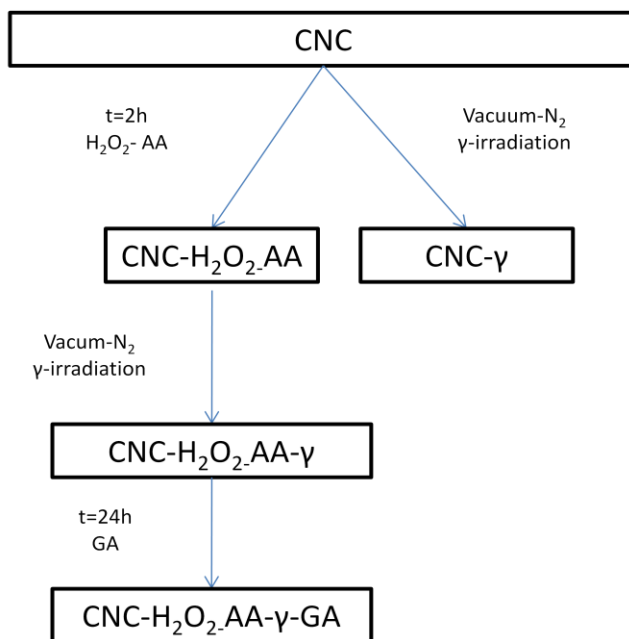


Fig. 12 Schema of treatments performed onto CNC

4.2.3 Ion Exchange (protonation) Treatment

CNC suspensions were treated to convert sodium carboxylate and sulfate ester groups into their protonated acid form. Aqueous suspensions were placed over Dowex® Marathon C™ cation-exchange resin and gently stirred for at least 2 h at room temperature. Resin beads were then removed by filtration with a Whatman GF/F glass microfibre filter (pore size 0.7 μm).

4.2.4 Characterization of CNCs by Fourier Transform Infrared (FTIR)

Characterization of native and CNCs derivatives were done by FTIR. A Spectrum One spectrophotometer (Perkin-Elmer, Woodbridge, ON, Canada) equipped with an attenuated total reflectance (ATR) device for solids analysis and a high linearity lithium tantalate (HLLT) detector was used for testing the freeze-dried samples. Spectra were analyzed using the Spectrum software within the spectral region of 4000 to 650 cm^{-1} with 64 scans recorded at a 4 cm^{-1} resolution. After attenuation of total reflectance and baseline correction, spectra were normalized at 1200 cm^{-1} with a limit ordinate of 1.5 absorbance units. The resulted FTIR spectra of CNCs, CNC- γ , CNC-H₂O₂-AA, CNC-

H₂O₂-AA-γ, CNC-H₂O₂-AA-γ-GA, were compared to evaluate the functional groups freshly introduced on CNCs.

4.2.5 Carboxylic Acid Content Determination by Conductometric Titration

The carboxyl content of the CNC samples was determined using conductometric titration according to a method derived for the titration of cellulosic fibres (Katz *et al.*, 1984). Suspensions of protonated CNCs containing 0.053 g of solid content were titrated with 0.01 M NaOH using a 809 Titrando automatic titrator (Metrohm, Canada) in the presence of 1.0 mM NaCl. Typical titration curves (**Fig. 13**) exhibit two discontinuities assigned to the presence of a strong acid (i.e., sulfate ester groups introduced during the CNCs production process) and a weak acid (i.e., carboxylic acid groups introduced during the irradiation/grafting process). Therefore, the carboxyl content of the sample is given by the following equation:

$$[\text{COOH}] = ((V_2 - V_1) * C_{\text{NaOH}}) / m_{\text{CNC}} \text{ in mmol/kg} \quad (11)$$

Where V_i is the volume of NaOH (in mL), C_{NaOH} is the exact NaOH concentration (in mol/L) and m_{CNC} is the dry weight of the sample (in kg).

4.2.6 Thermo Gravimetric Analysis (TGA)

The dried CNCs (15 mg) were pressed by hand in a home-made mold to generate cylinder-shape pellets fitting into the TGA platinum pans. The pellet dimensions were 6.6 mm in diameter and ~4 mm in height. Experiments were conducted in the thermogravimetric analyzer Q5000IR (TA Instruments, New Castle, DE, USA). An air vector gas flow rate of 20 mL/min was used. Runs were performed from 50°C to 600°C at a heating rate of 10°C/min. Data processing was performed using Universal Analysis™ software.

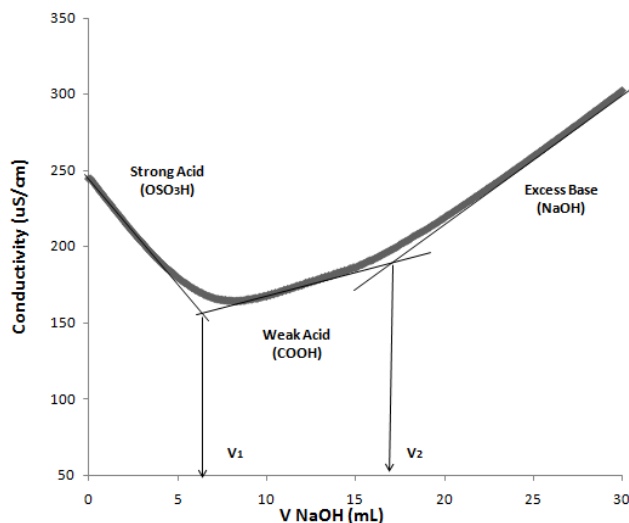


Fig. 13 Example of conductometric titration curve of protonated CNC containing weak acid groups

4.2.7 Free Radical Scavenger Properties

Radical scavenger properties of CNC solutions were evaluated in accordance with the procedure described by Han *et al.* (2011) using N,N-diethyl-p-phenylenediamine sulfate salt (DPPD) reagent. A volume of 200 µL of each CNCs derivative was placed in an electrolytic cell (platinum electrodes) containing 3 mL of NaCl (0.15 M), then submitted to electrolysis for 1 min (10 mA DC, 400 V). After electrolysis, a 200 µL aliquot of the electrolyte was added to 2 mL of DPPD (2.5% w/v) solution. The generated reactive oxygen species (ROS) such as superoxide anions ($\cdot\text{O}_2^-$), singlet oxygen ($^1\text{O}_2$), hydroxyl radicals ($\cdot\text{OH}$) and their by-products (H_2O_2 and OCl^-) instantly react with DPPD to generate a red coloration measured at 515 nm with a Cary 1 UV-visible spectrophotometer (Varian Canada Inc., Mississauga, ON, Canada). The colorimetric reaction is calibrated in a percentage scale using i) a negative control of the non-electrolyzed NaCl solution with 200 µL of ethanol solution 30% (v/v) ascribed to 100% radical scavenging (absence of ROS) and ii) a positive control ascribed to 0% scavenging i.e. the electrolyzed NaCl with 200 µL of ethanol 30% (v/v) solution (maximum concentration of ROS). From these considerations, the DPPD scavenging percentage is calculated using the following equation:

$$\text{DPPD Scavenging (\%)} = [1 - [(A_{\text{sample}} - A_{(-)}) / (A_{(+)} - A_{(-)})]] \times 100\% \quad (12)$$

in which $A_{(-)}$ is the absorbance of negative control and $A_{(+)}$ the absorbance of positive control. The antiradical activity of either CNCs derivative or antioxidant film was estimated from a standard curve by plotting DPPD scavenging vs. 1-4 mM of 6-hydroxy-2,5,7,8-tetramethylchroman-2-carboxylic acid (Trolox[®]). DPPD scavenging capacity was expressed in mM Trolox eq/mg of solution (RS/mg CNC).

A mass of 100 mg of each dried packaging film was used to evaluate the effect of antioxidant CNCs that were embedded into the gellan-based film.

Packaging films preparation

A gellan gum solution of 1% (w/w) containing 1% (w/w) of glycerol was prepared in distilled water. Different concentrations of antioxidant CNCs ((0-20%) w/w gellan gum in dry basis) were mixed with this polymer solution. A volume of 20 mL of the film formulation was spread onto Petri dishes and after 3 days drying at 25°C ($\pm 1^\circ\text{C}$), 2 mL of calcium chloride solution at 1.5 % (w/v) was spread over the pre-dried films and let to air dry for 24 h. Afterwards, the dried films were stored at room temperature (25 \pm 1°C) for at least 24 h in a desiccator containing saturated NaBr solution to ensure a stabilized atmosphere of 56% RH.

4.2.8 Mechanical Properties of Films

Film Thickness and Width

Thickness of gellan based-film containing CNCs or CNC-H₂O₂-AA- γ -GA was measured by using Mitutoyo digimatic indicator (Mitutoyo MFG Co. Ltd, Tokyo, Japan) with a resolution of 0.001 mm, at five random positions around the film.

Tensile Strength, Tensile Modulus and Elongation at break

The tensile strength (TS), tensile modulus (TM), and elongation at break (Eb) of gellan-based films were evaluated. Films were cut in a rectangular shape with a width of approximately 12 mm. The width was then measured using a Traceable[®] Carbon Fiber Digital Caliper (resolution of 0.1 mm; Fisher Scientific, ON, Canada), at three random positions. Mechanical properties were carried out measured according to the ASTM D638-99 method (1999) using a Universal Testing Machine (model H5KT; Tinius Olsen Testing Machine Co., Inc., Horsham, PA, USA), equipped with a 100 N-load cell (type FBB) and 1.5 kN-specimen grips. TS (MPa), TM (MPa), and Eb (%) values were

automatically collected after the film break due to elongation, using Test Navigator® 7 software.

4.2.9 Water Vapor Permeability (WVP) of Films

The WVP tests were conducted gravimetrically using the ASTM (1983) procedure. CNCs and CNC-H₂O₂-AA-γ-GA loaded gellan films were mechanically sealed onto vapometer cells (No. 68-1, Thwing-Albert Instrument Company, West Berlin, NJ) containing 30 g of anhydrous calcium chloride (0% RH). The cells were initially weighed and placed in a Shellab 9010 L controlled humidity chamber (Sheldon Manufacturing, Cornelius, OR, USA) maintained at 25°C and 60% RH for 24 h, corresponding to a vapor pressure of 3.282 kPa. The cells were weighed before and after 24 h and the WVP was calculated as shown in equation (13)

$$\text{WVP (g}\cdot\text{mm/m}^2\cdot\text{day}\cdot\text{kPa)} = \Delta w \cdot x / A \cdot \Delta P \quad (13)$$

Where ΔP corresponds to differential vapor pressure of the water through the film (3.282 kPa at 25 °C and 60% RH) and Δw refers to the difference between final and initial weight. A is the area of exposed surface of the film ($31.67 \times 10^{-4} \text{ m}^2$) and x the film thickness expressed in mm.

4.3 Statistical Analysis

Analysis of variance ANOVA and Duncan's multiple-range test were used to perform statistical analysis for each experiment, using PASW Statistics Base 16 software (SPSS Inc., Chicago, IL, USA). Differences between means were considered to be significant when $p \leq 0.05$.

4.4 Results

4.4.1 FTIR analysis

The formation of novel functional groups on CNCs were studied by analyzing the FTIR spectra of CNCs, CNC-γ, CNC-AA-H₂O₂, CNC-H₂O₂-AA-γ, CNC-H₂O₂-AA-γ-GA freeze-dried at pH 7.0 (**Fig. 14**). The absorption peaks of native CNCs are mainly assignable to the stretching vibrations of hydroxyl groups at 3600-3200 cm⁻¹ and the C-H stretching vibration of aliphatic chains at 2930 cm⁻¹ as it was described by Huq *et al.* (2012). In addition, an increased intensity of the peak at 1650 cm⁻¹ corresponds to the carbonyl

vibration of carboxylate anions (overlapped with adsorbed water) introduced onto cellulose nanocrystals. It is important to highlight that this band was able to be detected due to the CNCs' pH (7) which allowed the observation of carboxylate moieties (Oomens and Steill, 2008) of CNCs compared to the carboxylic acid groups (COOH) observed at lower pH (Landgraf *et al.*, 1998) and observed at 1750 cm^{-1} . It was also noticed that peaks from $1382\text{--}1375\text{ cm}^{-1}$ correspond to C-H bending, while $1300\text{--}1100\text{ cm}^{-1}$ are due to the C-O-C stretch vibration of the ether linkage of the pyranose ring. After treatment of CNCs either with irradiation or RP a new stretching band appears at 1730 cm^{-1} related to the introduction of C=O groups onto native CNCs.

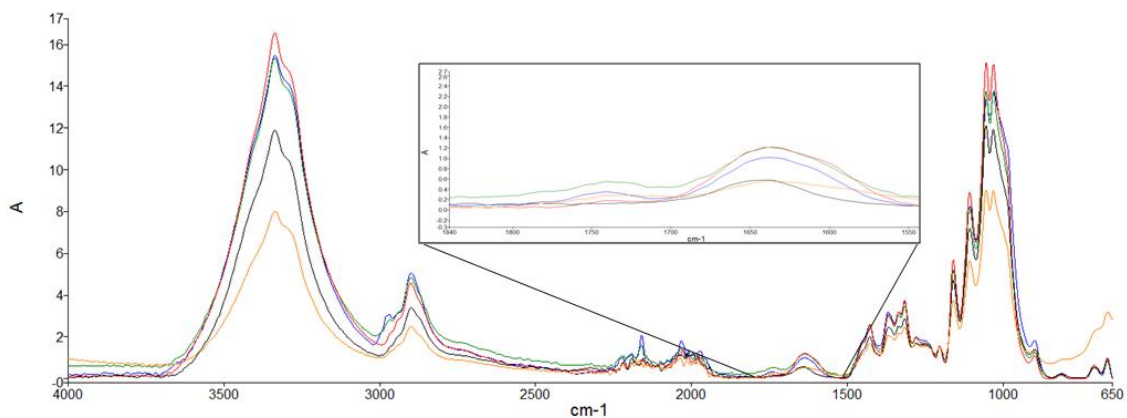


Fig. 14 FTIR spectra of CNC (Black), CNC-H₂O₂-AA (Green), CNC- γ (Yellow), CNC-H₂O₂-AA- γ (Blue) and CNC-H₂O₂-AA- γ -GA (Red)

The presence of these carbonyl groups can be explained by the introduction of aldehyde, ketone or ester functionalities mostly due to irradiation and/or chemical treatment with RP. Compared to irradiated CNCs (CNC- γ) at dose rate of 20 kGy followed by the CNC-H₂O₂-AA- γ , native CNCs showed a low intensity absorbance detected by FTIR analysis. At the same wavelength high intensities were observed when redox pair, gamma-irradiation and gallic acid were used. Therefore, modifications of CNC were supported by the formation of new bonds related to carbonyl new linkages which will be supported by further analysis.

4.4.2 Conductometric Titration of CNCs

Concentration of carboxylic acid groups of CNCs was determined by conductometric titration and the results are shown in **Table 4**. Native CNC exhibits a concentration of carboxylic acid groups on its surface of 49 mmol/kg. A 173% concentration increase was observed following the gamma-irradiation treatment. It is important to highlight that CNCs treated with the redox group presented as well a higher concentration of COOH groups (128 mmol COOH/kg CNC) compared to native CNCs. Concentration of COOH groups in CNC-H₂O₂-AA (128 mmol COOH/kg CNC) was close to the value observed in CNC-H₂O₂-AA-γ (121 mmol COOH/kg CNC), showing that irradiation treatment performed after reaction with RP did not introduce additional acidic groups. It can be suggested that formation of new carboxylic groups on modified CNCs observed in **Table 4** was related to different types of oxidation. Oxidation of cellulose by gamma-irradiation has been already discussed in literature (Bouchard *et al.*, 2006; Henniges *et al.*, 2012; Baccaro *et al.*, 2013) suggesting that high irradiation doses induces the formation of carbonyl groups and scission of cellulose chains. Similar to gamma-irradiation, it was also observed by Li *et al.* (2019) that cellulosic fibers were oxidized by a mechanism called Fenton reaction where ferrous ions are oxidized by hydrogen peroxide and reaction result in a production of hydroxyl radicals. It is suggested by Li *et al.* (2019) that this reaction carried in fibers lead to a decrease of degree of polymerization (DP from 800 to 200) of the fibers and the formation of carboxyl groups. Oxidation of ascorbic acid (AA) by hydrogen peroxide (H₂O₂) (Deutsch, 1998) has also reported the formation hydroxyl radicals (Kitagawa and Tokiwa, 2006; Spizzirri *et al.*, 2009) which might explain the increase of carboxyl groups found in CNCs treated with the reagents. When the sample was subsequently treated with gallic acid (CNC-H₂O₂-AA-γ-GA), a slight increase in the amount of carboxylic groups was also observed (from 121 up to 132 mmol COOH/kg CNC). This observation supports the grafting of a small amount of gallic acid onto the surface of the crystals. However, even if this amount is below the FTIR detection limit and could not be seen, the antioxidant properties of the grafted CNCs were significantly improved.

Table 4 Concentration of carboxylic acid groups introduced onto CNC surface

Sample	-COOH (mmol/kg CNC)
CNC	49
CNC-H ₂ O ₂ -AA	128
CNC- γ	134
CNC-H ₂ O ₂ -AA- γ	121
CNC-H ₂ O ₂ -AA- γ -GA	132

4.4.3 Thermogravimetric Analysis

Thermogravimetric analysis (TGA) of CNCs and their derivatives is presented in **Fig. 15**. They exhibit a small weight loss of 3% due to the water evaporation at temperatures from 50 °C to 100 °C. Native CNCs start to degrade above 250 °C. CNCs derivatives are less thermally stable as they start to degrade at lower temperatures. For example at 240 °C, CNC- γ showed a 17 % mass loss compared to 2% for native CNCs. The influence of the reaction of CNCs with the RP on the thermal properties is less marked than that of gamma-irradiation procedure. As it was shown in **Table 4**, the gamma-irradiation of CNCs leads to a higher content in carboxylic acid groups compared to the CNCs treated with the RP. Carboxylic groups are known to be detrimental to CNCs and speed-up the degradation process of CNCs with increasing temperature. Sharma and Varma (2014) were in agreement with these results suggesting that cellulose derivatives containing carboxylic acid functionalities exhibited lower temperature of decomposition (T_{onset}) compared to the non-modified cellulose. For instance, 2, 3 dicarboxycellulose had a T_{onset} of 184°C compared to 254°C observed for cellulose. This phenomenon was explained by the capacity of the carboxyl groups to be released at heating, causing acceleration on cellulose degradation.

It can be suggested that gamma-irradiation leads to changes on CNCs surface. Again, it can be shown that reaction of CNCs with RP followed by irradiation (CNC-H₂O₂-AA- γ) give similar thermal properties to CNC-H₂O₂-AA, confirming the results found by conductometric titration. When GA reacts with CNC after treatment of RP and irradiation, an intermediate thermal behavior is observed.

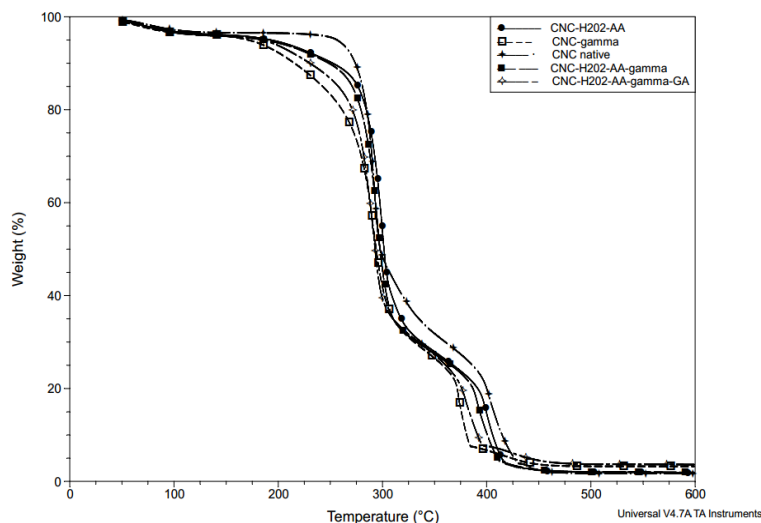


Fig. 15 Thermogravimetric analysis (TGA) of native CNC and its derivatives

Because its mass loss is lower than the one observed on irradiated CNCs, it can be suggested that the gallic acid present on CNCs acts as a protector, on its surface, when CNCs are under the effect of higher temperatures. Hence, it can be suggested that the higher thermal degradation observed at lower temperatures might be due to the introduction of new functional groups when ascorbic acid/peroxide oxygen, gamma-irradiation and gallic acid are used in treated CNCs.

4.4.4 Radical Scavenging (RS) Capacity of CNCs

Antiradical properties of CNCs derivatives (results expressed in mM Trolox eq/mg CNC) are shown in **Table 5**. Gallic acid has been shown to add some antiradical characteristics to native particles. Indeed, **Table 5**, shows that once CNCs were reacted with AA and H₂O₂, a significant increase from 0.024 mM Trolox eq/mg CNC with native CNCs to 0.317 mM Trolox eq/mg CNC for CNC-H₂O₂-AA. When gamma-irradiation treatment is performed, this value increased up to 1.920 mM Trolox eq/mg CNC for CNC-γ. In literature, it has been investigated that gamma-irradiation exhibits scission of cellulose chains (Henniges *et al.*, 2012). As it is known, cellulose is linked by β (1-4) D-glucose units. However, contrary to the rest of the chain this polysaccharide has at its right extremity a free reducing aldehyde group (Lapointe, 2000).

Table 5 Radical scavenging properties (mM Trolox eq/mg CNC) of CNCs derivatives

Sample	mM Trolox eq/mg CNC	±St Dev
CNC	0.024	0.001
CNC-H ₂ O ₂ -AA	0.317	0.050
CNC-H ₂ O ₂ -AA-γ	0.934	0.058
CNC-γ	1.920	0.065
CNC-H ₂ O ₂ -AA-γ-GA	8.212	0.130

It is then suggested that the gamma-irradiation exposure on CNCs decreases CNCs molar mass distribution, thus having a high exposure on aldehyde groups. Depending on the molecular structures, aldehyde functionalities are found to have an antiradical activity, which can be similar or lower than their acid counterparts. This phenomenon was studied by Bountagkidou *et al.* (2010) that found syringaldehyde and vallinin are required at 0.16 and 0 mol/mol DPPH to inhibit 50% of the radical level, respectively. Counterparts of syringic and vanillic acid showed both 0.28 mol/mol DPPH. When O-H bond dissociation energy are tested in phenolic compounds, low values are found due to the easy H-atom transfer (Borgohain *et al.*, 2015), however when CHO groups are present in these compounds the withdrawing effect can be reduced, thus showing a lower degree of antiradical activity compared to phenolic acids (Di Majo *et al.*, 2011). It has to be noted that phenolics acids such as gallic acid are known for their capacity to preserve food due to their antioxidant and antimicrobial properties (Gutiérrez-Larraínzar *et al.*, 2012). Exposure of the pretreated CNC-H₂O₂-AA-γ to gallic acid led to an important increase of RS properties with 0.934 mM Trolox eq/mg CNC found in CNC-H₂O₂-AA-γ. However, by comparing this value with 8.212 mM Trolox eq/mg CNC obtained for CNC-H₂O₂-AA-γ-GA, it can be concluded the GA has an important effect. Similar results were observed by Curcio *et al.* (2009) in relation with the grafting of gallic acid on chitosan. Results obtained by the group led to conclude that chitosan RS properties increased from 14% to 92% when GA was grafted to the polysaccharide. Other research groups have shown the antioxidant character of gallic acid (Yilmaz and Toledo, 2004; Pasanphan and Chirachanchai, 2008; Cho *et al.*, 2011), which mechanism was explained by Ji *et al.* (2006) as an easy deprotonation of GA to form GA

anion and thus a radical scavenger. In conclusion, it can be noted that the contribution of gallic acid, even if present in small amount, has a strong impact on the antiradical properties of CNCs.

4.4.5 Radical Scavenging (RS) Properties of Gellan-based Films

Results of radical scavenging capacity of gellan-based films containing native CNCs or CNC-H₂O₂-AA-γ-GA are shown in **Fig. 16**. Results show a significant ($p \leq 0.05$) increase of the RS capacity when CNC-H₂O₂-AA-γ-GA is added at a concentration of 20% (w/w polymer dry basis) as compared to samples containing native CNCs. Adding 20% (w/w polymer dry basis) of CNC-H₂O₂-AA-γ-GA to the gellan films can increase the RS value from 2.51 to 3.75 ($p \leq 0.05$). Values of RS of 2.81 and 3.31 mM Trolox were respectively observed at a CNCs concentration of 5% and 10% of CNC-H₂O₂-AA-γ-GA in gellan-based films, which is in accordance with the increase of antiradical CNCs. In addition, no significance ($p > 0.05$) was observed with the control and concentrations of 5%.

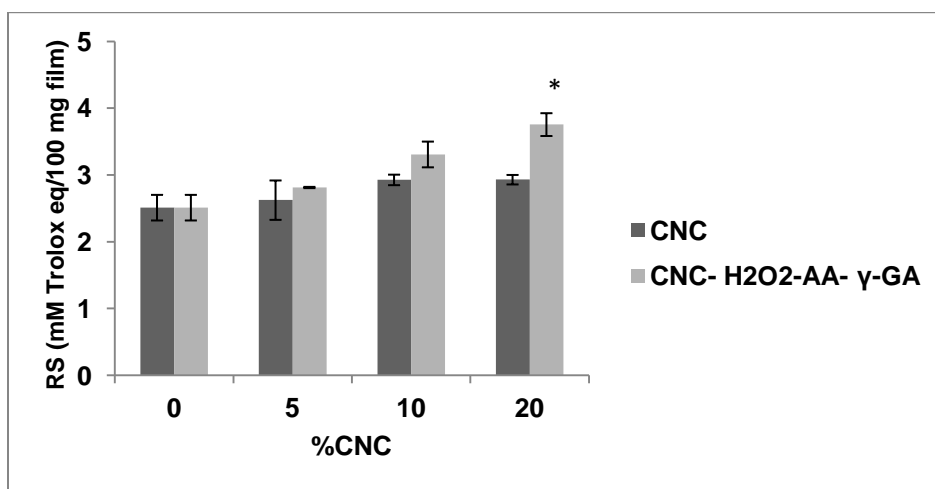


Fig. 16 Radical scavenging capacity (RS in mM Trolox eq/100 mg of film) of 1% (w/v) gellan-based films with native CNC or CNC- H₂O₂-AA-γ-GA at different concentrations. The asterisk indicates the difference with respect to the control

4.4.6 Effect of Modified CNC on Mechanical Properties of Gellan Films

The effect of CNCs addition on the tensile strength (TS) of gellan based film is shown in **Fig. 17**. Gellan films were tested with native and modified CNCs. Results show no significant differences between both types of formulations ($p > 0.05$). However, the TS of gellan film increased by increasing the concentration of CNCs or CNC-H₂O₂-AA-γ-GA. TS values increased from 37 MPa to 49 MPa by adding 20% of either native or modified

CNCs ($p \leq 0.05$). This gain in strength corresponds to an increase of the film stiffness by 31%. No significant difference ($p > 0.05$) was found between films containing 10% and 20% CNCs, indicating that 10% of CNC is the optimal concentration for TS.

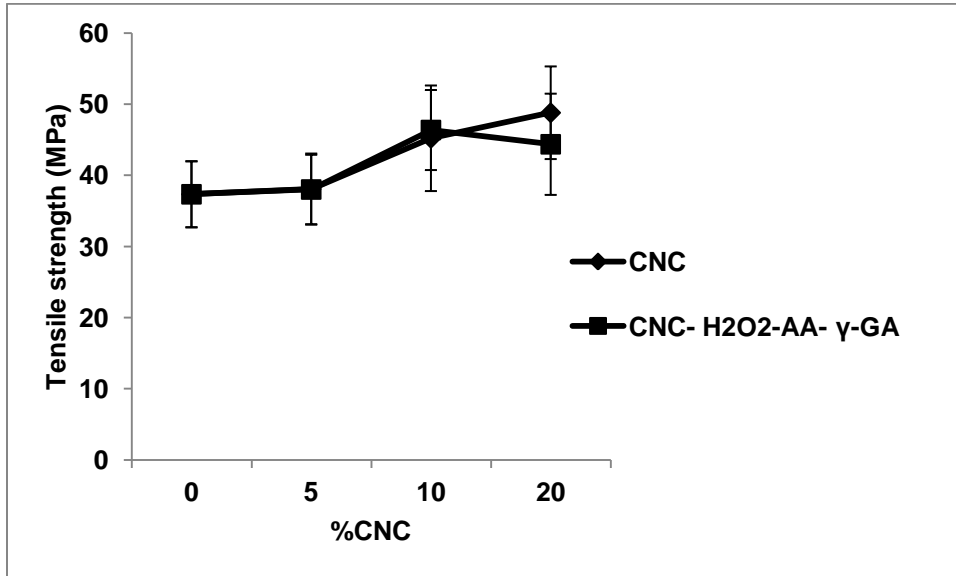


Fig. 17 Tensile strength (MPa) for gellan gum films containing CNC or CNC-H₂O₂-AA-γ-GA

For tensile modulus (TM) a significant increase of the TM was observed when the concentration of CNC or CNC-H₂O₂-AA-γ-GA was higher than 10% (**Fig. 18**). A maximum value of 990 MPa was obtained when 20% of CNC or CNC-H₂O₂-AA-γ-GA was added showing an increase of 51% of the TM compared to the films in absence of the particle. Khan *et al.* (2012) also observed a significant increase of the TM by adding 5% of CNC in chitosan-based films. The authors observed an increase from 1590 MPa to 2971 MPa when concentrations of CNC increased from 0 to 5% respectively. Ureña-Benavides *et al.* (2010) also studied the effect of the nanocomposites CNCs in alginate fibers and they observed an increase of 123 MPa in the TM by adding 10% CNCs in the films. In agreement with the loading of CNCs in the polymer matrix, it can be explained that increasing the CNC concentration led to a better interaction with the polymer matrix. It can be suggested, that a decrease of the mobility of polymer segments is induced and thus a higher value of tensile strength and tensile modulus can be observed.

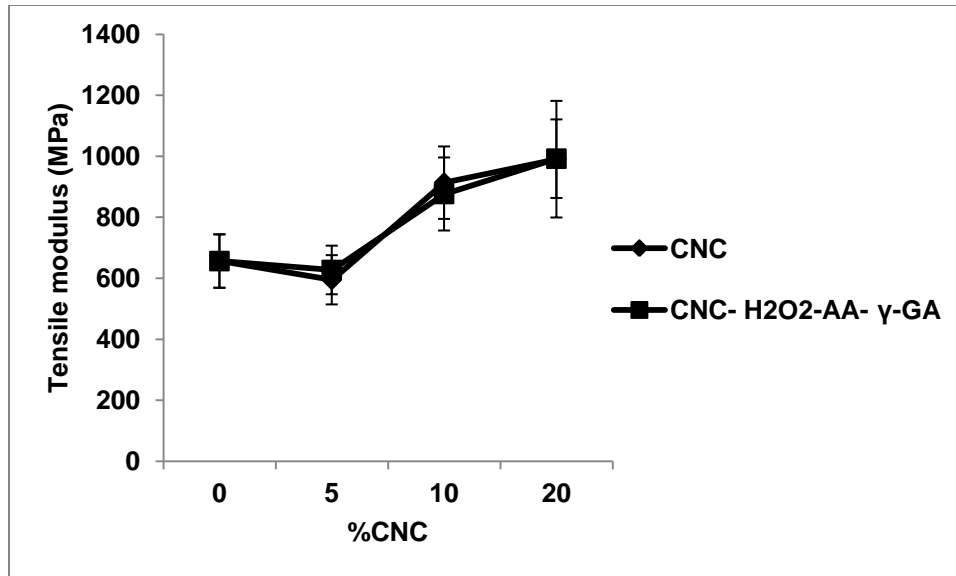


Fig. 18 Tensile modulus (MPa) for gellan gum films containing CNC or CNC-H₂O₂-AA-γ-GA

Results of elongation at break (Eb) of gellan-based films are shown in **Fig. 19**. A decrease of the elongation at break by increasing the concentration of CNCs was observed at concentrations higher than 5% ($p \geq 0.05$). A decrease of the elongation at break of 27% and 40% was noticed at concentrations of 10% and 20% of CNCs, showing respective values of 9.32% and 6.82% compared to 11.4% for the control without CNCs, respectively. Similar to TM and TS results, no influence on the elongation at break of the films was found when gallic acid was attached to CNCs. Similar results were obtained by Khan *et al.* (2012) who found that adding CNCs into chitosan-based films decreases the elongation at break by 8.5% until achieving stable value of 3.9% at concentrations of CNCs at 10% w/w of chitosan on a dry basis. This behavior might be correlated with the fact that CNC particles interact with the gellan matrix, thus creating a resistance to molecule arrangements when external strength is applied to the material. According to Azizi Samir *et al.* (2005) and Azeredo *et al.* (2010), the increase of the CNCs loading in polymer matrices, allows the CNC to create interactions with their surrounding molecules. Thus, gellan-based films containing CNCs contribute to the reinforcement in the mechanical properties due to the presence of CNC. Hence, an enhancement of TM and TS values can be observed with a decrease of Eb, indicating higher film stiffness with addition of CNCs.

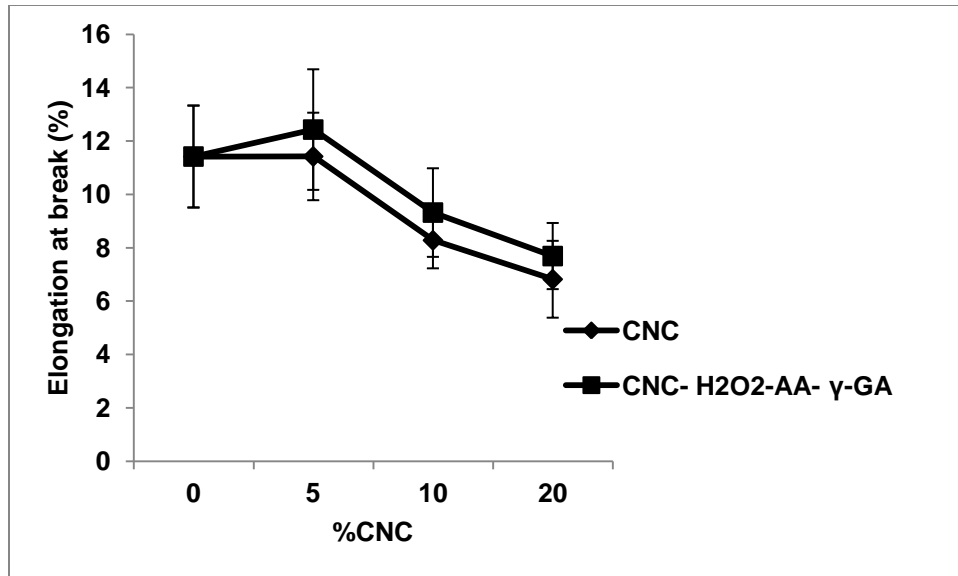


Fig. 19 Elongation at break (%) of gellan gum films containing CNC or CNC-H₂O₂-AA-γ-GA

4.4.7 Water Vapor Permeability (WVP)

The WVP results of the gellan films with native CNCs and modified CNCs are presented in **Fig. 20**. Results show no significant difference ($p > 0.05$) between films containing native and modified CNCs when added at the same concentrations. A significant reduction of WVP was noticed when 20% of CNCs or CNC-H₂O₂-AA-γ-GA was added into gellan films as compared to films containing from 0 to 10% CNCs or CNC-H₂O₂-AA-γ-GA ($p \leq 0.05$). Azeredo *et al.* (2009) found similar correlation in their mango puree edible films containing cellulose nanofiber (CNF) loadings. A decrease of 0.99 g·mm/m²·day·pKa of the WVP in films was observed by the group at 36 g of CNF/100g of mango puree, dry basis. In this study, a decrease of 1.51 g·mm/m²·day·pKa was observed in presence of 20% CNCs in gellan-based films.

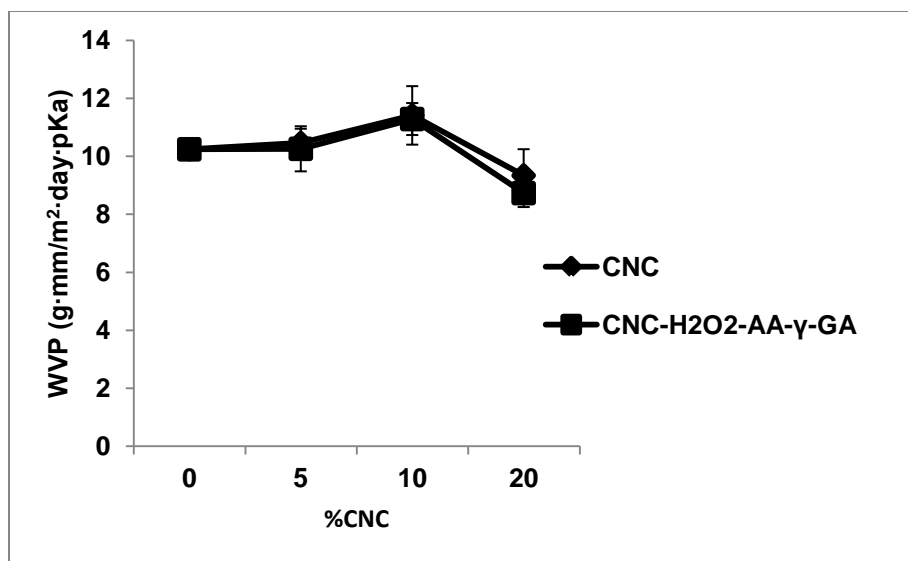


Fig. 20 Water vapor permeability (WVP in g·mm/m²·day·pKa) of gellan films containing CNCs or CNC-H₂O₂-AA-γ-GA

Thus, CNCs reinforcement on gellan-based films water vapor permeability is decreased and no effect was noticed for native or modified particles. It can be suggested that, adding CNC in polymer matrices creates tortuosities between the film components and this phenomenon can enhance significantly the barrier properties (Azeredo *et al.*, 2010).

4.5 Conclusions

This study has permitted to demonstrate the synergistic effect between gamma-irradiation and a hydrogen peroxide-ascorbic acid redox pairing as radical initiators to interact with the antioxidant gallic acid for functionalizing CNCs. Thus, modification of the CNC structure is presented by FTIR and confirmed by TGA. In addition, a significant increase of loaded carboxylic acid groups onto CNCs was analyzed by conductometric titration confirming changes on CNCs. Modified CNCs were then added to a gellan-based matrix and its antiradical properties were enhanced compared to gellan-based films loaded with native CNCs. Adding CNC or CNC-H₂O₂-AA-γ-GA improved significantly the mechanical and barriers properties of gellan-based films and a concentration of 20% showed antioxidant films.

The development of antioxidant-based films represents an important potential to stabilize food color and taste by the prevention of oxidation of food components like polyphenols or polyunsaturated fatty acids.

4.6 Acknowledgements

This research was supported by the National Science and Engineering Research Council of Canada (NSERC) and FPInnovations (Pointe-Claire, Canada) through the RDC program. Authors are grateful to the International Atomic Energy Agency (IAEA) for financial support to offer a fellowship (IAEA project code: PHI/13002) and for the coordinated Research Project No. F22051 entitled "Radiation Curing of Composites for enhancing their features and utility". Special thanks to Anie Day De Castro Asa, IAEA scholar and Damien Mauran for their valuable technical support and expertise for the development on this research work.

4.7 References

- ASTM, 1999. Standard test method for tensile strength of plastics. In Annual book of ASTM standards. ASTM International Method D, pp. 638- 699.
- ASTM, 1983. Standard test method for water vapor transmission of materials. Method 15.09: E96. American Society for Testing and Material. Philadelphia, PA.
- Azeredo, H.M.C. de, 2009. Nanocomposites for food packaging applications. *Food Res. Int.* 42, 1240–1253. <http://dx.doi.org/10.1016/j.foodres.2009.03.019>.
- Azeredo, H.M.C., Mattoso, L.H.C., Avena-Bustillos, R.J., Filho, G.C., Munford, M.L., Wood, D., McHugh, T.H., 2010. Nanocellulose reinforced chitosan composite films as affected by nanofiller loading and plasticizer content. *J. Food Sci.* 75, N1–N7. <http://dx.doi.org/10.1111/j.1750-3841.2009.01386.x>.
- Azeredo, H.M.C., Mattoso, L.H.C., Wood, D., Williams, T.G., Avena-Bustillos, R.J., McHugh, T.H., 2009. Nanocomposite Edible films from mango puree reinforced with cellulose nanofibers. *J. Food Sci.* 74, N31–N35. <http://dx.doi.org/10.1111/j.1750-3841.2009.01186.x>.
- Azizi Samir, M.A.S., Alloin, F., Dufresne, A., 2005. Review of recent research into cellulosic whiskers, their properties and their application in nanocomposite field. *Biomacromolecules* 6, 612–626. <http://dx.doi.org/10.1021/bm0493685>.
- Baccaro S., Carewska M., Casieri C., Cemmi A., Lepore A., 2013. Structure modifications and interaction with moisture in γ -irradiated pure cellulose by thermal analysis and infrared spectroscopy. *Polym Degrad Stab* 98:2005–2010. <http://dx.doi.org/10.1016/j.polymdegradstab.2013.07.011>.
- Bautista-Baños, S., Hernández-Lauzardo, A.N., Velázquez-del Valle, M.G., Hernández-López, M., Ait Barka, E., Bosquez-Molina, E., Wilson, C.L., 2006. Chitosan as a potential natural compound to control pre and postharvest diseases of horticultural commodities. *Crop Prot.* 25, 108–118. <http://dx.doi.org/10.1016/j.cropro.2005.03.010>.
- Borghain, R., Guha, A.K., Pratihari, S., Handique, J.G., 2015. Antioxidant activity of some phenolic aldehydes and their diimine derivatives: a DFT study. *Comput. Theor. Chem.* 1060, 17–23. <http://dx.doi.org/10.1016/j.comptc.2015.02.014>.
- Bouchard J., Méthot M., Jordan B., 2006. The effects of ionizing radiation on the cellulose of woodfree paper. *Cellulose* 13:601–610. <http://dx.doi.org/10.1007/s10570-005-9033-0>.
- Bountagkidou, O.G., Ordoudi, S.A., Tsimidou, M.Z., 2010. Structure–antioxidant activity relationship study of natural hydroxybenzaldehydes using in vitro assays. *Food Res. Int.* 43, 2014–2019. <http://dx.doi.org/10.1016/j.foodres.2010.05.021>.
- Cho, Y.-S., Kim, S.-K., Ahn, C.-B., Je, J.-Y., 2011. Preparation, characterization, and antioxidant properties of gallic acid-grafted-chitosans. *Carbohydr. Polym.* 83, 1617–1622. <http://dx.doi.org/10.1016/j.carbpol.2010.10.019>.
- Curcio, M., Puoci, F., Iemma, F., Parisi, O.I., Cirillo, G., Spizzirri, U.G., Picci, N., 2009. Covalent insertion of antioxidant molecules on chitosan by a free radical grafting procedure. *J. Agric. Food Chem.* 57, 5933–5938. <http://dx.doi.org/10.1021/jf900778u>.

- Di Majo, D., LaNeve, L., La Guardia, M., Casuccio, A., Giammanco, M., 2011. The influence of two different pH levels on the antioxidant properties of flavonols, flavan-3-ols, phenolic acids and aldehyde compounds analysed in synthetic wine and in a phosphate buffer. *J. Food Compos. Anal.* 24, 265–269. <http://dx.doi.org/10.1016/j.jfca.2010.09.013>.
- Dong, X.M., Revol, J-F, Gray, D.G., (1998). Effect of microcrystallite preparation conditions on the formation of colloid crystals of cellulose. *Cellulose* 5, 19–32. <http://dx.doi.org/10.1023/A:1009260511939>
- Dufresne, A., 2012. *Nanocellulose: from nature to high performance tailored materials.* de Gruyter W, Berlin.
- Dwibedy, P., Dey, G.R., Naik, D.B., Kishore, K., Moorthy, P.N., 1999. Pulse radiolysis studies on redox reactions of gallic acid: one electron oxidation of gallic acid by gallic acid–OH adduct. *Phys. Chem. Chem. Phys.* 1, 1915–1918. <http://dx.doi.org/10.1039/A809147A>.
- Erdohan, Z.Ö., Turhan, K.N., 2005. Barrier and mechanical properties of methylcellulose–whey protein films. *Packag. Technol. Sci.* 18, 295–302. <http://dx.doi.org/10.1002/pts.700>.
- Gutiérrez-Larraínzar, M., Rúa, J., Caro, I., de Castro, C., de Arriaga, D., García-Armesto, M.R., del Valle, P., 2012. Evaluation of antimicrobial and antioxidant activities of natural phenolic compounds against foodborne pathogens and spoilage bacteria. *Food Control* 26, 555–563. <http://dx.doi.org/10.1016/j.foodcont.2012.02.025>.
- Han, J., Britten, M., St-Gelais, D., Champagne, C.P., Fustier, P., Salmieri, S., Lacroix, M., 2011. Effect of polyphenolic ingredients on physical characteristics of cheese. *Food Res. Int.* 44, 494–497. <http://dx.doi.org/10.1016/j.foodres.2010.10.026>.
- Henniges, U., Okubayashi, S., Rosenau, T., Potthast, A., 2012. Irradiation of cellulosic pulps: understanding its impact on cellulose oxidation. *Biomacromolecules* 13, 4171–4178. <http://dx.doi.org/10.1021/bm3014457>.
- Huq, T., Salmieri, S., Khan, A., Khan, R.A., Le Tien, C., Riedl, B., Frascini, C., Bouchard, J., Uribe-Calderon, J., Kamal, M.R., Lacroix, M., 2012. Nanocrystalline cellulose (NCC) reinforced alginate based biodegradable nanocomposite film. *Carbohydr. Polym.* 90, 1757–1763. <http://dx.doi.org/10.1016/j.carbpol.2012.07.065>.
- Ji, H.-F., Zhang, H.-Y., Shen, L., 2006. Proton dissociation is important to understanding structure-activity relationships of gallic acid antioxidants. *Bioorg. Med. Chem. Lett.* 16, 4095–4098. <http://dx.doi.org/10.1016/j.bmcl.2006.04.096>.
- Kanai, S., Okano, H., 1998. Mechanism of the protective effects of sumac gall extract and gallic acid on the progression of CCl₄-induced acute liver injury in rats. *Am. J. Chin. Med.* 26, 333–341. http://dx.doi.org/10.1142/S0192415_98000373.
- Katz, S., Beatson, P.R.M.S.A., 1984. The determination of strong and weak acidic groups in sulfite pulps. *Sven. Papperstidning* 87, 48–53.
- Khan, A., Huq, T., Khan, R.A., Riedl, B., Lacroix, M., 2014. Nanocellulose-based composites and bioactive agents for food packaging. *Crit. Rev. Food Sci. Nutr.* 54, 163–174. <http://dx.doi.org/10.1080/10408398.2011.578765>.

- Khan, A., Khan, R.A., Salmieri, S., Le Tien, C., Riedl, B., Bouchard, J., Chauve, G., Tan, V., Kamal, M.R., Lacroix, M., 2012. Mechanical and barrier properties of nanocrystalline cellulose reinforced chitosan based nanocomposite films. *Carbohydr. Polym.* 90, 1601–1608. <http://dx.doi.org/10.1016/j.carbpol.2012.07.037>.
- Kitagawa, M., Tokiwa, Y., 2006. Polymerization of vinyl sugar ester using ascorbic acid and hydrogen peroxide as a redox reagent. *Carbohydr. Polym.* 64, 218–223. <http://dx.doi.org/10.1016/j.carbpol.2005.11.029>.
- Klemm, D., Schumann, D., Kramer, F., Heßler, N., Koth, D., Sultanova, B., 2009. Nanocellulose materials – different cellulose, different functionality. *Macromol. Symp.* 280, 60–71. <https://dx.doi.org/10.1002/masy.200950608>.
- Landgraf, M.D., da Silva, S.C., de O. Rezende, M.O., 1998. Mechanism of metribuzin herbicide sorption by humic acid samples from peat and vermicompost. *Anal. Chim. Acta* 368, 155–164. [http://dx.doi.org/10.1016/S0003-2670\(98\)00049-X](http://dx.doi.org/10.1016/S0003-2670(98)00049-X).
- Lapointe, R.E., 2000. *Précis de Chimie de la Cellulose*, second ed. Cégep de Trois-Rivières, Trois-Rivières.
- Larpent, C., Tadros, T.F., 1991. Preparation of microlatex dispersions using oil-in-water microemulsions. *Colloid Polym. Sci.* 269, 1171–1183. <http://dx.doi.org/10.1007/BF00654125>.
- Li, Q., Wang, A., Long, K., He, Z., Cha, R., 2019. Modified Fenton oxidation of cellulose fibers for cellulose nanofibrils preparation. *ACS Sustain. Chem. Eng.* 7, 1129–1136. <http://dx.doi.org/10.1021/acssuschemeng.8b04786>.
- Liu, J., Lu, J., Kan, J., Tang, Y., Jin, C., 2013. Preparation, characterization and antioxidant activity of phenolic acids grafted carboxymethyl chitosan. *Int. J. Biol. Macromol.* 62, 85–93. <http://dx.doi.org/10.1016/j.ijbiomac.2013.08.040>.
- Liu, J., Wen, X., Lu, J., Kan, J., Jin, C., 2014. Free radical mediated grafting of chitosan with caffeic and ferulic acids: structures and antioxidant activity. *Int. J. Biol. Macromol.* 65, 97–106. <http://dx.doi.org/10.1016/j.ijbiomac.2014.01.021>.
- Ludueña, L.N., Alvarez, V.A., Vazquez, A., 2007. Processing and microstructure of PCL/clay nanocomposites. *Mater. Sci. Eng. A* 460–461, 121–129. <http://dx.doi.org/10.1016/j.msea.2007.01.104>.
- Lu, Z., Nie, G., Belton, P.S., Tang, H., Zhao, B., 2006. Structure-activity relationship analysis of antioxidant ability and neuroprotective effect of gallic acid derivatives. *Neurochem. Int.* 48, 263–274. <http://dx.doi.org/10.1016/j.neuint.2005.10.010>.
- Oomens, J., Steill, J.D., 2008. Free carboxylate stretching modes. *J. Phys. Chem. A* 112, 3281–3283. <http://dx.doi.org/10.1021/jp801806e>.
- Pasanphan, W., Chirachanchai, S., 2008. Conjugation of gallic acid onto chitosan: an approach for green and water-based antioxidant. *Carbohydr. Polym.* 72, 169–177. <http://dx.doi.org/10.1016/j.carbpol.2007.08.002>.
- Ratnam, C.T., Abdullah, Z., Ismail, H., 2006. Electron beam irradiation of EVA/ENR blend. *Polym.-Plast. Technol. Eng.* 45, 555–559. <http://dx.doi.org/10.1080/03602550600554133>.

- Ray, S., Quek, S.Y., Easteal, A., Chen, X.D., 2006. The potential use of polymer-clay nanocomposites in food packaging. *Int. J. Food Eng.* 2. <http://dx.doi.org/10.2202/1556-3758.1149>.
- Rhim, J.-W., Park, H.-M., Ha, C.-S., 2013. Bio-nanocomposites for food packaging applications. *Prog. Polym. Sci.* 38, 1629–1652. <http://dx.doi.org/10.1016/j.progpolymsci.2013.05.008>.
- Seifried, H.E., Anderson, D.E., Fisher, E.I., Milner, J.A., 2007. A review of the interaction among dietary antioxidants and reactive oxygen species. *J. Nutr. Biochem.* 18, 567–579. <http://dx.doi.org/10.1016/j.jnutbio.2006.10.007>.
- Sharma, P.R., Varma, A.J., 2014. Thermal stability of cellulose and their nanoparticles: Effect of incremental increases in carboxyl and aldehyde groups. *Carbohydr. Polym.* 114, 339–343. <http://dx.doi.org/10.1016/j.carbpol.2014.08.032>.
- Shih, C.-M., Shieh, Y.-T., Twu, Y.-K., 2009. Preparation and characterization of cellulose/chitosan blend films. *Carbohydr. Polym.* 78, 169–174. <http://dx.doi.org/10.1016/j.carbpol.2009.04.031>.
- Singh, A., Silverman, J., 1992. *Radiation processing of polymers*, Carl Hanser Verlag GmbH & Co, München.
- Spizzirri, U.G., Iemma, F., Puoci, F., Cirillo, G., Curcio, M., Parisi, O.I., Picci, N., 2009. Synthesis of antioxidant polymers by grafting of gallic acid and catechin on gelatin. *Biomacromolecules* 10, 1923–1930. <http://dx.doi.org/10.1021/bm900325t>.
- Spizzirri, U.G., Parisi, O.I., Iemma, F., Cirillo, G., Puoci, F., Curcio, M., Picci, N., 2010. Antioxidant–polysaccharide conjugates for food application by eco-friendly grafting procedure. *Carbohydr. Polym.* 79, 333–340. <http://dx.doi.org/10.1016/j.carbpol.2009.08.010>.
- Sun, D., Zhou, L., Wu, Q., Yang, S., 2007. Preliminary research on structure and properties of nano-cellulose. *J. Wuhan Univ. Technol.-Mater Sci. Ed.* 22, 677–680. <http://dx.doi.org/10.1007/s11595-006-4677-7>.
- Suyatma, N.E., Tighzert, L., Copinet, A., Coma, V., 2005. Effects of hydrophilic plasticizers on mechanical, thermal, and surface properties of chitosan films. *J. Agric. Food Chem.* 53, 3950–3957. <http://dx.doi.org/10.1021/jf048790>.
- Ureña-Benavides, E.E., Brown, P.J., Kitchens, C.L., 2010. Effect of jet stretch and particle load on cellulose nanocrystal alginate nanocomposite fibers. *Langmuir* 26, 14263–14270. <http://dx.doi.org/10.1021/la102216v>.
- Woods, R.J., Pikaev, A.K., 1994. *Applied Radiation Chemistry: Radiation Processing*. John Wiley & Sons, New York.
- Ye, D., Farriol, X., 2006. Factors influencing molecular weights of methylcelluloses prepared from annual plants and juvenile eucalyptus. *J. Appl. Polym. Sci.* 100, 1785–1793. <http://dx.doi.org/10.1002/app.23071>.
- Yilmaz, Y., Toledo, R.T., 2004. Major flavonoids in grapeseeds and skins: antioxidant capacity of catechin, epicatechin, and gallic acid. *J. Agric. Food Chem.* 52, 255–260. <http://dx.doi.org/10.1021/jf030117h>.

- Zaharescu, T., Chipară, M., Postolache, M., 1999. Radiation processing of polyolefin blends II. Mechanical properties of EPDM-PP blends. *Polym. Degrad. Stab.* 66, 5–8. [http://dx.doi.org/10.1016/S0141-3910\(99\)00045-2](http://dx.doi.org/10.1016/S0141-3910(99)00045-2).
- Zivanovic, S., Chi, S., Draughon, A.F., 2005. Antimicrobial activity of chitosan films enriched with essential oils. *J. Food Sci.* 70, M45–M51. <http://dx.doi.org/10.1111/j.1365-2621.2005.tb09045.x>.

5. PUBLICATION 2: GAMMA-IRRADIATION OF CELLULOSE NANOCRYSTALS (CNCs): INVESTIGATION OF PHYSICOCHEMICAL AND ANTIOXIDANT PROPERTIES

Published in Cellulose (2017), 24: 2111-2124

**Paula Criado^a, Carole Fraschini^b, Majid Jamshidian^a, Stephane Salmieri^a, Agnès
Safrany^c, Monique Lacroix^{a*}**

^aResearch Laboratories in Sciences Applied to Food, Canadian Irradiation Center,
INRS–Institute Armand-Frappier, Institute of Nutraceutical and Functional Foods, 531
boulevard des Prairies, Laval, Quebec, H7V 1B7, Canada.

^bFPInnovations, 570 boulevard Saint Jean, Pointe-Claire, Quebec, H9R 3J9, Canada.

^cInternational Atomic Energy Agency (IAEA), Division of Nuclear Sciences and
Applications, Department of Physical and Chemical Sciences, Section of Industrial
Applications and Chemistry, Vienna International Centre, POB: 100, A-1400 Vienna,
Austria A2371.

*Corresponding author: Professor Monique Lacroix, Tel: +1 (450) 687-5010 #4489,
Fax: +1 (450) 686-5501. E-mail: monique.lacroix@iaf.inrs.ca

The number of figures and tables were adjusted in this article in order to follow the sequence of the thesis document. The style of references was presented according to the guidelines of the journal.

CONTRIBUTION OF AUTHORS

This research work was performed under supervision of Dr. Carole Fraschini, Pr. Monique Lacroix and Dr. Majid Jamshidian. All experiments were performed in the laboratory by Paula Criado and discussions of results and protocols were assisted by Stéphane Salmieri. The article was written by Paula Criado, while corrections and revisions were carried out by Stéphane Salmieri, Dr. Majid Jamshidian, Dr. Carole Fraschini, and Pr. Monique Lacroix. This research work was done in collaboration with IAEA under the supervision of Dr. Agnès Safrany.

RÉSUMÉ

L'irradiation gamma est un procédé communément utilisé, principalement pour la stérilisation contre la croissance bactérienne. Cependant, lorsque le procédé est appliqué sur un matériau, des changements physiques et chimiques peuvent en altérer l'intégrité et le comportement. Le but de cette étude était d'observer l'effet de l'irradiation gamma sur la chimie de surface des nanocristaux de cellulose (CNCs). La concentration en groupements carbonyles (fonctions acides carboxyliques et aldéhydes) a été mesurée afin d'étudier l'influence de la dose d'irradiation. La stabilité thermique, la mouillabilité et les propriétés antioxydantes ont également été mesurées. Un titrage conductimétrique a démontré que la concentration en acides carboxyliques (COOH) est passée de 43 mmol COOH/kg pour les CNCs natifs (0 kGy) à 631 mmol COOH/kg après application d'une dose d'irradiation de 80 kGy. Ces changements ont été confirmés par analyse FTIR et spectroscopie de fluorescence. À une dose d'irradiation élevée, une diminution significative du degré de polymérisation des chaînes de cellulose d'environ 30% a été observée, tandis que la concentration en groupements aldéhydes a été augmentée jusqu'à 379 mmol CHO/kg du à la rupture des liaisons glycosidiques. Ces changements physicochimiques ont conduit à une amélioration des propriétés antioxydantes des CNCs.

ABSTRACT

Gamma irradiation is a common process mostly used for sterilization against bacteria growth. However, when the process is applied to a material, physical and chemical changes may alter its integrity and behaviour. The aim of this study was to observe the effect of γ -irradiation on the surface chemistry of CNCs. The carbonyl content (both carboxylic acid and aldehyde functionalities) was followed to investigate the influence of the irradiation dose. Thermal stability, wettability and antioxidant properties were also measured. Conductometric titration showed that the carboxylic acid groups content (COOH) was increased from 43 mmol COOH/kg CNCs for native CNCs to 631 mmol COOH/kg CNCs when a dose of 80 kGy was applied. These changes were confirmed by FTIR and fluorescence spectroscopy. At high irradiation doses, a significant decrease of approximately 30 % was observed in the cellulose degree of polymerization while the aldehyde groups content was increased to 379 mmol CHO/kg CNCs due to the cleavage of glycosidic linkages. These physicochemical changes led to enhanced antioxidant properties of CNCs.

5.1 Introduction

γ -irradiation, also called ionizing radiation, is a source of energy that leads to a collision between the radiation beam and the atoms that compose the material to be irradiated. In living organisms, this transfer of energy mostly results in a disruption of microorganism cells, and this fact is one of the reasons why γ -irradiation has been considered as a non-thermal process for sterilization (Sintzel *et al.* 1997). Nevertheless, when a polymeric material is subjected to irradiation, degradation can occur, resulting in a change of its chemical, physical, and mechanical properties.

In order to understand the interaction of γ -irradiation on materials some authors stated that γ -rays are able to produce free radicals issued from water hydrolysis (O'Neill 1987; LaVerne 2000; Huq *et al.* 2012). In fact, radical active species such as hydroxyl radicals have the capacity to create macroradicals on polymer units, resulting on either chain scission (Huq *et al.*, 2012) or cross-linking. Studies indicate that at low irradiation doses, cross-linking occurs in polymers when free radicals are formed, but when the doses are increased, γ -irradiation has an effect on the degradation of the material (Takács *et al.* 1999; Henniges *et al.* 2012).

Despite the negative effect observed in polymer structure at high doses, industry has shown a great interest in producing oligomers by γ -irradiation. One advantage of this procedure relies on the production of low molecular weight molecules that bring higher biodegradability capacity with applications such as growth-promoting in plants (Hien *et al.* 2000; Xuan Tham *et al.*, 2001). Irradiated polymers also exhibit other properties such as antioxidant, giving them the ability to scavenge radicals and to catalyze a radical chain reactions (Huang *et al.*, 2005), reactions that are responsible for rancidity and consequent food spoilage. For example, studies reported that irradiated carrageenan or chitosan show antioxidant properties (Feng *et al.* 2008; Abad *et al.* 2013) with increasing irradiation doses. Many authors (Xie *et al.* 2001; Lin and Chou 2004; Xing *et al.* 2005) have established the interest of using chitosan due to its biological activities, including antioxidant properties. Scavenging properties of native chitosan are due to the active hydrogen offered by the free amino and hydroxyl groups of the polysaccharide. However, Feng *et al.* (2008) have demonstrated that those scavenging properties can be improved from 16.6 to 63.8 % by irradiating 1 % chitosan solution at doses ranging from 0 to 20 kGy.

This study focused on cellulose nanocrystals (CNCs) which are a nanomaterial constituted of linear homopolymer chains of β -(1 \rightarrow 4) linked D-glucose units. CNCs are extracted from naturally occurring cellulose sources such as wood pulp, cotton, bacteria, and tunicates (sea animals). The wide variety of sources leads to CNCs of different dimensions for instance, with lengths from 100 to 1000 nm and cross sectional dimensions from 3 to 15 nm for softwood plants and tunicate, respectively (Habibi *et al.* 2010). Within the wood nanofibrils, native cellulose consists of alternating amorphous and crystalline regions. CNCs are obtained by well-defined strong acid hydrolysis conditions, which preferentially dissolve the amorphous cellulosic parts present along the cellulosic fibers, thus, releasing the unaffected crystalline parts in the aqueous medium. The use of sulfuric acid imparts negatively charged acidic sulfate ester groups located at the surface of the crystals (sulfated CNCs).

The effects of γ -irradiation have been already studied on cellulosic materials (Takács *et al.*, 1999; Bouchard *et al.*, 2006; Khan *et al.*, 2006; Henniges *et al.*, 2012; Baccaro *et al.*, 2013). All the authors have stated that irradiation induces to a decrease of the degree of polymerization and increase of carbonyl content and other changes in the physical and chemical composition of cellulose, especially at high irradiation doses. Khan *et al.* (2006) mentioned that an increase in the irradiation dose led to a decrease in the molecular weight of lignocellulosic material when irradiated at high dose. Breakage of glycosidic bonds and formation of carbonyl groups can also occur (Bouchard *et al.* 2006; Baccaro *et al.* 2013). In addition, Baccaro *et al.* (2013) revealed an existing relationship between the dose absorbed by the cellulose bulk and the formation of carbonyl groups as well as the oxidative degradation of cellulose.

So far, no study has been reported on the effects of γ -irradiation on CNCs. In this work, the main objective was to evaluate the effect of increasing doses on the physicochemical structure of native and γ -irradiated CNCs in terms of formation of new functional groups, thermal stability, and hydrophilic character. Antioxidant properties of irradiated CNCs were also analyzed using the DPPH and total antioxidant capacity methods comparing CNCs with two reference compounds such as ascorbic acid (AA) and Trolox.

5.2 Materials

Aqueous CNC suspensions were prepared in the FPIInnovations' pilot plant from a dry commercial bleached softwood kraft pulp according to a procedure modified from the literature (Dong *et al.*, 1998). Milled dried pulp (2 kg o.d.) was added to 64 wt.% sulfuric acid (17.5 L) heated to 45°C with mixing at 200 rpm for 25 min. The reaction was quenched with deionized water (200 L) at room temperature, centrifuged and subjected to multiple passes through a hollow fibre membrane to remove acid and soluble carbohydrates and increase the solid content of the CNC suspension which was then homogenized and filtered (1 µm) to ensure a good dispersion. The acidic suspension was then neutralized using sodium hydroxide and spray-dried. This extraction confers to the surface of CNCs anionic half-sulfate ester groups which allow CNCs to have better stability within aqueous suspensions.

Sodium hydroxide solution (0.02 N), methanol, tetrahydrofuran (THF) and dimethyl sulfoxide (DMSO) were obtained from Anachemia (Montreal, QC, Canada). Dialysis membrane tubes having a molecular weight cut-off of 12-14 kDa were purchased from Spectrum Labs (Ottawa, ON, Canada). Dowex[®] Marathon C[™] cation-exchange resin, phenyl isocyanate (PIC), Purpald[®] reagent, 6-hydroxy-2,5,7,8-tetramethylchroman-2-carboxylic acid (Trolox), ascorbic acid, 2,2-diphenyl-1-picrylhydrazyl (DPPH), sulfuric acid, sodium phosphate and ammonium molybdate were obtained from Sigma Aldrich (Oakville, ON, Canada). All chemicals were used as received.

5.3 Methods

5.3.1 Preparation of CNCs Suspensions

A 125 mL solution of 0.5 % (w/w) CNCs in deionized water was magnetically stirred and sonicated (Fisher Scientific, Ottawa, ON, Canada). The solution was then flushed with nitrogen gas for 1 min to eliminate oxygen, followed by γ -irradiation treatment at different doses (0, 10, 20, 40, 80 kGy) with a dose rate of 16.536 kGy/h. Samples were irradiated at the Canadian Irradiation Center (CIC) using an underwater irradiator 15A equipped with a ⁶⁰Co source (Nordion Inc., Kanata, ON, Canada). Irradiated CNCs suspensions were then dialyzed using membrane tubes of MWCO of 12-14 kDa against running deionized water for three days.

5.3.2 Carboxylic Acid Content Determination by Conductometric Titration

Samples were protonated with a cation-exchange resin before conductometric titration. Aqueous suspensions of irradiated CNCs were placed over Dowex[®] Marathon C[™] cation-exchange resin (12 g resin/g CNCs) followed by a gentle stirring for at least 2 h at room temperature. The quantification of the total carboxylic acid content was determined using conductometric titration. Suspensions of protonated CNCs (0.15 g o.d.) were titrated against 0.01 M NaOH using a 809-Titrando automatic titrator (Metrohm, Mississauga, ON, Canada) in the presence of 1 mM NaCl.

Typical titration curves (**Fig. 13**) exhibit two discontinuities assigned to the presence of a strong acid (*i.e.* half-sulfate ester groups introduced during the CNCs production process) and a weak acid (*i.e.* carboxylic acid groups introduced during the γ -irradiation process). Therefore, the carboxyl content of the sample in mmol/kg CNC can usually be calculated using **Eq. 11**:

$$[\text{COOH}] = ((V_2 - V_1) \cdot C_{\text{NaOH}}) / m_{\text{CNC}} \quad (11)$$

Where V_i is the volume of NaOH (mL), C_{NaOH} is the exact NaOH concentration (mol/L) and m_{CNC} is the dry weight of CNC (kg).

However, it has been found that a high content in weak acid groups usually leads to an overestimation of the strong acid content. In light of this artifact, a more accurate value of the half-sulfate ester content, expressed in mmol S/kg CNCs, was obtained using inductively coupled plasma atomic emission spectroscopy (ICP-AES). The total content of carboxylic acid groups can now be calculated using **Eq. 14**:

$$[\text{COOH}] = ((V_2 \cdot C_{\text{NaOH}}) / m_{\text{CNC}}) - [\text{OSO}_3\text{H}]_{\text{ICP-AES}} \quad (14)$$

Where V_2 is the total volume of NaOH (mL), C_{NaOH} is the exact NaOH concentration (mol/L), m_{CNC} is the dry weight of CNC (kg) and $[\text{OSO}_3\text{H}]_{\text{ICP-AES}}$ is the total content of half-sulfate ester groups obtained by ICP-AES (mmol/kg CNCs).

5.3.3 Aldehyde Content Determination by Purpald[®] Reagent

Determination of the aldehyde content was performed with a colorimetric method based on the oxidation of the aldehyde-purpald adduct which turns purple in the presence of an oxidant (Quesenberry and Lee 1996). A volume of 200 μL of a Purpald[®] reagent solution 1 % (w/v) in NaOH 1M was mixed in a 96-well microplate with 20 μL of irradiated CNCs

suspensions at 0.28 % at pH 7. The microplate containing the samples was kept under shaking for 1h to complete the reaction. Measurement of absorbance was done immediately at 550 nm using a microplate reader (EL800UV, BioTek, Winooski, VT, USA). The standard calibration curve was prepared with formaldehyde as the aldehyde-containing reference.

5.3.4 Fourier Transform Infrared (FTIR) Spectroscopy

FTIR spectra of dried protonated native and irradiated CNCs were recorded by a Spectrum One spectrophotometer (Perkin-Elmer, Woodbridge, ON, Canada). Acidic samples were preferred to neutral samples to avoid the overlap of the carbonyl and adsorbed water bands ($\sim 1642\text{ cm}^{-1}$). Attenuated total reflectance (ATR) accessory equipped with a diamond crystal was used to analyze the samples. Spectra wavelength was chosen from region of 4000 to 650 cm^{-1} with 64 scans recorded at a 4 cm^{-1} resolution and all spectra were analyzed using the Spectrum software. After measurement, the attenuation of total reflectance (ATR) correction was applied and spectra were normalized at 1160 cm^{-1} .

5.3.5 Fluorescence Spectroscopy

The fluorescence emission of irradiated CNCs at concentration of 0.35% was recorded using a spectrofluorometer Infinite M10000 Pro (Tecan US Inc, Morrisville, NC, USA). A volume of 250 μL of each sample was introduced into a 96-well microplate and the samples were firstly excited from a wavelength range from 200 to 800 nm. Intensity of the emission spectra was recorded at 280 nm where irradiated CNCs showed a fluorescent behavior. Fluorescence intensity was expressed as arbitrary units (a.u.).

5.3.6 Cellulose Degree of Polymerization Determination

Cellulose Carbanilation Procedure

The used procedure is based on the conditions proposed to achieve a complete carbanilation reaction (three phenyl isocyanate groups per anhydroglucose unit) while minimizing cellulose depolymerization (Schroeder and Haigh 1979; Evans *et al.* 1989; Lapierre and Bouchard 1999). 25 mg of dried cellulosic sample were weighed into a vial

to which 10 mL of DMSO were added, followed by 1 mL of PIC. Samples were manually stirred for a few minutes and then kept at 70°C for 40h under intermittent agitation. The reaction was stopped by adding 2 mL of methanol to react with the excess PIC. Methanol was then evaporated out from the DMSO solution.

Gel Permeation Chromatography (GPC)

After appropriate dilution (0.05 wt.%) of the soluble cellulose tricarbaniolate (CTC) sample in THF, 50 µL of the diluted CTC was injected and eluted using THF (0.7 mL/min) through three columns connected in series and kept at 55°C (Shodex KF-806L, KF-805L and KF-804L (polystyrene exclusion limits from 4×10^6 to 2×10^7 Da)). Detection was done using a concentration-sensitive UV detector (Shimadzu, SPD-20A) working at a wavelength of 254 nm. The weight-average degree of polymerization (DP_w) was calculated from the DP distribution using polystyrene standards (Scientific Polymer Products, USA) calibration curve.

Mathematical deconvolutions of bimodal DP distribution curves were done using Peak Fit v4 software. The curves were fitted to two Gaussian distributions which were reprocessed as new independent chromatograms, and their respective DP distributions and averages were calculated (Lapierre and Bouchard 1999).

5.3.7 Chain Scission Number (CSN)

The chain scission number (CSN) represents the average number of glycosidic bonds broken per cellulose chain and is calculated using the degree of polymerization (DP_w), as follows (Bouchard *et al.* 2006):

$$CSN = \left[\frac{1}{DP} - \frac{1}{DP_0} \right] DP_0 \quad (15)$$

Where, DP_0 and DP are the initial degree of polymerization before and after γ -irradiation treatment, respectively.

5.3.8 Thermogravimetric Analysis (TGA)

Freeze-dried neutral sample pellets (about 15 mg) were analyzed with a Q5000IR thermogravimetric analyzer (TA Instruments, New Castle, USA). Pellets of dimensions of

6.6 mm in diameter and around 4 mm in height were set in platinum pans. Experiments were carried out under an air flow with a constant heating rate of 10°C/min and 25 mL/min. TG curves were recorded between 50°C and 600°C and data processing was done using the Universal Analysis™ software.

5.3.9 Contact Angle

Pure CNC films were prepared by casting a dispersed suspension of irradiated CNCs at pH 7 (550 mg o.d.) on a Petri dish at room temperature. The films were then placed in an oven at 100°C until a stable weight was reached. Finally, films were conditioned in a controlled humidity room (50% RH and 23°C) before testing. A water droplet of approximately 0.25 µL was deposited at the surface of the film and analyzed by the T100 Theta Lite Optical Contact Angle Meter (Biolin Scientific, Inc. Linthium Heights, MD, USA) with a water droplet. A number of 10 measurements per film were averaged to approximate the contact angle value.

5.3.10 Transmission Electron Microscopy (TEM)

After freeze-drying, CNCs neutralized with sodium hydroxide were re-suspended in deionized water (~0.005 % wt.). A drop of the CNC suspension was deposited on a carbon coated copper grid and stained with uranyl acetate. Morphology and dispersion state of CNCs was then assessed using a transmission electron microscope (Phillips FEI Tecnai 12 BioTwin) equipped with an AMT XR80C CCD camera system at accelerating voltage of 120 kV.

5.3.11 Antiradical Properties

DPPH Scavenging Test

A solution of the stable radical DPPH was prepared at a concentration of 40 µM in pure methanol and kept in the dark. For standard calibration curves, ascorbic acid, and Trolox were used as reference antioxidants. To measure the radical scavenging properties, irradiated CNCs (0-80 kGy) suspensions were prepared at the same concentration and pH (0.28 % w/w and pH 7). Then, a volume of 250 µL of the sample was mixed with 1 mL of DPPH solution and let to react for 1 h. A 1 mL aliquot of the suspension was

sampled and absorbance was measured in a UV spectrometer at a wavelength of 517 nm.

Standard calibration curves were done with known concentrations of ascorbic acid and Trolox scavenging inhibition power (SP) was calculated using the following equation (**Eq. 16**)

$$SP (\%) = \frac{Abs_{control} - Abs_{sample}}{Abs_{control}} * 100 \quad (16)$$

Total Antioxidant Capacity (TAC)

Total Antioxidant Capacity or Global Antioxidant Activity assay is based on the reduction of phosphomolybdenum from Mo (VI) to Mo (V) by an antioxidant under acidic pH conditions. The subsequent complex of green-blue phosphate/Mo (V) formed is determined by spectrophotometric analysis at λ_{max} of 695 nm. Measurement was done using the procedure described by Dasgupta and De (2004). 100 μ L of irradiated CNCs and 1 mL of reagent solution of phosphomolybdate (0.6 M sulphuric acid, 28 mM sodium phosphate and 4 mM of ammonium molybdate) were mixed and kept in the dark to preserve the activity of the solution.

The sample and reagent solutions were mixed in tubes hermetically closed with Parafilm and then immersed in a water bath at 95°C for 90 min. Then the solutions were cooled down before the absorbance was read at 695 nm. Standard calibration curve was done with ascorbic acid solution.

5.4 Statistical Analysis

Radical scavenging properties differences were analyzed by using statistical analysis. Analysis of variance (ANOVA) and Tamhane's multiple range tests were employed for the antioxidant results at each irradiation dose. PASW statistics base 16 software (SPSS Inc. Chicago, IL, USA) was used for data processing. Differences between means were considered to be significant at $p \leq 0.05$.

5.5 Results

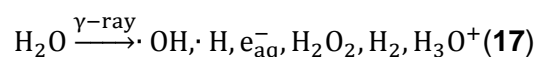
5.5.1 Determination of Carboxyl Groups Content by Conductometric Titration

The content of carboxylic acid after γ -irradiation of CNCs is presented in **Table 6**. A direct relationship was found between the content of carboxylic acid groups and the irradiation dose applied. The surface of native CNCs exhibits a carboxylic acid group (-COOH) content of approximately 43 mmol per kg of CNCs, while the concentration is raised up to 631 mmol per kg of CNCs when irradiation dose is increased to 80 kGy according to **Eq. 14**.

Table 6 Physicochemical characteristics of native and irradiated CNCs suspensions

kGy	0	10	20	40	80
Conductometric titration					
<i>Total carboxylic content in mmol COOH/kg CNC using Eq. 14</i>	43	156	229	312	631
Purpald[®] reaction					
<i>Total Aldehyde determination in mmol CHO/kg CNC</i>	20 ± 4	109 ± 2	173 ± 10	262 ± 21	379 ± 19
Elemental analysis (ICP-AES)					
<i>Total S content in mmol S/kg CNC</i>	254	225	201	202	155

These results were in accordance with Baccaro *et al.* (2013) who found a proportional relationship between the formation of carbonyl groups and the dose of γ -irradiation applied for paper samples. It has been reported in numerous studies (Henniges *et al.* 2012; Ponomarev and Ershov 2014), that ionizing radiation causes water radiolysis in aqueous dispersed solutions (**Eq.17**). This reaction induces the formation of cellulose macroradicals which leads to glycosidic bond cleavage and further formation of new functional groups.



Some of the carbonyl groups formed in cellulose, might include either aldehyde or carboxylic groups. Henniges *et al.* (2012) reported the effect of γ -irradiation on

carbonylgroup (CO) formation on bleached beech sulfite (BSP) cellulose pulp. An augmentation in carbonyl groups of BSP from 25 to 35 mmol CO per kg pulp was observed at applied irradiation doses of 1-10 kGy, respectively, associated with a decrease of 25% of the average molar mass (M_w) with regard to the starting material. The authors also reported that the formation of carbonyl groups was expected on the low molar mass chains of cellulose where new reducing end groups can be formed.

5.5.2 Determination of Aldehyde Content by the Purpald® Method

Table 6 shows the effect of irradiation on the aldehyde content of irradiated CNCs. The formation of aldehyde groups seems to follow the same trend observed for carboxylic acid groups.

It has been confirmed that increasing γ -irradiation doses leads to a cleavage of glycosidic bonds in dispersed cellulose solutions (**Fig. 21**) (Henniges *et al.* 2012; Ponomarev and Ershov 2014). In fact, water radiolysis leads to the formation of reactive species ($\cdot\text{OH}$; $\cdot\text{H}$) and intermediate products as previously shown in **Eq. 17**. Such radicals react rapidly on anhydroglucose units leading to cleavage of C-H bonds and formation of cellulose radicals (von Sonntag 1980; Sultanov and Turaev 1996; Ponomarev and Ershov 2014) (**Fig. 21**). Subsequent reaction such as propagation of radicals can be one of the main causes of cleavage of glycosidic bonds and polymer breakdown.

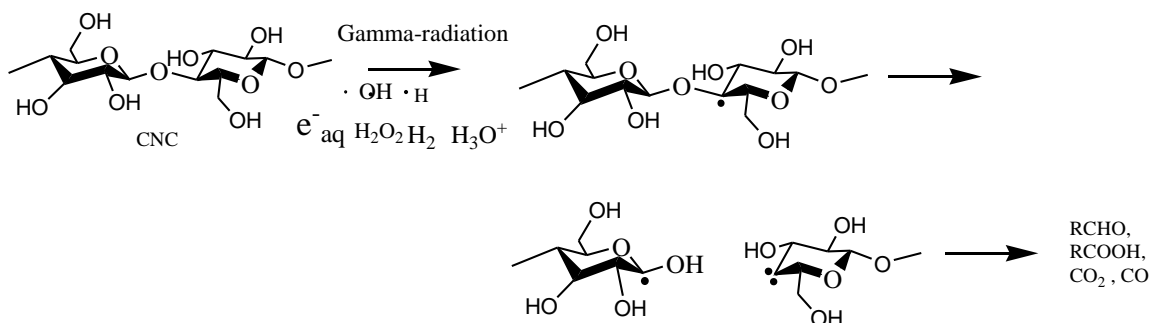


Fig. 21 Proposed reaction pathway of gamma-rays on C₁ and C₄ of CNCs adapted from (Sokhey and Hanna 1993; Sultanov and Turaev 1996; Sánchez Orozco *et al.* 2012; Ponomarev and Ershov 2014).

According to literature (Ershov and Klimentov 1984; Khan *et al.* 2006; Sánchez Orozco *et al.* 2012; Henniges *et al.* 2012; Ponomarev and Ershov 2014), ultimate radiolysis

compounds of cellulose released by γ -irradiation might include aldehydes, carboxylic acids, carbon dioxide, and carbon monoxide. Other studies performed on carbohydrates also confirmed the aldehyde formation which corroborates our results (Feng *et al.* 2008; Abad *et al.* 2009, 2013). For instance, Abad *et al.* (2009) found that a 1% aqueous solution of κ -carrageenan showed an increase of 14% of its reducing units when an irradiation dose of 50 kGy is applied.

5.5.3 Determination of Total Sulphur Content by ICP-AES

Table 6 shows that gamma irradiation has a negative impact on the half-sulfate ester content of CNCs. Native CNCs show an initial total S concentration of 254 mmol/kg CNC which is in accordance with the values found in the literature. Depending on the experimental conditions of acid hydrolysis, the initial concentration of half-sulfate ester content in bleached kraft pulp can vary from 210 to 270 mmol/kg CNC (Hamad and Hu 2010). **Table 6** shows that irradiation treatment leads to a decrease of half-sulfate ester content to 155 mmol/kg CNC when the irradiation dose is increased to 80 kGy. Other studies on irradiation of polymers reported a similar desulfation phenomenon. For instance, Relleve and Abad (2015), Relleve *et al.* (2005) and Abad *et al.* (2009) demonstrated that radiation induced to desulfation of carrageenan with the proposed following reaction:



5.5.4 Fourier Transform Infrared (FTIR) Spectroscopy of Irradiated CNCs

FTIR spectra of structural changes of irradiated CNCs are presented in **Fig. 22**. The intensity of 1733 cm^{-1} peak corresponding to C=O stretching mode (Takács *et al.*, 1999; Łojewska *et al.*, 2005, 2006), increased with increasing irradiation dose which confirms the presence of carboxylic acid and aldehydes groups.

Alongside with carbonyl group formation, changes in the adsorbed water peak at 1642 cm^{-1} is also observed (Baccaro, 2013; Maréchal and Chanzy, 2000; Hatakeyama *et al.*, 2000; Hofstetter *et al.*, 2006). **Fig. 22** exhibits an increase in the amount of absorbed water when doses of 40 to 80 kGy were applied. This phenomenon was correlated with the formation of new hydrophilic groups (Baccaro, 2013) such as carboxylic acid groups. Henniges *et al.* (2012) and Baccaro *et al.* (2013) observed that at low irradiation doses,

a crosslinking reaction occurs between cellulose chains, reducing their water retention capacity. Baccaro *et al.* (2013) also mentioned that irradiation at high dose (>128 kGy) led to an increase in the amount of absorbed water caused by a progressive degradation of cellulose chains. The glycosidic bond cleavage led to the formation of new hydrophilic groups, thus facilitating the adsorption of water molecules on cellulose chains (Kovalev and Bugaenko, 2003).

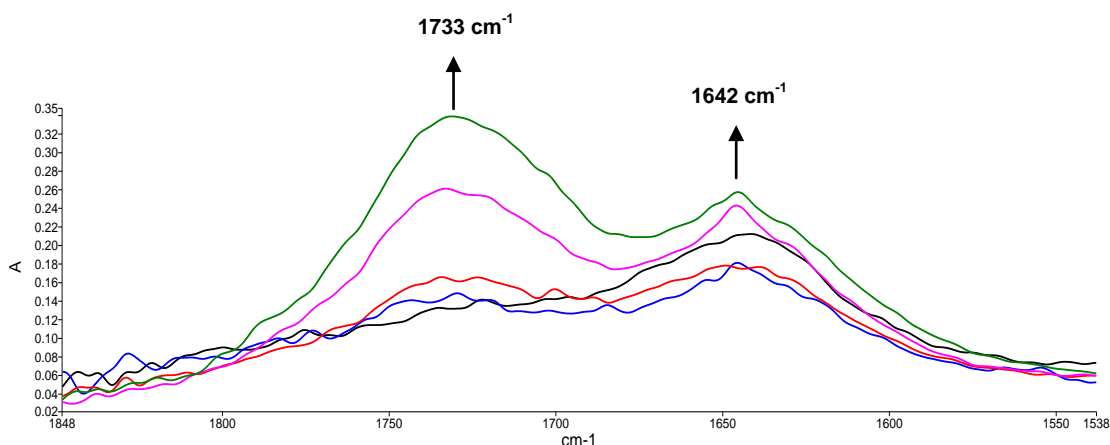


Fig. 22 FTIR spectra of acid freeze-dried CNCs irradiated at 0 kGy (Black), 10 kGy (Blue), 20 kGy (Red), 40 kGy (Pink), 80 kGy (Green)

5.5.5 Fluorescence Spectroscopy of Irradiated CNCs

Fig. 23 shows a fluorescent emission peak for CNCs at 307 nm on excitation at wavelength 208 nm. It was observed that increasing irradiation decreases the fluorescence intensity of irradiated CNCs. Thus, native (0 kGy) and sample irradiated at a dose of 80 kGy exhibit a decreasing behavior of fluorescence light intensity from 7×10^4 a.u. to 3×10^3 a.u. respectively. Khan *et al.* (2006) found a significant reduction (i.e., 56%) of the peak intensity when a sample of lignocellulose was irradiated at 50 kGy. In addition, Castellán *et al.* (2007) observed a decrease of the fluorescence intensity either in solid and dissolved acetylated microcrystalline cellulose. In order to understand the effect of irradiation on the fluorescence intensity, many authors agree that the reduction of fluorescence indicates the presence of carbonyl and carboxyl groups (Takács *et al.*, 1999, 2000; Khan *et al.*, 2006) which is in a good agreement with our findings.

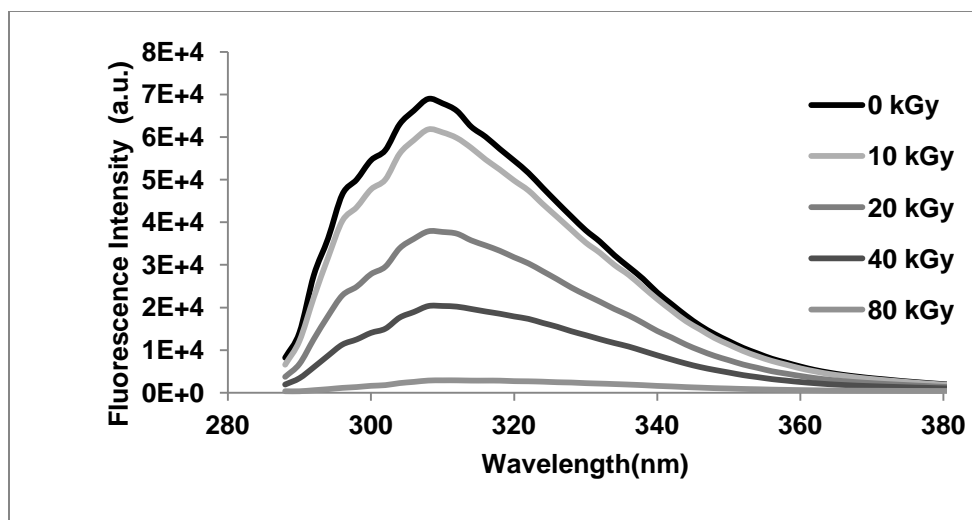


Fig. 23 Fluorescence spectroscopy of irradiated CNCs

5.5.6 Degree of Polymerization of Cellulose Chains

The effect of irradiation dose on degree of polymerization of cellulose chains is illustrated in **Fig. 24**. As expected, high energy levels led to a decrease of the degree of polymerization (DP_w), from 137 for native CNCs, down to 109 and 95 for CNCs irradiated at doses of 40 and 80 kGy, respectively.

Henniges *et al.* (2012) reported that an irradiation dose of 10 kGy caused a relative decrease of the molar mass (M_w) between 25 to 63% for plant pulps. Similar results were also reported by Bouchard *et al.* (2006) who demonstrated a decrease of DP from 3162 to 200 in cotton chromatographic paper when electron beam was applied from 0 to 240 kGy at 10 MeV. These results confirm the degradation action of γ -irradiation on CNCs via a chain scission mechanism.

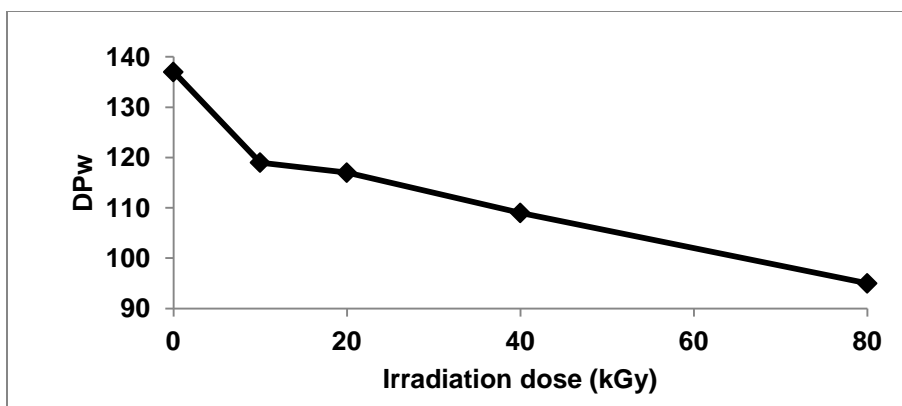


Fig. 24 Molar mass distribution of CNCs irradiated at different doses

5.5.7 Effect of Irradiation on the Chain Scission Number (CSN)

Fig. 25 shows the linear relationship between the irradiation dose and the chain scission number. These results strongly suggest that γ -irradiation treatment of CNCs samples led to a cleavage of the glycosidic bonds of the cellulose chains, thus exposing CNC reducing end units, which is in good agreement with the observed increased concentration of aldehydes. Similar observations were found by Bouchard *et al.* (2006) after electron beam irradiation of paper sheets (20-240 kGy). γ -rays are so energetic that they can ionize atoms throughout the irradiated material, resulting sometimes in a disruption of molecular bonds.

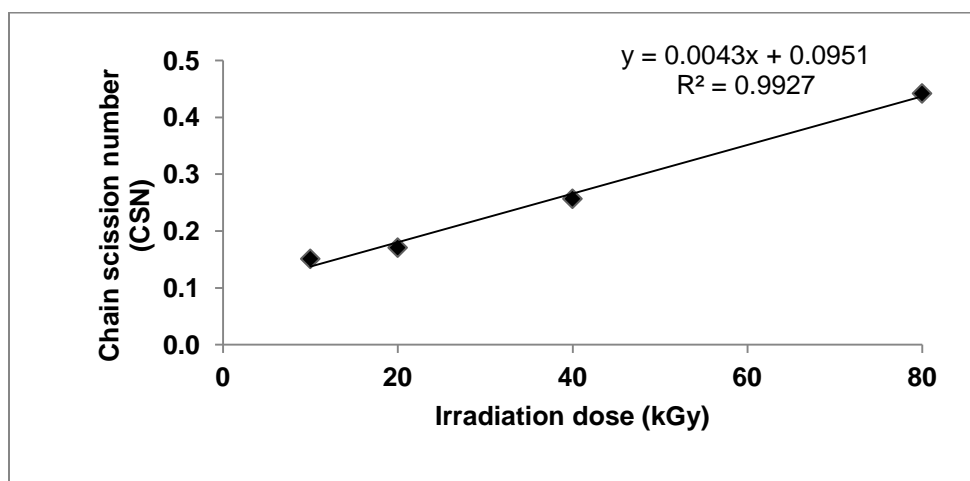


Fig. 25 Chain scission number (CSN) as a function of γ -irradiation dose

5.5.8 Thermogravimetric Analysis (TGA)

The introduction of new functional groups can sometimes be detrimental to the thermal stability of the material. For example, the presence of carboxyl groups can lead to decarbonation (Fukuzumi *et al.* 2010). Even a low level of protonated sulfate ester groups can catalyze the cellulose depolymerization further followed by dehydration to volatile levoglucosan (Roman and Winter 2004). **Fig. 26** shows the weight loss of irradiated CNCs as a function of the temperature.

Four distinctive regions can be observed on the thermal profiles of irradiated cellulose: 1) an initial region corresponding to water loss (100 °C), 2) the region of de-polymerization (around 250 °C), 3) the region of cellulose thermal decomposition (350 °C), and 4) the region of char residual ($\geq 400^{\circ}\text{C}$). The weight loss starting below 100°C corresponds to the evaporation of adsorbed (bulk) water, as already reported by Baccaro *et al.* (2013). It is clearly seen that an increase in the irradiation dose caused a gradual decrease in the thermal stability of the irradiated samples from 265°C down to 180°C. The mass loss shift towards lower temperatures is typical of oxidized cellulose (Varma and Chavan 1995). For example, the mass loss at 250°C is found to be 6.2, 8.4, 11.7, and 19.5% for irradiation doses of 10, 20, 40, and 80 kGy, respectively. Distinct thermal patterns were also observed by other authors (Baccaro *et al.* 2013; Moise *et al.* 2013), for samples irradiated at low irradiation doses ($\leq 30\text{kGy}$) compared to native polymer but high irradiation doses (500 kGy) led to a significant decrease of cellulose weight.

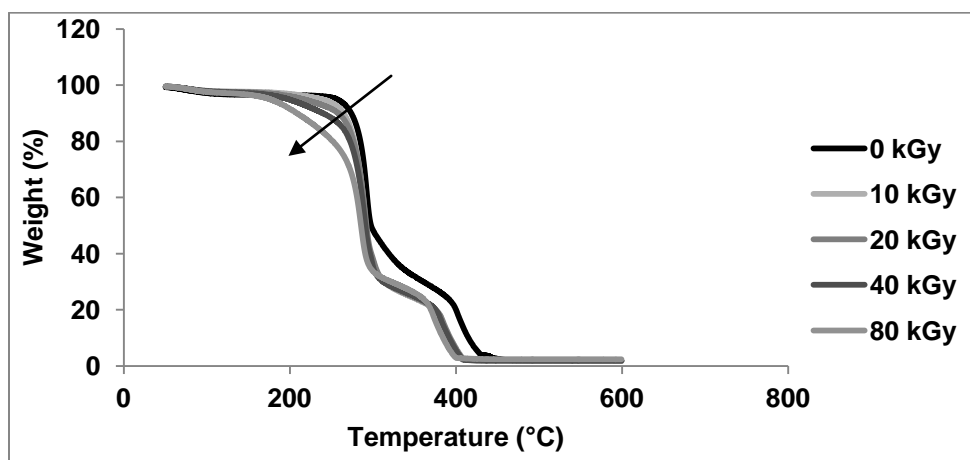


Fig. 26 Thermogravimetric curves of freeze-dried irradiated CNCs

Higher temperatures (> 300°C) led to the formation of intermediate products such as levoglucosan, which participates in two competitive reactions: decomposition to form volatile compounds and dehydration to form char (Soares *et al.* 1995). Char residuals remained at high temperatures (about 400 °C) (Moise *et al.* 2013).

5.5.9 Hydrophilic Character of Irradiated CNCs by Contact Angle

Contact angle measurements of CNC film could provide reliable understanding about the wettability of the CNC surface. **Fig. 27** shows the morphology of the water droplet at the surface of irradiated CNC films and the resulting contact angle measured. A significant decrease of the contact angle of CNC film surface was observed when increasing the dose of irradiation. Native CNC films have a contact angle of $61^\circ \pm 3$ which decreases to around $45^\circ \pm 7$ and $34^\circ \pm 6$ for CNC films treated at 40 and 80 kGy, respectively. The greater hydrophilic behavior of irradiated CNCs can be directly related to the carboxylic acid group content. It can be suggested that wettability was supported by the intermolecular interaction of the water droplet with the presence of a higher number of carboxylic acid groups.



Fig. 27 Contact angle measurements of films of irradiated CNCs

Surface chemistry of the material plays an important role in the determination of the contact angle (Bee *et al.* 1992). Rodionova *et al.* (2012) found that the contact angle of TEMPO-oxidized cellulose nanofibers-coated PET sheets decreased by 15-20° for carboxylate contents of 700-800 mmol/kg. In summary, as demonstrated by Kovalev and Bugaenko (2003), the hydrophilic character found in irradiated CNCs showed an improvement of the water-adsorbing capacity with high γ -irradiation doses.

5.5.10 Transmission Electron Microscopy (TEM)

The morphology of native and irradiated CNCs was recorded by TEM after re-suspension of the crystals in deionized water and all images show agglomeration of a few particles (**Fig. 28**).

This phenomenon was also reported by Jiang *et al.* (2010) when imaging of desulfated CNCs was performed by AFM. However, this agglomeration could also be an artifact due to the possible interaction between the CNCs and the supporting material of the grid as well as the sample preparation procedure used (Kaushik *et al.* 2015). Dispersibility of never-dried vs. dried CNCs samples has been a subject of study for many authors over the years, all suggesting that the freeze-drying procedure might lead to a poor dispersion of CNCs in water due to the formation of intermolecular hydrogen bonds during the drying process (Liang and Marchessault 1959). In order to overcome this drawback, it has been found that neutralization of CNCs with different counterions prior to drying can significantly improve the state and homogeneity of the dispersion (Dong and Gray 1997; Shimizu *et al.* 2014).

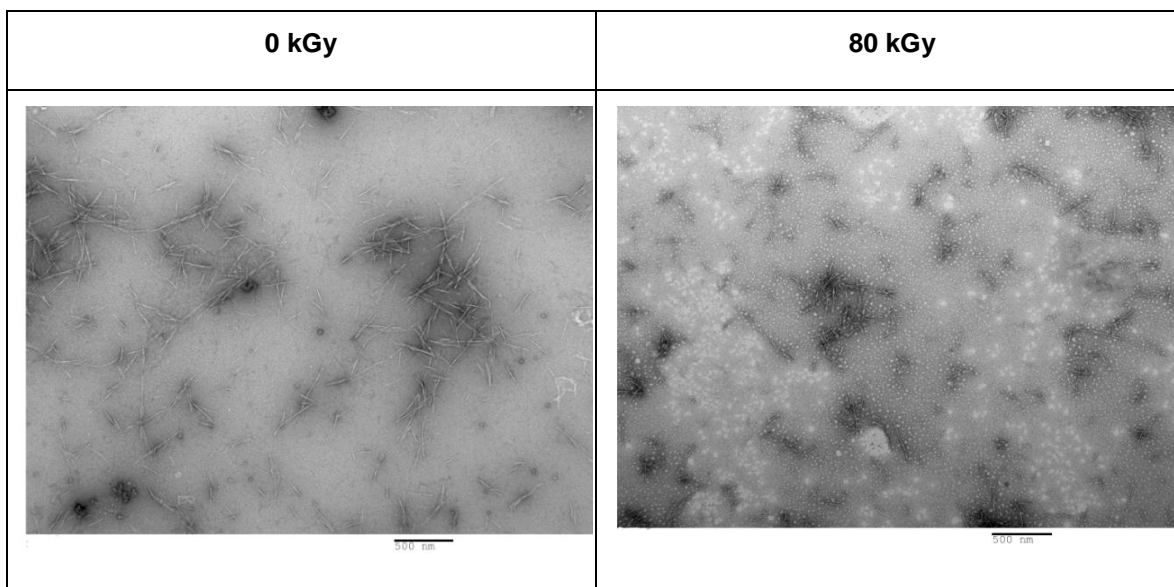


Fig. 28 TEM images (11,000x) of re-suspended native and irradiated CNCs neutralized with NaOH. The scale bar represents 500 nm

5.5.11 Radical Scavenging Properties of Irradiated CNCs

As Determined by DPPH Method

The radical scavenging properties of irradiated CNCs were evaluated by the action of the (1,1-diphenyl-2-picrylhydrazyl) DPPH radical. Two reference antioxidants (*i.e.* ascorbic acid and Trolox) were used for comparison purposes as shown in **Table 7**. Irradiated CNCs exhibit enhanced radical scavenging properties by showing 49 Trolox equivalent (eq) (μM) when a 80 kGy dose was applied compared to 4 Trolox eq (μM) for native CNCs. Similar antiradical activity trend was also observed for ascorbic acid (AA).

Table 7 Radical scavenging properties of irradiated CNC expressed as ascorbic acid and Trolox equivalents (eq) in μM

kGy	μM Trolox \pm St Dev	μM AA \pm St Dev
0	4.16 \pm 1.53 a	3.40 \pm 1.25 a
10	10.55 \pm 0.66 b	8.62 \pm 0.53 b
20	13.46 \pm 2.23 b	11.00 \pm 1.82 b
40	25.96 \pm 2.47 c	21.21 \pm 2.01 c
80	49.05 \pm 4.24 d	40.08 \pm 3.46 d

Lower case letters in each column means significant difference at the 0.05 level

It is generally considered that antioxidant properties of biopolymers are enhanced by irradiation. Abad *et al.* (2013) found an augmentation of κ -carrageenan scavenging capacity of 80% with respect to the control when an irradiation dose of 20 kGy was applied to the polymer with a concentration of 2000 $\mu\text{g}/\text{mL}$. In order to explain the phenomenon, they compared the antioxidant activity observed after irradiation on a solid and aqueous solution of κ -carrageenan. They found that an irradiation dose of 20 kGy in the liquid state gives better antioxidant properties than a dose of 100 kGy in the solid state. It was explained that the lower antioxidant capacities found in solid irradiated κ -carrageenan are due to the low amount of reducing end units formed during irradiation. Thus, the reported new reducing units in biopolymers were showed to improve scavenging activities.

Literature also tends to show that low molecular weight can have a direct influence on the radical scavenging properties. Like carrageenan (Abad *et al.* 2009), other irradiated

polymers such as laminarin (Choi *et al.* 2011), polysaccharides extracted from seaweed (Choi *et al.* 2009), chitosan (Feng *et al.* 2008), and hyaluronic acid (Kim *et al.* 2008) have also exhibited irradiation dose dependence on increased antioxidant properties.

In the case of irradiated CNCs, the improvement of antioxidant properties can be explained either by the increased amount of aldehyde groups, or a lower molecular weight or a combination of the two.

As Determined by Total Antioxidant Capacity Assay

Since similar results were found by comparing irradiated CNCs in terms of ascorbic acid eq and Trolox eq, comparison of two antiradical tests (total antioxidant capacity and DPPH scavenging) was performed with ascorbic acid as the standard compound as shown in **Fig. 29**.

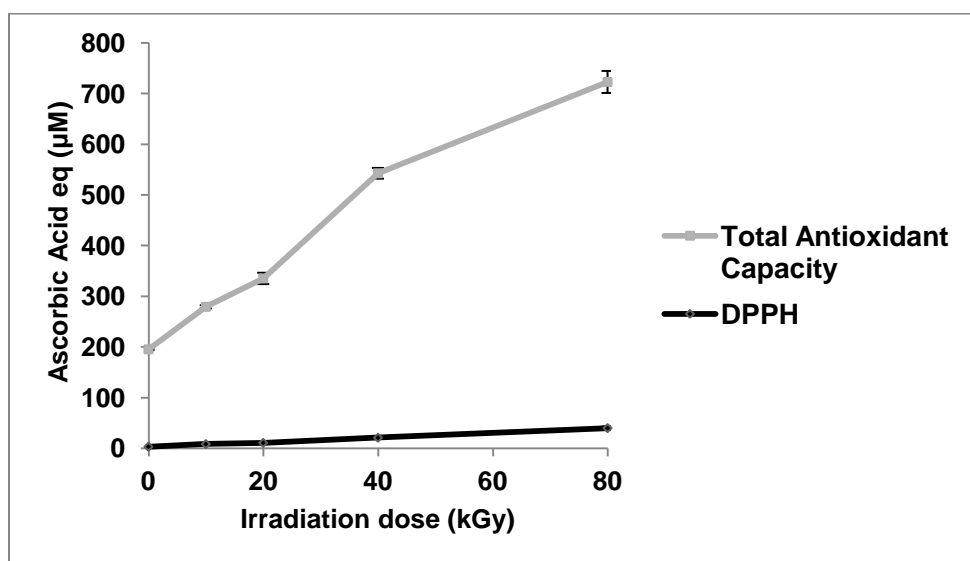


Fig. 29 Total antioxidant capacity and DPPH radical scavenging tests comparison performed in irradiated CNCs

It was observed that antioxidant properties were significantly higher when total antioxidant capacity tests were performed. For example, at a dose of 80 kGy, irradiated CNCs exhibited an antioxidant activity equivalence of 800 µM AA eq. by the total antioxidant capacity test compared to 40 µM by DPPH.

The total antioxidant capacity test is based on an electron transfer reaction that occurs between the probe (oxidant) and the tested molecule (Huang *et al.* 2005). It is assumed that this electron transfer to the molybdenum complex can be easily reduced, showing

the overall antioxidant capacity. The study carried by Megdiche-Ksouri *et al.* (2015) was in concordance with the ability of reduction observed in total antioxidant capacity assay. The authors analyzed the antioxidant effect of *Artemisia* essential oil, corroborating that total antioxidant capacity was twice than that obtained via DPPH test. DPPH, on the other hand, is a stable and commercially available radical that has a maximum absorption at 515 nm (Sharma and Bhat 2009). The chemical reaction involves the transfer of a hydrogen atom to the DPPH, giving the reduced form of the compound DPPHH. It can be suggested that irradiated CNCs might have a hydrogen donating effect. It has been reported in literature that compounds conjugated with hydroxyl and aldehyde (reducing compound) groups exhibit antioxidant properties (Abad *et al.* 2013; Motsa *et al.* 2015). As it was cited by Xue *et al.* (1998), the hydroxyl groups in carrageenan might enhance hydrogen transfer to DPPH radical, thus showing antioxidant activities. Foti *et al.* (2004) also reported that residual acids or bases present in the solvent may have an influence on the performance of antioxidant phenolic compounds and DPPHH.

Despite the differences found in both methods, it seems clear that the antioxidant properties of irradiated CNCs depend directly on the irradiation doses applied.

5.6 Conclusions

Antioxidant capacity of irradiated CNCs was confirmed upon γ -irradiation of dispersed suspensions of CNCs. Increase of γ -irradiation doses has a positive effect on the formation of new chemical functionalities (e.g., carboxylic and aldehyde groups) combined with a decrease in the molecular weight of cellulose chains leading to improved antioxidant properties. Scavenging properties of CNCs were analyzed by DPPH and total antioxidant capacity tests demonstrating equivalent concentration of 80 and 700 μ M of ascorbic acid, respectively. The presence of additional carboxylic acid groups also enhances the CNCs affinity for moisture.

Introduction of irradiated CNCs in active biodegradable polymeric materials might be interesting for potential applications in the packaging area. Due to their wettability and scavenging properties, irradiated CNCs could bring easy interaction with aqueous biopolymer matrices (e.g. alginate) for increasing stability in foods, especially for preventing lipids from oxidation. Further *in situ* studies must be done in order to evaluate the efficiency to inhibit thiobarbituric acid and other reactive substances considered as

by-products of lipid peroxidation.

5.7 Acknowledgements

The authors are thankful to Nordion Inc. for irradiation work, Natural Sciences and Engineering Research Council of Canada (NSERC) for funding and FPIInnovations for providing the CNC material and their scientific support. We also would like to thank Myriam Méthot and Damien Mauran for their technical help with GPC and TGA analysis. This work was done under the framework of the Coordinated Research Project (CRP) on *Application of Radiation Techniques in Development of Advanced Packaging Materials for Food Products*, IAEA research agreement No 17675.

5.8 References

- Abad LV, Kudo H, Saiki S et al (2009) Radiation degradation studies of carrageenans. *Carbohydr Polym* 78:100–106. doi: 10.1016/j.carbpol.2009.04.009
- Abad LV, Relleve LS, Racadio CDT et al (2013) Antioxidant activity potential of gamma irradiated carrageenan. *Appl Radiat Isot* 79:73–79. doi: 10.1016/j.apradiso.2013.04.035
- Baccaro S, Carewska M, Casieri C et al (2013) Structure modifications and interaction with moisture in γ -irradiated pure cellulose by thermal analysis and infrared spectroscopy. *Polym Degrad Stab* 98:2005–2010. doi: 10.1016/j.polymdegradstab.2013.07.011
- Bee TG, Cross EM, Dias AJ et al (1992) Control of wettability of polymers using organic surface chemistry. *J Adhes Sci Technol* 6:719–731. doi: 10.1163/156856192X01060
- Bouchard J, Méthot M, Jordan B (2006) The effects of ionizing radiation on the cellulose of woodfree paper. *Cellulose* 13:601–610. doi: 10.1007/s10570-005-9033-0
- Castellan A, Ruggiero R, Frollini E et al (2007) Studies on fluorescence of celluloses. *Holzforschung* 61:504–508. doi: 10.1515/HF.2007.090
- Choi J, Kim H-J, Kim J-H et al (2009) Application of gamma irradiation for the enhanced physiological properties of polysaccharides from seaweeds. *Appl Radiat Isot* 67:1277–1281. doi: 10.1016/j.apradiso.2009.02.027
- Choi J, Kim H-J, Lee J-W (2011) Structural feature and antioxidant activity of low molecular weight laminarin degraded by gamma irradiation. *Food Chem* 129:520–523. doi: 10.1016/j.foodchem.2011.03.078
- Dasgupta N, De B (2004) Antioxidant activity of *Piper betle* L. leaf extract in vitro. *Food Chem* 88:219–224. doi: 10.1016/j.foodchem.2004.01.036
- Dong XM, Gray DG (1997) Effect of counterions on ordered phase formation in suspensions of charged rodlike cellulose crystallites. *Langmuir* 13:2404–2409. doi: 10.1021/la960724h
- Dong, XM, Revol, J-F, Gray, DG, (1998). Effect of microcrystallite preparation conditions on the formation of colloid crystals of cellulose. *Cellulose* 5, 19–32. doi: 10.1023/A:1009260511939
- Ershov BG, Klimentov AS (1984) The radiation chemistry of cellulose. *Russ Chem Rev* 53:1195–1207. doi: 10.1070/RC1984v053n12ABEH003148
- Evans R, Wearne RH, Wallis AFA (1989) Molecular weight distribution of cellulose as its tricarbonyl by high performance size exclusion chromatography. *J Appl Polym Sci* 37:3291–3303. doi: 10.1002/app.1989.070371202
- Feng T, Du Y, Li J et al (2008) Enhancement of antioxidant activity of chitosan by irradiation. *Carbohydr Polym* 73:126–132. doi: 10.1016/j.carbpol.2007.11.003
- Foti MC, Daquino C, Geraci C (2004) Electron-transfer reaction of cinnamic acids and their methyl esters with the DPPH(*) radical in alcoholic solutions. *J Org Chem* 69:2309–2314. doi: 10.1021/jo035758q

- Fukuzumi H, Saito T, Okita Y, Isogai A (2010) Thermal stabilization of TEMPO-oxidized cellulose. *Polym Degrad Stab* 95:1502–1508. doi: 10.1016/j.polymdegradstab.2010.06.015
- Habibi, Y., Lucia, L.A., & Rojas, O.J. (2010). Cellulose nanocrystals: chemistry, self-assembly, and applications. *Chem. Rev.*, 110, 3479–3500. <https://doi.org/10.1021/cr900339w>
- Hamad WY, Hu TQ (2010) Structure–process–yield interrelations in nanocrystalline cellulose extraction. *Can J Chem Eng* 88:392–402. doi: 10.1002/cjce.20298
- Hatakeyama T, Nakamura K, Hatakeyama H (2000) Vaporization of bound water associated with cellulose fibres. *Thermochim Acta* 352–353:233–239. doi: 10.1016/S0040-6031(99)00471-2
- Henniges U, Okubayashi S, Rosenau T, Potthast A (2012) Irradiation of cellulosic pulps: understanding its impact on cellulose oxidation. *Biomacromolecules* 13:4171–4178. doi: 10.1021/bm3014457
- Hien NQ, Nagasawa N, Tham LX et al (2000) Growth-promotion of plants with depolymerized alginates by irradiation. *Radiat Phys Chem* 59:97–101. doi: 10.1016/S0969-806X(99)00522-8
- Hofstetter K, Hinterstoisser B, Salmén L (2006) Moisture uptake in native cellulose – the roles of different hydrogen bonds: a dynamic FT-IR study using Deuterium exchange. *Cellulose* 13:131–145. doi: 10.1007/s10570-006-9055-2
- Huang D, Ou B, Prior RL (2005) The chemistry behind antioxidant capacity assays. *J Agric Food Chem* 53:1841–1856. doi: 10.1021/jf030723c
- Huq T, Khan A, Dussault D et al (2012) Effect of gamma radiation on the physico-chemical properties of alginate-based films and beads. *Radiat Phys Chem* 81:945–948. doi: 10.1016/j.radphyschem.2011.11.055
- Jiang F, Esker AR, Roman M (2010) Acid-catalyzed and solvolytic desulfation of H₂SO₄-hydrolyzed cellulose nanocrystals. *Langmuir* 26:17919–17925. doi: 10.1021/la1028405
- Kaushik M, Putaux JL, Fraschini C, et al (2015) Transmission electron microscopy for the characterization of cellulose nanocrystals. *Intech*, p 129,163
- Khan F, Ahmad SR, Kronfli E (2006) γ -radiation induced changes in the physical and chemical properties of lignocellulose. *Biomacromolecules* 7:2303–2309. doi: 10.1021/bm060168y
- Katz S, Beatson, P R, M SA (1984) The determination of strong and weak acidic groups in sulfite pulps. *Sven Papperstidning* 87:48–53.
- Kim JK, Srinivasan P, Kim JH et al (2008) Structural and antioxidant properties of gamma irradiated hyaluronic acid. *Food Chem* 109:763–770. doi: 10.1016/j.foodchem.2008.01.038
- Kovalev GV, Bugaenko LT (2003) On the crosslinking of cellulose under exposure to radiation. *High Energy Chem* 37:209–215. doi: 10.1023/A:1024790415083
- Lapierre L, Bouchard J (1999) Molecular weight determination of softwood kraft cellulose: effects of carbanilation solvent, hemicelluloses, and lignin. *Adv Lignocellul Charact Tappi Press Atlanta* 239–262.

- LaVerne JA (2000) OH Radicals and oxidizing products in the gamma radiolysis of water. *Radiat Res* 153:196–200. doi: 10.1667/0033-7587(2000)153[0196:ORAOPI]2.0.CO;2
- Liang CY, Marchessault RH (1959) Infrared spectra of crystalline polysaccharides. I. Hydrogen bonds in native celluloses. *J Polym Sci* 37:385–395. doi: 10.1002/pol.1959.1203713209
- Lin H-Y, Chou C-C (2004) Antioxidative activities of water-soluble disaccharide chitosan derivatives. *Food Res Int* 37:883–889. doi: 10.1016/j.foodres.2004.04.007
- Łojewska J, Lubańska A, Miśkowiec P, et al (2006) FTIR in situ transmission studies on the kinetics of paper degradation via hydrolytic and oxidative reaction paths. *Appl Phys A* 83:597–603. doi: 10.1007/s00339-006-3529-9
- Łojewska J, Miśkowiec P, Łojewski T, Proniewicz LM (2005) Cellulose oxidative and hydrolytic degradation: In situ FTIR approach. *Polym Degrad Stab* 88:512–520. doi: 10.1016/j.polymdegradstab.2004.12.012
- Maréchal Y, Chanzy H (2000) The hydrogen bond network in I β cellulose as observed by infrared spectrometry. *J Mol Struct* 523:183–196. doi: 10.1016/S0022-2860(99)00389-0
- Megdiche-Ksouri W, Trabelsi N, Mkadmini K et al (2015) *Artemisia campestris* phenolic compounds have antioxidant and antimicrobial activity. *Ind Crops Prod* 63:104–113. doi: 10.1016/j.indcrop.2014.10.029
- Moise IV, Stanculescu I, Meltzer V (2013) Thermogravimetric and calorimetric study of cellulose paper at low doses of gamma irradiation. *J Therm Anal Calorim* 115:1417–1425. doi: 10.1007/s10973-013-3476-6
- Motsa NM, Modi AT, Mabhaudhi T et al (2015) Influence of agro-ecological production areas on antioxidant activity, reducing sugar content, and selected phytonutrients of orange-fleshed sweet potato cultivars. *Food Sci Technol Camp* 35:32–37. doi: 10.1590/1678-457X.6443
- O'Neill P (1987) The chemical basis of radiation biology. *Int J Radiat Biol Relat Stud Phys Chem Med* 52:976–976. doi: 10.1080/09553008714552571
- Ponomarev AV, Ershov BG (2014) Radiation-induced high-temperature conversion of cellulose. *Mol Basel Switz* 19:16877–16908. doi: 10.3390/molecules191016877
- Quesenberry MS, Lee YC (1996) A rapid formaldehyde assay using purpald reagent: application under periodation conditions. *Anal Biochem* 234:50–55. doi: 10.1006/abio.1996.0048
- Relleve L, Abad L (2015) Characterization and antioxidant properties of alcoholic extracts from gamma irradiated κ -carrageenan. *Radiat Phys Chem* 112:40–48. doi: 10.1016/j.radphyschem.2015.02.028
- Relleve L, Nagasawa N, Luan LQ, et al (2005) Degradation of carrageenan by radiation. *Polym Degrad Stab* 87:403–410. doi: 10.1016/j.polymdegradstab.2004.09.003
- Rodionova G, Eriksen Ø, Gregersen Ø (2012) TEMPO-oxidized cellulose nanofiber films: effect of surface morphology on water resistance. *Cellulose* 19:1115–1123. doi: 10.1007/s10570-012-9721-5

- Roman M, Winter WT (2004) Effect of sulfate groups from sulfuric acid hydrolysis on the thermal degradation behavior of bacterial cellulose. *Biomacromolecules* 5:1671–1677. doi: 10.1021/bm034519+
- Sánchez Orozco R, Balderas Hernández P, Flores Ramírez N et al (2012) Gamma irradiation induced degradation of orange peels. *Energies* 5:3051–3063. doi: 10.3390/en5083051
- Schroeder L., Haigh F. (1979) Cellulose and wood pulp polysaccharides. Gel permeation chromatographic analysis.
- Sharma OP, Bhat TK (2009) DPPH antioxidant assay revisited. *Food Chem* 113:1202–1205. doi: 10.1016/j.foodchem.2008.08.008
- Shimizu M, Saito T, Isogai A (2014) Bulky quaternary alkylammonium counterions enhance the nanodispersibility of 2,2,6,6-Tetramethylpiperidine-1-oxyl-oxidized cellulose in diverse solvents. *Biomacromolecules* 15:1904–1909. doi: 10.1021/bm500384d
- Sintzel MB, Merkli A, Tabatabay C, Gurny R (1997) Influence of irradiation sterilization on polymers used as drug carriers—A review. *Drug Dev Ind Pharm* 23:857–878. doi: 10.3109/03639049709148693
- Soares S, Camino G, Levchik S (1995) Comparative study of the thermal decomposition of pure cellulose and pulp paper. *Polym Degrad Stab* 49:275–283. doi: 10.1016/0141-3910(95)87009-1
- Sokhey, A.S., Hanna, M.A. (1993). Properties of Irradiated Starches. *Food Struct.* 12: 397–410.
- Sultanov K, Turaev AS (1996) Mechanism of the radiolytic transformation of cellulose. *Chem Nat Compd* 32:728–733. doi: 10.1007/BF01375125
- Takács E, Wojnárovits L, Borsa J, et al (1999) Effect of γ -irradiation on cotton-cellulose. *Radiat Phys Chem* 55:663–666. doi: 10.1016/S0969-806X(99)00245-5
- Takács E, Wojnárovits L, Földvály C, et al (2000) Effect of combined gamma irradiation and alkali treatment on cotton–cellulose. *Radiat Phys Chem* 57:399–403. doi: 10.1016/S0969-806X(99)00409-0
- Varma AJ, Chavan VB (1995) Thermal properties of oxidized cellulose. *Cellulose* 2:41–49. doi: 10.1007/BF00812771
- von Sonntag C (1980) Free-radical reactions of carbohydrates as studied by radiation techniques. In: Horton RST and D (ed) *Advances in Carbohydrate Chemistry and Biochemistry*. Academic Press, pp 7–77
- Xie W, Xu P, Liu Q (2001) Antioxidant activity of water-soluble chitosan derivatives. *Bioorg Med Chem Lett* 11:1699–1701. doi: 10.1016/S0960-894X(01)00285-2
- Xing R, Yu H, Liu S, et al (2005) Antioxidant activity of differently regioselective chitosan sulfates in vitro. *Bioorg Med Chem* 13:1387–1392. doi: 10.1016/j.bmc.2004.11.002
- Xuan Tham L, Nagasawa N, Matsushashi S et al (2001) Effect of radiation-degraded chitosan on plants stressed with vanadium. *Radiat Phys Chem* 61:171–175. doi: 10.1016/S0969-806X(00)00388-1

Xue C, Yu G, Hirata T et al (1998) Antioxidative activities of several marine polysaccharides evaluated in a phosphatidylcholine-liposomal suspension and organic solvents. *Biosci Biotechnol Biochem* 62:206–209. doi: 10.1271/bbb.62.206

**6. PUBLICATION 3: EFFECT OF CELLULOSE NANOCRYSTALS
ON THYME ESSENTIAL OIL RELEASE FROM ALGINATE BEADS:
STUDY OF ANTIMICROBIAL ACTIVITY AGAINST LISTERIA
INNOCUA AND GROUND MEAT SHELF LIFE IN COMBINATION
WITH GAMMA IRRADIATION**

Published in Journal Cellulose (2019), 26 (9): 5247–5265

**Paula Criado^a, Carole Frascini^b, Majid Jamshidian^a, Stephane Salmieri^a, Natacha
Desjardins^a, Affef Sahraoui^a, Monique Lacroix^{a†}**

^aResearch Laboratories in Sciences Applied to Food, Canadian Irradiation Centre,
INRS–Institut Armand-Frappier, Institute of Nutraceutical and Functional Foods, 531
Blvd des Prairies, Laval, Quebec, H7V 1B7, Canada

^bFPIInnovations, 570 Blvd Saint-Jean, Pointe-Claire, Quebec, H9R 3J9, Canada

[†]Corresponding author: Professor Monique Lacroix, Tel: +1 (450)687-5010 #4489,
Fax: +1 (450)686-5501, E-mail: monique.lacroix@iaf.inrs.ca

The number of figures and tables were adjusted in this article in order to follow the sequence of the thesis document. The style of references was presented according to the guidelines of the journal.

CONTRIBUTION OF AUTHORS

This research work was performed under the supervision of Pr. Monique Lacroix, Dr. Carole Fraschini and Dr. Majid Jamshidian.

Paula Criado and Natacha Desjardins carried out the laboratory experiments of the release of essential oil in simulating solvent and the evaluation of antimicrobial activity of beads on pathogenic bacteria. The protocols of the experiments were previously established with Pr. Lacroix and Dr. Fraschini and the obtained results were discussed with Dr. Jamshidian and Stephane Salmieri. Affef Sahraoui participated on the tests of mesophilic total flora growth in combination with the beads and gamma irradiation. This article was written by Paula Criado under supervision of Pr. Lacroix, Dr. Fraschini and Dr. Jamshidian.

RÉSUMÉ

Des billes d'alginate contenant de l'huile essentielle (EO) de thym (1-3%) et des nanocristaux de cellulose (CNCs) (0-40%, base sèche) ont été préparées afin d'étudier le profil de relargage d'EO dans un milieu simulé ainsi que l'effet antimicrobien des billes contre *Listeria innocua* par des tests *in vitro* et *in situ*. L'introduction de CNCs de 0 à 30% dans des billes d'alginate a permis une augmentation de l'efficacité d'encapsulation d'EO de 62% à 82% et une diminution de la constante cinétique de relargage (k) de 9.85 à 6.77 lorsque les billes ont été préparées avec 3% d'EO de thym. Ces concentrations optimales ont été sélectionnées dans le but d'examiner l'efficacité antimicrobienne des billes à éliminer *Listeria innocua* et à réduire la flore totale mésophile (MTF) dans la viande hachée durant l'entreposage. Les résultats ont montré une réduction de 2 log UFC/g de *L. innocua* pendant plus de 10 jours dans la viande hachée contenant les billes d'alginate bioactives par rapport aux échantillons témoins. L'influence du traitement d'irradiation gamma a été étudiée sur la MTF de la viande. Les résultats ont montré une réduction de 4 log UFC/g pendant 14 jours dans la viande traitée avec les billes d'alginate contenant 3% d'EO de thym. Une synergie entre la présence d'EO de thym et l'irradiation a été observée en termes d'élimination de *Listeria innocua* et d'extension de la durée de conservation de la viande.

ABSTRACT

Thyme essential oil (EO) loaded alginate beads (1-3%) containing cellulose nanocrystals (CNCs) (0-40% polymer dry basis) were prepared in order to study EO release profile in simulating solvent and the antimicrobial effect against *Listeria innocua* via *in vitro* and *in situ* tests. Introduction of CNCs from 0 to 30% in alginate beads exhibited an increase of EO encapsulation efficiency from 62 to 82% and a kinetic release constant (k) decrease from 9.85 to 6.77 when beads were prepared with 3% thyme EO, respectively. These optimal concentrations were selected in order to assess the antimicrobial efficiency to eliminate *Listeria innocua* and to reduce the mesophilic total flora (MTF) on ground meat during storage. Results showed that ground meat containing active alginate beads showed a 2 log reduction CFU/g of *L. innocua* during more than 10 days as compared to the control. The influence of gamma-irradiation treatment was studied on MTF of ground meat, allowing a 4 log reduction during 14 days when alginate beads containing 3% thyme EO were added. A synergy between thyme EO and irradiation was observed in terms of *Listeria innocua* elimination and shelf-life extension.

6.1 Introduction

Food safety is an important issue that agri-food industry faces when food needs to be treated and stored. Factors such as appearance, colour, sense perception, microbiological quality, and safety are critical to determine product shelf-life (Labuza 1996) as well as its quality criteria for commercialization. Animal-origin foods are highly favourable towards bacteria growth due to their high water activity, high content in nutrients and suitable pH value. In food, for instance, pathogenic bacteria such as *Salmonella*, *Escherichia coli*, *Campylobacter jejuni*, *Listeria monocytogenes*, and *Staphylococcus aureus*, represent the main causes of food-borne illnesses (Adams and Moss 2000). The total number of Canadians affected by food poisoning rises up to 4 million per year (Public Health Agency of Canada 2015) causing, thus, a reinforcement from the Canadian Food Inspection Agency on its food policies and standards. Therefore, in order to prevent food from any bacterial growth, antimicrobial and antioxidant agents are nearly always the most frequent adopted strategy by food manufacturers. However, with the increased demand from consumers to eliminate synthetic antimicrobial agents, research has developed methods and formulations based on natural compounds.

Thus, essential oils which are aromatic compounds with antimicrobial potential, mainly extracted from plants (leaves, bark or fruits), have been commonly proposed as natural food additives (Oussalah *et al.* 2007). They are principally constituted of hydrocarbons (terpenes, sesquiterpenes) and oxygenated compounds such as alcohols, esters, ethers, aldehydes, ketones, lactones, phenols, and phenol ethers. Studies showed that individual compounds found in essential oils exhibit repellent (Nerio *et al.* 2010), antifungal (Hossain *et al.* 2016) and antibacterial properties (Donsi *et al.* 2011). Briefly, essential oils are characterized for their particular activity. Their mechanism of action on bacteria is based on the production of pores on cell membrane, inducing cytoplasmic leakage and a decrease of ATP activity (Oussalah *et al.* 2006). In addition, Caillet *et al.* (2006) have demonstrated the effect of oregano essential oil and gamma irradiation on *Listeria monocytogenes* exoskeleton, or also called murein sacculus or peptidoglycan. It was reported that concentrations of essential oil of 0.02 and 0.025% led to degradation and modification of muropeptides as well as a decrease of intracellular ATP. The high efficiency of thyme essential oil on *Listeria* strains and its potential utilisation in food preservation has been discussed by many authors. Rasooli *et al.* (2006), for instance,

have reported that thyme essential oil had similar or higher effects on *Listeria* cell walls compared to those treated with nisin or with electric field intensity above 40 kV/cm.

Other procedures can be jointly applied to reinforce their properties against food-borne bacteria. Gamma irradiation is a non-thermal pasteurization process when applied to spoiled food that causes DNA-bacteria damage and cell death. It can be highlighted that gamma irradiation has proven a synergistic action when applied in combination with essential oils (Caillet *et al.* 2005). Caillet *et al.* (2005) have concluded that intracellular ATP decrease of bacteria count was even more important when oregano oil was combined to irradiation.

Even though gamma irradiation does not affect the integrity of essential oil (Kim *et al.* 2005), some drawbacks might be overcome. When exposed to external factors (e.g., oxygen, temperature and light), essential oils lack stability, resulting in volatilization or unpleasant transformations caused by oxidation, isomerisation, cyclization or dehydrogenation reactions. This is the reason why many authors have explored the possibility to encapsulate essential oils in polymeric matrices via emulsions (Salvia-Trujillo *et al.* 2013), films (Tunç and Duman 2011) or beads (Huq *et al.* 2015) to protect their bioactivity as well as to control their release during food processing and the storage time required during commercialization periods. The antimicrobial performance of essential oils or other types of antimicrobial compounds relies on their rate of release. A slow release rate might not be enough to prevent microbial growth while a high release rate might not have a sustained bacterial inhibition over time (Li *et al.* 2006). Thus, in order to avoid "dose dumping" of compound delivery, a study of the polymer physicochemical properties (Campos-Requena *et al.* 2015) and interactions between polymeric and antimicrobial materials must be considered (Cha *et al.* 2003).

Alginate is a polysaccharide extracted from brown algae and composed of guluronic and mannuronic acid residues. Due to their biodegradability, alginate polymers have been applied to different fields such as tissue engineering, food, drug delivery, and wound-dressing materials (Sussman 2006). The hydrophilic character and easy gelation properties with alkaline metals such as Mg^{2+} , Ca^{2+} , Sr^{2+} , and Ba^{2+} allows alginate to produce different types of gels with different shapes (capsules, films, and wound-dressing). There are some limitations of native alginate such as its hydrophilic behaviour and the introduction of long alkyl ester groups has been proposed to overcome this

problematic. However, in this study dispersion of thyme essential oil by an emulsification process has been proposed.

CNCs have been defined by Health Canada (Government of Canada National Research Council Canada 2014) as biodegradable and practically nontoxic nanomaterials which have demonstrated outstanding mechanical properties (Huq *et al.* 2012), for stabilization of emulsions (Zhu *et al.* 2015), gel formation (Yang *et al.* 2014), and promoting the viability of probiotic bacteria (*L. rhamnosus*) during storage periods. Because of their nanometric size, CNCs have the ability to create tortuous pathways in polymer matrices. Thus, they can be potentially used to delay the diffusion of chemical compounds in which they have been dispersed (Kaboorani *et al.* 2016).

The main objective of this study was to evaluate the antimicrobial effect of thyme oil encapsulated in alginate beads and study their release rate in food matrices when different concentrations of CNCs were added to alginate beads. The effect of parameters such as concentrations of thyme EO and CNCs were studied. Further testing was performed in order to characterize their antimicrobial properties via *in vitro* test against *Listeria innocua*. Finally, optimized beads were chosen for *in situ* testing on ground meat packed under vacuum in combination with gamma irradiation.

6.2 Materials and Methods

6.2.1 Materials

Alginic acid sodium salt from brown algae with mannuric and guluronic contents of ~5-35% and ~65-70% respectively, tween 80, calcium chloride (CaCl₂), and potassium bromide (KBr) were purchased from Sigma Aldrich Canada Ltd (Oakville, ON, Canada). Cellulose nanocrystals extracted from softwood were kindly supplied by FPIInnovations (Pointe Claire, QC, Canada). Glycerol and phosphate buffer saline (PBS) solution (sodium chloride, potassium chloride, potassium dihydrogen phosphate, and sodium hydrogen phosphate) were all purchased from Laboratory Mat (Quebec city, QC, Canada). PALCAM agar, peptone water, trypto soy broth (TSB), and trypto soy agar were obtained from Alpha Bioscience Inc. (Baltimore, MD, USA). *Thymus vulgaris* EO also known as common thyme was purchased from Aliksir (Grondines, QC, Canada) and ground lean pork (~15% fat content) was bought in a local IGA grocery store (Montreal, QC, Canada).

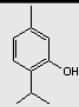
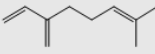
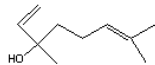
6.2.2 Bacteria Strain

Listeria innocua ATCC 51742 (Cederlane, ON, Canada) was stored at -80°C in TSB with 10-15% (w/w) of glycerol. Before use, two propagations of 24 h at 37°C were carried in 9 mL of TSB under aerobic conditions. The bacterium was diluted in peptone water from an initial concentration of 10^9 CFU/mL to a final concentration of 10^7 or 10^5 CFU/mL according to the required concentrations either for *in vitro* and *in situ* testing.

6.2.3 Preparation of Alginate Emulsion Loaded with Different Concentrations of Thyme EO and CNCs

Firstly, an alginate solution with concentration of 2.7% w/w was prepared in distilled water at room temperature, followed by overnight stirring. In order to prepare oil-in-water stock emulsion, thyme EO was introduced at 1 and 3% w/w and an equal mass ratio (1:1) with respect to tween 80 was added to the final emulsion. Then previously dispersed CNCs solution was mixed with alginate-based emulsion in order to obtain 0, 10, 20, 30, and 40% CNCs with respect to polymer dry basis. Final concentrations were 2% for alginate, and 1 and 3% for thyme EO emulsion. The mixture of compounds was then followed by homogenization of the solutions using a homogenizer Ultra-Turrax (IKA, Ottawa, ON, Canada) at 15,000 rpm and then microfluidized using 3 cycles at 15,000 psi in a Microfluidizer M-110P (Microfluidics Inc., Newton, MA, USA). Principal components of thyme EO represented in **Table 8** were analyzed by the company with a gas chromatograph equipped with FID detector and with column HP INNOWAX length 60 m, internal diameter 0.5 mm, film thickness 0.25 μm . The temperature in the system was set at 250°C, starting from 50°C with a gradient of 2°C/min for 6 min, and heating until set temperature was reached. The vector gas used for the analysis was Helium at 22 psi.

Table 8 Principal components of *Thymus vulgaris* (thyme) EO analyzed by the provider via gas chromatography

Structure	Compound (concentration, %)	Structure	Compound (concentration, %)
	thymol (35%)		myrcene (2%)
	γ -terpinene (20%)		linalol (2%)
	p-cymene (19%)		α -terpinene (2%)
	carvacrol (3%)	others (17%)	

6.2.4 Preparation of Thyme Oil Loaded Beads

Beads were prepared by pouring 10 mL of the specific emulsion dropwise into a 100 mL calcium chloride solution (5% w/w). The suspension was magnetically stirred at 300 rpm for 20 min at room temperature, to allow complete gelation of beads. Finally, the beads were filtered, rinsed with distilled water and then gently dried on a wipe paper.

6.2.5 Particle Size of Alginate Emulsions

Particle size measurement of alginate emulsions was determined by Dynamic Light Scattering using a Malvern Zetasizer Nano-ZS (Model ZEN3600) from Malvern Instruments Inc. (Westborough, MA, USA). Measurements were performed from 100-fold dilution and each solution was analyzed in triplicate.

6.2.6 Encapsulation Efficiency and Loading Capacity of Thyme EO in Alginate Beads

Concentration of loaded thyme oil in alginate beads was determined by dissolving 0.1 g of beads in 20 g of phosphate buffer saline solution (pH 7.4). After 24 h, the beads were completely dissolved and the suspension was vigorously stirred until homogenization. The supernatant was then filtered (0.45 μm) and the thyme oil concentration was quantified by UV-spectrophotometry (S-3100 UV-vis Spectrophotometer, Scinco co, Seoul, Korea) at $\lambda_{max} = 274 \text{ nm}$.

To characterize the yield of the procedure, encapsulation efficiency (EE%) (**Eq. 19**) was calculated. EE% represents the total quantity of EO recovered from the encapsulation procedure with respect to the initial quantity loaded to the emulsion. Additionally, loading capacity (LC%) (**Eq. 20**) was calculated and expressed in terms of the percentage of EO that was encapsulated in the beads.

$$\text{Encapsulation Efficiency (EE\%)} = \frac{\text{Total weight of loaded thyme EO}}{\text{Initial weight of thyme oil}} * 100 \text{ (19)}$$

$$\text{Loading capacity (LC\%)} = \frac{\text{Total weight of loaded thyme EO}}{\text{Weight of alginate beads}} * 100 \text{ (20)}$$

6.2.7 *In vitro* Release Study of Thyme EO in Food Simulating Solvent for Ground Meat (Ethanol 10% v/v)

To study the migration of thyme EO in contact with food, different simulating conditions have been proposed by European Commission (2007) or Food and Drug Administration (Center for Food Safety and Applied Nutrition 2009). Various simulating liquids are available depending on food type, which is divided in 3 main categories: aqueous and acidic food (ethanol 10% v/v), alcohol beverages (ethanol 50% v/v), and fatty food (edible or synthetic oil). Thus, ethanol 10% v/v was chosen as a simulating solvent to evaluate the *in vitro* release of thyme EO into ground meat. Following the procedure established by Jamshidian *et al.* (2012), a quantity of 0.1 g of thyme EO loaded alginate beads with different concentrations of CNCs was introduced into tubes containing 10 g of ethanol 10% v/v. The tubes were sealed and placed at 4°C for a period of 7 days. Measurements were taken at least twice a day with prior homogenization of the supernatant by pipetting up and down the suspensions 5-6 times. To quantify the amount of thyme oil released, absorbance of the supernatant was taken at $\lambda_{max} = 274$ nm by using a Photodiode Array (PDA) UV-Vis spectrophotometer (Scinco, S-3100, Toronto, ON, Canada).

Profile results were fitted to the suitable empirical model Korsmeyer-Peppas described in **Eq. 21**. Results were expressed in terms of cumulative release vs. time:

$$\frac{M_t}{M_\infty} = kt^n \text{ (21)}$$

Where M_t and M_∞ are the absolute cumulative amount of thyme EO released at time t and infinite time, respectively, n and k values represent the release exponent indicative

of the mechanism and the release constant, respectively. As explained by Peppas and Sahlin (1989) this equation can be used to analyze the first 60% release curve, regardless of the geometric shape of the analyzed object. The kinetics constants were calculated by linear regression of log release (%) vs. log time (h) and results showing a correlation coefficient (R^2) higher than 0.9 were analyzed.

6.2.8 *In vitro* "Agar Diffusion Assay"

Thyme EO diffusion was evaluated according to the protocol described by Soliman *et al.* (2013). Tryptic Soy Agar Media was prepared and poured in Petri dishes. Once the agar has cooled down, 100 μ L of *Listeria innocua* (10^7 CFU/mL) was spread on its surface. An 8 mm-well was then cut out from the center of each agar where the prepared beads containing thyme oil emulsion (0-3 %) were placed. The inhibition and the ring diameter were reported after 24 h incubation at 37°C. The diameter was measured by using a carbon fiber digital caliper (resolution 0.1 mm; accuracy \pm 0.2 mm; Fisher Scientific, Ottawa, ON, Canada).

6.2.9 Volume of Alginate Beads

In order to determine the final volume of the beads, 50 beads prepared from a 3% thyme oil emulsion (with and without CNCs) were randomly picked. The volume of each bead was approximated to a spheroid and calculated as shown in **Eq. 22**:

$$v = \frac{4}{3}\pi * w^2 * l \quad (22)$$

Where w is the equatorial radius and l is the polar radius, both measured with a carbon fiber digital caliper (resolution 0.1 mm; accuracy \pm 0.2 mm; Fisher Scientific).

6.2.10 Transmission Electron Microscopy (TEM) of Alginate Beads

The cross-section of alginate beads prepared from 3% thyme oil emulsion in presence (30% CNCs) and absence of CNCs (0% CNCs) was observed by TEM (Hitachi H-7100, Hitachi Ltd.) at 2,000 \times magnification. The beads were dehydrated with serial concentrations of acetone (25, 50, 75 and 95%) for 15-30 mins in each solution. Dehydrated beads were embedded first in a mixed Spurr resin: acetone (1:1, v/v) solution for 16-18 h then immersed in the SPURR resin for a total of 4 h. Polymerization of the resin was allowed by letting the samples at 60-65°C for 20-30 h. Samples were

then cut in thin sections and placed on Formvar-copper-grids (200 mesh). Staining procedure was done with uranyl acetate at 5% (w/v) dissolved in ethanol 50% for 20-25 min and then in lead citrate solution for 5-7 min. Prepared samples were then analyzed.

6.2.11 Fourier Transform Infrared Spectroscopy Analysis of Alginate Beads

Air-dried alginate beads containing 0-30% CNCs and 0-3% of thyme EO were milled with KBr powder (spectrophotometric grade) in a ratio of 1:10. Pellets were prepared and spectra were recorded using a Spectrum One spectrometer (Perkin-Elmer, Woodbridge, ON, Canada). The samples were analyzed using the Spectrum software within the spectral region of 4000 to 650 cm^{-1} and for each spectrum, 64 scans were recorded at a 4 cm^{-1} resolution.

6.2.12 In situ Test of Optimized Beads Introduced in Ground Meat

Activity of 3% thyme EO emulsion encapsulated in alginate beads was tested *in situ* against *Listeria innocua* growth. The optimized beads showing the highest antimicrobial effect and the best controlled released were chosen for observation *in situ*. Thus, 15 g of beads were introduced in 25 g previously treated at 45 kGy sterilized ground meat samples. Once the beads were completely spread on meat, a volume of 500 μL of *L. innocua* (10^5 CFU/mL) diluted working culture was mixed with meat in order to reach a final concentration of 10^3 CFU/mL. Samples were sealed under vacuum atmosphere and stored for 14 days at 4°C. Serial dilutions were done in peptone water and meat samples were homogenized with a mechanical homogenizer for 2 min at 230 rpm before inoculation into PALCAM agar.

6.2.13 Gamma Irradiation and Thyme EO Combined Treatment

To observe the synergistic effect of thyme EO with gamma irradiation on ground meat, the samples were prepared, as described in the previous section, followed by gamma irradiation treatment (0.5-3 kGy). The irradiation procedure was done at the Canadian Irradiation Centre (CIC) in an underwater UC-15A SS canister (Nordion Int. Inc.) at a dose rate of 12.52 kGy/hr. Samples were then analyzed during the following 14 day storage period for microbial growth analysis.

6.2.14 Mesophilic Total Flora (MTF) of Ground Meat

Evaluation of shelf-life of irradiated (0-3 kGy) ground meat loaded with alginate beads was determined based on the concentration of Mesophilic Total Flora (MTF) bacteria for a period of 14 days. The samples (25 g) were previously weighed in sterile filter bags (Whirl-Pak, Nasco, Fort Atkinson, WI, USA) and mixed with 15 g of 3% thyme EO emulsion prepared beads (0-30% CNCs). Samples were sealed under vacuum conditions and stored at 4°C. On each day of analysis, the samples were diluted 4-fold in peptone water and then homogenized. Then, a 10-fold serial dilution of the homogenized samples was performed prior to adding 1 mL of the diluted sample to tryptic soy agar into Petri dishes. To enumerate the MTF, the samples were incubated for 48 h at 37°C under aerobic conditions.

6.3 Statistical Analysis

In order to evaluate the emulsion size, *in vitro* release tests, and *in situ* tests two replicates were prepared and for each replicate, three samples were analyzed. Analysis of variance (ANOVA) and Duncan's multiple-range test for equal variances and Tamhane's test for unequal variances were performed for statistical analysis using the SPSS 16.0 software (SPSS Inc. Chicago, IL, USA). Differences between means were considered to be significant at a 5% level.

6.4 Results and Discussion

6.4.1 Effect of Microfluidization on Thyme Emulsion Particle Size

The effect of CNC concentration upon microfluidization on the particle size of emulsion is shown in **Fig. 30**. Microfluidization of oil-in-water emulsions containing 1% or 3% of thyme EO demonstrated that emulsion droplet size decreased for all tested CNCs concentrations when 3 cycles at a pressure of 15,000 psi were applied. The preparation of nanoemulsions has already been studied by several authors showing the positive effect of microfluidization compared to hand blender and ultrasonic techniques. For instance, Salvia-Trujillo *et al.* (2013) demonstrated the effect of the pressure (50 to 150 MPa) and the number of cycles (1-10) on the reduction of particle size of emulsion based on lemongrass-alginate. The authors found that particle size was drastically reduced after microfluidization (>2 cycles) compared to the initial size. Similar to our results,

Salvia-Trujillo *et al.* (2013) found that the application of high pressure such as 150 MPa (21,000 psi) in emulsions always exhibited the lowest particle size in their overall study. Indeed, it is suggested that emulsification process at high pressure promotes droplet disruption by applying either shear stress or turbulent flow (Schultz *et al.* 2004). Our results showed that particle sizes smaller than 200 nm were achieved by microfluidization process after 3 cycles and 15,000 psi.

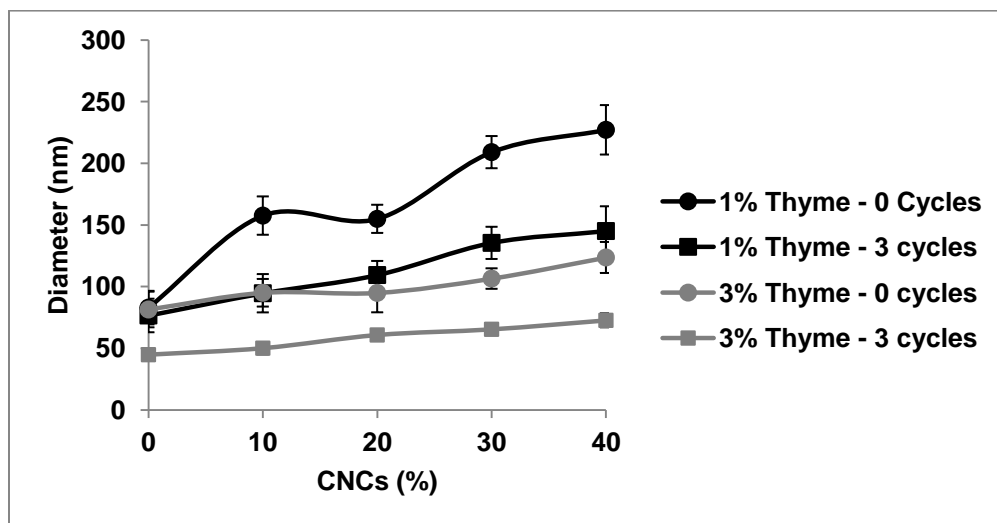


Fig. 30 Effect of CNCs concentration (0-40 % wt. polymer dry weight) on homogenization (0 and 3 cycles at 15,000 psi) of 1 and 3% thyme EO emulsion.

In addition, the effect of two thyme oil concentrations was evaluated (1-3%) before and after 3 cycles of microfluidization, showing that 1% thyme oil emulsions had higher particle sizes compared to 3% loading (**Fig. 30**). As it is described in the preparation procedure, a ratio 1:1 of tween 80 and thyme oil was used to stabilize oil-in-water emulsions. Thus, the increase of thyme oil content in the emulsion led to an increase of the amount of surfactant (tween 80). Since a surfactant has the capability to be absorbed at interfaces, its role was to reduce the superficial tension between the oily and aqueous phase. Previous studies (Qian and McClements 2011) have reported that increasing the amount of surfactants in emulsions had an advantageous influence on parameters such as lower light scattering and decreased turbidity as a response of small droplet formation. This trend was explained by the authors as the facility of surfactant to cover and to be absorbed onto the oil droplet, then producing small particles. As

compared to other research studies, our results suggest that the increase of surfactant enhances a decrease of the oil droplet size.

Another fact that was noticed in both 1 and 3% thyme essential oil EO was that an increase of CNCs concentrations led to formation of larger droplet size. For instance, after microfluidization of 1% thyme EO emulsion containing 0% CNCs showed a 77 nm droplet size which was significantly different from 145 nm observed in 40% CNCs loaded solutions. It is known that CNCs have the ability to be adsorbed at the interface of immiscible liquids, forming the so-called Pickering emulsions (Kalashnikova *et al.* 2012). The advantage of using CNCs besides other surfactants relies on the fact that low concentrations are required in order to stabilize emulsions. However, when CNC concentration is increased, it has been observed that nanoparticles tend to aggregate into clusters and in homogeneous dispersion (Kalashnikova *et al.* 2012) which is in accordance with our results.

6.4.2 Encapsulation Efficiency and Loading Capacity

The results of encapsulation efficiency and loading capacity are shown in **Table 9**. Results show that when no CNCs were used, 64% of thyme EO was encapsulated from the emulsion formulation containing 1% thyme EO in the alginate beads. However, when CNCs were introduced in beads formulations, encapsulation efficiency increased from 64 to 83% in the presence of 40% CNCs. Similar trend was found in alginate beads loaded with emulsion formulation containing 3% thyme oil where maximal encapsulation efficiency was attributed to the sample containing 30 and 40% CNCs. It is suggested that the presence of CNCs enhances intermolecular bonding in alginate network in combination with the calcium cations. This can be explained by the negative charges of CNCs generating ionic interaction with positive calcium ions and improving hydrogen bonding within alginate matrices (Kevadiya *et al.* 2010). It was established by Mohammed *et al.* (2015) that CNC-alginate beads improve the absorption of cationic methylene blue ink because of its attraction to positive charges present in the ink. Indeed, in our study, positive charges from calcium cations improve interactions either with alginate carboxylate groups and CNCs negative charges, thus encountering a better encapsulation. Like in CNCs, other authors have observed direct relationship between the added content of organic clays and encapsulation efficiency of drugs or bio-compounds in alginate beads (Zhang *et al.* 2010). Most of the beads studied in literature

in which clays were used (e.g., hydroxyapatite (Zhang *et al.* 2010) or montmorillonite (MMT) (Abou Taleb *et al.* 2012)) showed that the matrices were prone to be more compact compared to the beads without clays.

Table 9 Encapsulation efficiency (%) and loading capacity (%) of different concentrations of thyme EO (prepared from 1 and 3% emulsion) in alginate beads containing 0-40% CNCs.

Encapsulation Efficiency (%)					
% Thyme	% CNCs				
	0	10	20	30	40
1	64.35±1.67 ^{a,A}	64.23 ±8.64 ^{a,A}	62.76±6.54 ^{a,A}	74.34±2.72 ^{b,A}	83.32±3.02 ^{c,A}
3	61.91±7.42 ^{a,A}	68.80±6.59 ^{a,A}	71.76±6.71 ^{a,A}	82.19±10.00 ^{b,A}	83.03±11.81 ^{b,A}
Loading Capacity (%)					
% Thyme	% CNCs				
	0	10	20	30	40
1	0.04±0.00 ^{a,A}	0.04±0.00 ^{ab,A}	0.04±0.00 ^{ab,A}	0.05±0.00 ^{bc,A}	0.05±0.00 ^{c,A}
3	0.12±0.02 ^{a,B}	0.14±0.01 ^{ab,B}	0.14±0.01 ^{b,B}	0.17±0.02 ^{c,B}	0.16±0.02 ^{c,B}

¹Means followed by the same uppercase letter in each column are not significantly different at the 5% level. Means followed by the same lowercase letter in each row for each property are not significantly different at the 5% level.

The concentration of thyme EO in alginate beads was expressed in terms of loading capacity (LC%) as shown in **Table 9**. As expected, alginate beads prepared from 3% thyme EO emulsion showed higher loadings of thyme oil compared to 1% thyme EO emulsion. For instance, at 20% CNCs, the loading of the EO in the alginate beads increased from 0.04 % to 0.14% by increasing from 1 to 3% the thyme oil concentration in the prepared emulsion, respectively. The increase of the LC% is directly related to the thyme concentration used in the emulsion. In addition, it was found that in presence of 40% and 30% of CNCs, high LC% was found respectively in 1 and 3% thyme EO

formulation for the prepared beads. According to Lertsutthiwong *et al.* (2008) the concentration of EO incorporated in alginate nanoparticles is directly proportional to their loading capacity. The authors have observed an increase of LC% from 0.78% to 1.62% (dry mass) by increasing turmeric oil from 0.1 to 0.25% in alginate nanocapsules.

6.4.3 *In vitro* Release Study

The profiles of EO released from alginate beads containing different concentrations of CNCs are depicted in **Figs. 31** and **32**. Graphs can be divided into an initial increasing release phase (Hosseini *et al.* 2013) -also called burst phase- attributed to the release of EO adsorbed at the surface of the alginate beads. In general, this release is associated to a linear diffusion of the EO during the early period of release. Besides, a second phase takes place when alginate beads achieve a time independent diffusion. This final stage was attributed to EO release from inner to outer part of the beads.

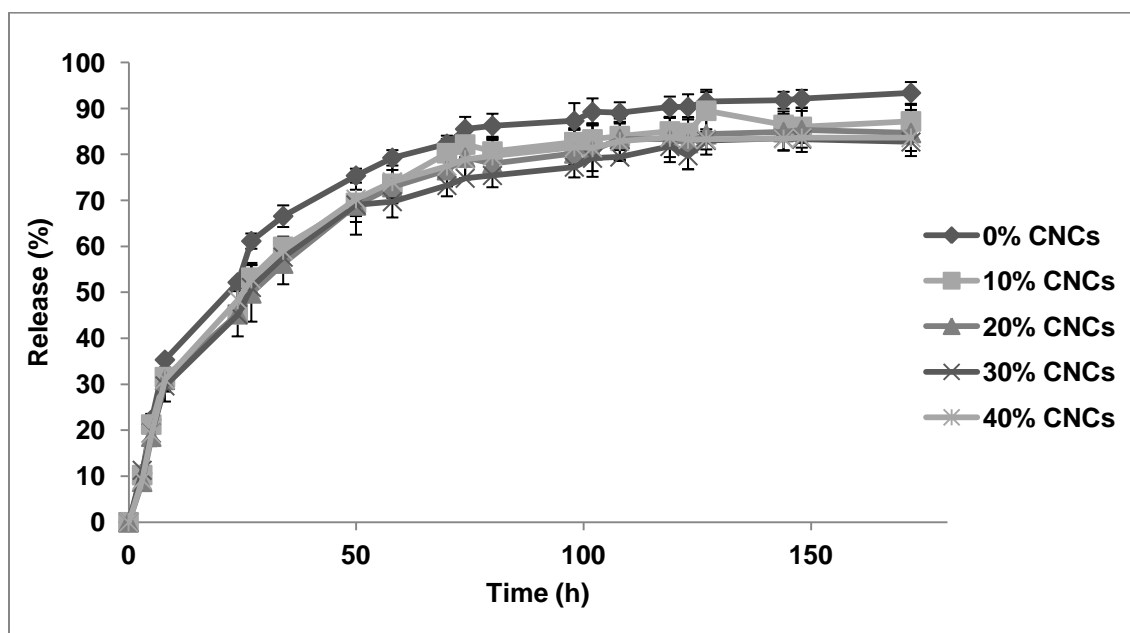


Fig. 31 *In vitro* thyme oil release profile of alginate beads prepared from 1% thyme EO emulsion and 0-40% CNCs.

Fig. 31 shows the release profile of beads prepared from 1% thyme EO emulsion at different concentrations of CNCs. Results showed that a reduction of thyme oil release can be achieved from alginate beads loaded with CNCs. After 80 h, alginate beads loaded with 10% CNCs showed a reduction on cumulative release of 6% with respect to beads without CNCs. This reduction was increased to 8 and 10% when concentrations

of CNCs were at 20 and 30%, respectively. According to Kevadiya *et al.* (2010) and Tunç and Duman (2011) the use of clays such as MMT can also delay bio-compounds release. Kevadiya *et al.* (2010) have also compared the release of diclofenac in loaded alginate beads containing MMT. Authors found that time independent phase of drug release profile in intestinal fluid was delayed by increasing the amount of MMT from 1.0 to 2.5% (w/w). It was suggested by Tunç and Duman (2011) that, as in this study, the addition of 60% MMT increases the diffusion path of carvacrol by releasing 50% of the compound from methylcellulose films after 15 days exposure at 15°C compared to 80% in films without MMT.

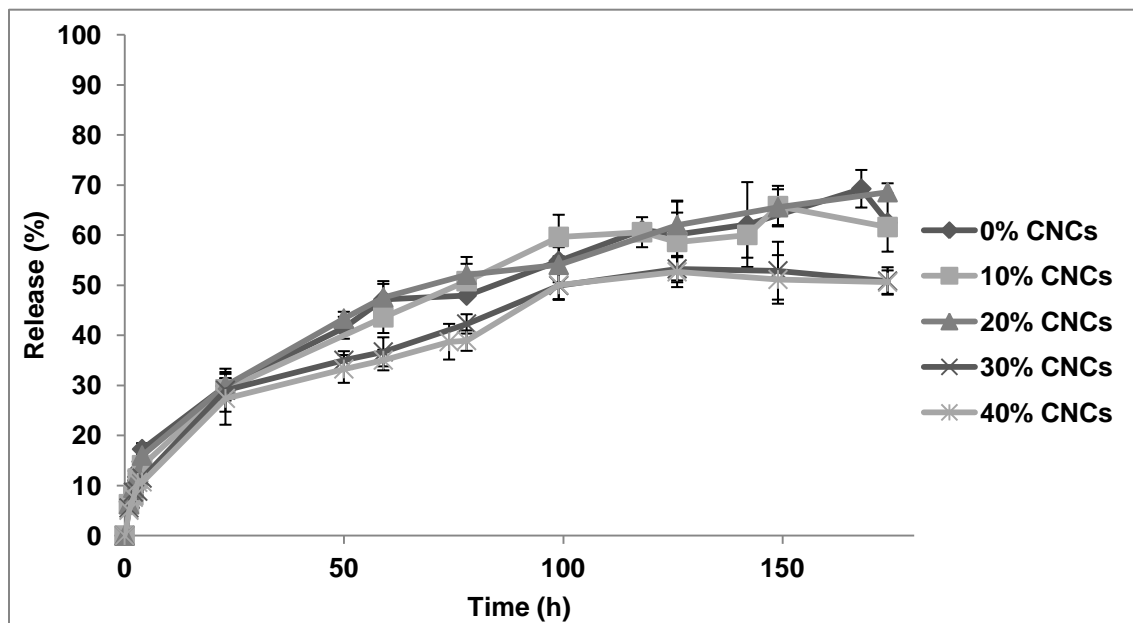


Fig. 32 *In vitro* thyme EO release profile of alginate beads prepared from 3% thyme oil emulsion and 0-40% CNCs.

Results of thyme release from beads prepared with higher concentrations (3%) of thyme EO emulsion are shown in **Fig. 32**. Firstly, an initial burst release during the first 100 hours was observed and by increasing the time of the test, it was observed that alginate beads loaded with 30% and 40% CNC showed a sustained release of 51% after 172 h (day 7). These results can corroborate the observations made in the loaded capacity (LC%) of alginate beads (**Table 9**), where it was noticed that increasing the thyme oil

concentration to 3% (LC 0.12%) leads to longer continuous release period compared to 1% (LC 0.04%). These results were in accordance with the observations made in **Fig. 31** in which the release of EO in simulating solvent was decreased due to the presence of CNCs in alginate beads prepared from 1% thyme EO emulsions.

Table 10 Release parameters of beads prepared from 1-3% thyme EO emulsion in simulating solvent (10% (v/v) ethanol). Parameters n and k represent exponent coefficient and release constant respectively.

Release parameters		
	n	k
1% Thyme - 0% CNCs	0.43	14.30
1% Thyme - 30% CNCs	0.44	11.61
3% Thyme - 0% CNCs	0.37	9.85
3% Thyme - 30% CNCs	0.43	6.77

With the aim to compare the release kinetics of both EO concentrations (1-3%) at the observed optimal conditions of CNCs (30%), the results were fitted to the Korsmeyer-Peppas semi-empirical model (Hosseini *et al.* 2013). Results given by the model are presented in **Table 10**. It was observed that all evaluated systems exhibit exponent coefficients (n) lower than 0.50, indicating that all beads followed a Fickian controlled diffusion. In addition, it was found that the release constant (k) obtained was indirectly proportional to the concentration of EO. For instance, for beads without CNCs, the release constant value decreased from 14.30 to 9.85 when the thyme EO in the emulsion increased from 1 (LC% 0.04) to 3% (LC% 0.12), respectively. Thus, the cumulative release decreased and extended to longer periods of time at higher concentration of EO. Hosseini *et al.* (2013) also observed a decrease of k from 28 to 17 while using 1 to 3% of EO in alginate microparticules. With respect to CNC concentrations and its effect on the release coefficient (k), it was observed that k decreased for all thyme oil loaded beads when CNCs were introduced. Similar observations were reported by Soppirnath and Aminabhavi (2002) who confirmed that the increase of time exposure to glutaraldehyde, a cross-linking agent, reduced the k values in guar gum and acrylamide hydrogels.

6.4.4 *In vitro* Test in "Agar Diffusion Assay" of Alginate Beads

Table 11 shows the *in vitro* antimicrobial evaluation of the beads prepared from 1 and 3% thyme EO emulsions with 0 and 30% CNCs. Neither pure alginate nor alginate + CNC control beads (without thyme oil) exhibited any antimicrobial effect against *Listeria innocua* (data not shown). Beads prepared from 1% thyme EO emulsions did not exhibit any inhibition diameter against the tested bacteria. However, higher concentration of EO (3%) showed a pronounced effect on the agar, showing a 13.19 mm inhibition diameter. Among all the principal constituents, thyme EO used in this study was composed mainly of 35% thymol, 20% γ -terpinene, and 19% *p*-cymene all components with demonstrated antioxidant and antimicrobial effectiveness. Several authors (Cosentino *et al.* 1999; Rota *et al.* 2008) have demonstrated that phenolic compounds play an important role on the antimicrobial activity in thyme EO. Indeed, the reaction mechanism of the phenol compound such as thymol was explained as an attack to the lipid membrane of bacteria when in contact with the EO (Marchese *et al.* 2016). These findings are in agreement with our *in vitro* tests results at 3% EO concentration.

Table 11 Agar diffusion assay of thyme oil loaded alginate beads inoculated with *Listeria innocua* on an initial well diameter of 8 mm.

Sample	Inhibition diameter (mm)
1% Thyme 0% CNCs	-
1% Thyme 30% CNCs	-
3% Thyme 0% CNCs	13.19±1.07
3% Thyme 30% CNCs	10.83±0.10

6.4.5 Volume of Alginate Beads

Volume of beads prepared from 3% thyme oil emulsion is illustrated in **Fig. 33**. Results show a direct correlation of the presence of CNCs on the increase of alginate beads volume. This behaviour was related to the increase of viscosity of the formulation by addition of CNCs (0.46 Pa·s at 0% CNCs and 1.11 Pa·s at 30% CNCs). Thus, introducing CNCs in the emulsion based on thyme EO (3%) led to a larger gelified bead volume (100 mm³) at 30% CNCs compared to bead without CNCs (81 mm³). Indeed,

Gershuny *et al.* (2016) explained that, in a stationary-state, the alginate beads dropping velocity and distance between beads decreased at high viscosities, resulting in a larger bead diameter.

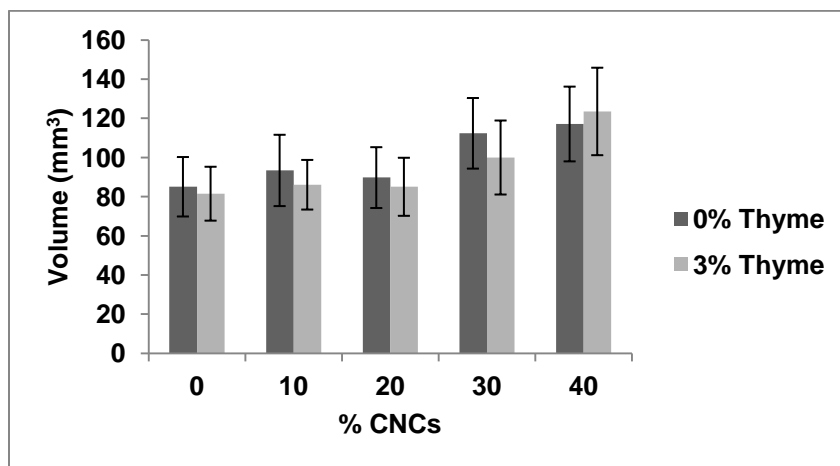


Fig. 33 Calculated volume of beads containing 0-40% CNCs prepared from 0 and 3% of thyme EO emulsions.

6.4.6 Transmission Electron Microscopy (TEM)

Beads with the highest antimicrobial and controlled release properties were chosen for studying their morphological properties. Thus, cross-section of alginate beads prepared from 3% thyme oil emulsion at 0% CNCs was compared to beads with 30% CNCs as illustrated in **Fig. 34**. A heterogeneous and porous matrix was observed in the absence of CNCs (**A**), while in the presence of CNCs (**B**), a homogenous matrix with drastically reduced pores was observed. In fact, these results were correlated with the findings in EE% and release studies from which an enhanced interconnection between alginate and nanocomposite were discussed (Yang *et al.* 2014). Even though the presence of submicron CNC particles were not visible within the alginate network, it can be suggested that the role of CNCs was to help forming a more compact inner bead due to the multiple binding sites with calcium ions and alginate carboxylate groups (Mohammed *et al.* 2015).

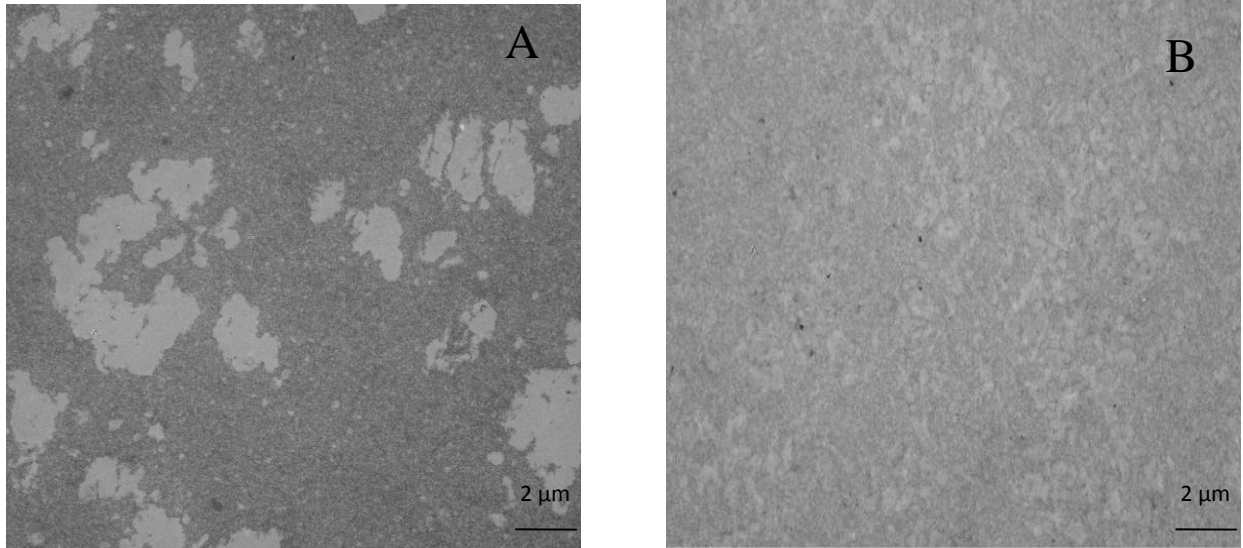


Fig. 34 TEM images (2,000×) of the cross section of alginate beads prepared from 3% thyme EO-loaded emulsion with 0% (A) and 30% CNCs (B).

6.4.7 Fourier Transform Infrared Spectroscopy

Fig. 35 shows the FTIR spectra of beads containing 0-30% CNCs and 0-3% thyme EO. All spectra exhibited six principal peaks at wavenumbers of 3374, 2925, 1616, 1433, 1291, and 1081 cm^{-1} . The strong broad absorption from 3600-3000 cm^{-1} bands represented stretching hydroxyl groups (O-H) belonging to the mannuronate and guluronate residues of alginate copolymer in the beads. Close to these hydroxyl groups, a "shoulder" appeared at wavelength of 2925 cm^{-1} , ascribed to the stretching band of C-H (Fujisawa *et al.* 2011). In the middle section of the spectrum, wavenumbers of 1615 and 1433 cm^{-1} demonstrated the presence of the asymmetrical and symmetrical stretch of carboxylate groups of alginate cross-linked by Ca^{+2} . As observed by Sartori *et al.* (1997) and Angadi *et al.* (2012), the presence of calcium ions in the beads shifts the symmetric stretching peak resulted from the bonding between the calcium ion and the oxygen atom of the carboxylate group from 1412 to 1431 cm^{-1} . As for the glycosidic bond (C-O-C) linking mannuronate and guluronate residues in alginate, the band remained at 1080 cm^{-1} as also observed by Lawrie *et al.* (2007).

Even though CNCs were included in alginate bead formulation, characteristic peaks of CNCs could not be distinguished in FTIR spectra, suggesting that these peaks were overlapped with those of alginate at the same region. Huq *et al.* (2012) who worked with

alginate based films containing CNCs observed similar findings where both materials were overlapped in the FTIR spectra.

FTIR spectra of alginate beads containing thyme EO are recognizable by the fingerprint region. Characteristic peaks of the used *Thymus vulgaris* EO showed a peak at 806 cm^{-1} corresponding to the C-H bond of the major aromatic groups of thymol. The peak observed at a wavenumber of 947 cm^{-1} was assigned to the CH_2 groups of the hydrocarbon chains in the isomeric cyclic γ -terpinenes contained in the EO (Schulz *et al.* 2005).

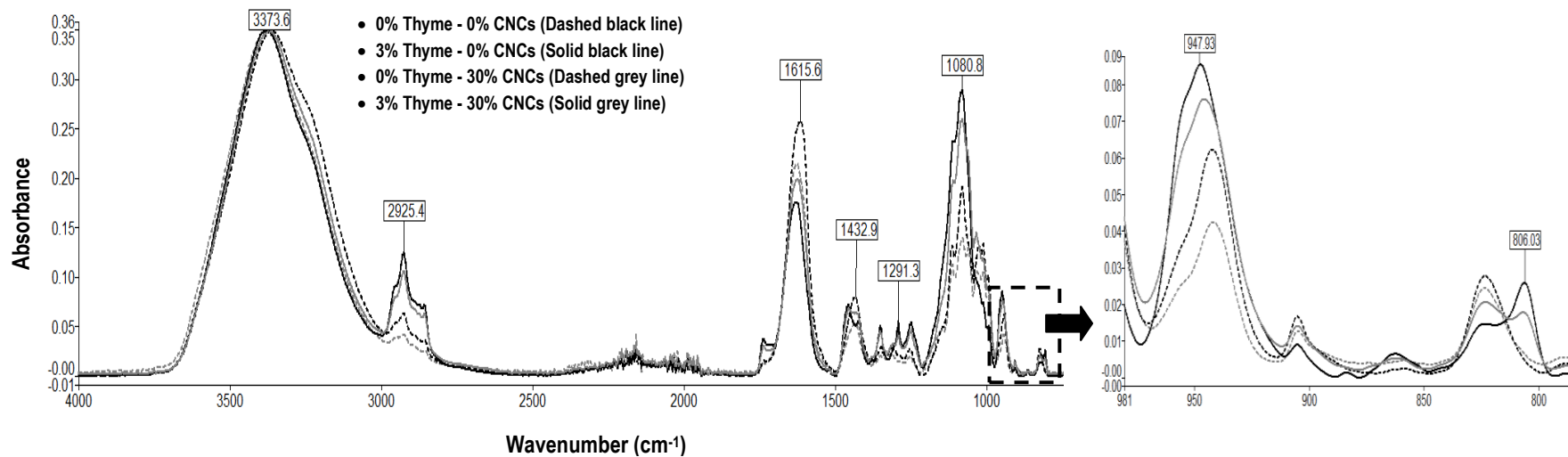


Fig. 35 Fourier Transform Infrared spectra of alginate beads containing 0-3% thyme EO - 0-30% CNCs.

6.4.8 Effect of Thyme EO loaded Alginate Beads and Gamma irradiation on *Listeria innocua* Inoculated Ground Meat

Table 12 presents the effect of thyme EO-loaded beads and gamma irradiation on the elimination of *Listeria innocua* in ground meat during storage. It was observed that meat samples (without beads) with an initial concentration of *Listeria innocua* of 3.81 log CFU/g showed a rapid increase to 6.86 log CFU/g at day 14. This increase was sustained from the first two days with a bacteria growth rate of 0.69 Ln CFU/g-day. When meat was mixed with thyme oil-loaded alginate beads, *Listeria* showed a significant reduction of 1 log CFU/g at day 6 and 2 log CFU/g reduction at day 10 and 14 compared to the control (without beads), respectively. After 6 days, inoculated meat mixed with thyme oil-loaded alginate beads showed higher antibacterial activity with a final concentration of 4.17 log CFU/g at day 14. The determined growth rate of samples containing alginate beads (0% CNCs) was found to be 0.14 Ln CFU/g-day, lower compared to meat samples without any beads. Additionally, results showed that when CNCs were included in alginate beads a sustained controlled growth of *Listeria* was observed during storage. However, it was noticed that samples containing CNCs showed a slower decrease of bacteria from day 6 to day 14 compared to the control beads without CNCs (0.17 and 0.14 Ln CFU/g.day, respectively). In fact, this behaviour was correlated with the results found in both diffusion assay and *in vitro* release tests in ethanol 10% v/v where CNCs contributed to a slow release of EO. It is suggested that beneficial effects of CNCs can be detected at even longer storage periods depending on the targeted food application. Related to literature, Tunç and Duman (2011) also noticed that the presence of 60% of MMT in methylcellulose films applied on sausage decreased the carvacrol release rate during storage time (21 days).

Table 12 *Listeria innocua* growth on ground meat mixed with alginate beads prepared from 3% thyme EO emulsion at 0% (Thyme) and 30% CNCs (Thyme+CNC) treated with gamma irradiation doses from 0 to 3 kGy.

Dose		Day				
		0	2	6	10	14
0 kGy	Control	3.81±0.05 ^{a,A}	3.89±0.05 ^{a,B}	4.85±0.07 ^{b,C}	6.27±0.11 ^{c,B}	6.86±0.11 ^{d,C}
	Thyme	3.74±0.06 ^{a,A}	3.62±0.09 ^{a,A}	3.57±0.2 ^{a,A}	4.08±0.2 ^{b,A}	4.17±0.12 ^{b,A}
	Thyme+CNC	3.76±0.10 ^{a,A}	3.67±0.03 ^{a,A}	4.13±0.23 ^{b,B}	4.25±0.11 ^{b,A}	4.71±0.09 ^{c,B}
0.5 kGy	Control	3.00±0.34 ^{a,C}	2.58±0.09 ^{a,B}	3.54±0.11 ^{b,C}	4.21±0.40 ^{c,B}	5.17±0.43 ^{d,B}
	Thyme	2.37±0.19 ^{c,B}	1.98±0.05 ^{b,A}	1.57±0.09 ^{a,A}	1.42±0.12 ^{a,A}	2.32±0.56 ^{bc,A}
	Thyme+CNC	2.25±0.29 ^{b,A}	2.07±0.29 ^{b,A}	2.34±0.05 ^{b,B}	1.59±0.27 ^{a,A}	2.08±0.41 ^{ab,A}
1 kGy	Control	2.20±0.20 ^{abc,B}	1.95±0.13 ^{abc,C}	1.94±0.06 ^{ab,B}	3.05±0.67 ^{bcd,B}	4.10±0.55 ^{cd,B}
	Thyme	1.32±0.25 ^{bc,A}	1.68±0.18 ^{d, B}	0.96±0.23 ^{abc,A}	0.66±0.20 ^{ab,A}	0.58±0.00 ^{ab,A}
	Thyme+CNC	1.27±0.16 ^{b,A}	0.88±0.00 ^{a,A}	0.92±0.23 ^{a,A}	0.70±0.16 ^{a,A}	ND
1.5 kGy	Control	0.81±0.31 ^{a,B}	0.58±0.00 ^{a,A}	0.00±0.00 ^{a,A}	0.58±0.00 ^a	0.58±0.00 ^a
	Thyme	0.58±0.00 ^{a,A}	ND	ND	ND	ND
	Thyme+CNC	0.58±0.00 ^{a,A}	ND	ND	ND	ND
3 kGy	Control	0.88±0.42 ^a	0.58±0.00 ^a	ND	ND	ND
	Thyme	ND	ND	ND	ND	ND
	Thyme+CNC	ND	ND	ND	ND	ND

¹Means followed by the same uppercase letter in each column are not significantly different at the 5% level. Means followed by the same lowercase letter in each row for each property are not significantly different at the 5% level.

²ND means not detected (<0.6 log CFU/g)

Synergistic response is demonstrated when combined effects of several methods induce a higher performance than the use of single methods separately (Bjergager *et al.* 2012). In this study, gamma irradiation was applied on ground meat mixed with thyme oil loaded alginate beads in order to study its effect on *Listeria* growth (**Table 12**). Results showed that gamma irradiation of meat samples enhanced the reduction of bacteria content at all applied doses. For instance, by treating meat with thyme EO-loaded beads and gamma irradiation at 0.5 kGy, *Listeria* concentration was reduced from 3.54 log CFU/g (no beads) to 1.57 log CFU/g after 6 days of storage. In addition, higher reduction of 3 log CFU/g was noticed in samples loaded with beads at day 6 with respect to control samples without any treatment (0 kGy). These results suggest a synergistic effect between thyme EO and gamma irradiation at low doses. Similar findings were discussed by other authors (Ouattara *et al.* 2002; Huq *et al.* 2015) who also observed a synergistic effect of EOs such as oregano, mustard, cinnamon, thyme oil with gamma irradiation. Huq *et al.* (2015) demonstrated that in order to reduce 1 log CFU/g of *Listeria monocytogenes* the required irradiation dose decreases from 0.54 to 0.45 when oregano EO encapsulated in beads was spread onto ham samples.

Considering alginate beads prepared with thyme EO and CNCs, it was observed that the combined treatment at 0.5 kGy at day 6 exhibited a 1 log CFU/g reduction with respect to meat without beads at the same irradiation dose. Results also demonstrated a 2 log CFU/g reduction with respect to the controls at 0 kGy.

In addition, it was observed that the 0.5 kGy treatment with alginate beads in presence of CNCs allows a sustained growth of bacteria from day 6 to day 14 compared to a bacteria increase (0.75 log CFU/g) observed in the system with beads without CNCs. Even though the influence of doses up to sterilizing conditions (25 kGy) on the alteration of composition of *Thymus vulgaris* EO (Haddad *et al.* 2007) is discarded, it can be hypothesized that the presence of the CNCs could have avoided a rapid release of the EO and preventing dump release.

By increasing the irradiation doses to 1 kGy, control samples (without any beads) showed an important reduction of 1.6 log CFU/g at day 0 compared to their control at 0 kGy. This reduction was even more important within storage period of 10 days where reduction was of 3 log CFU/g compared to the control without any treatment at day 10. This phenomenon can be explained by the fact that gamma irradiation is a cold process that induces DNA double strand to break and lead to bacterial death (Hussain *et al.*

2014). In addition, at 1 kGy, samples with beads loaded with thyme EO showed a reduction of *Listeria* of 2.6 and 3.2 log CFU/g when beads were prepared without and with CNCs, respectively.

Although, when meat without any beads was treated at 1.5 kGy, *Listeria* was still detected at day 14. On the contrary, when treated at 3 kGy a complete elimination of *Listeria* was observed after 2 days of storage. It is important to highlight that treatments with thyme EO loaded beads and γ -irradiation at 1.5 kGy and 3 kGy allowed a decrease of *Listeria innocua* of 3.2 log CFU/g and 3.7 log CFU/g with respect to their control (without beads and without irradiation) at day 0 (**Table 12**). By applying gamma-irradiation at a dose of 1.5 kGy in presence of active alginate beads, no detectable *Listeria* was observed from day 2 until the end of the experiment (**Table 12**). Treatment at 3 kGy with alginate beads did not reveal any *Listeria* formation from day 0.

In comparison with other studies done at similar doses, a reduction of 4 log CFU/g in meat inoculated with *Listeria monocytogenes* was observed when irradiation doses of 2.5 kGy were applied (Monk *et al.* 1994).

6.4.9 Effect of Combined Treatment in Mesophilic Total Flora (MTF) on Ground Meat

The results of the shelf-life of meat samples are shown on **Figs. 36-38**. According to Ministère de l'Agriculture, des Pêcheries et de l'Alimentation du Québec (MAPAQ 2009) limited concentration of MTF is an important criteria for the determination of a product's shelf-life. In meat, this concentration should be lower than 6 log CFU/g before the product loses its freshness and risk affects the consumer.

In this study, results depicted in **Fig. 36** for control meat samples (without beads at 0 and 0.5 kGy) exhibited an MTF level of 5.6 log CFU/g, exceeding, thus, its acceptable limit of MTF after only 0 days of storage. At doses of 1 and 1.5 kGy, MTF level in meat demonstrated a reduction of ~2 log CFU/g compared to control samples (0 kGy) at day 0. It was observed in these samples that meat shelf-life was about 10 days at which point MTF achieved 6.4 and 6 log CFU/g for 1 and 1.5 kGy, respectively. At 3 kGy dose, MTF level exhibited a reduction of 4 log CFU/g with respect to the control (no beads and 0 kGy) during the whole storage. Therefore, high dose of 3 kGy was the only dose that allows an increase of shelf-life for meat longer than 14 days.

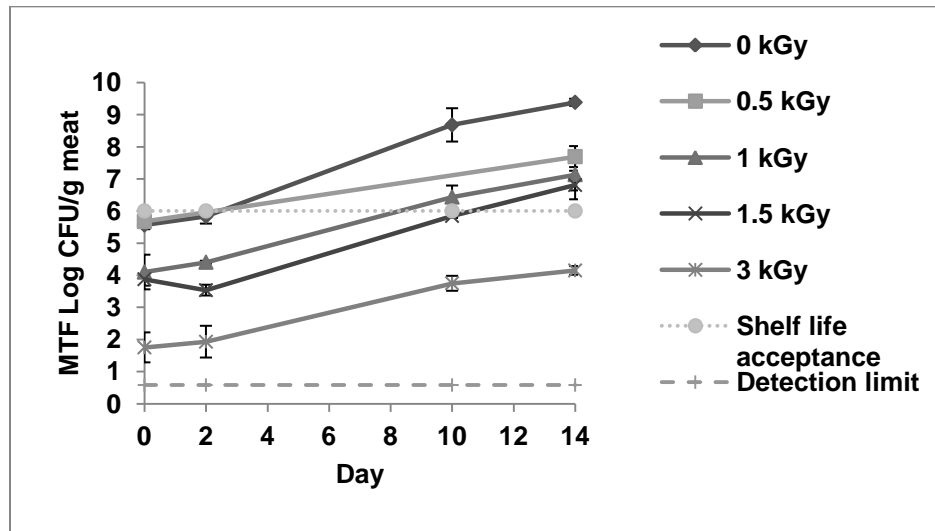


Fig. 36 Mesophilic Total Flora (MTF) growth on ground meat without beads as a function of gamma irradiation doses (0-3 kGy).

Results of the effect of active beads (without CNCs) and γ -irradiation on meat shelf-life are represented in **Fig. 37**. Similar to the behaviour observed in meat without beads, meat samples with active beads irradiated at 0 and 0.5 kGy showed a rapid end of shelf-life (>0 days). Remarkable synergistic effects were observed at doses ≥ 1 kGy where MTF level in meat samples with the active beads showed lower values than meat without beads or γ -treatment. For instance, meat irradiated at 1 kGy with active beads, showed an MTF concentration of 6 log CFU/g rather than 6.8 log CFU/g found in samples without beads tested at day 14. Compared to the increasing MTF level observed from day 2 (1.9 log CFU/g) to 14 (4.1 log CFU/g) in samples without any bead, 3 kGy treatment in presence of active beads allowed a long meat shelf-life of 14 days with MTF of 2 log CFU/g.

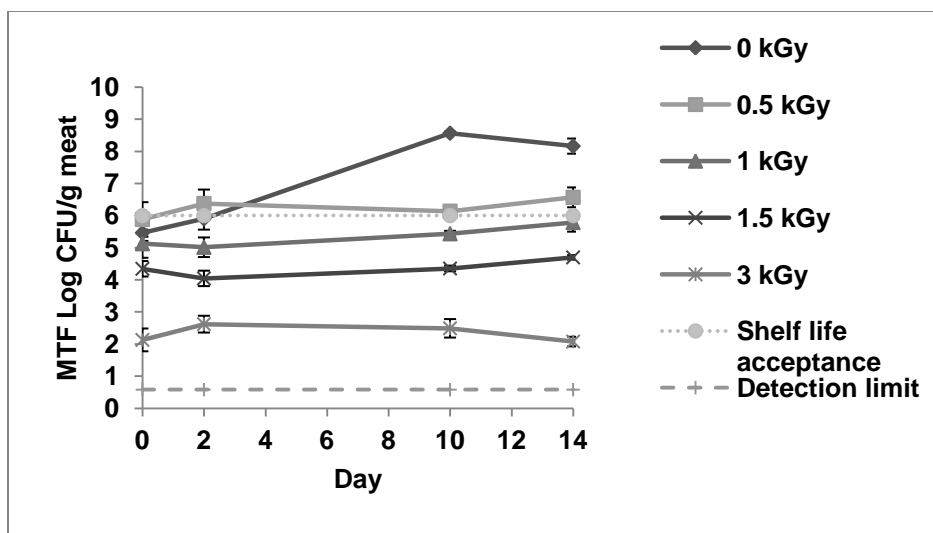


Fig. 37 Mesophilic Total Flora (MTF) growth on ground meat mixed with alginate beads (prepared from 3% thyme EO emulsion and 0% CNCs) as a function of gamma irradiation doses (0-3 kGy).

Synergistic effects were also found by Dussault *et al.* (2012) who showed that a dose of 1.5 kGy extended the shelf-life of fresh pork sausages to 14 days compared to 7 days in the untreated control. In this study, a dose of 1.5 kGy showed a stable level of MTF at a 4 log CFU/g during the whole storage period (13 days) of sausages. This extension of sausage shelf-life is probably due to the addition of preservatives such as salt and spices which have already demonstrated an effect on bacteria growth rate and an influence with gamma irradiation (Sommers and Fan 2003).

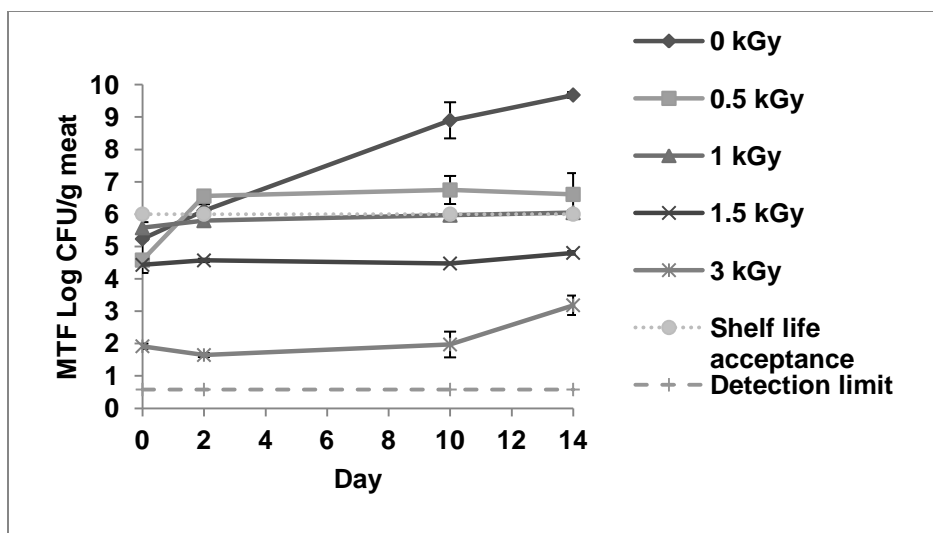


Fig. 38 Mesophilic Total Flora (MTF) growth on ground meat mixed with alginate beads (prepared from 3% thyme EO emulsion and 30% CNCs) as a function of gamma irradiation doses (0-3 kGy).

Mesophilic Total Flora (MTF) growth showed different behaviour when samples were treated with thyme EO beads containing CNCs and gamma irradiation (**Fig. 38**). It was observed that meat samples treated at irradiation doses range of 0-1 kGy and alginate beads exceed MTF limits from day 2. Also, from day 0 it was observed that samples treated at 3 kGy exhibited a 4 log CFU/g reduction and bacteria stability until 10 days. In addition, samples irradiated at 3 kGy with active beads and CNCs maintained a lower concentration from 2 log CFU/g until 3.2 log CFU/g observed at day 14.

Even though this study was mainly focused on the effect of gamma irradiation and active beads on MTF, it has been shown by Molins *et al.* (1987), Thayer *et al.* (1993), and Ye *et al.* (2017) that predominately gram-positive *Lactobacillus* spp, *Micrococcus* spp or gram-negative *Pseudomonas* spp, and *Enterobacteriaceae* spp are flora related to pork meat spoilage. Based on the species and the environmental conditions, these bacteria can create off-flavours, off-odours and slime production during storage time of meat product.

6.5 Conclusions

Alginate beads were prepared by ionic gelation procedure with various concentrations of thyme essential oil and CNCs. It was found that preparation of alginate beads containing high concentrations of CNCs (10-40%) led to increased EE% and LC% at two tested concentrations of essential oil. Moreover, *in vitro* test studies in simulated solvent demonstrated a reduced cumulative release of thyme essential oil when CNCs concentrations higher than 30% w/w (polymer dry weight) were used. Antimicrobial activity of thyme loaded alginate beads and gamma irradiation showed an existing synergistic effect against *Listeria innocua* and MTF. *In situ* results demonstrated a complete inhibition of *Listeria* from day 0 when doses of 3 kGy were applied on the samples loaded with the active alginate beads. In addition, synergistic effect was also observed to sustain the shelf-life of ground meat irradiated at 1 kGy with alginate beads prepared with thyme essential oil, which was extended to 14 days compared to 2 days when meat was treated without either gamma-irradiation or antimicrobial beads.

6.6 Acknowledgements

This research was supported by Natural Sciences and Engineering Research Council of Canada (NSERC) and FPInnovations (Pointe-Claire, QC, Canada) through a collaborative research project. This research was also supported by the International Atomic Energy Agency (IAEA) contract no: F22063 and by NSERC, discovery program. The authors would also like to thank Nordion Int. Inc. for irradiation treatments.

6.7 References

- Abou Taleb MF, Hegazy DE, Ismail SA (2012) Radiation synthesis, characterization and dye adsorption of alginate–organophilic montmorillonite nanocomposite. *Carbohydr Polym* 87: 2263–2269. <https://doi.org/10.1016/j.carbpol.2011.10.058>
- Adams MR, Moss MO (2000) Bacterial agents of foodborne illness. In: *Food Microbiology*. pp 184–271.
- Angadi SC, Manjeshwar LS, Aminabhavi TM (2012) Novel composite blend microbeads of sodium alginate coated with chitosan for controlled release of amoxicillin. *Int J Biol Macromol* 51: 45–55. <https://doi.org/10.1016/j.ijbiomac.2012.04.018>
- Bjergager M-BA, Hanson ML, Solomon KR, Cedergreen N (2012) Synergy between prochloraz and esfenvalerate in *Daphnia magna* from acute and subchronic exposures in the laboratory and microcosms. *Aquat Toxicol* 110–111:17–24. <https://doi.org/10.1016/j.aquatox.2011.12.001>
- Caillet S, Lacroix M (2006) Effect of gamma radiation and oregano essential oil on murein and ATP concentration of *Listeria monocytogenes*. *J Food Prot* 69: 2961–2969. <https://doi.org/10.1111/j.1750-3841.2009.01368>
- Caillet S, Shareck F, Lacroix M (2005) Effect of gamma radiation and oregano essential oil on murein and ATP concentration of *Escherichia coli* O157:H7. *J Food Prot* 68: 2571–2579. <https://doi.org/10.4315/0362-028X-68.12.2571>
- Campos-Requena VH, Rivas BL, Pérez MA, et al (2015) Polymer/clay nanocomposite films as active packaging material: Modeling of antimicrobial release. *Eur Polym J* 71: 461–475. <https://doi.org/10.1016/j.eurpolymj.2015.08.018>
- Center for Food Safety and Applied Nutrition (2009) *Ingredients, Additives, GRAS & Packaging - Guidance for industry: Recommendations for submission of chemical and technological data for direct food additive petitions*. <https://www.fda.gov/Food/GuidanceRegulation/GuidanceDocumentsRegulatoryInformation/IngredientsAdditivesGRASPackaging/ucm124917.htm>. Accessed 20 Aug 2017
- Cha DS, Cooksey K, Chinnan MS, Park HJ (2003) Release of nisin from various heat-pressed and cast films. *LWT - Food Sci Technol* 36: 209–213. [https://doi.org/10.1016/S0023-6438\(02\)00209-8](https://doi.org/10.1016/S0023-6438(02)00209-8)
- Cosentino S, Tuberoso CIG, Pisano B, et al (1999) In-vitro antimicrobial activity and chemical composition of Sardinian Thymus essential oils. *Lett Appl Microbiol* 29: 130–135. <https://doi.org/10.1046/j.1472-765X.1999.00605.x>
- Donsì F, Annunziata M, Sessa M, Ferrari G (2011) Nanoencapsulation of essential oils to enhance their antimicrobial activity in foods. *LWT - Food Sci Technol* 44: 1908–1914. <https://doi.org/10.1016/j.lwt.2011.03.003>
- Dussault D, Benoit C, Lacroix M (2012) Combined effect of γ -irradiation and bacterial-fermented dextrose on microbiological quality of refrigerated pork sausages. *Radiat Phys Chem* 81: 1098–1102. <https://doi.org/10.1016/j.radphyschem.2011.11.031>
- European Commission (2007) *Commission Directive 2007/19/EC of 2 April 2007 amending Directive 2002/72/EC relating to plastic materials and articles intended to come into contact with food and Council Directive 85/572/EEC laying down the*

- list of simulants to be used for testing migration of constituents of plastic materials and articles intended to come into contact with foodstuffs. https://www.fsai.ie/uploadedFiles/Legislation/Legislation_Update/Cor_to_Dir2007_19.pdf. Accessed 20 Oct 2018
- Fujisawa S, Okita Y, Fukuzumi H, et al (2011) Preparation and characterization of TEMPO-oxidized cellulose nanofibril films with free carboxyl groups. *Carbohydr Polym* 84: 579–583. <https://doi.org/10.1016/j.carbpol.2010.12.029>
- Gershuny V, Walter J, Washburn A (2016) Effect of viscosity on bead shape of polydimethylsiloxane fluid flowing down a fiber. *J Fluid Mech* 1–9
- Government of Canada National Research Council Canada (2014) CNC-1: Cellulose Nanocrystal powder certified reference material - national research council canada. https://www.nrc-cnrc.gc.ca/eng/solutions/advisory/crm/certificates/cnc_1.html. Accessed 22 Oct 2018
- Haddad M, Herent M-F, Tilquin B, Quetin-Leclercq J (2007) Effect of gamma and e-beam radiation on the essential oils of *Thymus vulgaris thymoliferum*, *Eucalyptus radiata*, and *Lavandula angustifolia*. *J Agric Food Chem* 55: 6082–6086. <https://doi.org/10.1021/jf063540+>
- Hossain F, Follett P, Dang Vu K, et al (2016) Evidence for synergistic activity of plant-derived essential oils against fungal pathogens of food. *Food Microbiol* 53, Part B:24–30. <https://doi.org/10.1016/j.fm.2015.08.006>
- Hosseini SM, Hosseini H, Mohammadifar MA, et al (2013) Incorporation of essential oil in alginate microparticles by multiple emulsion/ionic gelation process. *Int J Biol Macromol* 62: 582–588. <https://doi.org/10.1016/j.ijbiomac.2013.09.054>
- Huq T, Salmieri S, Khan A, et al (2012) Nanocrystalline cellulose (NCC) reinforced alginate based biodegradable nanocomposite film. *Carbohydr Polym* 90: 1757–1763. <https://doi.org/10.1016/j.carbpol.2012.07.065>
- Huq T, Vu KD, Riedl B, et al (2015) Synergistic effect of gamma (γ)-irradiation and microencapsulated antimicrobials against *Listeria monocytogenes* on ready-to-eat (RTE) meat. *Food Microbiol* 46: 507–514. <https://doi.org/10.1016/j.fm.2014.09.013>
- Hussain PR, Omeera A, Suradkar PP, Dar MA (2014) Effect of combination treatment of gamma irradiation and ascorbic acid on physicochemical and microbial quality of minimally processed eggplant (*Solanum melongena* L.). *Radiat Phys Chem* 103: 131–141. <https://doi.org/10.1016/j.radphyschem.2014.05.063>
- Jamshidian M, Tehrany EA, Desobry S (2012) Release of synthetic phenolic antioxidants from extruded poly lactic acid (PLA) film. *Food Control* 28: 445–455. <https://doi.org/10.1016/j.foodcont.2012.05.005>
- Kaboorani A, Auclair N, Riedl B, Landry V (2016) Physical and morphological properties of UV-cured cellulose nanocrystal (CNC) based nanocomposite coatings for wood furniture. *Prog Org Coat* 93: 17–22. <https://doi.org/10.1016/j.porgcoat.2015.12.009>
- Kalashnikova I, Bizot H, Bertoncini P, et al (2012) Cellulosic nanorods of various aspect ratios for oil in water Pickering emulsions. *Soft Matter* 9: 952–959. <https://doi.org/10.1039/C2SM26472B>

- Kevadiya BD, Patel HA, Joshi GV, et al (2010) Montmorillonite-alginate composites as a drug delivery system: intercalation and in vitro release of diclofenac sodium. *Indian J Pharm Sci* 72: 732–737. <https://doi.org/10.4103/0250-474X.84582>
- Kim H-J, Jo C, Lee N-Y, et al (2005) Effect of gamma irradiation on physiological activity of citrus essential oil. *J Korean Soc Food Sci Nutr* 34: 797–804. <https://doi.org/10.3746/jkfn.2005.34.6.797>
- Labuza TP (1996) Introduction to active packaging for foods. *Food technology (USA)*
- Lawrie G, Keen I, Drew B, et al (2007) Interactions between alginate and chitosan biopolymers characterized using FTIR and XPS. *Biomacromolecules* 8: 2533–2541. <https://doi.org/10.1021/bm070014y>
- Lertsutthiwong P, Noomun K, Jongaroonngamsang N, et al (2008) Preparation of alginate nanocapsules containing turmeric oil. *Carbohydr Polym* 74: 209–214. <https://doi.org/10.1016/j.carbpol.2008.02.009>
- Li B, Kennedy JF, Peng JL, et al (2006) Preparation and performance evaluation of glucomannan–chitosan–nisin ternary antimicrobial blend film. *Carbohydr Polym* 4: 488–494. <https://doi.org/10.1016/j.carbpol.2006.02.006>
- MAPAQ (2009) Lignes directrices et normes pour l'interprétation des résultats analytiques en microbiologie alimentaire. Ministère de l'Agriculture, des Pêcheries et de l'Alimentation du gouvernement de Québec. <https://www.mapaq.gouv.qc.ca/fr/Publications/recueil.pdf>
- Marchese A, Orhan IE, Daglia M, et al (2016) Antibacterial and antifungal activities of thymol: A brief review of the literature. *Food Chem* 210: 402–414. <https://doi.org/10.1016/j.foodchem.2016.04.111>
- Mohammed N, Grishkewich N, Berry RM, Tam KC (2015) Cellulose nanocrystal–alginate hydrogel beads as novel adsorbents for organic dyes in aqueous solutions. *Cellulose* 22: 3725–3738. <https://doi.org/10.1007/s10570-015-0747-3>
- Molins RA, Kraft AA, Marcy JA (1987) Extension of the shelf-life of fresh ground pork with polyphosphates. *J Food Sci* 52: 513–514. <https://doi.org/10.1111/j.1365-2621.1987.tb06661.x>
- Monk JD, Clavero MRS, Beuchat LR, et al (1994) Irradiation inactivation of *Listeria monocytogenes* and *Staphylococcus aureus* in low- and high-fat, frozen and refrigerated ground beef. *J Food Prot* 57: 969–974. <https://doi.org/10.4315/0362-028X-57.11.969>
- Nerio LS, Olivero-Verbel J, Stashenko E (2010) Repellent activity of essential oils: A review. *Bioresour Technol* 101: 372–378. <https://doi.org/10.1016/j.biortech.2009.07.048>
- Ouattara B, Giroux M, Yefsah R, et al (2002) Microbiological and biochemical characteristics of ground beef as affected by gamma irradiation, food additives and edible coating film. *Radiat Phys Chem* 63: 299–304. [https://doi.org/10.1016/S0969-806X\(01\)00516-3](https://doi.org/10.1016/S0969-806X(01)00516-3)
- Oussalah M, Caillet S, Saucier L, Lacroix M (2007) Inhibitory effects of selected plant essential oils on the growth of four pathogenic bacteria: *E. coli* O157:H7, *Salmonella Typhimurium*, *Staphylococcus aureus* and *Listeria monocytogenes*. *Food Control* 18: 414–420. <https://doi.org/10.1016/j.foodcont.2005.11.009>

- Oussalah M, Caillet S, Saucier L, Lacroix M (2006) Antimicrobial effects of selected plant essential oils on the growth of a *Pseudomonas putida* strain isolated from meat. *Meat Sci* 73: 236–244. <https://doi.org/10.1016/j.meatsci.2005.11.019>
- Peppas NA, Sahlin JJ (1989) A simple equation for the description of solute release. III. Coupling of diffusion and relaxation. *Int J Pharm* 57: 169–172. [https://doi.org/10.1016/0378-5173\(89\)90306-2](https://doi.org/10.1016/0378-5173(89)90306-2)
- Public Health Agency of Canada (2015) Yearly food-borne illness estimates for Canada. In: aem. <https://www.canada.ca/en/public-health/services/food-borne-illness-canada/yearly-food-borne-illness-estimates-canada.html>. Accessed 20 Oct 2018
- Qian C, McClements DJ (2011) Formation of nanoemulsions stabilized by model food-grade emulsifiers using high-pressure homogenization: Factors affecting particle size. *Food Hydrocoll* 25: 1000–1008. <https://doi.org/10.1016/j.foodhyd.2010.09.017>
- Rasooli I, Rezaei MB, Allameh A (2006) Ultrastructural studies on antimicrobial efficacy of thyme essential oils on *Listeria monocytogenes*. *Int J Infect Dis* 10: 236–241. <https://doi.org/10.1016/j.ijid.2005.05.006>
- Rota MC, Herrera A, Martínez RM, et al (2008) Antimicrobial activity and chemical composition of *Thymus vulgaris*, *Thymus zygis* and *Thymus hyemalis* essential oils. *Food Control* 19: 681–687. <https://doi.org/10.1016/j.foodcont.2007.07.007>
- Salvia-Trujillo L, Rojas-Graü MA, Soliva-Fortuny R, Martín-Belloso O (2013) Effect of processing parameters on physicochemical characteristics of microfluidized lemongrass essential oil-alginate nanoemulsions. *Food Hydrocoll* 30: 401–407. <https://doi.org/10.1016/j.foodhyd.2012.07.004>
- Sartori C, Finch DS, Ralph B, Gilding K (1997) Determination of the cation content of alginate thin films by FT-IR spectroscopy. *Polymer* 38: 43–51. [https://doi.org/10.1016/S0032-3861\(96\)00458-2](https://doi.org/10.1016/S0032-3861(96)00458-2)
- Schultz S, Wagner G, Urban K, Ulrich J (2004) High-Pressure homogenization as a process for emulsion formation. *Chem Eng Technol* 27: 361–368. <https://doi.org/10.1002/ceat.200406111>
- Schulz H, Özkan G, Baranska M, et al (2005) Characterisation of essential oil plants from Turkey by IR and Raman spectroscopy. *Vib Spectrosc* 39: 249–256. <https://doi.org/10.1016/j.vibspec.2005.04.009>
- Soliman EA, El-Moghazy AY, El-Din MSM, Massoud MA (2013) Microencapsulation of essential oils within alginate: formulation and in vitro evaluation of antifungal activity. *J Encapsulation Adsorpt Sci* 03: 48–55. <https://dx.doi.org/10.4236/jeas.2013.31006>
- Sommers C, Fan X (2003) Gamma irradiation of fine-emulsion sausage containing sodium diacetate. *J Food Prot* 66: 819–824. <https://doi.org/10.4315/0362-028X-66.5.819>
- Soppirnath KS, Aminabhavi TM (2002) Water transport and drug release study from cross-linked polyacrylamide grafted guar gum hydrogel microspheres for the controlled release application. *Eur J Pharm Biopharm* 53: 87–98. [https://doi.org/10.1016/S0939-6411\(01\)00205-3](https://doi.org/10.1016/S0939-6411(01)00205-3)

- Sussman G (2006) Management of the wound environment with dressings and topical agents. In: Wound Care Treatment & Management: Medical Care, Surgical Care, Future and Controversies. pp 250–267
- Thayer DW, Boyd G, Jenkins RK (1993) Low-dose gamma irradiation and refrigerated storage *in vacua* affect microbial flora of fresh pork. J Food Sci 58: 717–719. <https://doi.org/10.1111/j.1365-2621.1993.tb09342.x>
- Tunç S, Duman O (2011) Preparation of active antimicrobial methyl cellulose/carvacrol/montmorillonite nanocomposite films and investigation of carvacrol release. LWT - Food Sci Technol 44: 465–472. <https://doi.org/10.1016/j.lwt.2010.08.018>
- Yang J, Han C, Xu F, Sun R (2014) Simple approach to reinforce hydrogels with cellulose nanocrystals. Nanoscale 6: 5934–5943. <https://doi.org/10.1039/C4NR01214C>
- Ye K, Wang K, Liu M, et al (2017) Mathematical modelling of growth of *Listeria monocytogenes* in raw chilled pork. Lett Appl Microbiol 64: 309–316. <https://doi.org/10.1111/lam.12721>
- Zhang J, Wang Q, Wang A (2010) In situ generation of sodium alginate/hydroxyapatite nanocomposite beads as drug-controlled release matrices. Acta Biomater 6: 445–454. <https://doi.org/10.1016/j.actbio.2009.07.001>
- Zhu W, Ma W, Li C, et al (2015) Well-designed multihollow magnetic imprinted microspheres based on cellulose nanocrystals (CNCs) stabilized Pickering double emulsion polymerization for selective adsorption of bifenthrin. Chem Eng J 276: 249–260. <https://doi.org/10.1016/j.cej.2015.04.084>

7. PUBLICATION 4: CELLULOSE NANOCRYSTALS (CNCS) LOADED ALGINATE FILMS AGAINST LIPID OXIDATION OF CHICKEN BREAST

This article will be submitted to Food Research International Journal

Paula Criado¹, Carole Frascini², Stéphane Salmieri¹, Monique Lacroix^{1*}

¹Research Laboratories in Sciences Applied to Food, Canadian Irradiation Centre,
INRS–Institut Armand-Frappier, Institute of Nutraceutical and Functional Foods, 531
Blvd des Prairies, Laval, Quebec, H7V 1B7, Canada

²FPIInnovations, 570 Blvd Saint-Jean, Pointe-Claire, Québec, H9R 3J9, Canada

*Corresponding author: Professor Monique Lacroix, Tel: +1 (450)687-5010 #4489,
Fax: +1 (450)686-5501, E-mail: monique.lacroix@iaf.inrs.ca

The number of figures and tables were adjusted in this article in order to follow the sequence of the thesis document. The style of references was presented according to the guidelines of the journal.

CONTRIBUTION OF AUTHORS

This research study was done by Paula Criado under supervision of Pr. Monique Lacroix and Dr. Carole Fraschini. During the experiments, Stephane Salmieri assisted with the analysis and oxygen permeability discussions. This article was written by Paula Criado and both Pr. Lacroix and Dr. Carole Fraschini were participating in discussions of the reported results and in the corrections of the manuscript.

RÉSUMÉ

Comparé à la viande de boeuf ou de porc, la poitrine de poulet est un produit qui se distingue par sa teneur élevée en acides gras polyinsaturés (PUFA). Cependant, lorsque ces acides gras présents dans les aliments entrent en contact avec l'oxygène ou les rayons UV, ils ont tendance à s'oxyder, et il en résulte l'apparition d'odeurs désagréables et de changements de couleur. Grâce à leur transparence et propriétés comestibles, les enrobages représentent une solution alternative pour protéger la viande contre des facteurs dommageables externes tels que l'humidité et l'oxygène.

Les nanocristaux de cellulose (CNCs) sont un produit dérivé de la cellulose possédant comme caractéristiques principales des dimensions nanométriques et un haut degré de cristallinité. Grâce à leur capacité à être dispersés en milieu aqueux, les CNCs ont été utilisés pour renforcer des matrices polymériques à base de polysaccharides. Dans cette étude, les CNCs ont été introduits à différentes concentrations (0-30%, base sèche) dans des films d'alginate avec pour objectif d'évaluer leur rôle d'agent de renforcement et leur capacité à prévenir l'oxydation des lipides dans la poitrine de poulet. L'effet barrière à la lumière UV et la perméabilité à l'oxygène (OP) des films d'alginate contenant 0-30% de CNCs ont été évalués dans des conditions d'humidité relative de 0, 50 et 70% RH. La concentration plus performante de CNCs a été déterminée et le film d'enrobage a été appliqué sur des poitrines de poulet. Le degré d'oxydation des lipides a été déterminé en utilisant les tests permettant de quantifier les valeurs d'hydroperoxydes (PV) et les substances réactives à l'acide thiobarbiturique (TBARS). Les résultats ont démontré un effet barrière notable à la lumière UV et une réduction d'OP de 25% à 70% RH lorsque 30% CNCs étaient ajoutés dans les films d'alginate. Les tests de PV et de TBARS ont également indiqué une diminution du degré d'oxydation des gras dans le poulet traité par les films d'alginate contenant 30% de CNCs aux jours 1 et 3 d'entreposage, sans indication d'oxydation démontrée par la couleur.

ABSTRACT

Compared to other types of meats such as beef or pork, chicken breast constitutes one of the foods with valuable amount of polyunsaturated fatty acid (PUFA). However, when these fatty acids present in food come into contact with oxygen or UV light they are prone to oxidation resulting in off-odours and off-colour. Because of their transparency and edible properties, coatings have been an alternative solution to meat for bringing protection against external damaging factors such as humidity and oxygen.

Cellulose nanocrystals (CNCs) are a product derived from lignocellulosic material with nanometric dimensions and high crystallinity as main characteristics. Because of their ability to be dispersed in aqueous solutions, CNCs have been used to reinforce polysaccharidic matrices. In this study, CNCs at different concentrations were introduced in alginate-based films with the aim to evaluate their reinforcing properties and their role against oxidation of fatty acids in chicken breast samples. For this purpose, UV barrier properties and the oxygen permeability (OP) of alginate-based films loaded from 0-30% CNCs (w/w polymer, dry basis) were evaluated at 0, 50, and 70% RH. The best performing film was used to coat chicken breasts and lipid oxidation was assessed during storage through lipid peroxide value (PV), thiobarbituric acid reagent substances (TBARS) quantification and color variability measurements. Results showed promising

UV barrier effects and 25% decrease of OP at 70% RH when 30% CNCs were loaded in alginate films. Edible coating on chicken breasts also demonstrated a decrease of PV and TBARS at day 1 and 3 when 30% CNCs were used and no oxidative changes were indicated by color.

7.1 Introduction

Chicken is one of the most consumed and one of the healthier lean protein sources in North America, along with beef and pork. It constitutes an important nutritional source of conjugated linoleic acid (CLA) and bioactive peptides (Cavani *et al.*, 2009; Gibbs *et al.*, 2010; Ryan *et al.*, 2011). However, because of the presence of a large amount of unsaturated fatty acids, oxidative reactions can easily take place resulting in off-colour and off-flavour side-reactions.

In matrices such as cheese (Nawar, 1996), oxidation might be desirable whereas in meat it can lead to a dissatisfied consumer. In meat, the main reactions taking place during lipid oxidation are autoxidation due to atmospheric triplet oxygen ($^3\text{O}_2$) through a free radical reaction mechanism attacking polyunsaturated fatty acids. In the presence of UV light, metals contained in meat can also induce a photosensitized oxidation reaction caused by the action of singlet oxygen. These two types of oxidation reactions will end up in the formation of lipid peroxides compounds that are rapidly decomposed to several by-products including aldehydes, ketones, alcohols, and hydrocarbons.

In order to reduce the impact of lipid oxidation in meat, the application of an edible coating has demonstrated promising antioxidant properties due to its protective role against oxygen transmission through the food matrix. According to Ustunol (2009), edible coatings are not intended for replacing synthetic packaging materials but for bringing a secondary protection to food once the primary packaging has been opened. The interest of using polysaccharides (gellan, alginate, pectin) is based on their acceptance as food additives, biodegradability and easy manufacturing processes. Examples found in literature revealed that biopolymers such as methylcellulose and whey protein exhibited lower oxygen permeability at room temperature and 50% RH compared to that of low density polyethylene (LDPE) and high density polyethylene (HDPE) (Miller and Krochta, 1997).

Even though biopolymers show good barrier properties, nanofillers can also be added to contribute or improve their properties without affecting their nature. First discovered by Rånby (1949), cellulose nanocrystals (CNCs) have been characterized for their non-toxicity, large surface area and nanometric dimensions (Lima and Borsali, 2004; Terech *et al.*, 1999) making them of significant big interest for applications for multiple fields including food packaging.

In biopolymers, CNCs have demonstrated a valuable contribution to the enhancement of oxygen barrier properties in matrices such as polylactic acid (PLA), collagen and whey protein (Karkhanis *et al.*, 2018; Long *et al.*, 2018; Sukyai *et al.*, 2018).

The aim of this study was to evaluate i) the reinforcing effect of CNCs on alginate based films and ii) their protective effect against lipid oxidation of chicken breast when added to the edible formulation. Light transmittance and oxygen permeability of films were studied and best performing films were chosen to serve as edible coating of chicken breast. Oxidative by-products such as thiobarbituric acid reagent substances (TBARS) and lipid hydroperoxides were quantified through TBARS and peroxide values tests, while color changes were determined by CIE LAB measurements during a storage period of 8 days.

7.2 Materials and Methods

7.2.1 Chemicals

Barium chloride dihydrate, ferrous sulfate heptahydrate, ammonium thiocyanate, and Whatman No. 1 filter paper were obtained from Fisher Scientific (Whitby, ON, Canada). Isopropanol, hexane, butanol, acetic acid, and synthetic glycerol were purchased from Laboratory MAT (Québec, QC, Canada). Methanol was bought from Greenfield Global - Les Alcools de Commerce (Boucherville, QC, Canada). Thiobarbituric acid, trichloroacetic acid, hydrochloric acid and alginic acid sodium salt from brown algae were purchased from Sigma Aldrich (Oakville, ON, Canada) and used without further purification. Finally, cellulose nanocrystals were kindly provided by FPIInnovations (Pointe Claire, QC, Canada).

7.2.2 Preparation of Alginate-based Films Loaded with Cellulose Nanocrystals (CNCs)

A 3.4% w/w sodium alginate solution was prepared in distilled water under overnight stirring. Meanwhile, a suspension of 1.5% w/w CNCs was then prepared dispersing a pre-weighed amount of CNCs in distilled water under constant stirring. A sonication procedure was then applied to a 200 mL suspension of CNCs using a 500 W and 20 kHz Qsonica sonicator (Fisher Scientific, ON, Canada). The suspensions were sonicated at 1000 J/g CNCs with 60% amplitude. The CNC suspension was then added to alginate solution at different concentrations (0, 10, 20, 30, and 40 % w/w CNCs based on polymer dry weight or corresponding to 0, 7, 14, and 19 % w/w in dry basis). Glycerol

was then added at a final concentration of 0.5% w/w and distilled water was added to adjust alginate solution final concentration to 2% w/w. All the suspensions were degassed overnight under vacuum and suspensions were casted in petri dishes and let to air dry.

7.2.3 Characterization of Alginate-based Films

Optical Transmittance of Alginate-based Films

The optical transmittance of alginate based films was measured using a Cary 100 Bio UV-visible spectrophotometer (Agilent Technologies Canada Inc.). The transmission spectra of films were recorded in the 200-800 nm wavelength range and background was recorded in air as proposed by Dai *et al.* (2016).

Differential Interference Contrast (DIC) Microscopy of Alginate-based Films

Alginate-, CNCs-based films and alginate-based films containing CNCs were cut and mounted on glass slides and sealed each of it with cover slips. Images of the films were recorded with a Zeiss LSM780 microscope equipped with an EC Plan-Neofluar 40x/1.30 Oil M27 objective and final images were analyzed with Zen 2011 software (Zeiss).

Birefringence of Alginate-based Solutions

Prepared solutions of alginate films in absence (0% CNCs) and in presence of 10 to 30% CNCs (w/w, equivalent to a suspension at 0.6% w/w) were observed through cross-polarizers under magnetic stirring in order to observe CNCs dispersibility in alginate solutions.

Oxygen Permeability of Alginate-based Films

An OX-TRAN Model 1/50 (Minneapolis, MN, USA) was used to measure the oxygen transmission rate of alginate films loaded with CNCs at 0 and 30% (w/w polymer, dry basis). Tests were performed by setting relative humidity to 0, 50, and 70% at temperature of 23°C under atmospheric conditions. The oxygen transmission rate (OTR) of films was expressed in $\text{cm}^3/\text{m}^2\cdot\text{day}$. The film area was adjusted to 5 cm^2 with an aluminum foil mask. In order to determine oxygen permeability (OP) OTR results were multiplied by the average thickness of each film measured at 5 random positions with a type ID-S112TX Mitutoyo micrometer (BDI Canada Inc., Laval, QC, Canada). For

consideration of repeatability of samples, at least two films per formulation were analyzed.

The oxygen permeability of alginate films loaded with CNCs was calculated according to **Eq. 23**:

$$OP_{30\% \text{ CNCs}} = OP_{2\% \text{ Alg}} - (\text{Concentration of CNCs in dry basis} * OP_{100\% \text{ CNCs}}) \quad (23)$$

7.2.4 Lipid Oxidation Tests of Food Matrices

Preparation of Coated Chicken Samples

Entire chicken breasts were freshly bought from a nearby IGA grocery store (Laval, QC, Canada). The samples were cut in pieces of approximately 10 g each and then stored in a plastic bag. The samples were coated on their upper surface with the edible coating film (0 and 30% w/w CNCs, polymer dry basis) and then placed on an aluminum foil to create a barrier underneath the sample. For comparison purposes, control samples were placed under the same storage conditions (8 days) without any edible coating films.

Extraction of Lipids

A given quantity of chicken breast (10 g) was ground until complete homogenization in 10 mL of isopropanol and 20 mL of hexane using an Ultraturrax tissue blender (IKA, Ottawa, ON, Canada). The mixture was then filtered through a Whatman No. 1 filter paper and then dried by flushing nitrogen gas. The fatty residue was dried until constant weight was achieved. The samples were kept for analysis of peroxide values.

Peroxide Value Determination

Peroxide formation in meat samples was determined according to the original international dairy federation standard method. The method is based on the oxidation of ferrous (Fe^{2+}) to ferric (Fe^{3+}) ions by peroxides and the peroxide value was measured through a colorimetric test using ammonium thiocyanate (7.5 g in 25 mL water) and iron solutions (0.8 % w/v of barium chloride solution added to 1% w/v iron sulfate solution and 1 mL of HCl (10N)). Thus, fat extracted from samples (approx. 5 mg) was re-suspended in 1.5 mL of methanol: butanol working solution (2:1 v/v) and vortexed until complete homogenization. Detection of lipid peroxides was performed by reacting 7 μL of ammonium thiocyanate followed by addition of 7 μL of iron solution. Samples were incubated for 20 min at room temperature and absorbance was read at 510 nm

wavelength using a S-3100 UV spectrometer (Scinco co, Toronto, ON, Canada). The peroxide value (PV) (mEq/kg) was determined according to **Eq. 24**.

$$PV = \frac{A_{\text{sample}} - A_{\text{blank}}}{m_o(\text{g}) * 2 * 55.84} * \text{slope} \quad (24)$$

Where A_{blank} is the absorbance of the working solvent with the respective reagents and the m_o is the weight of the lipid extract used for peroxide value determination. The standard curve was prepared using different concentrations of iron (0 - 1.9 μg) and the slope was calculated using a linear regression protocol, resulting in a value of 0.035 ($R^2 = 0.99$).

Water Retention of Alginate based Film Loaded with CNCs

Water loss of meat was evaluated during storage period. The given weight of meat (g) with and without coating taken at day x (1, 3, 6, and 8) was compared to the initial weight at day 0 as shown in **Eq. 25**:

$$\text{Meat water loss (\%)} = \frac{\text{Weight meat}_{\text{day 0}} - \text{Weight meat}_{\text{day x}}}{\text{Weight meat}_{\text{day 0}}} * 100 \quad (25)$$

Coated samples were selected with the aim to measure the water retention capacity of the film. Thus, the water retention percentage was defined as the capacity of the system (meat + film) to retain weight from day 0 compared to weight at day X, as it is shown in **Eq. 26** :

$$\text{Water retention percentage (\%)} = \frac{\text{Weight (meat+film)}_{\text{day X}}}{\text{Weight (meat+film)}_{\text{day 0}}} * 100 \quad (26)$$

Thiobarbituric Acid Reagent Substances (TBARS)

Lipid oxidation of control and coated chicken samples was determined according to the method described by Oussalah *et al.* (2004). Briefly, an amount of approx. 5 g chicken breast was blended with 25 mL of distilled water and 5 mL trichloroacetic acid solution (15% w/w). The mixture was then centrifuged and the supernatant (2 mL) was mixed with 0.5 mL of the thiobarbituric acid solution for 90 min at 95°C. After incubation, the absorbance was measured at 520 nm in a S-3100 UV spectrometer (Scinco co, Toronto,

ON, Canada). Because the interaction of malondialdehyde (MDA) with protein (Igene *et al.*, 1980) might lead to TBARS value underestimation, a third-derivative calculation was applied to the spectrum in order to eliminate muscle interactions with protein and baseline tilts (Botsoglou *et al.*, 1994). The third derivative spectra were calculated using an online derivative application tool (<https://www.nwlifescience.com/sg>) with three as value parameter for both polynomial and derivative order.

Color of Chicken Breast

Color of chicken breast is considered as one of the primary attribute for consumer selection in its uncooked state (Fletcher, 2002). In raw poultry breast, a pale pink color is expected and desirable while in raw thigh and leg meat a dark red color is expected. It has been studied by Miller (1994) that the presence of myoglobin is the main reason for the color of meat, and it can differ depending on the animal species, muscle types, and age. For instance, it was demonstrated that old poultry meat had the lowest myoglobin content (0.01 mg myoglobin/g meat), followed by 26-week male poultry chicken breast (0.10 mg/g) and 26-week male poultry dark meat (1.50 mg/g) (Fletcher, 2002). These values are lower compared to young lamb (2.50 mg/g), dark meat fish species (5.3-24.4 mg/g) or old beef (16-20 mg/g).

Chicken breast meat color for coated and uncoated samples was examined using a standard CIE LAB color system with a Colormet colorimeter (Instrumar limited, St John's, NF, Canada). As explained in previous sections, cut pieces of chicken breast samples were coated with the respective alginate film on the top surface. In order to evaluate the colour, both lightness (L) and redness (a^*) were measured at day 0 and 8 and a number of 10 samples were analyzed for each group.

7.3 Statistical Analysis

The tests peroxide value and TBARS were done in duplicate and for each replicate at least three samples were analyzed and for color tests the number of replicates analyzed was ten. In order to evaluate the differences between groups at identical storage period, the variance (ANOVA) test was performed. The software PASW statistics base 16 (SPSS Inc. Chicago, IL, USA) was used for processing the data and differences within samples were identified at $p \leq 0.05$.

7.4 Results

7.4.1 Light Transmittance, Morphology of Films, and Birefringence of Alginate Solutions Loaded with CNCs

The optical transmittance of alginate-based films loaded with 0-30% CNCs in wavelength range of 200-800 nm is illustrated in **Fig. 39**. For all UV regions, UVC (100 - 280 nm), UVB (280 - 320 nm), and UVA (320 - 400 nm) showed that increasing the concentration of CNCs in the film leads to a decrease of the optical transmittance. It is known that at wavelength range of 315 to 400 nm 98% of the UV radiation reaches earth (Padera, 2013). Thus, at 400 nm, it was observed that the formulation with no CNCs shows a light transmission value of 83% compared to 72% when 30% CNCs were added to the films. At 320 nm wavelength (UVB range) a similar trend was observed with a 70% of transmittance when film with 0% CNCs was used compared to 55% when film was loaded with 30% CNCs.

The difference in the optical properties of films is related to the presence of CNCs and their inherent properties for scattering light. Similar decreasing effect was obtained when other nanoparticles such as TiO₂ (Ren *et al.*, 2015) were used. CNCs can play the role of UV filters which would find potential applications in food packaging (Mestdagh *et al.*, 2005; Van *et al.*, 2001) but also in photographic lenses (Lindfors and Ylianttila, 2016) or sunscreen creams (Dondi *et al.*, 2006).

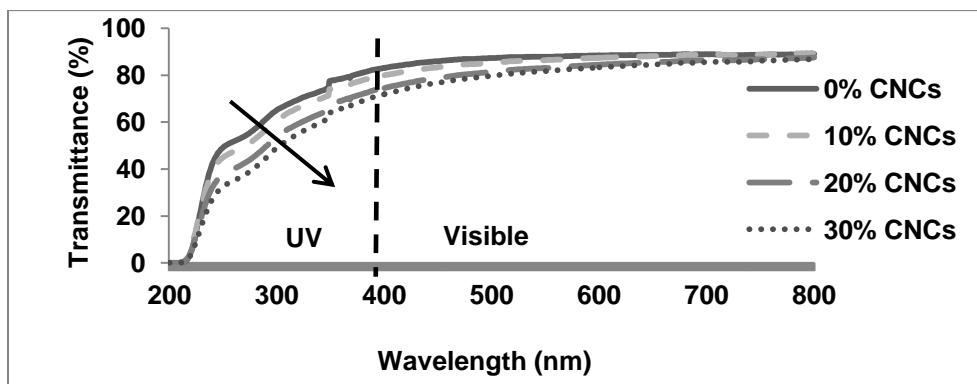


Fig. 39 Optical transmittance of alginate-based films loaded with cellulose nanocrystals (CNCs)

DIC microscopy images demonstrated a rough surface when pure CNCs films were observed in DIC microscopy (**Fig. 40A**). On the contrary, alginate-based films showed a

flat and smooth surface (**Fig. 40B**) that was changing from translucent to a more dense appearance as the CNCs loading was gradually increased (**Fig. 40C-E**). In order to confirm the nanoscale dispersion of CNCs in alginate film, birefringence of the initial solutions containing CNCs was assessed and results are presented in **Fig. 41**. Dispersibility of CNCs has been the focus of numerous studies to confirm CNCs homogeneous dispersion in various media (Fleming *et al.*, 2000, 2001; Viet *et al.*, 2007). The nanoparticles have the ability to self-assembly into chiral nematic structures in a certain range of concentrations under shear. When the pitch of the chiral nematic structure is similar to the wavelength of the visible light, the particles are able to reflect light giving an iridescent appearance to the solution that can be observed through cross-polarizers (de Vries, 1951; Pan *et al.*, 2010; Revol *et al.*, 1992).

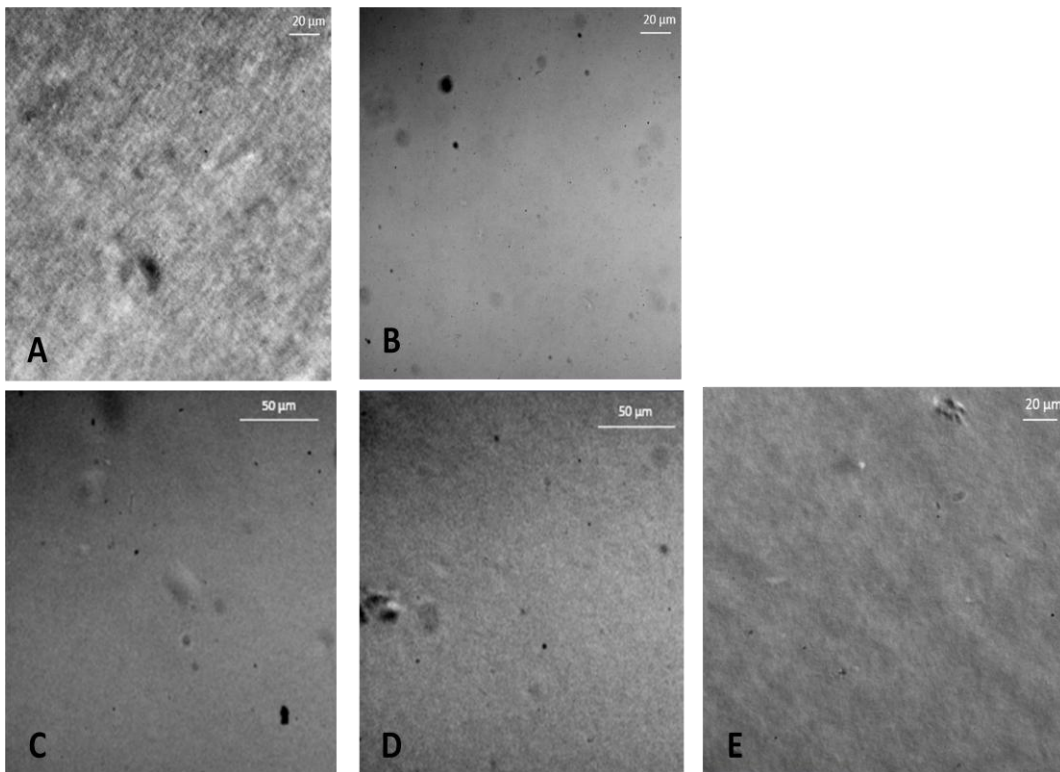


Fig. 40 DIC microphotographs of CNCs films (A) and alginate films loaded with 0% CNCs (B), 10% CNCs (C), 20% CNCs (D), and 30% CNCs (E)

As observed in **Fig. 41**, CNCs suspension (**Fig. 41A**) demonstrated an iridescent appearance characteristic of CNCs liquid crystalline order. When alginate solutions were observed through cross-polarizers no birefringence was detected (**Fig. 41B**). However, when CNCs were added to the polymer solution from 10% to 30% CNCs (**Figs. 41C-E**)

the suspension recovered its birefringence due to the addition of CNCs and high visual effects were obtained at 10% and 20% of the nanomaterial. On the other hand, no clear effect was observed at 30% loaded CNCs and rather an opaque suspension was obtained at this concentration which can be ascribed to the high viscosity (770 mPa·s). Although in our study glycerol was added to the solutions for plasticizing purposes, similar results were observed by Ureña-Benavides *et al.* (2010) in 1% sodium alginate solution loaded with CNCs. The authors Ureña-Benavides *et al.* (2010) described the effect of birefringence of CNCs in the suspensions as a representation of the particles remaining in order within the suspension.

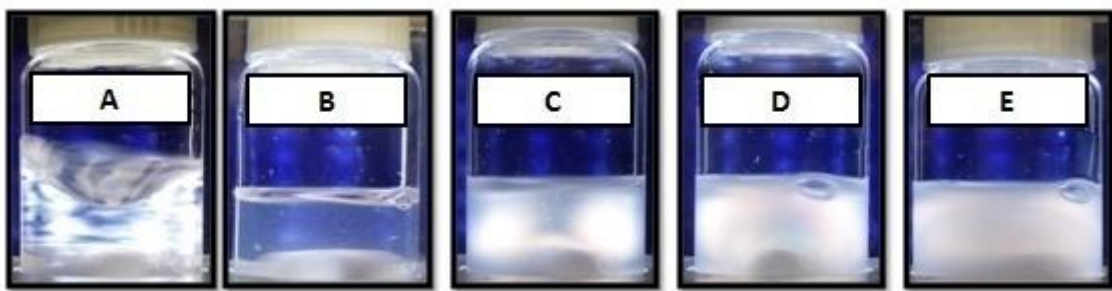


Fig. 41 Birefringence of CNC suspension at 0.6% w/w (A), alginate solution (B) and alginate solution with dispersed CNCs at 10% (C), 20% (D), and 30% w/w (E) as observed through cross-polarizers under magnetic stirring

7.4.2 Oxygen Permeability of Alginate-based Films Loaded with Cellulose Nanocrystals (CNCs)

Oxygen permeability results of alginate based-films loaded with 0, 30, and 100% CNCs-based films are shown in **Table 13**. Results show that oxygen permeability is proportional to relative humidity. Alginate-based films without CNCs at 0% RH exhibited an OP of $125 \text{ cm}^3 \cdot \mu\text{m}/\text{m}^2 \cdot \text{day}$, lower compared to the homologue film tested at 70% RH for which OP was approximately $1748 \text{ cm}^3 \cdot \mu\text{m}/\text{m}^2 \cdot \text{day}$.

Other studies also confirmed the exponential increase of oxygen permeability with %RH in materials like ethylene vinyl alcohol (Gontard *et al.*, 1996) or in cellulosic materials (Aulin *et al.*, 2010; Cozzolino *et al.*, 2016; Miettinen *et al.*, 2014; Zhang *et al.*, 2015). In fact, it has been suggested that the presence of water in films creates a plasticizing effect, softening the polymer chains and improving the gas diffusion through the matrix.

Table 13 Oxygen permeability (OP) ($\text{cm}^3 \cdot \mu\text{m}/\text{m}^2 \cdot \text{day}$) of pure CNCs-based and alginate-based films containing 0 and 30% CNCs at characterized at different relative humidity (%) and comparison with the calculated OP values according to Eq. 23.

Oxygen Permeability ($\text{cm}^3 \cdot \mu\text{m}/\text{m}^2 \cdot \text{day}$)			
Films	Relative Humidity (%)		
	0%	50%	70%
Alginate 2% - 0% CNCs	125 ± 16	361 ± 10	1748 ± 53
CNCs 100%	111 ± 16	373 ± 26	1071 ± 63
Alginate 2% - 30% CNCs _{exp}	105 ± 8	229 ± 7	1300 ± 126
Alginate 2% - 30% CNCs _{cal}	92	250	1427

In food, as water activity (a_w) relates to the free content of water but also to the relative humidity surrounding the product, taking into consideration this key parameter will be important. For example, a_w of tomato and lettuce is 0.95, raw poultry 0.70, white bread 0.35, and salami 0.30.

With respect to the effect of CNCs in alginate-based films, it was shown in **Table 13** that the oxygen permeability evaluated at 70% RH loaded with 30% CNCs was lower ($1300 \text{ cm}^3 \cdot \mu\text{m}/\text{m}^2 \cdot \text{day}$) as compared to the control film without CNCs ($1748 \text{ cm}^3 \cdot \mu\text{m}/\text{m}^2 \cdot \text{day}$) ($p \leq 0.05$). A similar trend was observed at 50% RH where the oxygen permeability of films exhibited a decrease from 361 to 229 $\text{cm}^3 \cdot \mu\text{m}/\text{m}^2 \cdot \text{day}$ with addition of 0% to 30% CNCs, respectively ($p \leq 0.05$). In addition, when the oxygen permeability of films loaded with CNCs was predicted (**Eq. 23**) from known OP of alginate and pure CNCs, it was perceived that calculated values were close to those calculated.

At 0% RH no difference in OP was noticed for both types of films, according to Wang *et al.* (2018), under these conditions (0% RH) the films become rigid and vitreous, reason why the effect of CNCs is no longer noticeable in alginate-based films. On the contrary, when water activity increases, with increased high relative humidity, it can be suggested that the films became viscous or soft, reason why a high oxygen permeability was obtained. Even though the relative humid conditions could have increased the oxygen permeability of the films, it can be suggested that the presence of CNCs could have brought more rigidity to the material and then improved the barrier properties (Fortunati *et al.*, 2012; Xing and Matuana, 2016). Sanchez-Garcia and Lagaron (2010) reported a similar trend of oxygen permeability of PLA films when measured at 80% RH. The authors mentioned that PLA films had an oxygen permeability of $1.37 \cdot 10^{-17}$

$\text{m}^3 \cdot \text{m} / \text{s} \cdot \text{m}^2 \cdot \text{Pa}$ which was decreased to $0.15 \cdot 10^{-17} \text{ m}^3 \cdot \text{m} / \text{s} \cdot \text{m}^2 \cdot \text{Pa}$ by the addition of 3 % wt of CNCs.

According to Huq *et al.* (2012) the addition of CNCs contributes to the crystallinity of alginate films as observed by X-Ray diffraction. This phenomenon was also reported by other authors as the reason for the improved oxygen barrier effects in starch-based films (Liu *et al.*, 2018) and poly(lactic acid)-based films (Karkhanis *et al.*, 2018).

7.4.3 Lipid Peroxide Values of Chicken Coated Samples

Fig. 42 shows the amount of lipid hydroperoxides formed in chicken breast during storage at 4°C. Starting from day 1, differences between samples coated with films loaded with 0% CNCs and with 30% CNCs can be noticed. The peroxide values (PV) demonstrated that samples coated with alginate films loaded with 0% CNCs had a significantly ($p \leq 0.05$) higher concentration of fat PV (0.01 mEq/kg) compared to the samples coated with alginate films loaded with 30% CNCs (0.001 mEq/kg). On the same day, no significant difference ($p > 0.05$) was noticed for the control (no coating) and samples coated with alginate-based film loaded with 0% CNCs samples. At day 3, similar effect was obtained where samples coated with alginate-based films loaded with 0% CNCs exhibited higher PVs (0.007 mEq/kg) compared to 30% CNCs loaded alginate films (0.002 mEq/kg). Finally, at day 8 it was observed that control samples exhibited the highest value of 0.003 mEq/kg compared to the coated samples where it was found absence of peroxide formation. During the 8 days of storage it was observed that control samples (without coating) showed increased values of PV compared to those loaded with CNCs.

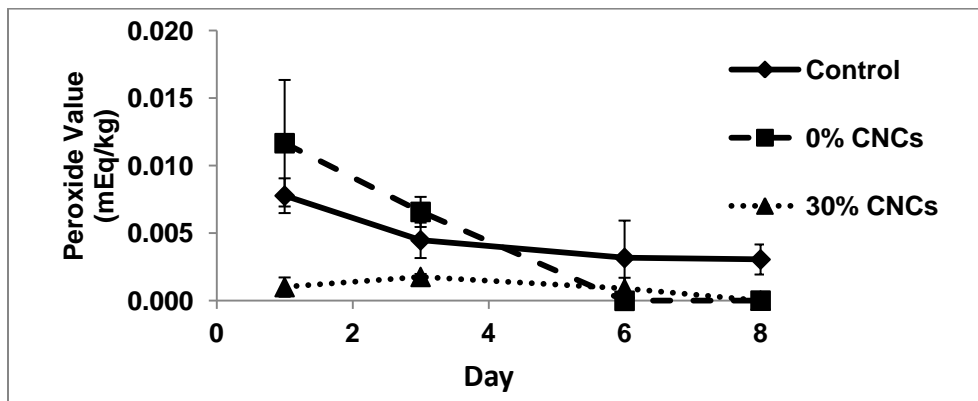


Fig. 42 Peroxide values (mEq/kg) of chicken coated with alginate-based films loaded at different concentrations of CNCs (control, 0, 30% CNCs)

Many studies have demonstrated the protecting role of film coatings against lipid oxidation of food matrices (Debeaufort *et al.*, 1998; Rodriguez-Turienzo *et al.*, 2012). Hence, some authors (Bolin, 1980; Labuza and Dugan, 1971) have studied the effect of moisture on food matrices oxidation. For instance, Labuza *et al.* (1969) reviewed the kinetics of oxidation of food and showed that lipid oxidation rate decreases with increasing the water activity. Other studies also showed that PV values in samples with low a_w such as nuts (a_w 0.6) exhibited lower PV concentrations (0.26 mEq/kg) compared to those exhibited in food with high a_w such as chicken (a_w 1.0) observed as 0.08 mEq/kg found in chicken breast samples (da Silva *et al.*, 2018).

Therefore, with the aim to evaluate the effect of water and understand the behavior observed in peroxide value results, the displacement of water in the studied samples (e.g., meat water loss and water retention of the meat+film system) was analyzed (Fig. 43). It was observed that meat coated with edible films lost approximately 20% of water compared to 3% water loss in control samples (without coating) (Fig. 43A). Nevertheless, the presence of the coating provides a physical barrier for retaining water in the system (meat and film) as observed in Fig. 43B.

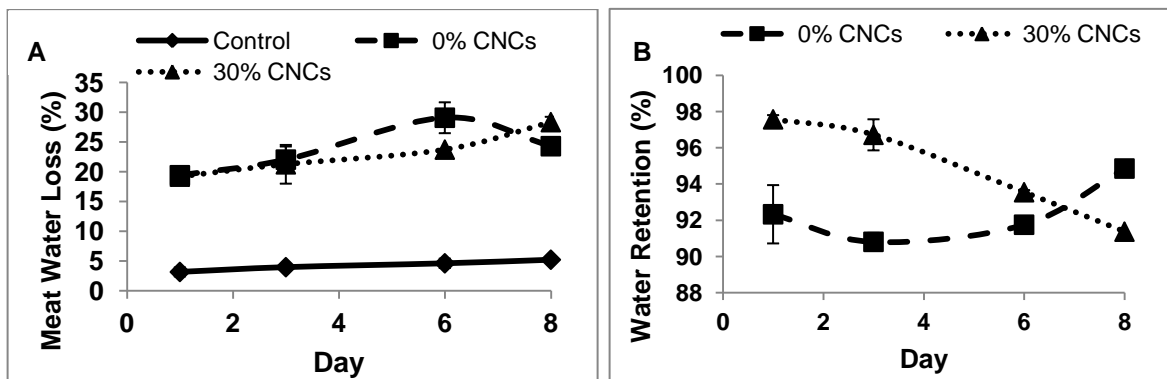


Fig. 43 Chicken meat water loss (%) without coating (control) and coated with alginate-based film (0% CNCs) and alginate based film loaded with CNCs (30% CNCs) (A). Water retention (%) of the system (meat and film) during storage of control and coated with film loaded with 0% and 30% CNCs (B)

It was then observed that samples coated with films with CNCs were capable of retaining close to 96% of water during the first 3 days (Fig. 43B). Lower water retention value was obtained in alginate-based films in absence of CNCs. Despite the fact that the

crystallinity of CNCs can prevent the permeation of water (Matuana-Malanda *et al.*, 1996; Stark, 2016), CNCs possess a hydrophilic character due to the numerous hydroxyl groups located on the surface of the crystals (Verlhac *et al.*, 1990, Mihranyan *et al.*, 2004, Habibi *et al.*, 2010). This could have allowed alginate-based films with CNCs to improve retention of water within the film and cause a delay in meat oxidation. Similar research results suggesting an increase of water affinity due to CNCs were mentioned by other authors (Rafieian *et al.*, 2014; Sukyai *et al.*, 2018; Wei *et al.*, 2018).

Increased water activity has been related to the decreasing behavior of fat oxidation (Salwin, 1960). Thus, it has been found that the water mechanism in the delay of the product oxidation is described by its i) interaction with the metallic compounds, decreasing their catalytic function and its ii) hydrogen bonding with hydroperoxides with no longer availability for further initiation oxidative reactions (Shafiur Rahman and Labuza, 2007). In our results, it can be suggested that water retention caused by edible films loaded with CNCs play a role on the delay of lipid peroxide formation of chicken breasts.

7.4.4 TBAR Substances of Chicken Breast Coated with Alginate Films

Malondialdehyde is one of the molecules produced during oxidation of polyunsaturated fatty acids and is considered the secondary product issued from lipid oxidation after lipid hydroperoxides. Thiobarbituric acid reactive substances (TBARS) test is commonly used for the quantification of malondialdehyde produced (Igene *et al.*, 1985). Concentration of TBARS formed during storage of chicken breast covered with alginate-based films is depicted in **Fig. 44**.

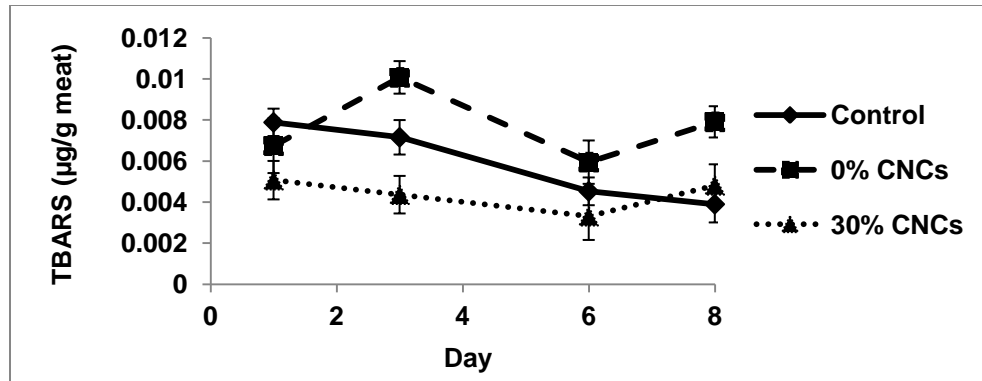


Fig. 44 Thiobarbituric Acid Reagent Substances (TBARS) content of chicken breast coated with alginate-based film containing 0% and 30% CNCs during storage for 8 days at 4°C, compared to the control without coating

Results showed that at day 1, concentration of TBARS demonstrated higher values for control compared to samples coated with film with 0% and 30% CNCs. At day 3, significant ($p \leq 0.05$) differences were observed in films with 30% loaded CNCs with respect to control and 0% CNCs. Thus, for instance, samples containing 30% CNCs showed 0.0043 $\mu\text{g TBARS/g meat}$ compared to 0.0072 $\mu\text{g TBARS/g meat}$ observed in control at day 3. Similar responses were obtained when the authors Abdollahi *et al.* (2014) added chitosan/clay films on the surface of silver carp fish and in accordance with our findings, it was stated that the reduction of TBARS formation was related to the protective and tortuous path created by the nanoparticle in the film. At day 6 and 9, no difference ($p > 0.05$) was obtained in control and samples coated with alginate-based films containing 30% CNCs. Contrary 30%, samples coated with film containing 0% CNCs showed increased TBARS response. As other authors have revealed, edible coating without presence of any clay or antioxidant result on high results of MDA. For instance, Vilarinho *et al.* (2018) evidenced that PLA packaging of salami compared to PLA-5%MMT packed samples had higher MDA concentration at days 15, 30, and 90. Also, Bermúdez-Oria *et al.* (2019) demonstrated that commercial or pectin-gelatin-based film showed increased MDA values in packed fresh beef samples compared to samples packed with phenol-derived antioxidant loaded films. Correlating these latter results with the reduced oxygen permeability values when films were loaded with CNCs, it can be suggested that presence of nanoparticles could have delayed production of oxidative products in chicken breast during storage. It is established that one of the conditions that influence lipid oxidation is the number of unsaturated fatty acids in the food matrix (Ahn

et al., 1992; Stoick *et al.*, 1991; Buckley *et al.*, 1995; Lee *et al.*, 1996). For instance, phospholipids, a class of lipids that constitute cell membranes are very prone to oxidation due to their composition based on unsaturated fatty acids. It was also observed by the authors Igene *et al.* (1980) and Pikul *et al.* (1984) that phospholipids are the main responsible compounds on the development of rancidity in model meat system during frozen storage. In meat, these effects might vary depending on the concentrations of unsaturated fatty acids found in the food matrix. Thus, chicken containing higher amount of polyunsaturated fatty acid is more prone to oxidize than pork, and similar tendency is observed for pork which tends to oxidize more easily than beef (Kadim and Mahgoub, 2007).

7.4.5 Color of Coated Chicken Breast

Figure 45 shows lightness (L^*) and redness (a^*) of chicken breast coated samples. Lightness (L^*) of all samples at day 1 demonstrated no significant ($p > 0.05$) difference within the values observed in all samples (control, coated with alginate-based films containing 0% and 30% CNCs), showing a value of approximately 81. At day 8, samples coated with alginate based-films containing 30% CNCs showed slight differences as compared to day 1 where it was noticed that L^* values decreased from 83 to 78.

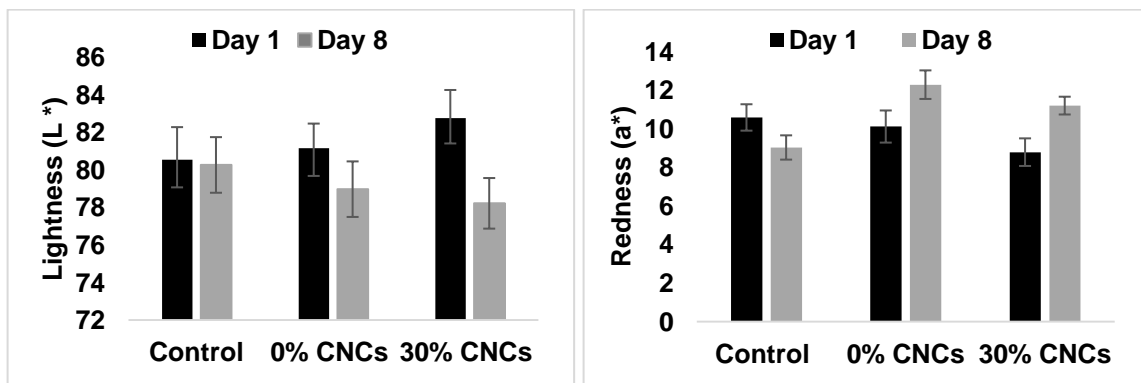


Fig. 45 Lightness (L^*) and redness (a^*) of chicken breast samples with and without alginate based coating loaded with 0 and 30% CNCs

Regarding the redness (a^*), all samples showed a^* values from 9-11 at day 1 which was in agreement with reported values in literature (Petrou *et al.*, 2012; Radha krishnan *et al.*, 2014). From day 1 to 8, redness increases by 27% in samples coated with alginate-

based films loaded with CNCs and by 22% in samples without CNCs. Contrary to coated chicken breast samples, the redness of the control showed a 15% decrease.

According to Jung *et al.* (2003), the decrease in redness in beef samples has been associated with the rate of myoglobin oxidation. In chicken, redness has also shown a direct correlation with myoglobin content as suggested by Le Bihan-Duval *et al.* (1999). In our study, it was observed that redness was increased in chicken breast coated with alginate films. This increase of redness was also observed by Holownia *et al.* (2003) who revealed that a^* values increased from 9 to 12 when antioxidant sodium nitrites was applied to chicken at a concentration of 1 ppm. The authors suggested that the presence of nitrite prevented the formation of oxidized metmyoglobin molecules, forming instead nitric oxide myoglobin. Nitrite, which is a well-known agent of preservation of meat and poultry products (Sindelar and Milkowski, 2011), is not the only compound that has demonstrated such effects of increasing results of a^* in chicken, but antioxidants such as chitosan films containing oregano were also effective to maintain and even increase the redness (Petrou *et al.*, 2012). Grape seed extracts with high content of phenolic compounds also showed an effect on the redness of cooked chicken hamburger during storage demonstrating thus an increase of approximately 90% with respect to control samples (Sáyago-Ayerdi *et al.*, 2009).

7.5 Conclusions

This study demonstrated the effect of CNCs in alginate based-films for the prevention of chicken breast oxidation during storage period. It was confirmed by this study that 30% CNCs loaded in alginate-based edible film allowed the prevention of UV light transmission and decreased the oxygen permeability of films at relative humidity of 50 and 70%. A prediction of oxygen permeability of the films was done for 30% CNCs loaded in alginate films, and the authors encourage the evaluation of different concentrations of CNCs in order to adjust the prediction to a variety of films. It was also observed that the presence of CNCs prevents the oxidation of lipids of chicken during the first 3 days of storage as shown by the peroxide values content of chicken fat. These results were in agreement with TBARS values that showed similar trend. With regard to

chicken breast color, no remarkable evidence due to oxidation was proven during storage from day 1 and 8.

7.6 Acknowledgements

This research study was part of a collaborative project supported by Natural Sciences and Engineering Research Council of Canada (NSERC) and FPInnovations (Pointe-Claire, QC, Canada). The authors would like to thank Kebba Technologies for the nitrogen flushing equipment and technical expertise about lipid oxidation and Jessy Tremblay for the support given on microscopy of films.

7.7 References

- Abdollahi, M., Rezaei, M., & Farzi, G. (2014). Influence of chitosan/clay functional bionanocomposite activated with rosemary essential oil on the shelf life of fresh silver carp. *Int. J. Food Sci. Technol.*, 49, 811–818. <https://doi.org/10.1111/ijfs.12369>.
- Ahn, D.U., Wolfe, F.H., Sim, J.S., & Kim, D.H. (1992). Packaging Cooked Turkey Meat Patties while Hot Reduces Lipid Oxidation. *J. Food Sci.*, 57, 1075–1115. <https://doi.org/10.1111/j.1365-2621.1992.tb11267.x>.
- Aulin, C., Gällstedt, M., & Lindström, T. (2010). Oxygen and oil barrier properties of microfibrillated cellulose films and coatings. *Cellulose*, 17, 559–574. <https://doi.org/10.1007/s10570-009-9393-y>.
- Bermúdez-Oria, A., Rodríguez-Gutiérrez, G., Rubio-Senent, F., Fernández-Prior, Á., & Fernández-Bolaños, J. (2019). Effect of edible pectin-fish gelatin films containing the olive antioxidants hydroxytyrosol and 3,4-dihydroxyphenylglycol on beef meat during refrigerated storage. *Meat Sci.*, 148, 213–218. <https://doi.org/10.1016/j.meatsci.2018.07.003>
- Bolin, H.R. (1980). Relation of moisture to water activity in prunes and raisins. *J. Food Sci.*, 45, 1190–1192. <https://doi.org/10.1111/j.1365-2621.1980.tb06518.x>.
- Botsoglou, N.A., Fletouris, D.J., Papageorgiou, G.E., Vassilopoulos, V.N., Mantis, A.J., & Trakatellis, A.G. (1994). Rapid, sensitive, and specific thiobarbituric acid method for measuring lipid peroxidation in animal tissue, food, and feedstuff samples. *J. Agric. Food Chem.*, 42, 1931–1937. <https://doi.org/10.1021/jf00045a019>.
- Buckley, D.J., Morrissey, P.A., & Gray, J.I. (1995). Influence of dietary vitamin E on the oxidative stability and quality of pig meat. *J. Anim. Sci.*, 73, 3122–3130. <https://doi.org/10.2527/1995.73103122x>.
- Cavani, C., Petracci, M., Trocino, A., & Xiccato, G. (2009). Advances in research on poultry and rabbit meat quality. *Ital. J. Anim. Sci.*, 8, 741–750. <https://doi.org/10.4081/ijas.2009.s2.741>.
- Cozzolino, C.A., Campanella, G., Türe, H., Olsson, R.T., & Farris, S. (2016). Microfibrillated cellulose and borax as mechanical, O₂-barrier, and surface-modulating agents of pullulan biocomposite coatings on BOPP. *Carbohydr. Polym.*, 143, 179–187. <https://doi.org/10.1016/j.carbpol.2016.01.068>.
- da Silva, S.L., Marangoni, C., Brun, D.S., Guidetti Vendruscolo, R., Silva, M.S., de Moura, H.C., Rampelotto, C., Wagner, R., de Menezes, C.R., Barin, J., Bastianello Campagnol, P.C., & Cichoski, A.J. (2018). Effect of dietary olive leaves on the lipid and protein oxidation and bacterial safety of chicken hamburgers during frozen storage. *Int. Food Res. J.*, 25, 383–391. [http://www.ifrj.upm.edu.my/25%20\(01\)%202018/\(51\).pdf](http://www.ifrj.upm.edu.my/25%20(01)%202018/(51).pdf) accessed 11 June 2019.
- Dai, L., Long, Z., Zhao, Y., Wang, B., & Chen, J. (2016). Comparison of hydroxypropyl and carboxymethyl guar for the preparation of nanocellulose composite films. *Cellulose*, 23, 2989–2999. <https://doi.org/10.1007/s10570-016-0998-7>.
- de Vries, H. (1951). Rotatory power and other optical properties of certain liquid crystals. *Acta Crystallogr.*, 4, 219–226. <https://doi.org/10.1107/S0365110X51000751>.

- Debeaufort, F., Quezada-Gallo, J.-A., & Voilley, A. (1998). Edible films and coatings: tomorrow's packagings: a review. *Crit. Rev. Food Sci. Nutr.*, 38, 299–313. <https://doi.org/10.1080/10408699891274219>.
- Dondi, D., Albini, A., & Serpone, N. (2006). Interactions between different solar UVB/UVA filters contained in commercial suncreams and consequent loss of UV protection. *Photochem. Photobiol. Sci.*, 5, 835–843. <https://doi.org/10.1039/b606768a>.
- Fleming, K., Gray, D., Prasannan, S., & Matthews, S. (2000). Cellulose crystallites: a new and robust liquid crystalline medium for the measurement of residual dipolar couplings. *J. Am. Chem. Soc.*, 122, 5224–5225. <https://doi.org/10.1021/ja000764e>.
- Fleming, K., Gray, D.G., & Matthews, S. (2001). Cellulose crystallites. *Chem. – Eur. J.* 7, 1831–1836. [https://doi.org/10.1002/1521-3765\(20010504\)7:9<1831::AID-CHEM1831>3.0.CO;2-S](https://doi.org/10.1002/1521-3765(20010504)7:9<1831::AID-CHEM1831>3.0.CO;2-S).
- Fletcher, D.L. (2002). Poultry meat quality. *World's Poult. Sci. J.*, 58, 131–145. <https://doi.org/10.1079/WPS20020013>.
- Fortunati, E., Peltzer, M., Armentano, I., Torre, L., Jiménez, A., & Kenny, J.M. (2012). Effects of modified cellulose nanocrystals on the barrier and migration properties of PLA nano-biocomposites. *Carbohydr. Polym.*, 90, 948–956. <https://doi.org/10.1016/j.carbpol.2012.06.025>.
- Gibbs, R.A., Rymer, C., & Givens, D.I. (2010). Postgraduate Symposium Long-chain n-3 PUFA: intakes in the UK and the potential of a chicken meat prototype to increase them: Conference on 'Over- and undernutrition: challenges and approaches.' *Proc. Nutr. Soc.*, 69, 144–155. <https://doi.org/10.1017/S0029665109991716>.
- Gontard, N., Thibault, R., Cuq, B., & Guilbert, S. (1996). Influence of relative humidity and film composition on oxygen and carbon dioxide permeabilities of edible films. *J. Agric. Food Chem.*, 44, 1064–1069. <https://doi.org/10.1021/jf9504327>.
- Habibi, Y., Lucia, L.A., & Rojas, O.J. (2010). Cellulose nanocrystals: chemistry, self-assembly, and applications. *Chem. Rev.*, 110, 3479–3500. <https://doi.org/10.1021/cr900339w>.
- Holownia, K., Chinnan, M.S., Reynolds, A.E., & Koehler, P.E. (2003). Evaluation of induced color changes in chicken breast meat during simulation of pink color defect. *Poult. Sci.*, 82, 1049–1059. <https://doi.org/10.1093/ps/82.6.1049>.
- Huq, T., Salmieri, S., Khan, A., Khan, R.A., Le Tien, C., Riedl, B., Frascini, C., Bouchard, J., Uribe-Calderon, J., Kamal, M.R., & Lacroix, M. (2012). Nanocrystalline cellulose (NCC) reinforced alginate based biodegradable nanocomposite film. *Carbohydr. Polym.*, 90, 1757–1763. <https://doi.org/10.1016/j.carbpol.2012.07.065>.
- Igene, J.O., Pearson, A.M., Dugan, L.R., & Price, J.F. (1980). Role of triglycerides and phospholipids on development of rancidity in model meat systems during frozen storage. *Food Chem.*, 5, 263–276. [https://doi.org/10.1016/0308-8146\(80\)90048-5](https://doi.org/10.1016/0308-8146(80)90048-5).
- Igene, J.O., Yamauchi, K., Pearson, A.M., Gray, J.I., & Aust, S.D. (1985). Evaluation of 2-thiobarbituric acid reactive substances (TBRS) in relation to warmed-over flavor

- (WOF) development in cooked chicken. *J. Agric. Food Chem.*, 33, 364–367. <https://doi.org/10.1021/jf00063a011>.
- Jung, S., Ghoul, M. & de Lamballerie-Anton, M. (2003). Influence of high pressure on the color and microbial quality of beef meat. *LWT - Food Sci. Technol.*, 36, 625–631. [https://doi.org/10.1016/S0023-6438\(03\)00082-3](https://doi.org/10.1016/S0023-6438(03)00082-3).
- Kadim, I.T., Mahgoub, O. (2007). Postharvest handling of red meat, In M. Shafiur Rahman (Ed.), *Handbook of Food Preservation* (pp. 173–202). Boca Ratón: Taylor & Francis Group.
- Karkhanis, S.S., Stark, N.M., Sabo, R.C. & Matuana, L.M. (2018). Water vapor and oxygen barrier properties of extrusion-blown poly(lactic acid)/cellulose nanocrystals nanocomposite films. *Compos. Part Appl. Sci. Manuf.*, 114, 204–211. <https://doi.org/10.1016/j.compositesa.2018.08.025>.
- Labuza, T.P. & Dugan, L.R. (1971). Kinetics of lipid oxidation in foods. *C R C Crit. Rev. Food Technol.*, 2, 355–405. <https://doi.org/10.1080/10408397109527127>.
- Labuza, T.P., Tsuyuki, H., & Karel, M. (1969). Kinetics of linoleate oxidation in model systems. *J. Am. Oil Chem. Soc.*, 46, 409–416. <https://doi.org/10.1007/BF02545625>.
- Le Bihan-Duval, E., Millet, N., & Remignon, H. (1999). Broiler meat quality: effect of selection for increased carcass quality and estimates of genetic parameters. *Poult. Sci.*, 78, 822–826. <https://doi.org/10.1093/ps/78.6.822>.
- Lee, S.K., Mei, L., & Decker, E.A. (1996). Lipid Oxidation in Cooked Turkey as Affected by Added Antioxidant Enzymes. *J. Food Sci.*, 61, 726–728. <https://doi.org/10.1111/j.1365-2621.1996.tb12190.x>.
- Lima, M.M. de S., & Borsali, R. (2004). Rodlike cellulose microcrystals: structure, properties, and applications. *Macromol. Rapid Commun.* 25, 771–787. <https://doi.org/10.1002/marc.200300268>.
- Lindfors, A.V., & Ylianttila, L. (2016). Visualizing Rayleigh Scattering through UV Photography. *Bull. Am. Meteorol. Soc.*, 97, 1561–1564. <https://doi.org/10.1175/BAMS-D-14-00260.1>.
- Liu, S., Li, X., Chen, L., Li, L., Li, B., & Zhu, J. (2018). Tunable D-limonene permeability in starch-based nanocomposite films reinforced by cellulose nanocrystals. *J. Agric. Food Chem.*, 66, 979–987. <https://doi.org/10.1021/acs.jafc.7b05457>.
- Long, K., Cha, R., Zhang, Y., Li, J., Ren, F., & Jiang, X. (2018). Cellulose nanocrystals as reinforcements for collagen-based casings with low gas transmission. *Cellulose*, 25, 463–471. <https://doi.org/10.1007/s10570-017-1569-2>.
- Matuana-Malanda, L., Park, C.B., & Balatinecz, J.J. (1996). Characterization of microcellular foamed PVC/Cellulosic-fibre composites. *J. Cell. Plast.*, 32, 449–469. <https://doi.org/10.1177/0021955X9603200503>.
- Mestdagh, F., De Meulenaer, B., De Clippeleer, J., Devlieghere, F., & Huyghebaert, A. (2005). Protective influence of several packaging materials on light oxidation of milk. *J. Dairy Sci.*, 88, 499–510. [https://doi.org/10.3168/jds.S0022-0302\(05\)72712-0](https://doi.org/10.3168/jds.S0022-0302(05)72712-0).

- Miettinen, A., Chinga-Carrasco, G., & Kataja, M. (2014). Three-dimensional microstructural properties of nanofibrillated cellulose films. *Int. J. Mol. Sci.*, 15, 6423–6440. <https://doi.org/10.3390/ijms15046423>.
- Mihiranyan, A., Llagostera, A.P., Karmhag, R., Strømme, M., & Ek, R. (2004). Moisture sorption by cellulose powders of varying crystallinity. *Int. J. Pharm.*, 269, 433–442. <https://doi.org/10.1016/j.ijpharm.2003.09.030>.
- Miller, K.S., & Krochta, J.M. (1997). Oxygen and aroma barrier properties of edible films: a review. *Trends Food Sci. Technol.*, 8, 228–237. [https://doi.org/10.1016/S0924-2244\(97\)01051-0](https://doi.org/10.1016/S0924-2244(97)01051-0).
- Miller, R. (1994). Quality characteristics. In Kinsman, D. M., Kotula, A.W., Breidenstein B. C. (Eds.), *Muscle foods; meat, poultry, and seafood technology* (pp. 296–332). New York: Chapman & Hall.
- Nawar, W.W. (1996). Lipids. In Fennema O. R. (Ed), *Food Chemistry* (pp. 225–314). New York: Marcel Dekker.
- Northwest life sciences specialities. Online derivative analysis. <https://www.nwlifescience.com/sq/accessed> 11 June 2019
- Oussalah, M., Caillet, S., Salmiéri, S., Saucier, L., & Lacroix, M. (2004). Antimicrobial and antioxidant effects of milk protein-based film containing essential oils for the preservation of whole beef muscle. *J. Agric. Food Chem.*, 52, 5598–5605. <https://doi.org/10.1021/jf049389q>.
- Padera, F. (2013). Measuring light transmittance and UVA and UVB of transparent materials using the PerkinElmer LAMBDA 35. Shelton, USA. https://www.perkinelmer.ca/CMSResources/Images/44-156246APP_Measuring_Light_Transmittance_and_UVA_and_UVB_of_Transparent_Materials_LAMBDA_35.pdf/accessed 11 June 2019.
- Pan, J., Hamad, W., & Straus, S.K. (2010). Parameters affecting the chiral nematic phase of nanocrystalline cellulose films. *Macromolecules*, 43, 3851–3858. <https://doi.org/10.1021/ma902383k>.
- Petrou, S., Tsiraki, M., Giatrakou, V., & Savvaidis, I.N. (2012). Chitosan dipping or oregano oil treatments, singly or combined on modified atmosphere packaged chicken breast meat. *Int. J. Food Microbiol.*, 156, 264–271. <https://doi.org/10.1016/j.ijfoodmicro.2012.04.002>.
- Pikul, J., Leszczynski, D.E., & Kummerow, F.A. (1984). Relative role of phospholipids, triacylglycerols, and cholesterol esters on malonaldehyde formation in fat extracted from chicken meat. *J. Food Sci.* 49, 704–708. <https://doi.org/10.1111/j.1365-2621.1984.tb13192.x>.
- Radha krishnan, K., Babuskin, S., Azhagu Saravana Babu, P., Sasikala, M., Sabina, K., Archana, G., Sivarajan, M., & Sukumar, M. (2014). Antimicrobial and antioxidant effects of spice extracts on the shelf life extension of raw chicken meat. *Int. J. Food Microbiol.*, 171, 32–40. <https://doi.org/10.1016/j.ijfoodmicro.2013.11.011>.
- Rafieian, F., Shahedi, M., Keramat, J., & Simonsen, J. (2014). Mechanical, thermal and barrier properties of nano-biocomposite based on gluten and carboxylated cellulose nanocrystals. *Ind. Crops Prod.*, 53, 282–288. <https://doi.org/10.1016/j.indcrop.2013.12.016>.

- Rånby, B.G. (1949). Aqueous colloidal solutions of cellulose micelles. *Acta Chemica Scandinavica*, 3, 649–650. <https://doi.org/10.3891/acta.chem.scand.03-0649>.
- Ren, J., Wang, S., Gao, C., Chen, X., Li, W., & Peng, F. (2015). TiO₂-containing PVA/xylan composite films with enhanced mechanical properties, high hydrophobicity and UV shielding performance. *Cellulose*, 22, 593–602. <https://doi.org/10.1007/s10570-014-0482-1>.
- Revol, J.-F., Bradford, H., Giasson, J., Marchessault, R. H., & Gray, D. G. (1992). Helicoidal self-ordering of cellulose microfibrils in aqueous suspension. *Int. J. Biol. Macromol.*, 14, 170–2. [https://doi.org/10.1016/S0141-8130\(05\)80008-X](https://doi.org/10.1016/S0141-8130(05)80008-X).
- Rodriguez-Turienzo, L., Cobos, A., & Diaz, O. (2012). Effects of edible coatings based on ultrasound-treated whey proteins in quality attributes of frozen Atlantic salmon (*Salmo salar*). *Innov. Food Sci. Emerg. Technol.*, 14, 92–98. <https://doi.org/10.1016/j.ifset.2011.12.003>.
- Ryan, J.T., Ross, R.P., Bolton, D., Fitzgerald, G.F., & Stanton, C. (2011). Bioactive peptides from muscle sources: meat and fish. *Nutrients*, 3, 765–791. <https://doi.org/10.3390/nu3090765>.
- Salwin, H. (1960). Defining minimum moisture contents for dehydrated foods. *Food Technol.* 13: 594-595.
- Sanchez-Garcia, M.D., & Lagaron, J.M. (2010). On the use of plant cellulose nanowhiskers to enhance the barrier properties of polylactic acid. *Cellulose*, 17, 987–1004. <https://doi.org/10.1007/s10570-010-9430-x>.
- Sáyago-Ayerdi, S.G., Brenes, A., & Goñi, I. (2009). Effect of grape antioxidant dietary fiber on the lipid oxidation of raw and cooked chicken hamburgers. *LWT - Food Sci. Technol.*, 42, 971–976. <https://doi.org/10.1016/j.lwt.2008.12.006>.
- Shafiur Rahman, M., & Labuza, T.P. (2007). Water activity and food preservation. In M. Shafiur Rahman (Ed.), *Handbook of Food Preservation* (pp. 447–476). Boca Raton: Taylor & Francis Group.
- Sindelar, J.J., & Milkowski, A.L. (2011). Sodium nitrite in processed meat and poultry meats: a review of curing and examining the risk/benefit of its use. *Am. Meat Sci. Assoc. White Pap. Ser.*, 3, 1-14. [https://meatscience.org/docs/default-source/publications-resources/white-papers/2011-11-amsa-nitrite-white-paper.pdf?sfvrsn=4232bbb3_8/accessed 11 June 2019](https://meatscience.org/docs/default-source/publications-resources/white-papers/2011-11-amsa-nitrite-white-paper.pdf?sfvrsn=4232bbb3_8/accessed%2011%20June%202019)
- Stark, N. (2016). Opportunities for cellulose nanomaterials in packaging films: a review and future trends. *J. Renew. Mater.*, 4, 313–326. <https://doi.org/10.7569/JRM.2016.634115>.
- Stoick, S.M., Gray, J.I., Booren, A.M., & Buckley, D.J. (1991). Oxidative stability of restructured beef steaks processed with oleoresin rosemary, tertiary butylhydroquinone, and sodium tripolyphosphate. *J. Food Sci.*, 56, 597–600. <https://doi.org/10.1111/j.1365-2621.1991.tb05337.x>.
- Sukyai, P., Anongjanya, P., Bunyahwuthakul, N., Kongsin, K., Harnkarnsujarit, N., Sukatta, U., Sothornvit, R., & Chollakup, R. (2018). Effect of cellulose nanocrystals from sugarcane bagasse on whey protein isolate-based films. *Food Res. Int.* 107, 528–535. <https://doi.org/10.1016/j.foodres.2018.02.052>.

- Terech, P., Chazeau, L., & Cavaille, J.Y. (1999). A small-angle scattering study of cellulose whiskers in aqueous suspensions. *Macromolecules*, 32, 1872–1875. <https://doi.org/10.1021/ma9810621>.
- Ureña-Benavides, E.E., Brown, P.J., & Kitchens, C.L. (2010). Effect of jet stretch and particle load on cellulose nanocrystal–alginate nanocomposite fibers. *Langmuir*, 26, 14263–14270. <https://doi.org/10.1021/la102216v>.
- Ustunol, Z. (2009). Edible films and coatings for meat and poultry. In Huber, K.C., Embuscado, M.E. (Eds.), *Edible Films and Coatings for Food Applications* (pp. 245–268) New York: Springer. https://doi.org/10.1007/978-0-387-92824-1_8.
- Verlhac, C., Dedier, J. & Chanzy, H. (1990). Availability of surface hydroxyl groups in valonia and bacterial cellulose. *J. Polym. Sci. Part Polym. Chem.*, 28, 1171–1177. <https://doi.org/10.1002/pola.1990.080280517>.
- Viet, D., Beck-Candanedo, S., & Gray, D.G. (2007). Dispersion of cellulose nanocrystals in polar organic solvents. *Cellulose*, 14, 109–113. <https://doi.org/10.1007/s10570-006-9093-9>.
- Vilarinho, F., Andrade, M., Buonocore, G.G., Stanzione, M., Vaz, M.F., & Sanches Silva, A. (2018). Monitoring lipid oxidation in a processed meat product packaged with nanocomposite poly(lactic acid) film. *Eur. Polym. J.*, 98, 362–367. <https://doi.org/10.1016/j.eurpolymj.2017.11.034>.
- Wang, J., Gardner, D.J., Stark, N.M., Bousfield, D.W., Tajvidi, M., & Cai, Z. (2018). Moisture and oxygen barrier properties of cellulose nanomaterial-based films. *ACS Sustain. Chem. Eng.*, 6, 49–70. <https://doi.org/10.1021/acssuschemeng.7b03523>.
- Wei, Z., Sinko, R., Keten, S., & Luijten, E. (2018). Effect of surface modification on water adsorption and interfacial mechanics of cellulose nanocrystals. *ACS Appl. Mater. Interfaces*, 10, 8349–8358. <https://doi.org/10.1021/acsmi.7b18803>.
- Xing, C. & Matuana, L.M. (2016). Epoxidized soybean oil-plasticized poly(lactic acid) films performance as impacted by storage. *J. Appl. Polym. Sci.* 133, 43201. <https://doi.org/10.1002/app.43201>.
- Zhang, C., Salick, M.R., Cordie, T.M., Ellingham, T., Dan, Y., & Turng, L.S. (2015). Incorporation of poly(ethylene glycol) grafted cellulose nanocrystals in poly(lactic acid) electrospun nanocomposite fibers as potential scaffolds for bone tissue engineering. *Mater. Sci. Eng. C Mater. Biol. Appl.*, 49, 463–471. <https://doi.org/10.1016/j.msec.2015.01.024>.

GENERAL DISCUSSION AND CONCLUSIONS

A large number of research studies in literature are focusing on the improvement of polymeric matrices performance such as the reinforcement of mechanical properties and the barrier properties induced by the presence of CNCs (Sanchez-Garcia *et al.*, 2010; Huq *et al.*, 2012; Khan *et al.* 2012; Karkanis *et al.*, 2018). However, these research studies have mainly concentrated on the characterization of the material itself and only a few of them have studied direct applications in food packaging (Long *et al.*, 2018; Fotie *et al.* 2018).

Studies carried out on chemical modification of CNCs have been performed with the main purpose of improving its affinity with hydrophobic matrices or to introduce new properties such as antimicrobial or antioxidant properties. However, these chemical reactions can sometimes lead to long reactions times combined to complex and time-consuming purification procedures. Physical treatments on the other hand, such as gamma irradiation, require shorter reaction times and purification is made easier to achieve similar behaviours. The purpose of the first part of this thesis was to use gamma irradiation as a physical treatment for CNCs modification.

Gamma irradiation has been applied for multiple purposes from bactericidal, grafting, and cross-linking at low doses to sterilization and oxidation at higher doses (Takács *et al.*, 1999; Henniges *et al.*, 2012; Baccaro *et al.*, 2013). At low irradiation doses, gamma irradiation of cellulosic derivatives have demonstrated the creation of active sites for further polymerization, grafting reactions or cross-linking (Kobayashi, 1961; Nasef and Hegazy, 2004) whereas at high doses, oxidative reactions are observed. With the aim to graft antioxidant molecules on CNCs surface, the first step of this project started with the use of a combination of gamma irradiation in the presence of a redox pair as a pre-treatment for the creation of active sites on CNCs surface, followed by the introduction of gallic acid, a molecule well-known for its antioxidant properties. It was observed that both pre-treatment and addition of gallic acid led to enhanced antiradical properties (Criado *et al.*, 2016).

However, when evaluating the changes in the concentration of carbonyl groups present at the surface of CNCs, we noticed that gamma irradiation alone also had a significant effect on the surface chemistry of CNCs. Results showed that an increase of gamma irradiation doses led to an increase of functional groups such as carboxylic acid and aldehyde groups. These results were in agreement with research studies done on cellulose backbone and because aldehyde groups have demonstrated reducing capacities, antiradical tests were performed and showed a significant improvement of bioactivity of CNCs irradiated at 80 kGy compared to non-modified CNCs.

The second part of this thesis deals with the controlled release of encapsulated active compounds in polymers reinforced with CNCs, a topic that has been introduced many times for implementation of long-lasting delivery of drugs for biomedical applications (Siegel and Rathbone, 2012). By introducing CNCs, this concept was applied to control the release of ionic antibiotics from cationic treated CNCs (Jackson *et al.*, 2011) or for encapsulation purposes (Akhlaghi *et al.*, 2015; Ooi *et al.*, 2016).

Similar research studies have been carried out on the use of nanofillers to bring protection to food additives (Almasi *et al.*, 2014; Shahmohammadi Jebel and Almasi 2016; Alizadeh Sani *et al.*, 2017; Campos-Requena *et al.*, 2017). Controlled release being an important concept for the delivery of bioactive compounds and the tortuosity a characteristic brought by CNCs in polymeric materials, the objective of the sixth chapter was to introduce CNCs in a cross-linked alginate bead system to observe their effect on the controlled release of essential oils.

In this study, it was observed in a calcium cross-linked alginate beads loaded with 3% thyme essential oil (EO) that the kinetic constant of EO release in a simulated solvent can be reduced by approximately 30%, when 30% CNCs were introduced. This formulation was tested in ground meat, where however, results showed that initial release of EOs was delayed which consequently led to unwanted bacterial growth. A sustained release and absence of pathogenic bacteria was then observed at day 14 when the beads loaded with EO were combined to gamma irradiation treatment (1 kGy) revealing a protecting behaviour of CNCs on EO. In addition, gamma irradiation and beads containing EO demonstrate a synergistic effect on decontamination. By imaging

the cross-section of the beads loaded with EO, it was demonstrated that CNCs lead to a homogenous and less porous morphological structure (Criado *et al.*, 2019). These results confirmed the fact that the nanoparticles formed a dense 3D network which was in agreement with the reinforced Young modulus capacity of beads with CNCs (291 MPa) compared to beads in their absence (173 MPa). In conclusion, these results aim to confirm the mechanical reinforcing contribution of CNCs in polymeric matrices as well as the protective role that CNCs brings to active compounds.

Finally, because of the easy ability of food to be oxidized when they are exposed to oxygen or light, the purpose of the seventh chapter was to study the capacity of the cellulose nanocrystals to decrease lipid oxidation in food by taking advantage of their ability to fill free spaces in polymeric systems. Alginate based films loaded at different concentrations of CNCs (0 to 30% CNCs) were prepared and barrier properties were evaluated under different relative humidity conditions (%RH). It was observed that the presence of 30% CNCs decreases the oxygen permeability (OP) by 36% at 50% RH. In addition, CNCs also showed a capability to scatter light, reducing the transmission of light through films in all the UV ranges. This latter property can result of potential applicability especially for UV sensitive food (Conrad *et al.*, 2005; Van *et al.*, 2001). Therefore, alginate films loaded with CNCs were tested on chicken breast, chosen as a food model, and results demonstrated a significant decrease of lipid oxidation byproduct formation during the first three days of storage. Color of coated chicken demonstrated, in addition, that redness was maintained in samples where CNCs were loaded compared to the non coated samples.

Perspectives

Considering that this study showed that gamma irradiation of CNCs can be used as a novel technology for modification of cellulose derivatives, it will be interesting to explore the advantages of adding other active compounds to CNCs or to favor grafting reactions or *in situ* polymerization of monomers such as acrylic acid, as exemple of a monomer used for several applications (El Salmawi *et al.* 2018) in presence of CNCs.

In the packaging field and with the aim to enhance sustainable release of bioactive compounds in presence of CNCs, the evaluation of other food matrices that achieve longer shelf-lives -such as ham, pastrami, sausages and others RTE food- are

recommended. Finally, since our studies brought a significant contribution of CNCs to the reduction of the lipid oxidation of food matrices, it should be interesting to evaluate the contribution of oxygen barrier of CNCs in different types of food matrices (different a_w and/or storage time). Since CNCs have demonstrated a barrier effect to oxygen in the coatings and with the lack of studies made on CO_2 , the study of the effect that CNCs has on this latter gas could add more value of CNCs as gas barrier agent. With the valuable contribution that modified atmosphere conditions have on food storage, it should be interesting to consider the effect of CNCs for this type of packaging. Finally, because it has been claimed the value of reusable, recyclable and biodegradable packaging, it should be of great interest to evaluate the contribution of CNCs to this field.

REFERENCES

- Abad, L.V., Relve, L.S., Racadio, C.D.T., Aranilla, C.T., De la Rosa, A.M., 2013. Antioxidant activity potential of gamma irradiated carrageenan. *Appl. Radiat. Isot.* 79, 73–79. <https://doi.org/10.1016/j.apradiso.2013.04.035>
- Aider, M., 2010. Chitosan application for active bio-based films production and potential in the food industry: review. *LWT - Food Sci. Technol.* 43, 837–842. <https://doi.org/10.1016/j.lwt.2010.01.021>
- Akhlaghi, S.P., Berry, R.M., Tam, K.C., 2015. Modified cellulose nanocrystal for vitamin c delivery. *AAPS PharmSciTech* 16, 306–314. <https://doi.org/10.1208/s12249-014-0218-4>
- Akkapeddi, M.K., Gervasi, J.A., 1989. Amorphous copolyamide article of manufacture with moisture-insensitive oxygen barrier properties. US4826955A.
- Alizadeh Sani, M., Ehsani, A., Hashemi, M., 2017. Whey protein isolate/cellulose nanofibre/TiO₂ nanoparticle/rosemary essential oil nanocomposite film: Its effect on microbial and sensory quality of lamb meat and growth of common foodborne pathogenic bacteria during refrigeration. *Int. J. Food Microbiol.* 251, 8–14. <https://doi.org/10.1016/j.ijfoodmicro.2017.03.018>
- Almasi, H., Ghanbarzadeh, B., Dehghannya, J., Entezami, A.A., Khosrowshahi Asl, A., 2014. Development of a novel controlled-release nanocomposite based on poly(lactic acid) to increase the oxidative stability of soybean oil. *Food Addit. Contam. - Part Chem. Anal. Control Expo. Risk Assess.* 31, 1586–1597. <https://doi.org/10.1080/19440049.2014.935962>
- Alvarado, N., Romero, J., Torres, A., López de Dicastillo, C., Rojas, A., Galotto, M.J., Guarda, A., 2018. Supercritical impregnation of thymol in poly(lactic acid) filled with electrospun poly(vinyl alcohol)-cellulose nanocrystals nanofibers: Development an active food packaging material. *J. Food Eng.* 217, 1–10. <https://doi.org/10.1016/j.jfoodeng.2017.08.008>
- Appendini, P., Hotchkiss, J.H., 2002. Review of antimicrobial food packaging. *Innov. Food Sci. Emerg. Technol.* 3, 113–126. [https://doi.org/10.1016/S1466-8564\(02\)00012-7](https://doi.org/10.1016/S1466-8564(02)00012-7)
- Araki, J., Wada, M., Kuga, S., 2001. Steric stabilization of a cellulose microcrystal suspension by poly(ethylene glycol) grafting. *Langmuir* 17, 21–27. <https://doi.org/10.1021/la001070m>
- Asahata, S., Hirai, Y., Ainoda, Y., Fujita, T., Okada, Y., Kikuchi, K., 2015. Fournier's gangrene caused by *Listeria monocytogenes* as the primary organism [WWW Document]. *Can. J. Infect. Dis. Med. Microbiol.* <https://doi.org/10.1155/2015/501386> (accessed 15.02.18)
- Azeredo, H.M.C. de, 2009. Nanocomposites for food packaging applications. *Food Res. Int.* 42, 1240–1253. <https://doi.org/10.1016/j.foodres.2009.03.019>

- Aziz, M., Karboune, S., 2018. Natural antimicrobial/antioxidant agents in meat and poultry products as well as fruits and vegetables: a review. *Crit. Rev. Food Sci. Nutr.* 58, 486–511. <https://doi.org/10.1080/10408398.2016.1194256>
- Baccaro S., Carewska M., Casieri C., Cemmi, A. 2013. Structure modifications and interaction with moisture in γ -irradiated pure cellulose by thermal analysis and infrared spectroscopy. *Polym. Degrad. Stab.* 98, 2005–2010. <https://doi.org/10.1016/j.polymdegradstab.2013.07.011>
- Balamatsia, C.C., Paleologos, E.K., Kontominas, M.G., Savvaidis, I.N., 2006. Correlation between microbial flora, sensory changes and biogenic amines formation in fresh chicken meat stored aerobically or under modified atmosphere packaging at 4 °C: possible role of biogenic amines as spoilage indicators. *Antonie Van Leeuwenhoek* 89, 9–17. <https://doi.org/10.1007/s10482-005-9003-4>
- Barriuso, B., Astiasarán, I., Ansorena, D., 2013. A review of analytical methods measuring lipid oxidation status in foods: a challenging task. *Eur. Food Res. Technol.* 236, 1–15. <https://doi.org/10.1007/s00217-012-1866-9>
- Bekhit, M., Arab-Tehrany, E., Kahn, C.J.F., Cleymand, F., Fleutot, S., Desobry, S., Sánchez-González, L., 2018. Bioactive films containing alginate-pectin composite microbeads with *Lactococcus lactis* subsp. *lactis*: physicochemical characterization and antilisterial activity. *Int. J. Mol. Sci.* 19, 574. <https://doi.org/10.3390/ijms19020574>
- Bengio, E.A., Tsentelovich, D.E., Behabtu, N., Kleinerman, O., Kesselman, E., Schmidt, J., Talmon, Y., Pasquali, M., 2014. Statistical length measurement method by direct imaging of carbon nanotubes. *ACS Appl. Mater. Interfaces* 6, 6139–6146. <https://doi.org/10.1021/am500424u>
- Bonilla, J., Poloni, T., Sobral, P.J.A., 2018. Active edible coatings with Boldo extract added and their application on nut products: reducing the oxidative rancidity rate. *Int. J. Food Sci. Technol.* 53, 700–708. <https://doi.org/10.1111/ijfs.13645>
- Bouchard J., Méthot M., Jordan B., 2006. The effects of ionizing radiation on the cellulose of woodfree paper. *Cellulose* 13, 601–610. <https://doi.org/10.1007/s10570-005-9033-0>
- Braconnot, H., 1825. *Annales de Chimie et Physique* 28, 173–178.
- Braconnot, H., 1811. *Recherches analytiques sur la nature des champignons* 79, 265–304.
- Bras, J., Viet, D., Bruzzese, C., Dufresne, A., 2011. Correlation between stiffness of sheets prepared from cellulose whiskers and nanoparticles dimensions. *Carbohydr. Polym.* 84, 211–215. <https://doi.org/10.1016/j.carbpol.2010.11.022>
- Brioude, M.M., Roucoules, V., Haidara, H., Vonna, L., Laborie, M.-P., 2015. Role of cellulose nanocrystals on the microstructure of maleic anhydride plasma polymer thin films. *Appl. Mater. Interfaces*, 7, 14079-14088. <https://doi.org/10.1021/acsami.5b03302>
- Brody, A.L., 2007. Nanocomposite technology in food packaging. *Food Technol.*
- Buesch, C., Smith, S.W., Eschbach, P., Conley, J.F., Simonsen, J., 2016. The microstructure of cellulose nanocrystal aerogels as revealed by transmission

- electron microscope tomography. *Biomacromolecules* 17, 2956–2962. <https://doi.org/10.1021/acs.biomac.6b00764>
- Bumbudsanpharoke, N., Choi, J., Ko, S., 2015. Applications of nanomaterials in food packaging. *J. Nanosci. Nanotechnol.* 15, 6357–6372. <https://doi.org/10.1166/jnn.2015.10847>
- Bumbudsanpharoke, N., Ko, S., 2015. Nano-Food packaging: an overview of market, migration research, and safety regulations. *J. Food Sci.* 80, R910–R923. <https://doi.org/10.1111/1750-3841.12861>
- Burat, K.M., Borzcut, O., 1996. Improvement of calibration curve for determining peroxide values of food lipids by the modified ferrous oxidation-xylenol orange method. *J. AOAC Int.* 74, 995–997.
- Butterfield, F.J., 1987. The potential long-term effects of gamma irradiation on paper. *Stud. Conserv.* 32, 181–191. <https://doi.org/10.2307/1506182>
- Caillet, S., Lacroix, M., 2006. Effect of gamma radiation and oregano essential oil on murein and ATP concentration of *Listeria monocytogenes*. *J. Food Prot.* 69, 2961–2969.
- Caillet, S., Millette, M., Salmiéri, S., Lacroix, M., 2006a. Combined effects of antimicrobial coating, modified atmosphere packaging, and gamma irradiation on *Listeria innocua* present in ready-to-use carrots (*Daucus carota*). *J. Food Prot.* 69, 80–85. <https://doi.org/10.4315/0362-028X-69.1.80>
- Caillet, S., Millette, M., Turgis, M., Salmieri, S., Lacroix, M., 2006b. Influence of antimicrobial compounds and modified atmosphere packaging on radiation sensitivity of *Listeria monocytogenes* present in ready-to-use carrots (*Daucus carota*). *J. Food Prot.* 69, 221–227. <https://doi.org/10.4315/0362-028X-69.1.221>
- Camarero-Espinosa, S., Kuhnt, T., Foster, E.J., Weder, C., 2013. Isolation of thermally stable cellulose nanocrystals by phosphoric acid hydrolysis. *Biomacromolecules* 14, 1223–1230. <https://doi.org/10.1021/bm400219u>
- Campos-Requena, V.H., Rivas, B.L., Pérez, M.A., Figueroa, C.R., Figueroa, N.E., Sanfuentes, E.A., 2017. Thermoplastic starch/clay nanocomposites loaded with essential oil constituents as packaging for strawberries – In vivo antimicrobial synergy over *Botrytis cinerea*. *Postharvest Biol. Technol.* 129, 29–36. <https://doi.org/10.1016/j.postharvbio.2017.03.005>
- Carlsson, D.O., Lindh, J., Nyholm, L., Strømme, M., Mhraryan, A., 2014. Cooxidant-free TEMPO-mediated oxidation of highly crystalline nanocellulose in water. *RSC Adv.* 4, 52289–52298. <https://doi.org/10.1039/C4RA11182F>
- Catalá, R., Gavara, R., 1996. Review: alternative high barrier polymers for food packaging revisión: polímeros de alta barrera para el envase de alimentos. *Food Sci. Technol. Int.* 2, 281–291. <https://doi.org/10.1177/108201329600200501>
- Cell Membrane Structure [WWW Document] AECBio11 Wiki. URL https://aebio11.fandom.com/wiki/1.2_Cell_Membrane_Structure (accessed 6.19.19).
- Ching, S.H., Bansal, N., Bhandari, B., 2017. Alginate gel particles—a review of production techniques and physical properties. *Crit. Rev. Food Sci. Nutr.* 57, 1133–1152. <https://doi.org/10.1080/10408398.2014.965773>

- Ciftci, D., Ozilgen, S., 2019. Evaluation of kinetic parameters in prevention of quality loss in stored almond pastes with added natural antioxidant. *J. Food Sci. Technol.* 56, 483–490. <https://doi.org/10.1007/s13197-018-3510-6>
- Choe, E., Min, D.B., 2005. Chemistry and reactions of reactive oxygen species in foods. *J. Food Sci.* 70, R142–R159. <https://doi.org/10.1111/j.1365-2621.2005.tb08329.x>
- Collins, C., Grange, J., Lyne, P., III, J.F., 2004. *Collins and Lyne's Microbiological Methods*, 8Ed, CRC Press, London.
- Conn, R.E., Kolstad, J.J., Borzelleca, J.F., Dixler, D.S., Filer, L.J., Ladu, B.N., Pariza, M.W., 1995. Safety assessment of polylactide (PLA) for use as a food-contact polymer. *Food Chem. Toxicol.* 33, 273–283. [https://doi.org/10.1016/0278-6915\(94\)00145-E](https://doi.org/10.1016/0278-6915(94)00145-E)
- Conrad, K.R., Davidson, V.J., Mulholland, D.L., Britt, I.J., Yada, S., 2005. Influence of PET and PET/PEN blend packaging on ascorbic acid and color in juices exposed to fluorescent and UV light. *J. Food Sci.* 70, E19–E25. <https://doi.org/10.1111/j.1365-2621.2005.tb09032.x>
- Cretu, M., I. Docan, A., Cristea, V., Vârlan, O.-G., Lorena, D., Guriencu, R., 2017. The effect of dietary supplementation with Sea-buckthorn (*Hippophae rhamnoides*) and Spirulina (*Spirulina platensis*) on the growth performance of some sturgeon hybrids. *AAFL Bioflux* 10, 1157-1163. <http://www.bioflux.com.ro/docs/2017.1157-1163.pdf>
- Criado, P., Frascini, C., Salmieri, S., Becher, D., Safrany, A., Lacroix, M., 2016. Free radical grafting of gallic acid (GA) on cellulose nanocrystals (CNCS) and evaluation of antioxidant reinforced gellan gum films. *Radiat. Phys. Chem., Ionizing Radiation and Polymers symposium, IRaP 2014* 118, 61–69. <https://doi.org/10.1016/j.radphyschem.2015.05.030>
- Criado, P., Frascini, C., Salmieri, S., Lacroix, M., 2019. Effect of cellulose nanocrystals on thyme essential oil release from alginate beads: study of antimicrobial activity against *Listeria innocua* and ground meat shelf life in combination with gamma irradiation. *Cellulose* (submitted 1st February 2019).
- da Silva, S.L., Marangoni, C., Brum, D.S., Vendruscolo, R.G., Silva, M.S., de Moura, H.C., Rampelotto, C., Wagner, R., de Menezes, C.R., Barin, J.S., Campagnol, P.C., Cichoski, A., 2018. Effect of dietary olive leaves on the lipid and protein oxidation and bacterial safety of chicken hamburgers during frozen storage. *Int Food Res J.* 25, 383–391.
- Danalache, F., Beirão-da-Costa, S., Mata, P., Alves, V.D., Moldão-Martins, M., 2015. Texture, microstructure and consumer preference of mango bars jellified with gellan gum. *LWT - Food Sci. Technol.* 62, 584–591. <https://doi.org/10.1016/j.lwt.2014.12.040>
- de Nooy, A.E.J., Besemer, A.C., Bekkum, H. van, 1994. Highly selective TEMPO mediated oxidation of primary alcohol groups in polysaccharides. *Recl. Trav. Chim. Pays-Bas* 113, 165–166. <https://doi.org/10.1002/recl.19941130307>
- De Souza Lima, M.M., Wong, J.T., Paillet, M., Borsali, R., Pecora, R., 2003. Translational and rotational dynamics of rodlike cellulose whiskers. *Langmuir* 19, 24–29. <https://doi.org/10.1021/la020475z>

- Dehghani, S., Hosseini, S.V., Regenstein, J.M., 2018. Edible films and coatings in seafood preservation: a review. *Food Chem.* 240, 505–513. <https://doi.org/10.1016/j.foodchem.2017.07.034>
- Del Toro-Sánchez, C.L., Ayala-Zavala, J.F., Machi, L., Santacruz, H., Villegas-Ochoa, M.A., Alvarez-Parrilla, E., González-Aguilar, G.A., 2010. Controlled release of antifungal volatiles of thyme essential oil from β -cyclodextrin capsules. *J. Incl. Phenom. Macrocycl. Chem.* 67, 431–441. <https://doi.org/10.1007/s10847-009-9726-3>
- Dhar, P., Bhardwaj, U., Kumar, A., Katiyar, V., 2015. Poly (3-hydroxybutyrate)/cellulose nanocrystal films for food packaging applications: barrier and migration studies. *Polym. Eng. Sci.* 55, 2388–2395. <https://doi.org/10.1002/pen.24127>
- Dhar, P., Gaur, S.S., Soundararajan, N., Gupta, A., Bhasney, S.M., Milli, M., Kumar, A., Katiyar, V., 2017. Reactive extrusion of polylactic acid/cellulose nanocrystal films for food packaging applications: influence of filler type on thermomechanical, rheological, and barrier properties. *Ind. Eng. Chem. Res.* 56, 4718–4735. <https://doi.org/10.1021/acs.iecr.6b04699>
- Dobarganes, M.C., Velasco, J., 2002. Analysis of lipid hydroperoxides. *Eur. J. Lipid Sci. Technol.* 104, 420–428. [https://doi.org/10.1002/1438-9312\(200207\)104:7<420::AID-EJLT420>3.0.CO;2-N](https://doi.org/10.1002/1438-9312(200207)104:7<420::AID-EJLT420>3.0.CO;2-N)
- Domard, A., Cartier, N., 1989. Preparation and characterization of fully deacetylated chitosan. *Int J Biol Macromol* 11, 297–302.
- Dong, X.M., Revol, J.-F., Gray, D.G., 1998. Effect of microcrystallite preparation conditions on the formation of colloid crystals of cellulose. *Cellulose* 5, 19–32. <https://doi.org/10.1023/A:1009260511939>
- Du, L., Arnholt, K., Ripp, S., Sayler, G., Wang, S., Liang, C., Wang, J., Zhuang, J., 2015. Biological toxicity of cellulose nanocrystals (CNCs) against the luxCDABE-based bioluminescent bioreporter *Escherichia coli* 652T7. *Ecotoxicol. Lond. Engl.* 24, 2049–2053. <https://doi.org/10.1007/s10646-015-1555-0>
- Dufresne, A., 2017. Cellulose nanomaterial reinforced polymer nanocomposites. *Curr. Opin. Colloid Interface Sci.* 29, 1–8. <https://doi.org/10.1016/j.cocis.2017.01.004>
- Dufresne, A., 2012. Nanocellulose: from nature to high performance tailored materials, in: de Gruyter, Berlin.
- El Achaby, M., El Miri, N., Hannache, H., Gmouh, S., Ben youcef, H., Aboulkas, A., 2018. Production of cellulose nanocrystals from vine shoots and their use for the development of nanocomposite materials. *Int. J. Biol. Macromol.* 117, 592–600. <https://doi.org/10.1016/j.ijbiomac.2018.05.201>
- El Salmawi, K.M., El-Naggar, A. A., Ibrahim, S.M., 2018. Gamma irradiation synthesis of carboxymethyl cellulose/acrylic acid/clay superabsorbent hydrogel. *Adv. Polym. Technol.* 37, 515–521. <https://doi.org/10.1002/adv.21690>
- Ertesvåg, H., Valla, S., 1998. Biosynthesis and applications of alginates, in: *Polym. Degrad. Stab., biodegradable polymers and macromolecules.* 59, 85–91. [https://doi.org/10.1016/S0141-3910\(97\)00179-1](https://doi.org/10.1016/S0141-3910(97)00179-1)

- Espinosa, S.C., Kuhnt, T., Foster, E.J., Weder, C., 2013. Isolation of thermally stable cellulose nanocrystals by phosphoric acid hydrolysis. *Biomacromolecules*, 14, 1223-1230. <https://doi.org/10.1021/bm400219u>
- Eustice, R., 2011. Food Irradiation: a global perspective & future prospects [WWW Document] URL <http://ansnuclearcafe.org/2011/06/09/food-irradiation-a-global-perspective-future-prospects/>. (accessed 10.24.18).
- Eymard, S., Genot, C., 2003. A modified xylenol orange method to evaluate formation of lipid hydroperoxides during storage and processing of small pelagic fish. *Eur. J. Lipid Sci. Technol.* 105, 497–501. <https://doi.org/10.1002/ejlt.200300768>
- Favier, V., Canova, G.R., Cavaillé, J.Y., Chanzy, H., Dufresne, A., Gauthier, C., 1995. Nanocomposite materials from latex and cellulose whiskers. *Polym. Adv. Technol.* 6, 351–355. <https://doi.org/10.1002/pat.1995.220060514>
- Feng, T., Du, Y., Li, J., Hu, Y., Kennedy, J.F., 2008. Enhancement of antioxidant activity of chitosan by irradiation. *Carbohydr. Polym.* 73, 126–132. <https://doi.org/10.1016/j.carbpol.2007.11.003>
- Filpponen, I., Argyropoulos, D.S., 2010. Regular linking of cellulose nanocrystals via click chemistry: synthesis and formation of cellulose nanoplatelet gels. *Biomacromolecules* 11, 1060–1066. <https://doi.org/10.1021/bm1000247>
- Fincke A., Maurer R., 1974 Verhalten von citronenöl bei der herstellung und lagerung citronenöhlhaltiger zuckerwaren. 2 Mitteilung: Lager-und herstellungsversuche. *Dtsch Lebensm Rdsch* 70: 100-104.
- Flores, S.C.P., 1976. Gamma radiation as fungicide and its effects on paper. *Bull. Am. Inst. Conserv.* 16, 15–44. <https://doi.org/10.1179/019713676806029384>
- Fotie, G., Limbo, S., Piergiovanni, L., 2018. Effectiveness of Cellulose Nanocrystals (CNCS) application as bio-based oxygen barrier for shelled walnuts shelf-life extension. *Ital. J. Food Sci.* 30, 1–6.
- Fraschini, C., Chauve, G., Bouchard, J., 2017. TEMPO-mediated surface oxidation of cellulose nanocrystals (CNCs). *Cellulose* 24, 2775–2790. <https://doi.org/10.1007/s10570-017-1319-5>
- Frérot, E., 2017. Fats and oils, in: Buettner, A. (Ed.) *Springer Handbook of Odor*, Springer Handbooks. Springer, Cham, pp. 31–32. https://doi.org/10.1007/978-3-319-26932-0_11
- Furtak-Wrona, K., Kozik-Ostrówka, P., Jadwiszczak, K., Maigret, J.E., Aguié-Béghin, V., Coqueret, X., 2018. Polyurethane acrylate networks including cellulose nanocrystals: a comparison between UV and EB- curing. *Radiat. Phys. Chem., Ionizing radiations and polymers, IRaP-2016* 142, 94–99. <https://doi.org/10.1016/j.radphyschem.2017.04.013>
- Gallois, A., Langlois, D., 1990. New results in the volatile odorous compounds of french cheeses. *Le Lait* 70, 89–106. <https://doi.org/10.1051/lait:199028>
- Gambale, W., Croce, J., Costam-Manso, E., Croce, M., Sales, M., 1993. Library fungi at the University of Sao Paulo and their relationship with respiratory allergy. *J. Investig. Allergol. Clin. Immunol.* 3, 45–50.
- García, M., Barsema, J., Galindo, R.E., Cangialosi, D., Garcia-Turiel, J., Zyl, W.E. van, Verweij, H., Blank, D.H.A., 2004. Hybrid organic inorganic nylon-6/SiO₂

- nanocomposites: Transport properties. *Polym. Eng. Sci.* 44, 1240–1246. <https://doi.org/10.1002/pen.20119>
- Garcia-Garcia, D., Lopez-Martinez, J., Balart, R., Strömberg, E., Moriana, R., 2018. Reinforcing capability of cellulose nanocrystals obtained from pine cones in a biodegradable poly(3-hydroxybutyrate)/poly(ϵ -caprolactone) (PHB/PCL) thermoplastic blend. *Eur. Polym. J.* 104, 10–18. <https://doi.org/10.1016/j.eurpolymj.2018.04.036>
- Gennadios, A., Hanna, M.A., Kurth, L.B., 1997. Application of edible coatings on meats, poultry and seafoods: a review. *LWT - Food Sci. Technol.* 30, 337–350. <https://doi.org/10.1006/fstl.1996.0202>
- Glegg, R.E., Kertesz, Z.I., 1957. Effect of gamma-radiation on cellulose. *J. Polym. Sci.* 26, 289–297. <https://doi.org/10.1002/pol.1957.1202611403>
- Gorshkova, T.A., Wyatt, S.E., Salnikov, V.V., Gibeaut, D.M., Ibragimov, M.R., Lozovaya, V.V., Carpita, N.C., 1996. Cell-wall polysaccharides of developing flax plants. *Plant Physiol.* 110, 721–729.
- Government of Canada, Canadian Food Inspection Agency, 2012. Former - Irradiated Foods [WWW Document] URL <http://www.inspection.gc.ca/food/labelling/former-food-labelling-for-industry/former-irradiated-foods/eng/1506563742546/1506563743124> (accessed 10.24.18).
- Government of Canada, 2013. Permitted synonyms for food additives table [WWW Document]. URL <http://www.inspection.gc.ca/food/labelling/food-labelling-for-industry/list-of-ingredients-and-allergens/table/eng/1369857665232/1369857767799> (accessed 3.11.18).
- Government of Canada, 2012. Recalls and safety alerts [WWW Document]. URL <http://www.healthycanadians.gc.ca/recall-alert-rappel-avis/index-eng.php> (accessed 3.5.18).
- Gralén, N., The Svedberg, 1943. Molecular weight of native cellulose. *Nature* 152, 625. <https://doi.org/10.1038/152625a0>
- Grau, A., Guardiola, F., Boatella, J., Barroeta, A., Codony, R., 2000. Measurement of 2-thiobarbituric acid values in dark chicken meat through derivative spectrophotometry: influence of various parameters. *J. Agric. Food Chem.* 48, 1155–1159. <https://doi.org/10.1021/jf990518q>
- Greene, B.E., 1969. Lipid oxidation and pigment changes in raw beef. *J. Food Sci.* 34, 110–113. <https://doi.org/10.1111/j.1365-2621.1969.tb00898.x>
- Grujic, R., Vukic, M., Gojkovic, V., 2017. Application of biopolymers in the food industry, in: *advances in applications of industrial biomaterials*. Springer. 103–119. https://doi.org/10.1007/978-3-319-62767-0_6
- Guidetti, G., Atifi, S., Vignolini, S., Hamad, W.Y., 2016. Flexible photonic cellulose nanocrystal films. *Adv. Mater.* 28, 10042–10047. <https://doi.org/10.1002/adma.201603386>
- Habibi, Y., Chanzy, H., Vignon, M.R., 2006. TEMPO-mediated surface oxidation of cellulose whiskers. *Cellulose* 13, 679–687. <https://doi.org/10.1007/s10570-006-9075-y>

- Habibi, Y., Lucia, L.A., Rojas, O.J., 2010. Cellulose nanocrystals: chemistry, self-assembly, and applications. *Chem. Rev.* 110, 3479–3500. <https://doi.org/10.1021/cr900339w>
- Hai, L.V., Bum Seo, Y., 2017. Characterization of cellulose nanocrystal obtained from electron beam treated cellulose fiber. *Nordic Pulp and Paper Research* 32.
- Hamad W.Y., Hu T. Q., 2010. Structure–process–yield interrelations in nanocrystalline cellulose extraction. *Can. J. Chem. Eng.* 88, 392–402. <https://doi.org/10.1002/cjce.20298>
- Hamad, W., 2017. Properties of cellulose nanocrystals, in: *Cellulose Nanocrystals*. John Wiley & Sons, Ltd. (pp. 65–137). <https://doi.org/10.1002/9781118675601.ch4>
- Ham-Pichavant, F., Sèbe, G., Pardon, P., Coma, V., 2005. Fat resistance properties of chitosan-based paper packaging for food applications. *Carbohydr. Polym.* 61, 259–265. <https://doi.org/10.1016/j.carbpol.2005.01.020>
- Hancock, D.D., Besser, T.E., Rice, D.H., Ebel, E.D., Herriott, D.E., Carpenter, L.V., 1998. Multiple sources of Escherichia coli O157 in feedlots and dairy farms in the northwestern USA. *Prev. Vet. Med.* 35, 11–19. [https://doi.org/10.1016/S0167-5877\(98\)00050-6](https://doi.org/10.1016/S0167-5877(98)00050-6)
- Harper, B.J., Clendaniel, A., Sinche, F., Way, D., Hughes, M., Schardt, J., Simonsen, J., Stefaniak, A.B., Harper, S.L., 2016. Impacts of chemical modification on the toxicity of diverse nanocellulose materials to developing zebrafish. *Cellul. Lond. Engl.* 23, 1763–1775. <https://doi.org/10.1007/s10570-016-0947-5>
- Hasanain, F., Guenther, K., Mullett, W.M., Craven, E., 2014. Gamma sterilization of pharmaceuticals—a review of the irradiation of excipients, active pharmaceutical ingredients, and final drug product formulations. *PDA J. Pharm. Sci. Technol.* 68, 113–137. <https://doi.org/10.5731/pdajpst.2014.00955>
- Hasegawa, M., Yagi, K., Iwakawa, S., Hirai, M., 2001. Chitosan induces apoptosis via caspase-3 activation in bladder tumor cells. *Jpn. J. Cancer Res.* 92, 459–466. <https://doi.org/10.1111/j.1349-7006.2001.tb01116.x>
- Hassanzadeh, P., Tajik, H., Rohani, S.M.R., Moradi, M., Hashemi, M., Aliakbarlu, J., 2017. Effect of functional chitosan coating and gamma irradiation on the shelf-life of chicken meat during refrigerated storage. *Radiat. Phys. Chem.* 141, 103–109. <https://doi.org/10.1016/j.radphyschem.2017.06.014>
- Health Canada, 2008. Vitamin D and calcium: updated dietary reference intakes [WWW Document]. URL <https://www.canada.ca/en/health-canada/services/food-nutrition/healthy-eating/vitamins-minerals/vitamin-calcium-updated-dietary-reference-intakes-nutrition.html#a15> (accessed 12.30.18).
- Health Canada, H., 2004. Food-Related Illnesses [WWW Document]. URL <https://www.canada.ca/en/health-canada/services/food-nutrition/food-safety/food-related-illnesses.html> (accessed 6.12.19).
- Health Canada, 2011. Policy on Listeria monocytogenes in ready-to-eat foods [WWW Document]. URL <https://www.canada.ca/en/health-canada/services/food-nutrition/legislation-guidelines/policies/policy-listeria-monocytogenes-ready-eat-foods-2011.html#appb> (accessed 12.19.18).

- Health Canada, 2005. Dietary reference intakes [WWW Document]. URL <https://www.canada.ca/en/health-canada/services/food-nutrition/healthy-eating/dietary-reference-intakes/tables/reference-values-elements-dietary-reference-intakes-tables-2005.html> (accessed 12.30.18).
- Helbert, W., Cavallé, J.Y., Dufresne, A., 1996. Thermoplastic nanocomposites filled with wheat straw cellulose whiskers. Part I: Processing and mechanical behavior. *Polym. Compos.* 17, 604–611. <https://doi.org/10.1002/pc.10650>
- Henniges, U., Okubayashi, S., Rosenau, T., Potthast, A., 2012. Irradiation of cellulosic pulps: understanding its impact on cellulose oxidation. *Biomacromolecules* 13, 4171–4178. <https://doi.org/10.1021/bm3014457>
- Horáková, H., Martinek, F., 1984. Desinfection of archive documents by ionizing radiation. *Restaurador* 6, 205–216.
- Horticulture and Forestry Science, Agri-Science queensland shelf-life extension and nutritional profile of irradiated strawberry. March 2012.
- Hossain, F., Follett, P., Vu, K.D., Salmieri, S., Fraschini, C., Jamshidian, M., Lacroix, M., 2018. Antifungal activity of combined treatments of active methylcellulose-based films containing encapsulated nanoemulsion of essential oils and γ -irradiation: in vitro and in situ evaluations. *Cellulose* <https://doi.org/10.1007/s10570-018-2135-2>
- Hosseini, S.M., Hosseini, H., Mohammadifar, M.A., Mortazavian, A.M., Mohammadi, A., Khosravi-Darani, K., Shojaee-Aliabadi, S., Dehghan, S., Khaksar, R., 2013. Incorporation of essential oil in alginate microparticles by multiple emulsion/ionic gelation process. *Int. J. Biol. Macromol.* 62, 582–588. <https://doi.org/10.1016/j.ijbiomac.2013.09.054>
- Hsieh, W.-C., Chang, C.-P., Gao, Y.-L., 2006. Controlled release properties of chitosan encapsulated volatile citronella oil microcapsules by thermal treatments. *Colloids Surf. B Biointerfaces* 53, 209–214. <https://doi.org/10.1016/j.colsurfb.2006.09.008>
- Huang, Y., Mei, L., Chen, X., Wang, Q., 2018. Recent developments in food packaging based on nanomaterials. *Nanomaterials* 8, 830. <https://doi.org/10.3390/nano8100830>
- Huq, T., Fraschini, C., Khan, A., Riedl, B., Bouchard, J., Lacroix, M., 2017. Alginate based nanocomposite for microencapsulation of probiotic: Effect of cellulose nanocrystal (CNC) and lecithin. *Carbohydr. Polym.* 168, 61–69. <https://doi.org/10.1016/j.carbpol.2017.03.032>
- Huq, T., Riedl, B., Bouchard, J., Salmieri, S., Lacroix, M., 2014. Microencapsulation of nisin in alginate-cellulose nanocrystal (CNC) microbeads for prolonged efficacy against *Listeria monocytogenes*. *Cellulose* 21, 4309–4321. <https://doi.org/10.1007/s10570-014-0432-y>
- Huq, T., Salmieri, S., Khan, A., Khan, R.A., Le Tien, C., Riedl, B., Fraschini, C., Bouchard, J., Uribe-Calderon, J., Kamal, M.R., Lacroix, M., 2012. Nanocrystalline cellulose (NCC) reinforced alginate based biodegradable nanocomposite film. *Carbohydr. Polym.* 90, 1757–1763. <https://doi.org/10.1016/j.carbpol.2012.07.065>
- Irimia, A., Ioanid, G.E., Zaharescu, T., Coroabă, A., Doroftei, F., Safrany, A., Vasile, C., 2017. Comparative study on gamma irradiation and cold plasma pretreatment for a cellulosic substrate modification with phenolic compounds. *Radiat. Phys. Chem.* 130, 52–61. <https://doi.org/10.1016/j.radphyschem.2016.07.028>

- Jackson, J.K., Letchford, K., Wasserman, B.Z., Ye, L., Hamad, W.Y., Burt, H.M., 2011. The use of nanocrystalline cellulose for the binding and controlled release of drugs. *Int. J. Nanomedicine* 6, 321–330. <https://doi.org/10.2147/IJN.S16749>
- Jeantet, R., Croguennec, T., Schuck, P., Brulé, G., Collectif, 2006a. *Science des aliments: Tome 1, Stabilisation biologique et physico-chimique*. Tec & Doc Lavoisier, Paris.
- Jeantet, R., Croguennec, T., Schuck, P., Brulé, G., Collectif, 2006b. *Science des aliments: Tome 2, Technologie des produits alimentaires*. Tec & Doc Lavoisier, Paris.
- Jensen, A., 1993. Present and future needs for algae and algal products. *Hydrobiologia* 260–261, 15–23. <https://doi.org/10.1007/BF00048998>
- Jeon, Y.-J., Park, P.-J., Kim, S.-K., 2001. Antimicrobial effect of chitooligosaccharides produced by bioreactor. *Carbohydr. Polym.* 44, 71–76. [https://doi.org/10.1016/S0144-8617\(00\)00200-9](https://doi.org/10.1016/S0144-8617(00)00200-9)
- Jiang, G., Zhang, M., Feng, J., Zhang, S., Wang, X., 2017. High oxygen barrier property of poly(propylene carbonate)/polyethylene glycol nanocomposites with low loading of cellulose nanocrystals. *ACS Sustain. Chem. Eng.* 5, 11246–11254. <https://doi.org/10.1021/acssuschemeng.7b01674>
- Karimirad, R., Behnamian, M., Dezhsetan, S., Sonnenberg, A., 2018. Chitosan nanoparticles-loaded Citrus aurantium essential oil: a novel delivery system for preserving the postharvest quality of *Agaricus bisporus*. *J. Sci. Food Agric.* 98, 5112–5119. <https://doi.org/10.1002/jsfa.9050>
- Karkhanis, S.S., Stark, N.M., Sabo, R.C., Matuana, L.M., 2018. Water vapor and oxygen barrier properties of extrusion-blown poly(lactic acid)/cellulose nanocrystals nanocomposite films. *Compos. Part Appl. Sci. Manuf.* 114, 204–211. <https://doi.org/10.1016/j.compositesa.2018.08.025>
- Karthika, J.S., Vishalakshi, B., 2015. Novel stimuli responsive gellan gum-graft-poly(DMAEMA) hydrogel as adsorbent for anionic dye. *Int. J. Biol. Macromol.* 81, 648–655. <https://doi.org/10.1016/j.ijbiomac.2015.08.064>
- Kaushik, M., Frascini, C., Chauve, G., Moores, J.-L.P. and A., 2015. Transmission electron microscopy for the characterization of cellulose nanocrystals. *Transm. Electron Microsc. - Theory Appl.* 129-163 <https://doi.org/10.5772/60985>
- Khan, A., Khan, R.A., Salmieri, S., Le Tien, C., Riedl, B., Bouchard, J., Chauve, G., Tan, V., Kamal, M.R., Lacroix, M., 2012. Mechanical and barrier properties of nanocrystalline cellulose reinforced chitosan based nanocomposite films. *Carbohydr. Polym.* 90, 1601–1608. <https://doi.org/10.1016/j.carbpol.2012.07.037>
- Khattak A. B. and Klopfenstein C. F., 1989. Effects of gamma irradiation on the nutritional quality of grain and legumes. I. Stability of niacin, thiamin, and riboflavin. *Cereal chem.* 66, 169-170
- Kirchmajer, D.M., Steinhoff, B., Warren, H., Clark, R., in het Panhuis, M., 2014. Enhanced gelation properties of purified gellan gum. *Carbohydr. Res.* 388, 125–129. <https://doi.org/10.1016/j.carres.2014.02.018>

- Klemm, D., Kramer, F., Moritz, S., Lindström, T., Ankerfors, M., Gray, D., Dorris, A., 2011. Nanocelluloses: a new family of nature-based materials. *Angew. Chem. Int. Ed.* 50, 5438–5466. <https://doi.org/10.1002/anie.201001273>
- Kobayashi, Y., 1961. Gamma-ray-induced graft copolymerization of styrene onto cellulose and some chemical properties of the grafted polymer. *J. Polym. Sci.* 51, 359–372. <https://doi.org/10.1002/pol.1961.1205115522>
- Kovacs, T., Naish, V., O'Connor, B., Blaise, C., Gagné, F., Hall, L., Trudeau, V., Martel, P., 2010. An ecotoxicological characterization of nanocrystalline cellulose (NCC). *Nanotoxicology* 4, 255–270. <https://doi.org/10.3109/17435391003628713>
- Kubat, J., Martin-Lof, S., De Ruvo, A., 1968. The effect of gamma radiation on some paper properties. *Sven. Papperstidningarg* 71, 851–856.
- Kubeczka K-H., 1993. Möglichkeiten und Grenzen der Qualitätsbeurteilung arzneilich verwendeter ätherischer Öle. In: Carle R (Ed.). *Ätherische Öle - Anspruch and Wirklichkeit*. Stuttgart, Germany: Wissenschaftliche Verlagsgesellschaft. p 85-102
- Kuga, S., Muto, N., Isogai, A., Usuda, M., 1989. Molecular weight distribution of native celluloses, in: *Cellulose, structure and functional aspects*. pp. 81–86.
- Kulkarni, S.G., Vijayanand, P., 2010. Effect of extraction conditions on the quality characteristics of pectin from passion fruit peel (*Passiflora edulis f. flavicarpa L.*). *LWT - Food Sci. Technol.* 43, 1026–1031. <https://doi.org/10.1016/j.lwt.2009.11.006>
- Kusumaningrum, H.D., Riboldi, G., Hazeleger, W.C., Beumer, R.R., 2003. Survival of foodborne pathogens on stainless steel surfaces and cross-contamination to foods. *Int. J. Food Microbiol.* 85, 227–236. [https://doi.org/10.1016/S0168-1605\(02\)00540-8](https://doi.org/10.1016/S0168-1605(02)00540-8)
- Kvien, I., Tanem, B.S., Oksman, K., 2005. Characterization of cellulose whiskers and their nanocomposites by atomic force and electron microscopy. *Biomacromolecules* 6, 3160–3165. <https://doi.org/10.1021/bm050479t>
- Labuza, T.P., Dugan Jr, L.R., 1971. Kinetics of lipid oxidation in foods. *C R C Crit. Rev. Food Technol.* 2, 355–405. <https://doi.org/10.1080/10408397109527127>
- Lagaron, J.M., Catalá, R., Gavara, R., 2004. Structural characteristics defining high barrier properties in polymeric materials. *Mater. Sci. Technol.* 20, 1–7. <https://doi.org/10.1179/026708304225010442>
- Larotonda, F., 2007. Biodegradable films and coatings obtained from carrageenan from *Mastocarpus stellatus* and starch from *Quercus suber*. Universidade do Porto.
- Le Moigne, N., Sonnier, R., El Hage, R., Rouif, S., 2017. Radiation-induced modifications in natural fibres and their biocomposites: Opportunities for controlled physico-chemical modification pathways? *Ind. Crops Prod.* 109, 199–213. <https://doi.org/10.1016/j.indcrop.2017.08.027>
- Lee, K.Y., Mooney, D.J., 2012. Alginate: properties and biomedical applications. *Prog. Polym. Sci.* 37, 106–126. <https://doi.org/10.1016/j.progpolymsci.2011.06.003>
- Lee, L.K., 1987. Radiation chemistry of biopolymers, in: *Radiation chemistry*. p. 497.

- Lee, S., Phillips, A.L., Liebler, D.C., Faustman, C., 2003. Porcine oxymyoglobin and lipid oxidation in vitro. *Meat Sci.* 63, 241–247. [https://doi.org/10.1016/S0309-1740\(02\)00076-1](https://doi.org/10.1016/S0309-1740(02)00076-1)
- Lemke, C.H., Dong, R.Y., Michal, C.A., Hamad, W.Y., 2012. New insights into nanocrystalline cellulose structure and morphology based on solid-state NMR. *Cellulose* 19, 1619–1629. <https://doi.org/10.1007/s10570-012-9759-4>
- Le-Tien, C., Millette, M., Lacroix, M., Mateescu, M.-A., 2004. Modified alginate matrices for the immobilization of bioactive agents. *Biotechnol. Appl. Biochem.* 39, 189–198. <https://doi.org/10.1042/BA20030054>
- Li, M., Tshabalala, M.A., Buschle-Diller, G., 2016. Formulation and characterization of polysaccharide beads for controlled release of plant growth regulators. *J. Mater. Sci.* 51, 4609–4617. <https://doi.org/10.1007/s10853-016-9775-0>
- Linnan, M.J., Mascola, L., Lou, X.D., Goulet, V., May, S., Salminen, C., Hird, D.W., Yonekura, M.L., Hayes, P., Weaver, R., 1988. Epidemic listeriosis associated with Mexican-style cheese. *N. Engl. J. Med.* 319, 823–828. <https://doi.org/10.1056/NEJM198809293191303>
- Little, C.L., Sagoo, S.K., Gillespie, I.A., Grant, K., McLauchlin, J., 2009. Prevalence and level of *Listeria monocytogenes* and other *Listeria* species in selected retail ready-to-eat foods in the United Kingdom. *J. Food Prot.* 72, 1869–1877.
- Liu, P., Guo, X., Nan, F., Duan, Y., Zhang, J., 2017. Modifying mechanical, optical properties and thermal processability of iridescent cellulose nanocrystal films using ionic liquid. *ACS Appl. Mater. Interfaces* 9, 3085–3092. <https://doi.org/10.1021/acsami.6b12953>
- Lizundia, E., Meaurio, E., & Vilas, J.L., 2016. Chapter 3 - Grafting of Cellulose Nanocrystals, in: Puglia, D., Fortunati, E., Kenny, J.M. (Eds.), *Multifunctional polymeric nanocomposites based on cellulosic reinforcements*. William Andrew Publishing, pp. 61–113. <https://doi.org/10.1016/B978-0-323-44248-0.00003-1>.
- Long, K., Cha, R., Zhang, Y., Li, J., Ren, F., Jiang, X., 2018. Cellulose nanocrystals as reinforcements for collagen-based casings with low gas transmission. *Cellulose* 25, 463–471. <https://doi.org/10.1007/s10570-017-1569-2>
- Louis, M.E.S., Morse, D.L., Potter, M.E., DeMelfi, T.M., Guzewich, J.J., Tauxe, R.V., Blake, P.A., Cartter, M.L., Petersen, L., Gallagher, K., Greenspan, J.R., Gensheimer, K.F., Dennis, D., Schwartz, E., Parkin, W.E., Rosenfeld, H., Schultz, S., Kondracki, S.F., Witte, E.J., Vogt, R.L., Pühr, N., Shipman, L., Hargrett-Bean, N., 1988. The emergence of grade a eggs as a major source of salmonella enteritidis infections: new implications for the control of salmonellosis. *JAMA* 259, 2103–2107. <https://doi.org/10.1001/jama.1988.03720140023028>
- Martínez-Pardo, M.E., Vera-Graziano, R., 1995. Gamma radiation induced crosslinking of polyethylene/ethylene—vinylacetate blends. *Radiat. Phys. Chem.* 45, 93–102. [https://doi.org/10.1016/0969-806X\(94\)E0004-3](https://doi.org/10.1016/0969-806X(94)E0004-3)
- Marx-Figini, M., 1969. On the biosynthesis of cellulose in higher and lower plants. *J. Polym. Sci. Part C Polym. Symp.* 28, 57–67. <https://doi.org/10.1002/polc.5070280108>

- Mastromatteo, M., Barbuzzi, G., Conte, A., Del Nobile, M.A., 2009. Controlled release of thymol from zein based film. *Innov. Food Sci. Emerg. Technol.* 10, 222–227. <https://doi.org/10.1016/j.ifset.2008.11.010>
- McDougall, G.J., 1993. Isolation and partial characterisation of the non-cellulosic polysaccharides of flax fibre. *Carbohydr. Res.* 241, 227–236. [https://doi.org/10.1016/0008-6215\(93\)80109-R](https://doi.org/10.1016/0008-6215(93)80109-R)
- Mead, P.S., Griffin, P.M., 1998. Escherichia coli O157:H7. *The Lancet* 352, 1207–1212. [https://doi.org/10.1016/S0140-6736\(98\)01267-7](https://doi.org/10.1016/S0140-6736(98)01267-7)
- Mehyar, G.F., Al Nabulsi, A.A., Saleh, M., Olaimat, A.N., Holley, R.A., 2018. Effects of chitosan coating containing lysozyme or natamycin on shelf-life, microbial quality, and sensory properties of Halloumi cheese brined in normal and reduced salt solutions. *J. Food Process. Preserv.* 42, n/a-n/a. <https://doi.org/10.1111/jfpp.13324>
- Menas, A.L., Yanamala, N., Farcas, M.T., Russo, M., Friend, S., Fournier, P.M., Star, A., Iavicoli, I., Shurin, G.V., Vogel, U.B., Fadeel, B., Beezhold, D., Kisin, E.R., Shvedova, A.A., 2017. Fibrillar vs crystalline nanocellulose pulmonary epithelial cell responses: cytotoxicity or inflammation? *Chemosphere* 171, 671–680. <https://doi.org/10.1016/j.chemosphere.2016.12.105>
- Miller, A.F., Donald, A.M., 2003. Imaging of anisotropic cellulose suspensions using environmental scanning electron microscopy. *Biomacromolecules* 4, 510–517. <https://doi.org/10.1021/bm0200837>
- Miller, K.S., Krochta, J.M., 1997. Oxygen and aroma barrier properties of edible films: a review. *Trends Food Sci. Technol.* 8, 228–237. [https://doi.org/10.1016/S0924-2244\(97\)01051-0](https://doi.org/10.1016/S0924-2244(97)01051-0)
- Mima, S., Miya, M., Iwamoto, R., Yoshikawa, S., 1983. Highly deacetylated chitosan and its properties. *J. Appl. Polym. Sci.* 28
- Min, D.B., Boff, J.M., 2002. Chemistry and reaction of singlet oxygen in foods. *Compr. Rev. Food Sci. Food Saf.* 1, 58–72. <https://doi.org/10.1111/j.1541-4337.2002.tb00007.x>
- Moritaka, H., Naito, S., Nishinari, K., Ishihara, M., Fukuba, H., 1999. Effects of gellan gum, citric acid and sweetener on the texture of lemon jelly. *J. Texture Stud.* 30, 29–41. <https://doi.org/10.1111/j.1745-4603.1999.tb00200.x>
- Morris, E.R., Nishinari, K., Rinaudo, M., 2012. Gelation of gellan – a review. *Food Hydrocoll.* 28, 373–411. <https://doi.org/10.1016/j.foodhyd.2012.01.004>
- Murray, E.G.D., Webb, R.A., Swann, M.B.R., 1926. A disease of rabbits characterised by a large mononuclear leucocytosis, caused by a hitherto undescribed bacillus *Bacterium monocytogenes* (n.sp.). *J. Pathol. Bacteriol.* 29, 407–439. <https://doi.org/10.1002/path.1700290409>
- Nasef, M.M., Hegazy, E.-S.A., 2004. Preparation and applications of ion exchange membranes by radiation-induced graft copolymerization of polar monomers onto non-polar films. *Prog. Polym. Sci.* 29, 499–561. <https://doi.org/10.1016/j.progpolymsci.2004.01.003>

- Näslund, P., Vuong, R., Chanzy, H., C. Jésior, J., 1988. Diffraction contrast transmission electron microscopy on flax fiber ultrathin cross sections. *Text. Res. J.* 58, 414–417. <https://doi.org/10.1177/004051758805800707>
- Nguyen, H., Morgan, D.A.F., Forwood, M.R., 2007. Sterilization of allograft bone: effects of gamma irradiation on allograft biology and biomechanics. *Cell Tissue Bank.* 8, 93–105. <https://doi.org/10.1007/s10561-006-9020-1>
- No, H., Meyers, S., 1997. Preparation of chitin and chitosan, in: *chitin handbook*. pp. 475–489
- Nourooz-Zadeh, J., Tajaddini-Sarmadi, J., Wolff, S.P., 1995. Measurement of hydroperoxides in edible oils using the ferrous oxidation in xylenol orange assay. *J. Agric. Food Chem.* 43, 17–21. <https://doi.org/10.1021/jf00049a005>
- O'Connor, B., Berry, R., Goguen, R., 2014. Chapter 10 - Commercialization of cellulose nanocrystal (NCC™) production: a business case focusing on the importance of proactive EHS management, in: Hull, M.S., Bowman, D.M. (Eds.), *Nanotechnology Environmental Health and Safety (Second Edition)*, Micro and Nano Technologies. William Andrew Publishing, Oxford, pp. 225–246.
- Odier, A., 1821. Structural diversity of chitosan and its complexes, 29–42.
- Official Journal of the European Communities, 2002. Commission Directive 2002/72/EC [WWW Document]. URL <https://eur-lex.europa.eu/legal-content/EN/TXT/PDF/?uri=CELEX:32002L0072&from=EN> (accessed 16.01.18)
- Oksman, K., Bondeson, D., Syre, P., 2008. Nanocomposites based on cellulose whiskers and cellulose plastics. US20080108772A1.
- Ooi, S.Y., Ahmad, I., Amin, M.C.I.M., 2016. Cellulose nanocrystals extracted from rice husks as a reinforcing material in gelatin hydrogels for use in controlled drug delivery systems. *Ind. Crops Prod., nanocellulose: production, functionalisation and applications* 93, 227–234. <https://doi.org/10.1016/j.indcrop.2015.11.082>
- Oussalah, M., Caillet, S., Saucier, L., Lacroix, M., 2006. Antimicrobial effects of selected plant essential oils on the growth of a *Pseudomonas putida* strain isolated from meat. *Meat Sci.* 73, 236–244. <https://doi.org/10.1016/j.meatsci.2005.11.019>
- Ouattara, B., Sabato, S.F., Lacroix, M., 2001. Combined effect of antimicrobial coating and gamma irradiation on shelf life extension of pre-cooked shrimp (*Penaeus* spp.). *Int. J. Food Microbiol.* 68, 1–9. [https://doi.org/10.1016/S0168-1605\(01\)00436-6](https://doi.org/10.1016/S0168-1605(01)00436-6)
- Pacelli, S., Paolicelli, P., Dreesen, I., Kobayashi, S., Vitalone, A., Casadei, M.A., 2015. Injectable and photocross-linkable gels based on gellan gum methacrylate: a new tool for biomedical application. *Int. J. Biol. Macromol.* 72, 1335–1342. <https://doi.org/10.1016/j.ijbiomac.2014.10.046>
- Pacelli, S., Paolicelli, P., Moretti, G., Petralito, S., Di Giacomo, S., Vitalone, A., Casadei, M.A., 2016. Gellan gum methacrylate and laponite as an innovative nanocomposite hydrogel for biomedical applications. *Eur. Polym. J.* 77, 114–123. <https://doi.org/10.1016/j.eurpolymj.2016.02.007>
- Pedersen, S.S., Kharazmi, A., Espersen, F., Høiby, N., 1990. *Pseudomonas aeruginosa* alginate in cystic fibrosis sputum and the inflammatory response. *Infect. Immun.* 58, 3363–3368. [https://doi.org/0019-9567/90/103363-06\\$02.00/0](https://doi.org/0019-9567/90/103363-06$02.00/0)

- Pettersen, R.C., 1984. The chemical composition of wood, in: Rowell, R. (Ed.), *The chemistry of solid wood*. American Chemical Society, Washington, DC, pp. 57–126. <https://doi.org/10.1021/ba-1984-0207.ch002>
- Ponomarev, A.V., Ershov, B.G., 2014. Radiation-induced high-temperature conversion of cellulose. *Mol. Basel Switz.* 19, 16877–16908. <https://doi.org/10.3390/molecules191016877>
- Preuss, F., 1964. Über photomechanische Veränderungen von Bestandteilen des Kümmerlöles. *Dtsch Apoth Ztg* 104, 1797–1803
- Prezotti, F.G., Cury, B.S.F., Evangelista, R.C., 2014. Mucoadhesive beads of gellan gum/pectin intended to controlled delivery of drugs. *Carbohydr. Polym.* 113, 286–295. <https://doi.org/10.1016/j.carbpol.2014.07.021>
- Public Health Agency of Canada, 2015. Yearly food-borne illness estimates for Canada [WWW Document]. URL <https://www.canada.ca/en/public-health/services/food-borne-illness-canada/yearly-food-borne-illness-estimates-canada.html> (accessed 3.1.18).
- Pujato, S.A., Quiberoni, A., Mercanti, D.J., 2019. Bacteriophages on dairy foods. *J. Appl. Microbiol.* 126, 14–30. <https://doi.org/10.1111/jam.14062>
- Rahman, M.S., 2007. Food preservation: overview, in: *Handbook of food preservation*. CRC Press, Boca Raton, FL, USA, pp. 3–18. <https://doi.org/10.1201/9781420017373>
- Rampazzo, R., Alkan, D., Gazzotti, S., Ortenzi, M.A., Piva, G., Piergiovanni, L., 2017. Cellulose nanocrystals from lignocellulosic raw materials, for oxygen barrier coatings on food packaging films. *Packag. Technol. Sci.* 30, 645–661. <https://doi.org/10.1002/pts.2308>
- Rånby, B.G., 1949. Aqueous colloidal solutions of cellulose micelles. *Acta Chemica Scandinavica* 3, 649–650.
- Ravindra, R., Krovvidi, K.R., Khan, A.A., 1998. Solubility parameter of chitin and chitosan. *Carbohydr. Polym.* 36, 121–127. [https://doi.org/10.1016/S0144-8617\(98\)00020-4](https://doi.org/10.1016/S0144-8617(98)00020-4)
- Rehm, B.H.A. (Ed.), 2009. Material properties of alginates, in: *alginates: biology and applications, microbiology monographs*. Springer-Verlag, Berlin Heidelberg, pp. 2–53.
- Revol, J.F., Bradford, H., Giasson, J., H Marchessault, R., G Gray, D., 1992. Helicoidal self-ordering of cellulose microfibrils in aqueous suspension. *Int. J. Biol. Macromol.* 14, 170–2. [https://doi.org/10.1016/S0141-8130\(05\)80008-X](https://doi.org/10.1016/S0141-8130(05)80008-X)
- Rhim, J.-W., Lee, J.-H., Hong, S.-I., 2006. Water resistance and mechanical properties of biopolymer (alginate and soy protein) coated paperboards. *LWT - Food Sci. Technol.* 39, 806–813. <https://doi.org/10.1016/j.lwt.2005.05.008>
- Rhoades, J., Roller, S., 2000. Antimicrobial actions of degraded and native chitosan against spoilage organisms in laboratory media and foods. *Appl. Environ. Microbiol.* 66, 80–86.
- Ricardo Machi, A., Rodrigues Mayne, R., Adriani Gava, M., Bergamin Arthur, P., Arthur, V., 2019. Gamma radiation sterilization dose of adult males in asian tiger mosquito pupae. *Insects* 10, 101. <https://doi.org/10.3390/insects10040101>

- Riedo, F.X., Pinner, R.W., Tosca, M. de L., Cartter, M.L., Graves, L.M., Reeves, M.W., Weaver, R.E., Plikaytis, B.D., Broome, C., 1994. A point-source foodborne listeriosis outbreak: documented incubation period and possible mild illness. *J. Infect. Dis.* 170, 693–696. <https://doi.org/10.1093/infdis/170.3.693>
- Roman, M., 2015. Toxicity of cellulose nanocrystals: a review. *Ind. Biotechnol.* 11, 25–33. <https://doi.org/10.1089/ind.2014.0024>
- Roman, M., Dong, S., Hirani, A., Lee, Y.W., 2009. Cellulose nanocrystals for drug delivery, in: Edgar, K.J., Heinze, T., Buchanan, C.M. (Eds.) *Polysaccharide materials: performance by design*, ACS Symposium Series. American Chemical Society, pp. 81–91. <https://doi.org/10.1021/bk-2009-1017.ch004>
- Roy, D., Semsarilar, M., Guthrie, J.T., Perrier, S., 2009. Cellulose modification by polymer grafting: a review. *Chem. Soc. Rev.* 38, 2046–2064. <https://doi.org/10.1039/B808639G>
- Ruiz, M.M., Cavallé, J.Y., Dufresne, A., Graillat, C., Gérard, J.-F., 2001. New waterborne epoxy coatings based on cellulose nanofillers. *Macromol. Symp.* 169, 211–222. [https://doi.org/10.1002/1521-3900\(200105\)169:1<211::AID-MASY211>3.0.CO;2-H](https://doi.org/10.1002/1521-3900(200105)169:1<211::AID-MASY211>3.0.CO;2-H)
- Rusli, R., Eichhorn, S.J., 2008. Determination of the stiffness of cellulose nanowhiskers and the fiber-matrix interface in a nanocomposite using Raman spectroscopy. *Appl. Phys. Lett.* 93, 033111. <https://doi.org/10.1063/1.2963491>
- Sacui, I.A., Nieuwendaal, R.C., Burnett, D.J., Stranick, S.J., Jorfi, M., Weder, C., Foster, E.J., Olsson, R.T., Gilman, J.W., 2014. Comparison of the properties of cellulose nanocrystals and cellulose nanofibrils isolated from bacteria, tunicate, and wood processed using acid, enzymatic, mechanical, and oxidative methods. *ACS Appl. Mater. Interfaces* 6, 6127–6138. <https://doi.org/10.1021/am500359f>
- Sadeghifar, H., Filpponen, I., Clarke, S.P., Brougham, D.F., Argyropoulos, D.S., 2011. Production of cellulose nanocrystals using hydrobromic acid and click reactions on their surface. *J. Mater. Sci.* 46, 7344–7355. <https://doi.org/10.1007/s10853-011-5696-0>
- Salajková, M., Berglund, L.A., Zhou, Q., 2012. Hydrophobic cellulose nanocrystals modified with quaternary ammonium salts. *J. Mater. Chem.* 22, 19798–19805. <https://doi.org/10.1039/C2JM34355J>
- Salunke, S.R., Patil, S.B., 2016. Ion activated in situ gel of gellan gum containing salbutamol sulphate for nasal administration. *Int. J. Biol. Macromol.* 87, 41–47. <https://doi.org/10.1016/j.ijbiomac.2016.02.044>
- Sanchez-Garcia, M.D., Lagaron, J.M., 2010. On the use of plant cellulose nanowhiskers to enhance the barrier properties of polylactic acid. *Cellulose* 17, 987–1004. <https://doi.org/10.1007/s10570-010-9430-x>
- Sánchez Orozco, R., Balderas Hernández, P., Flores Ramírez, N., Roa Morales, G., Saucedo Luna, J., Castro Montoya, A.J., 2012. Gamma irradiation induced degradation of orange peels. *Energies* 5, 3051–3063. <https://doi.org/10.3390/en5083051>
- Sapalidis, A.A., Katsaros, F.K., Steriotis, T.A., Kanellopoulos, N.K., 2012. Properties of poly(vinyl alcohol)—bentonite clay nanocomposite films in relation to polymer—

- clay interactions. *J. Appl. Polym. Sci.* 123, 1812–1821. <https://doi.org/10.1002/app.34651>
- Satin, M., 1993. Food irradiation, in: *Food irradiation: a guidebook*. Technomic Pub., pp. 1-22.
- Schneider, N., Werkmeister, K., Pischetsrieder, M., 2011. Analysis of nisin A, nisin Z and their degradation products by LCMS/MS. *Food Chem.* 127, 847–854. <https://doi.org/10.1016/j.foodchem.2011.01.023>
- Şengül, B., Dilsiz, N., 2014. Barrier properties of polylactic acid/layered silicate nanocomposites for food contact applications. *Polym. Sci. - Ser. A* 56, 896–906. <https://doi.org/10.1134/S0965545X14060194>
- Serrano-León, J.S., Bergamaschi, K.B., Yoshida, C.M.P., Saldaña, E., Selani, M.M., Rios-Mera, J.D., Alencar, S.M., Contreras-Castillo, C.J., 2018. Chitosan active films containing agro-industrial residue extracts for shelf life extension of chicken restructured product. *Food Res. Int.* 108, 93–100. <https://doi.org/10.1016/j.foodres.2018.03.031>
- Severino, R., Vu, K.D., Donsì, F., Salmieri, S., Ferrari, G., Lacroix, M., 2014. Antimicrobial effects of different combined non-thermal treatments against *Listeria monocytogenes* in broccoli florets. *J. Food Eng.* 124, 1–10. <https://doi.org/10.1016/j.jfoodeng.2013.09.026>
- Shahmohammadi Jebel, F., Almasi, H., 2016. Morphological, physical, antimicrobial and release properties of ZnO nanoparticles-loaded bacterial cellulose films. *Carbohydr. Polym.* 149, 8–19. <https://doi.org/10.1016/j.carbpol.2016.04.089>
- Shin, E., Choi, S., Lee, J., 2018. Fabrication of regenerated cellulose nanoparticles/waterborne polyurethane nanocomposites. *J. Appl. Polym. Sci.* 135. <https://doi.org/10.1002/app.46633>
- Shoseyov, O., Paltiel, Y., Yochelis, S., Baruch-Sharon, S., Nevo, Y., 2015. Coating layers of a nanocomposite comprising a nano-cellulose material and nanoparticles. US20150017432A1.
- Shvedova, A.A., Kisin, E.R., Yanamala, N., Farcas, M.T., Menas, A.L., Williams, A., Fournier, P.M., Reynolds, J.S., Gutkin, D.W., Star, A., Reiner, R.S., Halappanavar, S., Kagan, V.E., 2016. Gender differences in murine pulmonary responses elicited by cellulose nanocrystals. *Part. Fibre Toxicol.* 13, 28. <https://doi.org/10.1186/s12989-016-0140-x>
- Siegel, R.A., Rathbone, M.J., 2012. Overview of controlled release mechanisms, in: Siepmann, J., Siegel, R.A., Rathbone, M.J. (Eds.), *Fundamentals and applications of controlled release drug delivery, advances in delivery science and technology*. Springer US, Boston, MA, pp. 19–43. https://doi.org/10.1007/978-1-4614-0881-9_2
- Šimon, P., Chaudhry, Q., Bakoš, D., 2008. Migration of engineered nanoparticles from polymer packaging to food – a physicochemical view. *J. Food Nutr. Res. Slovak Repub.* [WWW Document]. URL <http://agris.fao.org/openagris/search.do?recordID=SK2008000245> (accessed 08.01.18)
- Sinco, P., 2000. Use of gamma rays in book conservation. *Nucl. News* 38–40.

- Sinki, G., Assaf, R., Lombardo, J., 1997. Flavor changes: a review of the principal causes and reactions. *Perfum Flavor* 22, 23–31.
- Skaugrud, O., Hagen, A., Borgersen, B., Dornish, M., 1999. Biomedical and pharmaceutical applications of alginate and chitosan. *Biotechnol. Genet. Eng. Rev.* 16, 23–40. <https://doi.org/10.1080/02648725.1999.10647970>
- Sokhey, A.S., Hanna, M.A., 1993. Properties of irradiated starches. *Food Structure* 12, 397–410.
- Soliman, E.A., El-Moghazy, A.Y., El-Din, M.S.M., Massoud, M.A., 2013. Microencapsulation of essential oils within alginate: formulation and in vitro evaluation of antifungal activity. *J. Encapsulation Adsorpt. Sci.* 03, 48–55. <http://dx.doi.org/10.4236/jeas.2013.31006>
- Sonje, A.G., Mahajan, H.S., 2016. Nasal inserts containing ondansetron hydrochloride based on chitosan–gellan gum polyelectrolyte complex: in vitro–in vivo studies. *Mater. Sci. Eng. C* 64, 329–335. <https://doi.org/10.1016/j.msec.2016.03.091>
- Sonnier, R., Otazaghine, B., Viretto, A., Apolinario, G., Lenny, P., 2015. Improving the flame retardancy of flax fabrics by radiation grafting of phosphorus compounds. *Eur. Polym. J.* 68, 313–325. <https://doi.org/10.1016/j.eurpolymj.2015.05.005>
- St Angelo, A.J., 1996. Lipid oxidation on foods. *Crit. Rev. Food Sci. Nutr.* 36, 175–224. <https://doi.org/10.1080/10408399609527723>
- Štuncová, A., Davies, G.R., Eichhorn, S.J., 2005. Elastic modulus and stress-transfer properties of tunicate cellulose whiskers. *Biomacromolecules* 6, 1055–1061. <https://doi.org/10.1021/bm049291k>
- Sultanov, K., Turaev, A.S., 1996. Mechanism of the radiolytic transformation of cellulose. *Chem. Nat. Compd.* 32, 728–733. <https://doi.org/10.1007/BF01375125>
- Syamila, M., Gedi, M.A., Briars, R., Ayed, C., Gray, D.A., 2019. Effect of temperature, oxygen and light on the degradation of β -carotene, lutein and α -tocopherol in spray-dried spinach juice powder during storage. *Food Chem.* 284, 188–197. <https://doi.org/10.1016/j.foodchem.2019.01.055>
- Sworn, G., Sanderson, G.R., Gibson, W., 1995. Gellan gum fluid gels. *Food Hydrocoll.* 9, 265–271. [https://doi.org/10.1016/S0268-005X\(99\)80257-9](https://doi.org/10.1016/S0268-005X(99)80257-9)
- Tahara, N., Tabuchi, M., Watanabe, K., Yano, H., Morinaga, Y., Yoshinaga, F., 1997. Degree of polymerization of cellulose from *Acetobacter xylinum* BPR2001 decreased by cellulase produced by the strain. *Biosci. Biotechnol. Biochem.* 61, 1862–1865. <https://doi.org/10.1271/bbb.61.1862>
- Takács, E., Wojnárovits, L., Borsa, J., Földváry, C., Hargittai, P., Zöld, O., 1999. Effect of γ -irradiation on cotton-cellulose. *Radiat. Phys. Chem.* 55, 663–666. [https://doi.org/10.1016/S0969-806X\(99\)00245-5](https://doi.org/10.1016/S0969-806X(99)00245-5)
- Takács, E., Wojnárovits, L., Borsa, J., Papp, J., Hargittai, P., Korecz, L., 2005. Modification of cotton-cellulose by pre-irradiation grafting. *Nucl. Instrum. Methods Phys. Res. Sect. B Beam Interact. Mater. At., Ionizing Radiation & Polymers* 236, 259–265. <https://doi.org/10.1016/j.nimb.2005.03.248>
- Tirado, C., Schmidt, K., 2001. WHO surveillance programme for control of foodborne infections and intoxications: preliminary results and trends across greater

- Europe. World Health Organization. *J. Infect.* 43, 80–84. <https://doi.org/10.1053/jinf.2001.0861>
- Toft, K., Grasdalen, H., Smidsrød, O., 1986. Synergistic gelation of alginates and pectins, in: *chemistry and function of pectins*, ACS Symposium Series. American Chemical Society, pp. 117–132. <https://doi.org/10.1021/bk-1986-0310.ch010>
- Turek, C., Stintzing, F.C., 2013. Stability of essential oils: a review. *Compr. Rev. Food Sci. Food Saf.* 12, 40–53. <https://doi.org/10.1111/1541-4337.12006>
- United States Department of Agriculture, 2010. 2010 Dietary guidelines advisory committee: systematic reviews of the sodium, potassium and water subcommittee [WWW Document]. URL https://www.cnpp.usda.gov/sites/default/files/usda_nutrition_evidence_flibrary/2010DGAC-SR-SodiumPotassiumWater.pdf (accessed 30.12.18)
- Urban, J., Santar, I., Sedlackova, J., Pipota, J., 1978. Use of gamma radiation for conservation purposes in Czechoslovakia, in: 5th Triennial Meeting. Presented at the ICOM Committee for Conservation, Zagreb.
- Valapa, R.B., Pugazhenti, G., Katiyar, V., 2015. Fabrication and characterization of sucrose palmitate reinforced poly(lactic acid) bionanocomposite films. *J. Appl. Polym. Sci.* 132. <https://doi.org/10.1002/app.41320>
- Van, A., Duncan, S.E., Marcy, J.E., Long, T.E., Hackney, C.R., 2001. Effectiveness of poly(ethylene terephthalate) and high-density polyethylene in protection of milk flavor. *J. Dairy Sci.* 84, 1341–1347. [https://doi.org/10.3168/jds.S0022-0302\(01\)70164-6](https://doi.org/10.3168/jds.S0022-0302(01)70164-6)
- Vanderfleet, O.M., Osorio D.A., Cranston E. D., 2018. Optimization of cellulose nanocrystal length and surface charge density through phosphoric acid hydrolysis. *Philos. Trans. R. Soc. Math. Phys. Eng. Sci.* 376, 20170041. <https://doi.org/10.1098/rsta.2017.0041>
- Velasco, J., Dobarganes, C., Márquez-Ruiz, G., 2003. Variables affecting lipid oxidation in dried microencapsulated oils. *Grasas aceites* 54, 304–314. <https://doi.org/10.3989/gya.2003.v54.i3.246>
- Villanova, J.C.O., Ayres, E., Carvalho, S.M., Patrício, P.S., Pereira, F.V., Oréface, R.L., 2011. Pharmaceutical acrylic beads obtained by suspension polymerization containing cellulose nanowhiskers as excipient for drug delivery. *Eur. J. Pharm. Sci.* 42, 406–415. <https://doi.org/10.1016/j.ejps.2011.01.005>
- Vital, A.C.P., Guerrero, A., Monteschio, J. de O., Valero, M.V., Carvalho, C.B., de Abreu Filho, B.A., Madrona, G.S., do Prado, I.N., 2016. Effect of edible and active coating (with rosemary and oregano essential oils) on beef characteristics and consumer acceptability. *PloS One* 11, e0160535. <https://doi.org/10.1371/journal.pone.0160535>
- Voda, K., Boh, B., Vrtačnik, M., Pohleven, F., 2003. Effect of the antifungal activity of oxygenated aromatic essential oil compounds on the white-rot *Trametes versicolor* and the brown-rot *Coniophora puteana*. *Int. Biodeterior. Biodegrad.* 51, 51–59. [https://doi.org/10.1016/S0964-8305\(02\)00075-6](https://doi.org/10.1016/S0964-8305(02)00075-6)
- Von Sonntag C., 1980. Free-radical reactions of carbohydrates as studied by radiation techniques, in: Horton, D. and Tipson R.S. (Eds.) *Advances in carbohydrate chemistry and biochemistry*. Academic Press, pp 7–77.

- Vu, K.D., Hollingsworth, R.G., Salmieri, S., Takala, P.N., Lacroix, M., 2012. Development of bioactive coatings based on γ -irradiated proteins to preserve strawberries. *Radiat. Phys. Chem., International Meeting on Radiation Processing* 81, 1211–1214. <https://doi.org/10.1016/j.radphyschem.2011.11.071>
- Vukić, M., Grujić, S., Odzaković, B., 2017. Application of edible films and coatings in food production, in: Pellicier, E., Nikolic D., Sort J., Baró M., Zivic F., Grujovic N., Grujic R., Pelemis S. (Eds.) *Advances in applications of industrial biomaterials*. Springer, Cham, pp. 121–138. https://doi.org/10.1007/978-3-319-62767-0_7
- Wang, F., Wen, Y., Bai, T., 2016. The composite hydrogels of polyvinyl alcohol–gellan gum- Ca^{2+} with improved network structure and mechanical property. *Mater. Sci. Eng. C* 69, 268–275. <https://doi.org/10.1016/j.msec.2016.06.084>
- Wang, J., Gardner, D.J., Stark, N.M., Bousfield, D.W., Tajvidi, M., Cai, Z., 2018. Moisture and oxygen barrier properties of cellulose nanomaterial-based films. *ACS Sustain. Chem. Eng.* 6, 49–70. <https://doi.org/10.1021/acssuschemeng.7b03523>
- Warren, H., in het Panhuis, M., 2015. Highly conducting composite hydrogels from gellan gum, PEDOT:PSS and carbon nanofibres. *Synth. Met.* 206, 61–65. <https://doi.org/10.1016/j.synthmet.2015.05.004>
- Watanabe, K., Tabuchi, M., Morinaga, Y., Yoshinaga, F., 1998. Structural features and properties of bacterial cellulose produced in agitated culture. *Cellulose* 5, 187–200. <https://doi.org/10.1023/A:1009272904582>
- Weiss J., Takhistov P., McClements D. J., 2006. Functional materials in food nanotechnology. *J. Food Sci.* 71, R107–R116. <https://doi.org/10.1111/j.1750-3841.2006.00195.x>
- Weiss, J., Gaysinsky, S., Davidson, M., McClements, J., 2009. Nanostructured encapsulation systems: Food Antimicrobials, in: Barbosa-Cánovas, G., Mortimer, A., Lineback, D., Spiess, W., Buckle, K., Colonna, P. (Eds.), *Global Issues in Food Science and Technology*. Academic Press, San Diego, pp. 425–479. <https://doi.org/10.1016/B978-0-12-374124-0.00024-7>
- Whiley, H., Ross, K., 2015. Salmonella and eggs: from production to plate. *Int. J. Environ. Res. Public Health* 12, 2543–2556. <https://doi.org/10.3390/ijerph120302543>
- Willey, J., Sherwood L.M., Woolverton C.J., 2016. A review of the chemistry of biological molecules, in: Willey J., Sherwood L., Woolverton C. (Eds.) *Prescott's Microbiology*. McGraw-Hill Education, New York, NY
- Wischke, C., Schwendeman, S.P., 2008. Principles of encapsulating hydrophobic drugs in PLA/PLGA microparticles. *Int. J. Pharm., Future Perspectives in Pharmaceutics Contributions from Younger Scientists* 364, 298–327. <https://doi.org/10.1016/j.ijpharm.2008.04.042>
- Yamamoto, K., Kumagai, H., Sakiyama, T., Song, C.-M., Yano, T., 1991. Inhibitory activity of alginate against the formation of calcium phosphate. *Biosci. Biotech. Biochem.* 56, 90–93. <https://doi.org/10.1271/bbb.56.90>
- Yang, X., Bakaic, E., Hoare, T., Cranston, E.D., 2013. Injectable polysaccharide hydrogels reinforced with cellulose nanocrystals: morphology, rheology, degradation, and cytotoxicity. *Biomacromolecules* 14, 4447–4455. <https://doi.org/10.1021/bm401364z>

- Yanishlieva, N.V., Marinova, E.M., Gordon, M.H., Raneva, V.G., 1999. Antioxidant activity and mechanism of action of thymol and carvacrol in two lipid systems. *Food Chem.* 64, 59–66. [https://doi.org/10.1016/S0308-8146\(98\)00086-7](https://doi.org/10.1016/S0308-8146(98)00086-7)
- Younes, I., Rinaudo, M., 2015. Chitin and chitosan preparation from marine sources. structure, properties and applications. *Mar. Drugs* 13, 1133–1174. <https://doi.org/10.3390/md13031133>
- Yu, J., Peñaloza-Vázquez, A., Chakrabarty, A.M., Bender, C.L., 1999. Involvement of the exopolysaccharide alginate in the virulence and epiphytic fitness of *Pseudomonas syringae* pv. *syringae*. *Mol. Microbiol.* 33, 712–720. <https://doi.org/10.1046/j.1365-2958.1999.01516.x>
- Yuan, J.-P., Chen, F., 1998. Degradation of ascorbic acid in aqueous solution. *J. Agric. Food Chem.* 46, 5078–5082. <https://doi.org/10.1021/jf9805404>
- Zeeb, B., Saberi, A.H., Weiss, J., McClements, D.J., 2015. Formation and characterization of filled hydrogel beads based on calcium alginate: factors influencing nanoemulsion retention and release. *Food Hydrocoll.* 50, 27–36. <https://doi.org/10.1016/j.foodhyd.2015.02.041>
- Zhang, D., Karkooti, A., Liu, L., Sadrzadeh, M., Thundat, T., Liu, Y., Narain, R., 2018. Fabrication of antifouling and antibacterial polyethersulfone (PES)/cellulose nanocrystals (CNC) nanocomposite membranes. *J. Membr. Sci.* 549, 350–356. <https://doi.org/10.1016/j.memsci.2017.12.034>
- Zhao, M., Moy, J., Paull, R.E., 1996. Effect of gamma-irradiation on ripening papaya pectin. *Postharvest Biol. Technol.* 8, 209–222. [https://doi.org/10.1016/0925-5214\(96\)00004-X](https://doi.org/10.1016/0925-5214(96)00004-X)
- Zhou, C., Wu, Q., 2012. Recent development in applications of cellulose nanocrystals for advanced polymer-based nanocomposites by novel fabrication strategies, in: Neralla, S. (Ed.), *Nanocrystals - Synthesis, Characterization and Applications*. InTech. <https://doi.org/10.5772/48727>
- Zografi, G., Kontny, M.J., 1986. The interactions of water with cellulose- and starch-derived pharmaceutical excipients. *Pharm. Res.* 3, 187–194. <https://doi.org/10.1023/A:1016330528260>

PUBLICATIONS AND CONTRIBUTIONS

- 1) Criado *et al.* (2019) Effect of cellulose nanocrystals on thyme essential oil release from alginate beads: study of antimicrobial activity against *Listeria innocua* and ground meat shelf life in combination with gamma irradiation. *Cellulose* 26, 9: 5247-5265.
- 2) Criado *et al.* (2016) Gamma-irradiation of cellulose nanocrystals (CNCs): investigation of physicochemical and antioxidant properties. *Cellulose* 24: 2111-2124.
- 3) Maherani *et al.* (2016) World market development and consumer acceptance of irradiation technology. *Foods* 5, 79.
- 4) Marra *et al.* (2016). Effect of PLA/ZnO packaging and gamma radiation on the content of *Listeria innocua*, *Escherchia coli* and *Salmonella enterica* on ham during storage at 4°C. *Journal of Food Science and Engineering* 6: 245-259.
- 5) Criado *et al.* (2016) Free radical grafting of gallic acid on cellulose nanocrystals (CNCs) and evaluation of antioxidant reinforced gellan gum films. *Radiation Physics and Chemistry* 118: 61-69.
- 6) Criado *et al.* (2014). Modification of nanocrystalline cellulose for bioactive loaded films. *Journal of Research Updates in Polymer Science* 3, 2.

Book Chapter

- 1) Criado *et al.* (2019) Cellulose nanocrystals in food packaging. Reference module in food sciences. Elsevier
- 2) Criado *et al.* (2017) Nanocellulose in food packaging. In: *Nanocomposites in Active Packaging*. United States. Scrivener Publishing LLC

Presentations

- 1) 5th Ed. Student Conference CRIBIQ 23rd Oct, 2018
Drummondville, QC, Canada
- 2) International Congress on Engineering and Food 14-18th June, 2018
Quebec city, QC, Canada